Universidade de Aveiro Departamento de Biologia
2012

Ana Cristina Esteves Oliveira Gomes

O efeito do stress ambiental na fidelidade da sintese de proteínas

The role of environmental stress on protein synthesis fidelity

Dissertação apresentada à Universidade de Aveiro para cumprimento dos requisitos necessários à obtenção do grau de Doutor em Bioquímica, realizada sob a orientação científica do Doutor Manuel António da Silva Santos, Professor Associado do Departamento de Biologia da Universidade de Aveiro.

Apoio financeiro da FCT e do POCTI/FSE no âmbito do III Quadro Comunitário de Apoio.

Tudo no mundo está dando respostas, o que demora é o tempo das perguntas.

José Saramago, *O Memorial do Covento* (1982)

o júri

presidente **Doutor Nelson Fernando Pacheco da Rocha**
Professor Catedrático da Universidade de Aveiro
em representação da Reitoria da Universidade de Aveiro

Doutora Maria da Conceição Lopes Vieira dos Santos
Professora Associada com agregação da Universidae de Aveiro

Doutor Manuel António da Silva Santos
Professor Associado da Universidade de Aveiro (Orientador)

Doutora Luisa Maria Ferreira Romão Loison
Investigadora Principal com habilitações do Instituto Nacional
de Saúde Dr. Ricardo Jorge

Doutora Margarida Gama Carvalho
Professora Auxiliar da Faculdade de Ciências da Universidade de Lisboa

Doutora Maria do Céu Gomes dos Santos
Professora Auxiliar Convidada da Universidade de Aveiro

Doutora Gabriela Maria Ferreira Ribeiro de Moura
Investigadora Auxiliar da universidade de Aveiro (Coorientadora)

Doutora Maria da Conceição Venâncio Egas
Investigadora do Biocant - Associação de Transferência de Tecnologia,
Parque Tecnológico de Cantanhede

agradecimentos

acknowledgements

I would first like to thank my advisor, Dr. Manuel Santos, for giving me the opportunity to work and grow in his laboratory. He was a source of knowledge and wisdom for which I will always be thankfull. I am greatfull for all the support and guidance that pushed me further along this path.

I would also like to thank all the present and past colleagues at the RNA biology laboratory. I am honored to have shared so much with such an amazing group of people. I am deeply greatfull to João Simões, Rita, Violeta, Marisa, Tobias, Ana, Jörg and João Paredes for the knowledge and all the friendship that always kept my spirits up. A special thanks to Patrícia, Céu and Laura, for so many advices and for always finding the right words to say. I am also thankfull to Catarina and Gabriela for all the help when I first arrived in the laboratory. Finally and foremost, I wish to thank Tatiana and Denisa, for being so special and for always being there for me.

I am greatfull to Dr. Philip Farabaugh, from UMBC in Baltimore, for how well he received me in his laboratory and for all our fruitfull discussions. I also wish to thank his group members, specially Ana Raman, Haritha, Susmitha and Emily for all the help performing the experiments and for making me feel so welcome.
I warmly thank Dr. Knud Nierhaus, from the Max Planck Institute for Molecular Genetics in Berlin, for how much he taught me during my short stay in his laboratory and for the many scientific advices.
I would also like to thank Dr. Tao Pan and Elizabeth, from the University of Chicago, for all the help with the yeast pulse labeling protocol and Clement Chan, from the Massachusetts Institute of Technology, for his contribution to the quantification of cytoplasmic tRNA modifications.

I want to acknowledge FCT for finantial support during my PhD.

I am indebted to all my friends, specially Elisabete, Maria João, Alexandra, Marta and Rui G. for their endless support. Thank you for bringing music, humour and so much joy into my life.

Mais do que tudo, quero agradecer à minha família, a quem devo toda a minha força. À minha irmã, que me segura desde o primeiro passo; aos meus pais, a quem dedico esta tese, que com dedicação e amor me ensinaram a persistir e a sonhar, mesmo quando tudo parece perdido. São vossas também, as minhas pequenas vitórias.

ab imo pectore

palavras-chave

Erros de tradução, mRNA, stress ambiental, supressão de terminação, resposta ao stress, agregação de proteína, mecanismos de controlo de qualidade do proteoma, modificações de tRNA.

resumo

Estudos recentes estabelecem uma ligação entre erros na tradução do mRNA e cancro, envelhecimento e neurodegeneração. RNAs de transferência mutantes que introduzem aminoácidos em locais errados nas proteínas aumentam a produção de espécies reactivas de oxigénio e a expressão de genes que regulam autofagia, ribofagia, degradação de proteínas não-funcionais e protecção contra o stress oxidativo. Erros na tradução do mRNA estão portanto relacionados com stress proteotóxico. Sabe-se agora que o mecanismo de toxicidade do crómio está associado à diminuição da fidelidade de tradução e à agregação de proteínas com malformações que destabilizam a sua estrutura terciária. Desta forma, é possível que os efeitos do stress ambiental ao nível da degeneração celular possam estar relacionados com a alteração da integridade da maquinaria da tradução.

Neste estudo procedeu-se a uma avaliação alargada do impacto do stress ambiental na fidelidade da síntese de proteínas, utilizando *S. cerevisiae* como um sistema modelo. Para isso recorreu-se a repórteres policistrónicos de luciferase que permitiram quantificar especificamente a supressão de codões de terminação e o erro na leitura do codão AUG em células exposta a concentações não letais de metais pesados, etanol, cafeína e H_2O_2. Os resultados sugerem que a maquinaria de tradução é na generalidade muito resistente ao stress ambiental, devido a uma conjugação de mecanismos de homeostase que muito eficientemente antagonizam o impacto negativo dos erros de tradução. A nossa abordagem quantitativa permitiu-nos a identificar genes regulados por uma resposta programada ao stress ambiental que são também essenciais para mitigar a ocorrência de erros de tradução, nomeadamente, *HSP12*, *HSP104* e *RPN4.* A exposição prolongada ao stress ambiental conduz à saturação dos mecanismos de homeostase, contribuindo para a acumulação de proteínas contendo erros de tradução e diminuindo a disponibilidade de proteínas funcionais directamente envolvidas na manutenção da fidelidade de tradução e integridade celular. Ao contrário de outras Hsps, a Hsp12p adopta normalmente uma localização membranar em condições de stress, que pode modular a fluidez e estabilidade membranar, sugerindo que a membrana plasmática é um alvo preferencial da perda de fidelidade da tradução.

Para melhor compreender as respostas celulares aos erros de tradução, células contendo deleções em genes codificadores das Hsps foram transformadas com tRNAs mutantes que introduzem alterações no proteoma. Os nossos resultados demonstram que para além da resposta geral ao stress, estes tRNAs induzem alterações a nível do metabolismo celular e um aumento de aminoacilação com Metionina em vários tRNAs, sugerindo um mecanismo de protecção contra espécies reactivas de oxigénio. Em conclusão, este estudo sugere um papel para os erros de tradução na gestão de recursos energéticos e na adaptação das células a ambientes desfavoráveis.

keywords

Mistranslation, mRNA, environmental stress, stop codon supression, stress response mechanisms, protein aggregation, proteome quality control mechanisms, tRNA modifications.

abstract

Recent studies link mRNA mistranslation to cancer, neurodegeneration, aging and metabolic imbalances. It was shown previously that mutant tRNAs that mutagenise the proteome via mRNA misreading increase production of reactive oxygen species and up-regulate the expression of oxidative stress, autophagy and ribophagy genes, indicating that mistranslation is an important cause of proteotoxic stress. Interestingly, chromium toxicity is linked to increased mistranslation and protein aggregation suggesting that environmental stressors may cause cell degeneration and human disease through deregulation of protein synthesis fidelity.

In this study, we investigate the impact of environmental on the fidelity of protein synthesis using *S.cerevisiae* as a model system. We used a dual luciferase reporter to quantify both AUG misreading and stop codon readthrough in cells exposed to sub-lethal concentrations of heavy metals, ethanol, caffeine and hydrogen peroxide. Our results suggest that the translational machinery is in general very resistant to environmental stress, due to a conjugation of homeostasis mechanisms that effectively antagonize the negative impact of protein synthesis errors to a level tolerated by cells. Additionally, our quantitative approach allowed us to identify genes under the control of the environmental stress response (ESR) that are essential to cope with induced amino acid misincorporation, namely *HSP12, HSP104* and *RPN4*. Prolonged stress exposure drives saturation of protein homeostasis mechanisms, which contributes to accumulation of mistranslated protein into the cytoplasm and thereby decreases the availability of functional proteins directly involved in translational fidelity and cellular integrity. Unlike all other Hsps, Hsp12p associates with the plasma membrane under stress, which may help modulate membrane fluidity and stability, suggesting that protein synthesis errors target membrane components.

To further understand the cellular responses to mistranslation and proteotoxic stress, cells harboring deletions in genes coding for small heat-shock proteins were transformed with a misreading tRNA. The data showed that besides a wide response to stress, constitutive mistranslation also promoted a shift in cellular metabolism. Finally, cells expressing misreading tRNAs show increased Met-misacylation, suggesting that methionine misincorporation into proteins protects against ROS. This study strongly supports a role for mistranslation in energy management and cell adaptation to suboptimal environmental conditions.

List of Contents

List of abbreviations

aaRS	Aminoacyl-tRNA synthetase
aa-tRNA	Aminoacyl-tRNA
APS	Ammonium persulphate
ATP	Adenosine triphosphatase
BCA	Bicinchoninic acid
cDNA	Complementary deoxyribonucleic acid
CFU	Colony forming units
Cy3	Cyanine 3
DHE	Dihydroethidium
DHR123	Dihydrorhodamine 123
DNA	Deoxyribonucleic acid
DTT	Dithiothreitol
EDTA	Ethylennediamine tetraacetic acid
ER	Endoplasmic reticulum
ESR	Environmental stress response
F-Luc	Firefly luciferase
GAAC	General amino acid control
GDP	Guanosine 5′-diphosphate
GFP	Green fluorescent protein
GTP	Guanosine 5′-triphosphate
HPLC	High-performance liquid chromatography
HSP	Heat shock protein
IPOD	Perivacuolar insoluble protein deposits
IRES	Internal ribosome entry site
JUNQ	Juxtanuclear quality-control compartments
kDa	kilodalton
LB	Lysogeny broth
LC – MS/MS	Liquid chromatography – coupled mass spectrometry
mA	milliampere
MetRS	Methionyl-tRNA synthetase
MM	Minimal medium
mRNA	messenger ribonucleic acid
NADH	Nicotinamide adenine dinucleotide
NADPH	Nicotinamide adenine dinucleotide phosphate

NMD	Nonsense-mediated decay
ORF	Open reading frame
PAB	Poly (A)-binding protein
PAGE	Polyacrylamide gel electrophoresis
PBS	Phosphate buffered saline
PCR	Polymerase chain reaction
PEG	Polyethylene glycol
PTC	Peptidyl-transferase centre
QQQ	Triple quadrupole mass spectrometer
R - Luc	*Renilla* luciferase
RLU	Relative luminescence units
RNA	Ribonucleic acid
RNAse	Ribonuclease
ROS	Reactive oxygen species
rpm	Revolutions per minute
S	Svedberg units
SDS	Sodium dodecyl sulphate
SECIS	Selenocysteine Insertion Sequence
sHSP	Small heat shock protein
TCA	Tricarboxylic acid
TEMED	Tetramethylethylenediamine
TMV	Tobacco Mosaic Virus
TPP	Thiamine pyrophosphate
Tris	Tris(hydroxymethyl)aminomethane
tRNA	transfer ribonucleic acid
UPR	Unfolded protein response
UPS	Ubiquitin proteasome system
V	volt
V/V	Volume/volume
W/W	Mass/mass
YPD	Yeast Extract Peptone Dextrose

List of Figures

List of Tables

Chapter 1

Introduction

1.1 Central Dogma of Molecular Biology

The information necessary for cell development, survival and division is contained in DNA and organized in genes. Dividing cells duplicate their genetic contend by DNA replication and the information is inherited and preserved by daughter cells. For all the fundamental processes in the cell to take place DNA must first be converted into messenger RNA (mRNA) that relocates to ribosomes where it can be used to produce unique sequences of amino acids. The final protein molecules lie at the heart of cellular metabolism and participate in virtually every process within cells. This understanding of how genetic information is transformed by the cell into a unique protein by an mRNA intermediate composes the Central Dogma of Molecular Biology.

1.2. Genetic Code and Overview of the Translation Steps

While DNA stores the information for protein synthesis and mRNA carries the genetic information copied from DNA, nearly all the activities in cells are accomplished by protein effectors. The rules that govern the transfer of genetic information from nucleic acids to proteins compose the genetic code. Three nucleotide residues of mRNA (one codon) are required to encode each amino acid and these triplets are read in a successive, non overlapping way by the ribosome, giving instructions for the incorporation of specific amino acids, resulting in synthesis of new protein.

Triplet combination of the 4 ribonucleosides (adenosine or A, uridine or U, guanosine or G, cytidine or C) results in the 64 different codons that compose the genetic code. Of these, 61 identify individual amino acids and three are stop codons (see Figure 1.1). Most amino acids are encoded by more than one codon and the different codons for a given amino acid are synonymous. Because of these redundancies, the genetic code is degenerate (Lodish et al., 2000).

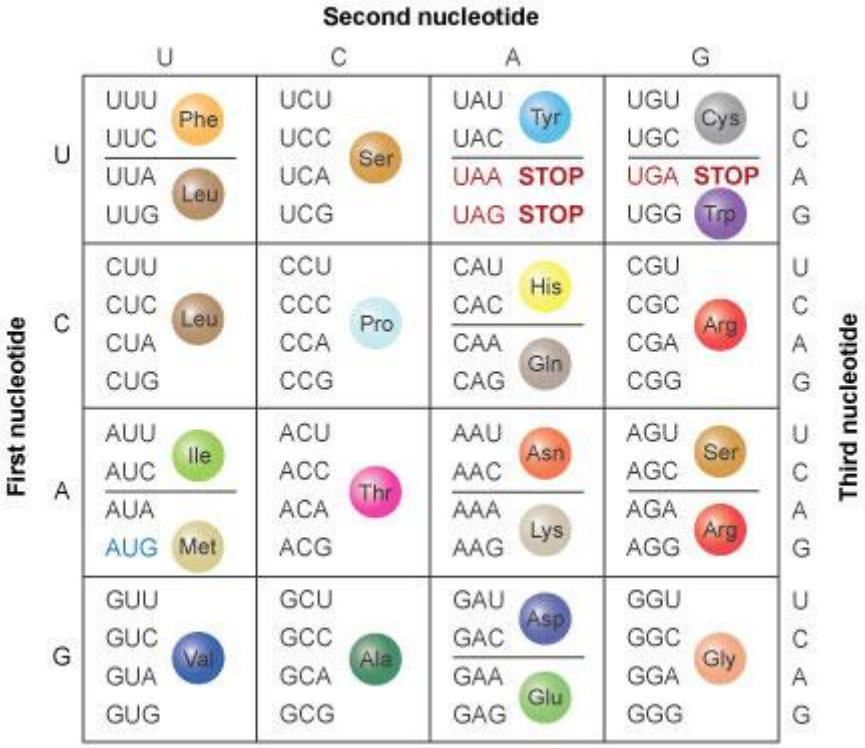

Figure 1.1 - The standard genetic code table is composed of 64 codons. Of these, 61 identify individual amino acids (represented in colors) and three are stop codons. Multiple codons can code for the same amino acid.

Translation is a cyclical process that takes place through four distinct stages in all living organisms, namely: Initiation, elongation, termination and recycling. The mechanisms and machinery are quite conserved, but have different features across the distinct branches of life.

1.2.1. Key mechanistic players in translation

Proteins have a leading role in cellular function, carrying out most of the biological activities. The accurate synthesis of proteins is thus vital to keep cellular homeostasis. The complexity of protein synthesis takes its shape by the distinct but cooperative contribution of at least three species of RNA: messenger RNA (mRNA), transfer RNA (tRNA) and ribosomal RNA (rRNA).

mRNA conveys sequence information from the genome to the protein synthesis machinery in the form of sequential codons, each one comprising three nucleotides that specify either one particular amino acid or synthesis termination. Ribosomal RNA (rRNA) intricate association with proteins forms ribosomes, complex structures that catalyze peptide bond formation and mediate mRNA/tRNA interactions. tRNAs function as adaptor molecules between mRNA and protein.

Anticodon interactions with the mRNA codon occur at one end of the tRNA and specifically assign an amino acid to the growing peptide chain, all in concerted action with another major partner, the ribosome. For every amino acid there is at least one tRNA and a specific aminoacyl-tRNA sintethase that recognizes the surface structure of each tRNA and assures that the cognate amino acid is charged. The resulting aminoacyl-tRNA then recognizes a codon in mRNA by complementary base pairing interactions and in that way carries its cognate amino acid to the growing polypeptide, ultimately linking the information on DNA to protein synthesis. The amino group of the amino acid is then involved in nucleophilic attack on the carbonyl group in the C-terminus of the growing peptide, culminating in formation of a new bond.

1.2.1.1. Ribosome

One of the key cellular players is the ribosome, which catalyzes the assembly of amino acids into proteins. In growing yeast there are nearly 200 000 ribosomes per cell, making it the most abundant cellular RNA-protein complex, composed of several different ribosomal RNA (rRNA) molecules and more than 50 proteins, organized into a large and a small subunit. rRNA makes up 80% of the total cellular RNA. Around 50% of RNA polymerase II transcription and 90% of mRNA splicing is devoted to ribosomal proteins (Warner, 1999).

A functionally competent ribosome consists of two subunits, one of them about twice the size of the other, and named according to their sedimentation coefficients, in Svedberg units (S). Ribosomes from prokaryotic and eukaryotic cells differ in the size

of the subunits, because of the distinct composition and length of RNA molecules and proteins (Lodish et al., 2000). In prokaryotes the large subunit contains two rRNAs (23S and 5S) and 34 proteins (L1-L34), while the small subunit contains only one rRNA (16S) and 21 proteins (S1-S21). In eukaryotes the ribosomes are homologous but larger and include a higher number of components. The large subunit contains three rRNAs (28S, 5.8S and 5S) and the small subunit one 18S rRNA.

Ribosomes actively catalyzing protein synthesis are 1:1 complexes of the two subunits that share mechanistic principles common to all organisms. Remarkably, the two subunits are functionally different. The small subunit mediates the codon-anticodon interaction and the large subunit contains the peptidyl-transferase centre (PTC), which catalyses the formation of peptide bonds in the growing polypeptide (Steitz, 2008). Remarkably, both subunits can carry out their specific functions independently, even when not incorporated in a 1:1 complex (Moore & Steitz, 2011). During protein synthesis the ribosome moves along the mRNA in one-codon steps, each corresponding to addition of one amino acid to the growing polypeptide. There are three binding sites for tRNA in the ribosome: the A-site for aminoacyl-tRNA, the P-site for peptidyl-tRNA and the E-site for the deacylated tRNA leaving the ribosome.

1.2.1.2. Transfer RNA

tRNA molecules function as adaptor molecules, linking protein synthesis with the information stored in the nucleic acids. tRNA binds to a specific amino acid (aminoacylation) and recognizes the nucleotide encoding that amino acid in mRNA through a three base sequence (anticodon). This culminates with amino acid transference to the growing polypeptide.

tRNA molecules consist of a single ribonucleic acid chain around 73 – 93 nucleotides long which can fold in short double helix regions stabilized by Watson-Crick base pairing (Holley, 1965). This arrangement defines several distinct stem-loops (D loop, anticodon loop and the TΨCG loop) together with an acceptor stem, so called because

it bears the 3′ single stranded CCA terminus, the site of aminoacylation. There is in addition a loop of variable size between the anticodon and the TΨCG that allows tRNAs categorization into two classes. tRNAs bearing a short variable loop of 4 or 5 nucleotide residues are classified as type I (almost almost all existing tRNAs), and those having a long variable stem-loop 10 to 24 bases long, as type II (eukaryotic leucine and serine tRNAs) (Brennan & Sundaralingam, 1976). A group of noncanonical tRNAs lacking the D or T loops exists in mitochondria. These molecules can only be charged by their cognate mitochondrial synthetases (Cavarelli & Moras, 1993).

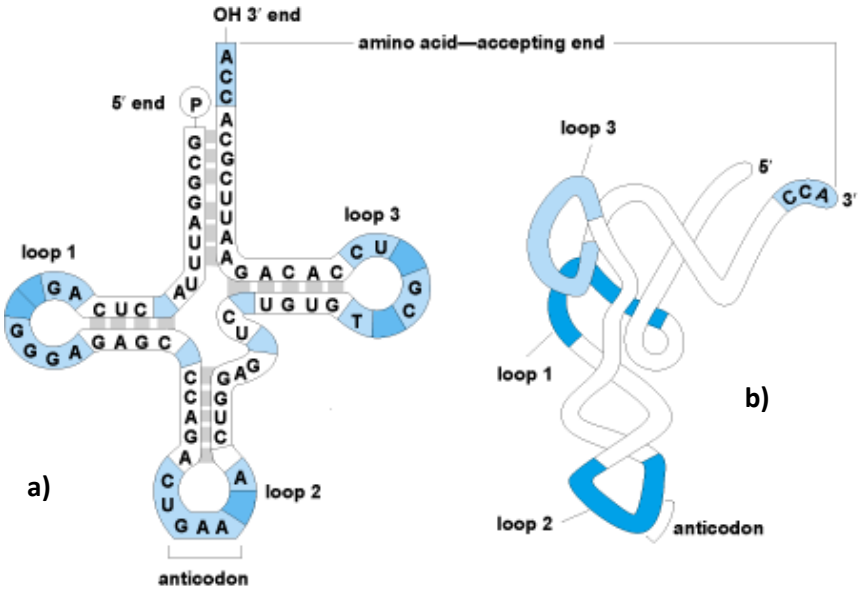

Figure 1.2 – The structure of tipical tRNA a) secondary structure (cloverleaf – like model) b) terciary L-shapped structure. **Loop 1** – D loop, **loop 2** – anticodon loop and **loop 3** - TΨCG loop.

In three dimensions the tRNA is folded in a compact L shape with the anticodon loop in coaxial stacking with the TΨCG loop and the acceptor stem forming two discrete structural domains positioned around 76Å opposite from each other (Schimmel & Ribas de, 1995). This arrangement allows both optimized fit into the P and A-sites of the ribosome and recognition by aminoacyl-tRNA synthetases. A number of hydrogen bonding interactions between base-phosphate, base-ribose, phosphate-ribose and

ribose-ribose are formed during the tRNA maturation process and contribute to stability of this tertiary structure (Holley, 1965; Schimmel, 1991)(see Figure 1.2).

1.2.1.2.a. tRNA synthesis and processing

In eukaryotes, polymerase III transcribes small untranslated RNAs required for transcription regulation or translation, like 5S rRNA and tRNAs. The first protein that binds to newly synthesized pre-tRNAs in the nucleus is the La autoantigen, a highly abundant phosphoprotein that facilitates maturation of the 3′ terminus in newly synthesized transcripts. The La protein may function as a chaperone, to promote the formation of the correctly folded pre-tRNA structure.

The 5′- leader sequence of pre-tRNAs is removed by RNase P, a ubiquitous ribonucleoprotein made up by a 350–450 nucleotides RNA component, which is accountable for the catalytic activity. At least nine protein subunits copurify with the nuclear RNAse P RNA subunit in Eukarya, being responsible for increased catalytic efficiency and substrate versatility (Hartmann & Hartmann, 2003; Mann et al., 2003).
The 3′-terminal sequence is removed in a process mediated by a specific combination of endoribonucleases and exoribonucleases that differ according to the pre-tRNA. The 3′-terminal sequence is capped with a CCA sequence, which in eukaryotes is synthesized in a template-independent manner by the enzyme ATP (CTP): tRNA nucleotidyltransferase, through AMP and CMP transfer from ATP and CTP to the 3′ ends of tRNA molecules. In *E.coli* this sequence is encoded in tRNA genes (Chen et al., 1990).

tRNA splicing occurs in Bacteria, Archaea, and Eukarya. In bacteria introns are self-splicing, a mechanism completely unrelated from the other branches of life (Biniszkiewicz et al., 1994). Around 25% of *Saccharomyces cerevisiae* tRNA families have introns, placed immediately 3′ to the anticodon and devoid of splice-site consensus sequences. Contradicting initial evidences, pre-tRNA intron removal in

yeast occurs in the cytoplasm and most of the tRNA splicing endonuclease activity is localized in the cytosolic surface of the outer mitochondrial membrane (Yoshihisa et al., 2003).

The reaction proceeds through three distinct steps, each one catalyzed by a different enzyme. In the first step the pre-tRNA is cleaved at its splice sites. Pre-tRNA molecules are then folded into a particular secondary structure similar to mature tRNAs. This brings the two intron-exon junctions into proximity, allowing for endonuclease recognition and subsequent intron excision to occur (Abelson et al., 1998). Instantly after, the resulting tRNA half-molecules are joined by a ligase, using one ATP and one GTP molecule (Phizicky et al., 1986). After this process is complete, a 2′ – phosphate remains at the ligation junction and is moved to a NAD molecule by a nicotinamide adenine dinucleotide (NAD)-dependent phosphotransferase, finishing the splicing (McCraith & Phizicky, 1991).

3′ and 5′ terminal maturation usually precedes splicing but for particular tRNAs the splicing might occur first, especially when yeast are grown at high temperature, linking the order of processing of at least some pre-tRNAs with growth conditions (Wolin & Matera, 1999).

In vertebrates, tRNA post-transcriptional processing generally occurs in the nucleus (Lund & Dahlberg, 1998). In yeast, experimental evidences implicate tRNA aminoacylation defects in nuclear accumulation of spliced tRNAs (Shaheen & Hopper, 2005), suggesting bidirectional movement of tRNAs between the nucleus and the cytoplasm (Shaheen & Hopper, 2005; Takano et al., 2005) (see Figure 1.3). This tRNA subcellular dynamics involves at least three members of the importin-β family: Los1, Msn5 and Mtr10.

Los1, a yeast nuclear pore protein, has been implicated in the export of newly transcribed end-matured tRNAs from the nucleus to the cytoplasm as well as in tRNA re-export processes (Shaheen & Hopper, 2005; Murthi et al., 2010). During translocation through the nuclear pore, Los1p directly binds to the tRNA in a complex with Ran-GTP, which upon GTP hydrolysis releases the tRNA in the cytoplasm

(Phizicky & Hopper, 2010). *LOS1* is not an essential gene in yeast, suggesting the existence of an alternative pathway involved in tRNA bidirectional movement. Mtr10, on the other hand, is implicated in retrograde tRNA nuclear import (Shaheen & Hopper, 2005), shown to be a constitutive process in yeast (Takano et al., 2005; Murthi et al., 2010). Msn5, a nutrient-responsive tRNA exportin, is primarily specialized in re-export of aminoacylated tRNAs (Eswara et al., 2009; Murthi et al., 2010).

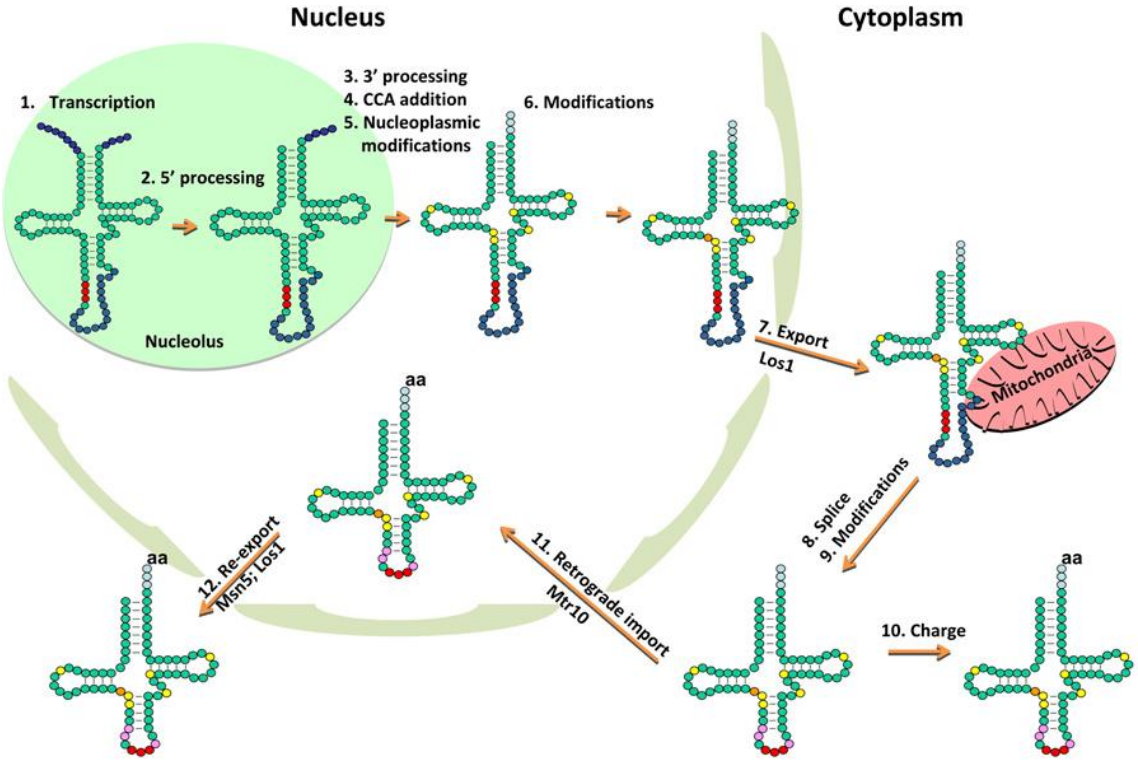

Figure 1.3 – Mechanisms of tRNA synthesis and processing in *S.cerevisiae*. tRNA transcription is followed by 5′ end-processing in the nucleolus. 3′ processing, CCA addition and some nucleoside modifications occur next, immediately before intron-containing pre-tRNAs are exported to the cytoplasm by Los1. In the cytoplasm, processing is completed by addition of new modifications and aminoacylation, just after pre-tRNA splicing on the cytoplasmic surface of mitochondria. Retrograde tRNA flow to the nucleus occurs constitutively or as a proofreading mechanism and is mediated by Mtr10. Re-export of nuclear tRNAs to the cytoplasm also occur as part of the retrograde process, mediated by both Los1 and Msn5. Red circles - anticodon, purple circles - 5′ and 3′ end sequences, dark-blue circles - intron sequence, light-blue circles - CCA end. Image adapted from Phizicky and Hopper, 2010.

This tRNA shuttling serves two major purposes. The first is proofreading, to avert defective tRNAs from interacting with the translation machinery (Shaheen & Hopper, 2005). In fact, a constitutive nucleus-located tRNA degradation system that recognizes aberrant tRNAs has been identified in yeast (Kadaba et al., 2004). Second, retrograde tRNA flow might work as a novel mechanism to regulate gene expression or as an element of regulatory response to certain physiological signals, such as amino acid starvation (Shaheen & Hopper, 2005; Phizicky, 2005). Indeed, under a low nutrient status, repression of tRNA transcription (Ciesla et al., 2007) is followed by increased tRNA retrograde movement, by which tRNAs that were once located in the cytoplasm rapidly accumulate in the nucleus (Shaheen & Hopper, 2005; Hurto et al., 2007; Whitney et al., 2007).

Finally, several of the ribonucleotides are covalently modified by a set of enzymes that recognize specific features of tRNA structure (Phizicky & Hopper, 2010).

1.2.1.2.b. tRNA modification: roles in translation and metabolism

More than 100 distinct chemical modifications of nucleosides have been identified in all the different types of RNAs, but particularly in noncoding RNAs, such as rRNAs and especially tRNAs, which hold around 80% of these modifications.
Some modifications can be found in all three domains of life and are conserved in specific tRNAs from organisms phylogenetically very distant. So far, 25 distinct ribonucleoside modifications have been identified in *S.cerevisiae*, targeting 34 different positions and giving an average of 13 modifications per tRNA species (Sprinzl & Vassilenko, 2005; Chernyakov et al., 2008). In parallel, 50 genes encoding tRNA modifying enzymes have been uncovered, many of them operating under a specific sequence of events, as part of large multi-enzyme complexes.

Modifications are positioned through the entire tRNA molecule, some in much conserved locations, but occur with particular frequency at positions 34 and 37, in the anticodon loop of the tRNA. The most prevalent tRNA modifications are simple base

or ribose methylations and isomerization of uridine into pseudouridine. Some are as complex as wybutosine, exhibiting highly branched conformations (Grosjean, 2009) (see Figure 1.4).

By contributing to an increase in molecular structural diversity, modified nucleosides afford highly selective molecular recognition of specific tRNAs and play important roles in regulating RNA function, stability and lifetime, also influencing genetic decoding by involvement in translation mechanisms (Moore & Steitz, 2011). tRNA modifications bring order to the internal loops and hairpin structures of RNA. For example, the modified nucleosides of the anticodon restrict its conformational dynamics and define its shape. Consequently, the effort of the ribosome to constrain or remodel each tRNA to fit the decoding site is reduced. This diminishes the entropic price for translation and explains the conservation of RNA modifications in general (Agris, 2008).

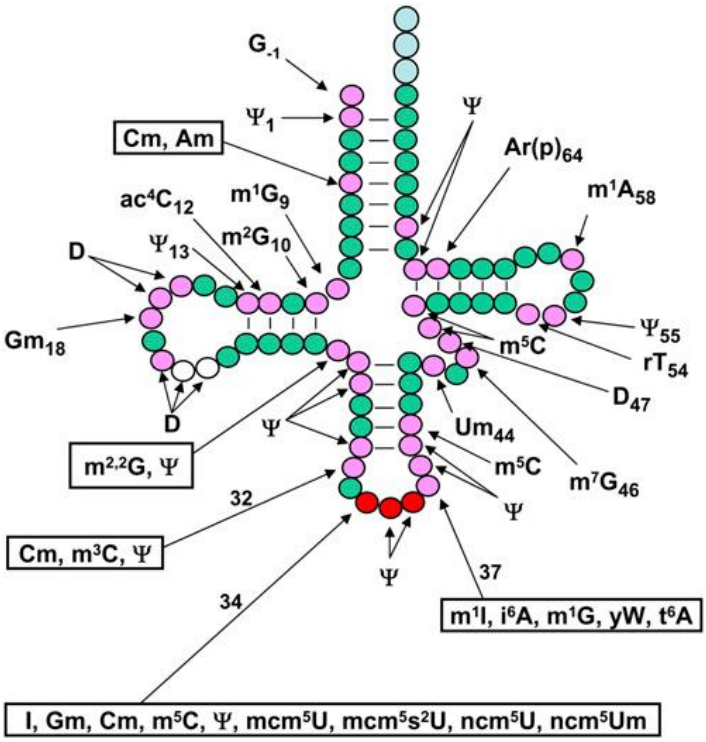

Figure 1.4 – Nucleoside modifications in the cytoplasmic tRNAs of *S. cerevisiae*. Although modifications are relatively spread alongside the tRNA molecule, many concentrate around the anticodon region, especially at positions 34 and 37. Image adapted from Phizicky E and Hopper A, 2010.

Many of the genes responsible for tRNA modifications in the anticodon region are vital for viability and cell growth, however, the great majority of the tRNA modification enzymes are not essential for life and deletion of individual modification enzymes shows no serious growth phenotypes (Alexandrov et al., 2006). The implication that modifications beyond the anticodon can also contribute to base pairing and decoding by promoting molecular flexibility suggests a high level of functional redundancy (Alexandrov et al., 2006).

Ribonucleoside secondary modifications occur both in the nucleus and the cytoplasm, being potentially involved in signaling for tRNA translocation or final cellular destination (Marechal-Drouard et al., 1988; Cavaille et al., 1999). Certain nucleotide modifications take place immediately on the newly synthesized pre-tRNA, some are added after 3′ and 5′ terminal maturation, and others occur only after splicing (Grosjean et al., 1997; Phizicky & Hopper, 2010).

tRNA modifications can be determined by the abundance level of tRNAs and activity or location of the modifying enzymes, occurring many times in a very specific order. A given modified nucleoside in a specific position may actually not be present in all the molecules of a tRNA population and the degree of modification may vary according to physiological conditions, like temperature or availability of metabolic intermediates, creating molecular heterogeneity. Organelle tRNAs and rRNAs contain their own set of modified nucleosides, some of which are not present in cytoplasmic RNAs of the eukaryotic host cell (Grosjean, 2009).

A hypomodified cognate tRNA is usually defective in the aminoacyl-tRNA (aa-tRNA) selection step and a wild type near-cognate tRNA can be accepted at the A-site instead. However, if a hypomodified tRNA is accepted at the A-site, the following nucleotide translocation into the P-site can eventually result in frameshifting. Therefore, tRNA modified nucleosides are vital for reading frame maintenance, improving the fidelity and efficiency of translation by regulating aa-tRNA selection rate and optimizing the fitness of the tRNA in the P-site (Bjork et al., 1999).

By definition, tRNA identity elements are ribonucleotides essencial for maintaining the specificity of the aminoacyl-tRNA synthetases recognition process. Several modifications play particular roles in this process. For example, *in vitro* transcribed and unmodified yeast $tRNA^{Asp}$ can still be charged with aspartate like the modified native tRNA, but it is also quite efficiently mischarged with arginine (Perret et al., 1990). Also in yeast, m^2G10 affects the kinetics of $tRNA^{Phe}$ aminoacylation by stabilizing tRNA terciary structure in order to feature it as a better substract for PheRS (Roe et al., 1973). Nevertheless, tRNA recognition by tRNA sinthethases may also involve the anticodon region and modifications in the surrounding nucleosides. An *E. coli* $tRNA^{Ile}$ has a modified nucleoside named lysidine (K^2C) in the first position of the anticodon (position 34), which is essential for the specific recognition of the codon AUA. The absence of this modification causes mischarging by methionyl-tRNA synthetase (MetRS) (Muramatsu et al., 1988).

Looking to a table representation of the genetic code, the first two codon letters create 16 possible combinations, each of which is displayed in a separate box. Eight of the codon boxes code for only a single amino acid (4-fold degenerate). The other 12 amino acids have codons in 2-fold degenerate codon boxes, like asparagine and lysine, or have only one codon, like methionine and tryptophan (Agris, 2004; Agris, 2008). Modified nucleosides in the anticodon region play an important role in the efficiency of codon reading by regulating conformational dynamics and wobbling. This happens by either restricting tRNA interaction to one or two codons or expanding the recognition to three or four synonymous codons by the same tRNA species. For example, mcm^5s^2U34 in yeast $tRNA^{Glu}$ limits the tRNA to pair with A. Also mnm^5s^2U, an *E.coli* wobble modification with similar structure found in $tRNA^{Gln}$ and $tRNA^{Lys}$, strongly favors base pair with A (Agris et al., 1973; Lustig et al., 1981). On the other hand, modified ribonucleosides at the wobble position might also extend the number of codons recognized by specific species of tRNA. For example, $tRNA^{Val}$, $tRNA^{Ser}$ and $tRNA^{Ala}$ from *E.coli* contain cmo^5U34, allowing interaction with codons that have A, U and G at the wobble position (Murao et al., 1982).

In conclusion, tRNA modifications favor specific recognition and binding of the anticodon to cognate and wobble codons. This efficiency results in accuracy and energy saving, which might be of major importance for a quick response to environmental signals and stress, assuring cell survival under challenging conditions (Agris, 2008).

1.2.1.3 Aminoacyl-tRNA synthetases

The genetic code is robustly established through aminoacyl-tRNA synthetases (aaRS), which integrate two levels of cellular organization: nucleic acids and proteins. Amino acids are specifically recognized by their cognate aminoacyl-tRNA synthetase (aaRS), which then catalyze the synthesis of aminoacyl-tRNA (aa-tRNA) by esterification to the appropriate tRNA. Aminoacylation is a two step reaction. In the first step, the amino acid is combined with an ATP molecule by α-phosphate attack, forming an aminoacyl adenylate intermediate and inorganic pyrophosphate. In the second step, the amino acid moiety is transferred to the 3'-terminal ribose of a tRNA molecule (Arnez & Moras, 1997).

Aminoacyl-tRNA synthetases catalyse the same basic reaction, but are nevertheless divided in two classes (class I and class II), each with 10 enzymes. Their classification is based on molecular size, quaternary structure (class I enzymes are usually monomers and the class II enzymes are organized in dimmers) and also on the existence of two different active sites, each with conserved sequence motifs and functional characteristics (Ludmerer & Schimmel, 1987; Cusack et al., 1990; Eriani et al., 1990).
Class I and class II enzymes approach the anticodon of their cognate tRNAs from opposite sides, binding the acceptor arm and the 3'-terminal CCA of tRNA in a mirror symmetric fashion. Class I enzymes are responsible for tRNA aminoacylation at the 2′ OH group of the terminal ribose while enzymes from the class II family add the amino acid to the 3′OH group (Cusack et al., 1990; Sankaranarayanan & and Moras, 2001); (Arnez & Moras, 1997).

Within each class, the synthetases can also be arranged into three subclasses representing enzymes that are more closely related to each other in the same class, mostly due to higher conservation in their sequence (Sankaranarayanan & and Moras, 2001).

The aminoacylation reaction is extremely specific, due to the existence of both pre-transfer and post-transfer editing pathways, encoded by a discrete domain that is distinct from the aminoacylation active site. Pre-transfer mechanisms involve the hydrolysis of misactivated aminoacyl adenylates, produced after the first step of the aminoacylation reaction (Baldwin & Berg, 1966), whereas post-transfer mechanisms determine the hydrolysis of the incorrect amino acid in mischarged tRNAs (Eldred & Schimmel, 1972; Martinis & Boniecki, 2010). Coexistence of pre- and post-transfer editing mechanisms within a single aaRS results in a redundancy of fidelity mechanisms. Defects in the editing activity cause mistranslation, which can be connected with mutagenicity and toxicity in bacteria as well as with severe pathologies in mammals (Lee et al., 2006). Therefore, it is thought that the efficiency of aaRSs was a determinant event during evolution by allowing sustainable cell homeostasis and consequently the development of the tree of life (Schimmel & Ribas de, 2000; Schimmel, 2008).

1.2.2. Translation Initiation

1.2.2.1. Prokaryotes

Before incorporation into a nascent peptide, amino acids are delivered to the ribosome by tRNAs. During the initiation stage of protein synthesis, the ribosome subunits are assembled with the mRNA in the start codon, with a methionyl initiator tRNA bound in the peptidyl P-site, forming the translation complex. The AUG methionine codon functions as the start codon in the vast majority of mRNAs. The GUG valine and UUG leucine codons are used as alternative start codons in prokaryotes, around 14% and 3% of the times, respectively, but also get translated as methionine (Blattner et al., 1997).

Bacteria and eukaryotes contain two different methionine tRNAs. One that can bind to the P-site in the ribosome and initiate protein synthesis (Met-$tRNA_i^{Met}$) and the other that only binds to the A-site in the ribosome, being responsible for methionine incorporation into growing protein chains. Both are charged by the same aminoacyl-tRNA synthetase (MetRS). In Met-$tRNA_i^{Met}$ from Bacteria the amino group of the methionine is modified by addition of a formyl group and is called fMet-$tRNA_i^{Met}$. However, Met-$tRNA_i^{Met}$ is usually used to designate the initiator tRNA in all cells (Lodish et al., 2000).

Assembly of the translation complex during initiation comprises two steps and involves interactions with specific proteins referred to as initiation factors. In bacteria, translation initiation involves the initiation factors IF1, IF2 and IF3. IF2 has GTPase activity and together with IF3 enhances specific binding of the initiator tRNA to the P-site in the small ribosomal subunit. Initially, IF3 binds strongly to the 30S subunit and prevents its association with the 50S subunit. At this point, IF1 is blocking the A-site of the small ribosomal subunit. Initiation factors then guide the small subunit and the initiator tRNA to a complementary sequence in the mRNA, the *Shine-Dalgarno* sequence. This sequence is located upstream and near the AUG start codon, is rich in purines and has on average six out of eight nucleotides complementary to the 3'-end sequence of 16S rRNA. This first step of initiation yields a 30S initiation complex. Following this process, IF1 is thought to induce a conformational change that prepares transition for subunit association. Addition of the large (50S) ribosomal subunit is then coupled with release of the IF1 and IF3 protein factors and hydrolysis of GTP bound to IF2, yielding elongation-competent 70S ribosomes (Ramakrishnan, 2002; Kapp & Lorsch JR, 2004).

1.2.2.2. Eukaryotes

The outcome of the Eukaryotic initiation process is the same as in bacteria, but the mechanisms and the machinery involved differ considerably, being much more complex. First, there is no Shine-Dalgarno sequence upstream of the initiation codon. Also, the mRNA has a 5' cap consisting of a guanine nucleotide connected to the

mRNA via an unusual triphosphate linkage, which ensures molecular stability. Finally, there are at least 12 initiation factors in eukaryotes, which consist of at least 23 different polypeptides. For many of those the function is not yet known (Kapp & Lorsch JR, 2004).

The first step of the Eukaryotic initiation process comprises the assembly of an eIF2-GTP-Met-$tRNA_i^{Met}$ ternary complex. At this point, the small (40S) ribosomal subunit binds simultaneously to eIF3, eIF1 and eIF1A. These initiation factors potentiate the binding of the ternary complex to the 40s ribosomal subunit, by increasing the stability of the resulting 43S preinitiation complex (Figure 1.5-1) (Pestova et al., 1998; Chaudhuri et al., 1999; Pestova et al., 2001). This is a crucial regulation point. When cells encounter stress conditions, protein kinases are activated to phosphorylate a serine residue on the eIF2 bound to GTP, causing a reduction of the eIF2-GTP-Met-$tRNA_i^{Met}$ ternary complex and protein synthesis inhibition (Sonenberg & Hinnebusch, 2009). Interaction of the 43s complex with the 5'-capped mRNA requires a set of factors that recognize and unwind secondary structures found in the 5'-untranslated region (UTR). This is accomplished through the ATP-dependent and cooperative action of eIF4F/eIF4B. eIF4F is a multiprotein complex tightly hold by eIF4G and bearing RNA helicase activity (eIF4A), cap-binding activity (eIF4E) as well as poly (A)-binding protein (PAB). eIF4F is also known to be associated with eIF3 (situated in the 43S complex). eIF4B promotes the ATPase activity and the ATP-dependent RNA unwinding activity of both eIF4-A.

When the Poly (A)-binding protein (PAB) comes to scene it immediately binds to the 3'-poly (A) tails of eukaryotic mRNAs (Preiss & Hentze, 2003). eIF4E is the rate-limiting member of the eIF4F complex (Mamane et al., 2004) and associates with the 5' cap structure of the mRNA, which contains the 7-methyl-GTP (m^7GTP) moiety. These interactions are responsible for the circularization of eukaryotic mRNAs, which in turn stimulates translation by facilitating loading of the 43S complex to the mRNA (Figure 1.5-3). This step also provides a quality control mechanism, since partially degraded mRNAs will not be translated efficiently (Jackson et al., 2010).

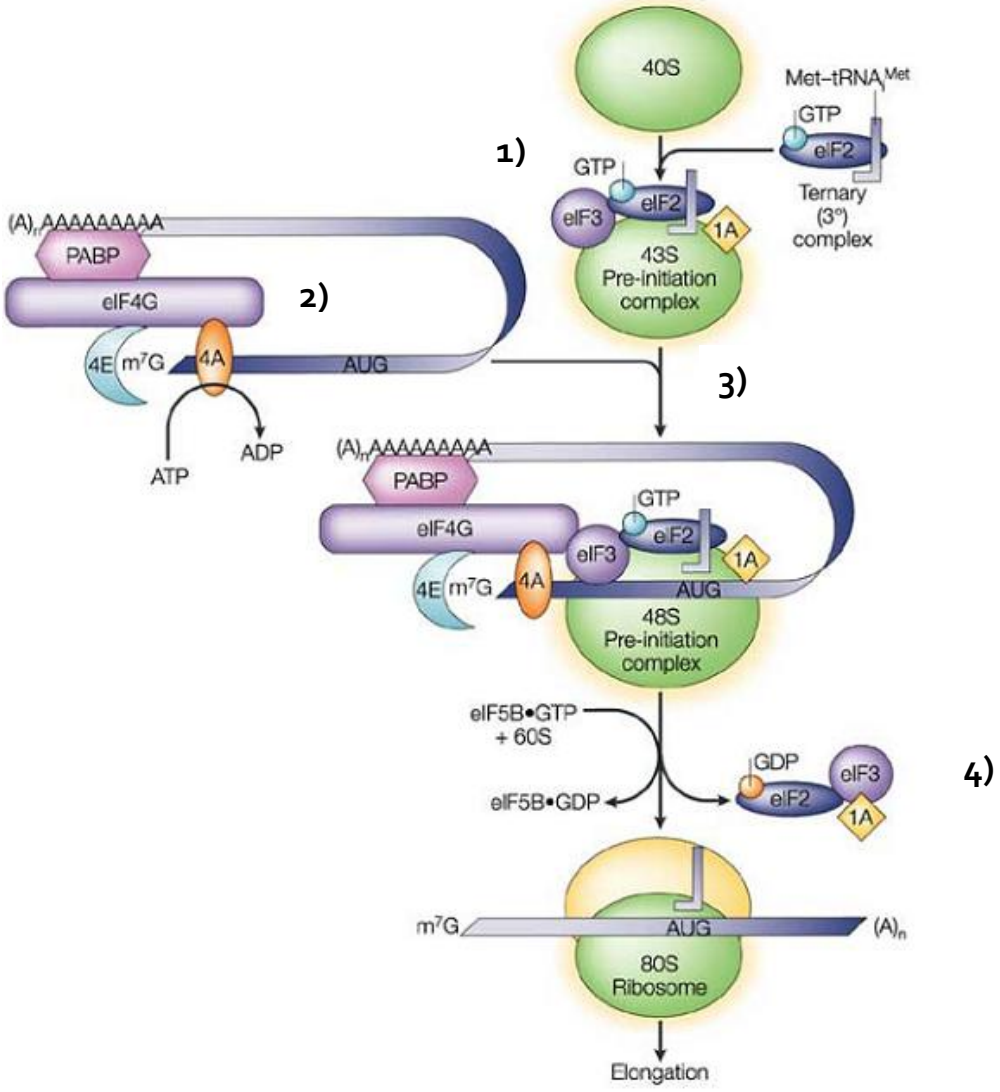

Figure 1.5 – Schematic representation of the Eukaryotic translation initiation and the role of the most important Initiation Factors (eIFs). eIF2–GTP–Met-tRNAiMet ternary complex associates with the 40S ribosomal subunit and with additional factors such as eIF3 and eIF1A (1A), which promote generation of a 43S pre-initiation complex. The eIF4F multiprotein complex unwinds the 5′ cap-proximal region of mRNA for ribosomal attachment eventually leading to circularization of eukaryotic mRNAs and promoting the binding of the 43S pre-initiation complex to the mRNA, producing a 48S pre-initiation complex. AUG scanning and GTP hydrolysis by eIF2 preclude the dissociation of factors from the 48S complex. Finally, eIF5B-GTP hydrolysis allows joining of the large (60s) subunit giving origin to elongation-competent 80S ribosomal complex. Image adapted from Klann and Dever, 2004.

After loading, the 43s complex slides along the mRNA in the 5′ to 3′ direction until recognition of the correct initiation codon. This is usually the first AUG codon in an optimum context, the consensus sequence GCC(A/G)CC**A**UGG, with a purine at the –3 and a G at the +4 positions (Kozak, 1999; Kozak, 2002). This favorable context sequences are called Kozak signal sequences. Efficiency of translation initiation at a certain AUG codon depends on the strength of the signal sequence, weaker meaning more different from the consensus sequence. Much less frequently, the preinitiation complex binds to internal ribosome entry sites (IRES) within the mRNA sequence, far downstream of the 5′ end, and from there scans downstream for an AUG start codon (Kapp & Lorsch, 2004; Jackson et al., 2010).

At this stage, eIF1 helps 43S complexes locating AUG codons that have a favorable context and also dissociates the ribosomal complexes that aberrantly assemble at such codons, therefore playing a key part in maintaining fidelity of initiation. Codon-anticodon base pairing between the initiation codon and the initiator tRNA in the ternary complex triggers GTP hydrolysis by eIF2, a reaction facilitated by the GTPase-activating protein (GAP) eIF5. Finally, after release of the Met-tRNA$_i$ into the P-site of the 40S subunit, eIF2-GDP, eIF1, eIF1A, eIF3, and eIF5 dissociate from the complex giving place to eIF2 and also eIF5B-GTP, a yeast homologue of bacterial IF2 (Kapp & Lorsch JR, 2004; Unbehaun et al., 2004). eIF5B not only facilitates the release of initiation factors from the complex but also the joining of the large (60s) subunit to the 40S subunit, probably by changes in the subunit's conformation (Pestova et al., 2000). GTP hydrolysis is not thought to be required for this assignment but instead, promotes the release of eIF5B from the 80S complex only after the subunit joining step has been complete and properly set up to start elongation (Figure 1.5 - 4) (Jackson et al., 2010).

1.2.3. Elongation

Elongation is much more conserved across the three kingdoms of life than termination or initiation. The mechanisms are basically the same in eukaryotes, bacteria and archaea (see Figure 1.6).

With an empty A-site and the initiating Met-tRNA$_i^{Met}$ bound at the P-site and base-paired with the AUG start codon in the mRNA, bacterial 70S or eukaryotic 80S ribosome are ready to move along the mRNA towards its 3'-end. The in-frame stepwise addition of amino acids can then begin. Again, a set of special proteins, the elongation factors (EFs), are required to carry out the process. In bacteria, each aminoacyl-tRNA approaches the ribosome as a ternary complex with an EF-Tu-GTP molecule (EF1A-GTP in eukaryotes). If the anticodon of the incoming aminoacyl-tRNA correctly matches the positioned mRNA codon, this will result in a tight binding at the A-site and trigger GTP hydrolysis by EF-Tu (Kapp & Lorsch JR, 2004; Moore & Steitz, 2011). Three 16S rRNA bases (A1492, A1493 and G530) are vital for decoding, greatly stabilizing the cognate tRNA-mRNA interaction at the A-site (Ogle et al., 2001). The tRNA then swings into the peptidyl transferase site, in a process called accommodation. Otherwise, the aminoacyl-tRNA simply diffuses away.

1.2.3.1 The kinetic proofreading model

It was initially thought that differences in the free energy of base-pairing were behind aa-tRNAs discrimination. However, the difference in free energy for binding between cognate and near-cognate tRNAs, which differ by a single codon-anticodon mismatch, is only - 3 kcal/mol. This value is insufficient to account for the observed translation fidelity (Uhlenbeck et al., 1971; Parker, 1989; Ogle & Ramakrishnan, 2005). The explanation for this discrepancy is presented by the kinetic proofreading model, which couples the rate of EF-Tu-dependent GTP hydrolysis to tRNA selection.

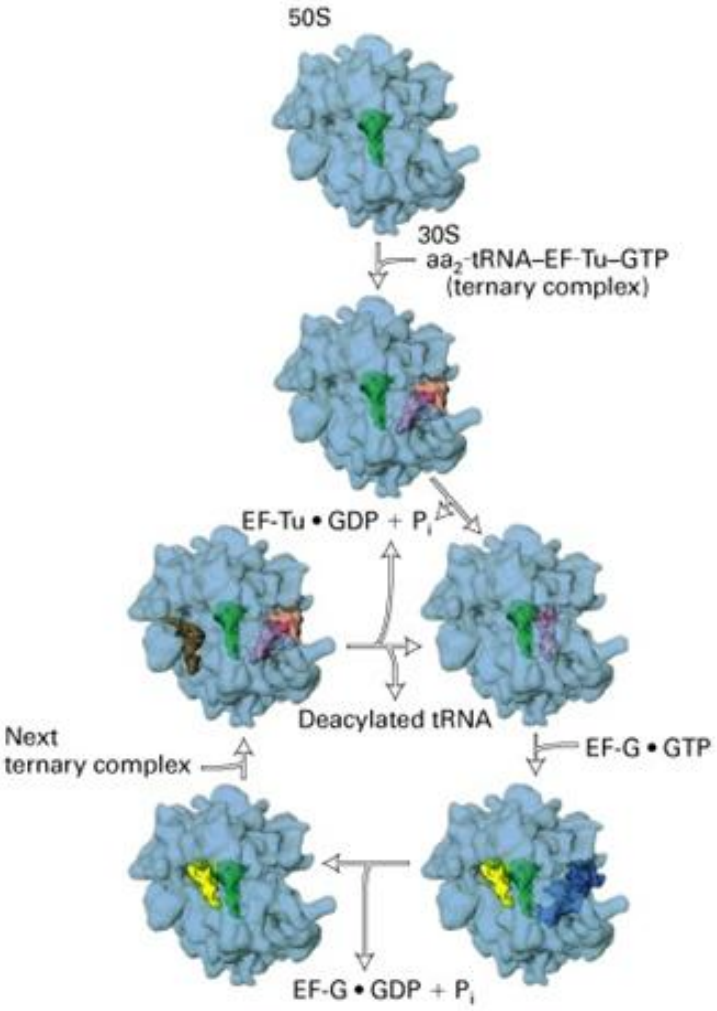

Figure 1.6 – Schematic representation of the elongation cycle in *E.Coli*. Elongation starts with 70S ribosome containing an empty A-site and the initiating Met-$tRNA_i^{Met}$ (green) bound at the P-site and base-paired with the AUG start codon. Each aminoacyl-tRNA (purple) approaches the ribosome as a ternary complex with an EF-Tu – GTP molecule (red). Codon–anticodon pairing activates the hydrolysis of GTP and propels the peptidyl-transferase reaction. The ribosome then shifts in the 3' mRNA direction to decode the next mRNA codon. Translocation is assisted by binding of the GTPase EF-G (dark blue), which allows the deacylated tRNA at the P-site (now yellow) to move to the E-site and the peptidyl-tRNA at the A-site to move to the P-site (now green). The deacylated tRNA in the E-site (now brown) is released on binding of the next aminoacyl-tRNA to the A-site. The ribosome is then ready for the next round of elongation. Image adapted from Lodish H *et al.*, 2000.

Higher selectivity can be achieved in any process if it involves two very selective steps separated by an irreversible step. The ribosome has an important role in aa-tRNAs decoding, actively discriminating between correct and incorrect aa-tRNAs. High accuracy is achieved because there are two opportunities to examine and discard incorrect aa-tRNAs in the ribosome (Hopfield, 1974; Ninio, 1975). The GTPase activity efficiently separates selection into two stages, initial selection and proofreading, allowing multiple opportunities for rejection of incorrect tRNAs (Thompson & Stone, 1977).

tRNA selection at the initial selection step is tightly kinetically controlled. GTPase rates for cognate tRNAs are four orders of magnitude higher than the rates for non-cognate tRNA (more than one codon mismatch) (Rodnina et al., 1996). This suggests that binding of cognate tRNA causes an increased rate of EF-Tu–dependent GTP hydrolysis, leading to preferential release of EF-Tu - GDP from ribosomes that contain cognate tRNA bound to the A-site (Pape et al., 1998). Discrimination against non-cognate ternary complexes can therefore take place preceding EF-Tu–dependent GTP hydrolysis, with essentially no energetic cost. Discrimination against near-cognate ternary complexes is more difficult and takes place in the subsequent proofreading step, after irreversible EF-Tu–dependent hydrolysis of GTP is stimulated but before peptide bond formation (Rodnina et al., 1996; Rodnina & Wintermeyer, 2001).
Remarkably, selection of cognate aminoacyl-tRNAs over near-cognate tRNAs can be accomplished by conformational changes in the decoding center, through an induced-fit mechanism (Pape et al., 1999; Rodnina & Wintermeyer, 2001; Ogle et al., 2002). Cognate tRNA binding induces global domain movements in the 30S subunit, changing the conformational arrangement of A1492, A1493 and G530, universally conserved bases of 16S RNA (Ogle et al., 2001; Ogle et al., 2002). These reorganizations in the ribosome structure ultimately boost GTPase activation rate and result in higher rates of accommodation, a process in which the acceptor arm of the aa-tRNA swings into the peptidyl transferase site after its release from EF-Tu (Pape et al., 1999; Rodnina & Wintermeyer, 2001; Ogle et al., 2001), paving the way to peptide bond formation. Therefore, there is a high probability that near-cognate aa-tRNA will

dissociate at this stage. A specific domain in the large subunit of the ribosome, previously implicated in the control of elongation fidelity, was also identified as a GTPase-activating center (Sanbonmatsu et al., 2005). Conformational changes are transmitted from the decoding center to the large ribosomal subunit through the tRNA body (Cochella & Green, 2005a). Therefore, tRNAs are not merely a substrate during protein synthesis, revealing a very active contribution for translation accuracy through a role in the induced fit mechanism (Weinger et al., 2004).

Remarkably, other ribosomal regions might have a role in the accuracy of codon recognition. According to a quite disputed allosteric model for ribosome function, the occupation of the E-site with a cognate tRNA decreases the affinity of the A-site, which under these conditions discriminates much more effectively against non-cognate tRNA species (Nierhaus, 2006).

1.2.3.2. Peptidyl Transferase and translocation

Following accommodation, peptide bond formation occurs instantaneously. The α-amino group of the A-site aminoacyl-tRNA amino acid attacks the ester bond between the peptide and the tRNA at the P-site, forming a new peptide bond. Peptide bond formation is catalyzed by ribozyme activity located in the peptidyl transferase center (Moore & Steitz, 2003) and is also substrate-assisted, due to participation of the 2′ hydroxyl group of A76 from the peptidyl-tRNA (Steitz, 2008). The ribosome conformation adjusts the position of the reacting groups relative to each other in order to decrease the activation entropy of this reaction and provides an optimal electrostatic environment by shielding the reaction environment against bulk water (Schmeing et al., 2005; Trobro & Aqvist, 2005).This process eventually results in deacylation of the P-site tRNA coupled with peptide chain transference to the A-site tRNA. Remarkably, the rate of the peptidyl transfer reaction is influenced by the nature of the amino acid side chain of the A-site substrate (Wohlgemuth et al., 2008).

Finally, in the last step of elongation, the tRNAs bound to the ribosome are translocated to the next adjacent position. Alongside, the mRNA is moved by three nucleotides, in order to place the next codon of the mRNA into the A-site. Ribosomal translocation does not occur at the same time in the large and small subunits (Moazed & Noller, 1989). During this process, the P-site bound tRNA changes to a hybrid state, with its acceptor end in the exit (E) site of the large ribosomal subunit and its anticodon end in the P-site of the small subunit. The A-site bound tRNA changes to a similar hybrid intermediate situation, with anticodon and acceptor end tilted between the P-site and the A-site of different subunits (Green & Noller, 1997). Complete translocation is catalyzed by EF-G - elongation factor 2 (EF2) in eukaryotes - at the expanse of GTP hydrolysis. By the end of this process the deacylated tRNA is moved to the exit (E) site on the ribosome and is released. The A-site becomes available for accepting another aminoacyl-tRNA, starting a new elongation round (Spiegel et al., 2007). The deacylated tRNA in the E-site is released on binding of the next aminoacyl-tRNA to the A-site. This cycle is repeated until an in frame stop codon is reached, which begins the termination process.

1.2.4. Termination

A stop codon occupying the ribosomal A-site is decoded by Release Factors (RF) through RNA-protein interactions that eventually promote the hydrolysis of the ester bond between the polypeptide chain and the P-site tRNA, culminating in release of the completed polypeptide (see Figure 1.7 a and b). This reaction is also catalyzed by the peptidyl transferase center of the ribosome, in the large ribosomal subunit. Evidences from crystallography studies in *E.coli* highlight the role of 23S rRNA as a catalytic entity in the peptidyl transferase center. Thus, rRNA plays an important role in maintaining the efficiency of translation termination just as it plays a central role in the decoding process during polypeptide elongation (Moore & Steitz, 2003; Steitz & Moore, 2003; Polacek & Mankin, 2005).

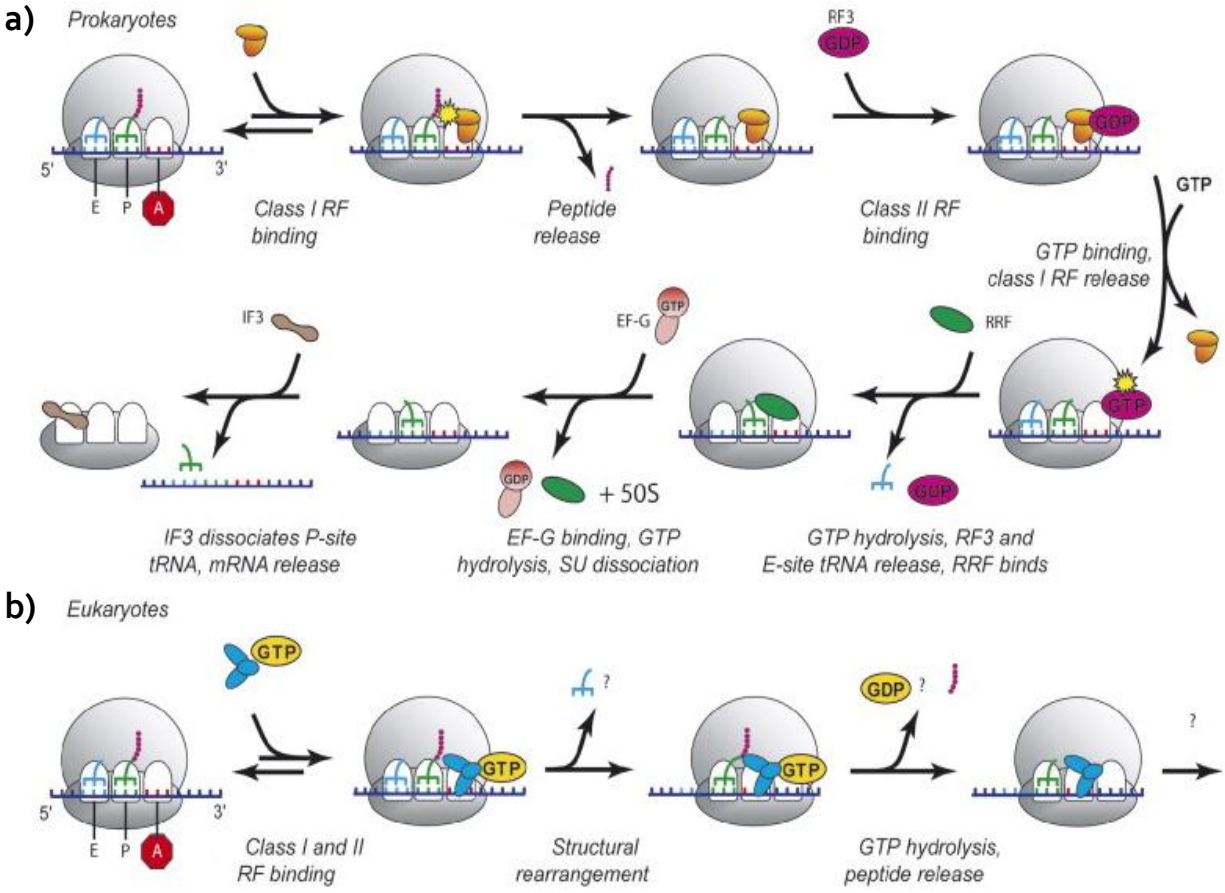

Figure 1.7 - Schematic representation of translation termination. Image adapted from Petry et al., 2008. a) Prokaryotes - When a stop codon reaches the A-site (red hexagon) it is decoded by either release factor-1 (RF1) or RF2, giving origin to peptide release from the tRNA in the P-site. Recruitment of RF3–GDP eventually results in RF1/2 release. RF3 is discharged due to exchange of GDP for GTP. The binding of ribosomal release factor (RRF) followed by EF-G elongation factor and GTP hydrolysis disassembles the ribosomal subunits. Initiation factor-3 (IF3) is required to dissociate the deacylated tRNA from the P-site. b) Eukaryotes - eRF1 acts cooperatively with eRF3 to allow polypeptide chain release from the ribosome. An eRF1–eRF3 complex binds to the A-site, where eRF1 directly interacts with the stop codon. This step induces structural rearrangements in the ribosome, eventually enhancing GTP hydrolysis by eRF3 and peptidyl-tRNA hydrolysis thereafter. It is not known how eukaryotic termination complexes are recycled for a new round of translation.

1.2.4.1. Prokariotes

In bacteria, translation termination is mediated by two class I release factors (RF1 and RF2) that functionally and structurally mimic tRNA molecules (Ito et al., 1996). Class I Release Factors recognize stop codons at the A-site and interact with the peptidyl transferase activity of the ribosome, thereby stimulating release of the completed polypeptide chain. RF3, a class II Release Factor, makes no contribution to catalysis of peptide release but enhances the activity of RF1 and RF2, also promoting their recycling from the termination complex by a mechanism involving GTP hydrolysis (Freistroffer et al., 1997; Zavialov et al., 2001) (see Figure 1.7 a).
RF1 decodes UAG and UAA stop codons with no difference in binding free energy, while RF2 decodes UGA and UAA codons with similar affinities but strongly discriminates against both the UAG (stop), due to a large energetic barrier (Scolnick et al., 1968; Kapp & Lorsch JR, 2004). The tripeptides Pro-Ala-Thr and Ser-Pro-Phe, hold respectively by RF1 and RF2, mediate the recognition and interaction with the stop codons. The first amino acid of the tripeptide discriminates the second purine base and the third amino acid independently discriminates the third purine base (Ito et al., 2001). However, there is indication that other domains of the release factors also help define the codon recognition ability, by influencing the structure of the tripeptide discriminator (Sund et al., 2010).

1.2.4.2. Eukaryotes

In Eukaryotic organisms, translation termination is mediated through the action of a single class I release factor (eRF1) that recognizes all three stop codons (UAG, UAA, and UGA) (Bertram et al., 2001; Kisselev et al., 2003). The eukaryotic class II release factor (eRF3) carries out GTP hydrolysis and ensures rapid and efficient peptide release by forming a stable heterodimer with eRF1 (Stansfield et al., 1995; Alkalaeva et al., 2006; Pisareva et al., 2006) (see Figure 1.7 b). The crystal structure of human and *Schizosaccharomyces pombe* eRF1–eRF3 complexes suggest that this physical

interaction results in eRF1 resemblance to a tRNA molecule (Cheng et al., 2009) (see Figure 1.8).

eRF1 proteins have three distinct functional domains. Domain 1 recognizes stop codons in the ribosomal A-site and contains the highly conserved TASNIKS motif. This heptapeptide cooperates with eRF3 to trigger conformational changes that enhance GTPase activity and thereby efficiently link stop codon recognition and peptide release (Frolova et al., 2002; Inagaki et al., 2002; Song et al., 2000). Domain 2 triggers peptidyl-tRNA hydrolysis by close interaction with the peptidyl transferase center of the large ribosome subunit (Frolova et al., 1999; Seit-Nebi et al., 2001; Song et al., 2000) and domain 3 mediates eRF3 binding (Eurwilaichitr et al., 1999; Ito et al., 1998) (see Figure 1.8).

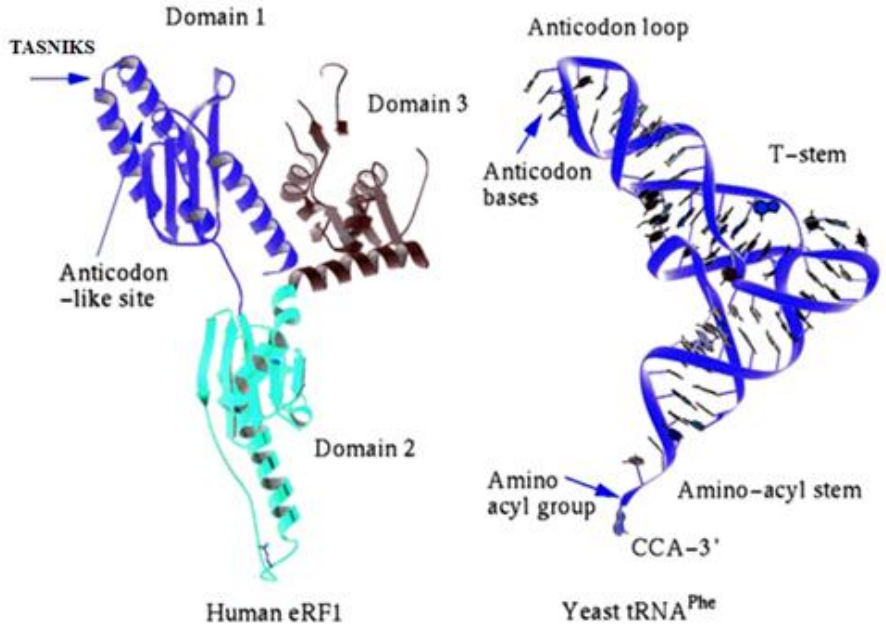

Figure 1.8 – Representation of eRF1 structure and evidences of molecular mimicry with tRNA molecules. The spatial arrangement of domains 1, 2, and 3 in the eRF1 corresponds to tRNA anticodon loop, aminoacyl stem, and T stem, respectively. Image adapted from Song et al., 2000.

It still remains obscure how eRF1 recognizes all three stop codons. Based on available experimental data, current models offer explanations that vacillate between stop

codon binding to the TASNIKS motif and the potential existence of cavities on eRF domain 1 that physically accommodate the stop codon (Merritt et al., 2010).
eRF1 and eRF3 bind to each other also in the absence of the ribosome, and this interaction is required for optimum efficiency of termination in *S. cerevisiae*. In contrast, no such cytosolic complex was observed between RFs 1 or 2 and RF_3 in bacteria (Stansfield et al., 1995; Ito et al., 1996).

Translation termination appears to be similar between eukaryotes and Archea, as confirmed by the high homology between aRF1 and eRF1. However, until this moment no equivalent was found for eRF_3 in Archea (Kapp & Lorsch, 2004).

1.2.5. Recycling

Translation is a cyclical process and therefore initiation is always preceded by recycling of post-termination ribosomal complexes (post-TCs), composed by the 80S ribosome still harboring the mRNA, as well as the P-site deacylated tRNA and eRF1. In eukaryotes, recycling is mediated by eIF_3, in cooperation with its associated eIF_3j subunit, eIF1 and eIF1A. The process starts with 60S and 40S dissociation. eIF1 and eIF_3j then respectively promote release of deacylated tRNA and mRNA from the 40S subunits (Fraser et al., 2007). The role of eIF_3, eIF1 and eIF1A is then to prevent re-association of ribosomal subunits, by remaining linked with recycled 40S subunits. The 40S subunit is not released back into the cytoplasm, but instead shuttled back to the 5-end of the mRNA smoothing the progress of translation reinitiation (Jackson et al., 2010).
In bacteria, post-TCs are recognized by ribosome release factor (RRF) that in conjunction with EF-G dependent GTP hydrolysis alters the structure of the ribosome, destabilizing the binding of tRNA and mRNA. IF_3 then binds and facilitates complete subunit dissociation and release of the tRNA and mRNA (Karimi et al., 1999; Lancaster et al., 2002).

1.3. The fidelity of the biological flow of information

Each of the steps from DNA replication to mRNA transcription and to protein synthesis must occur with considerable accuracy to ensure cell survival and viability. To maintain genome sequence stability organisms developed a variety of mechanisms, namely DNA proofreading, which ensure very low rates of genomic mutations during replication (10^{-10}- 10^{-11} nucleotide exchanges per base pair in eukaryotes) (Kunkel & Bebenek, 2000; Goldsmith & Tawfik, 2009).Therefore, an almost error-free genome replication is possible, but perfectly synthesized proteomes never occur. In fact, the mechanisms leading to the synthesis of functional proteins are intrinsically error prone.

The mutation rates of mRNA transcription and translation are 5 and 6 orders of magnitude higher, respectively, than that of DNA replication. The error rate for transcriptional misincorporation is estimated between 2×10^{-6} (*in vitro*) and 10^{-4} (*E.coli*) per position, due to an apparent lack of proofreading and repair mechanisms in transcription. Inaccuracies in the process of transcription by the RNA polymerase, producing a flawed mRNA template then translated by the ribosomes, can be an important contribution for the total translation error rate (Goldsmith & Twafik, 2009). However, the eukaryotic cell has various mechanisms to deal with mRNAs that direct aberrant protein synthesis. Remarkably, mRNAs incorrectly processed because of gene mutations or defective synthesis can be very easily identified and eliminated by distinct quality control mechanisms—nonsense-mediated mRNA decay, nonstop mRNA decay or no-go mRNA decay (Isken & Maquat, 2007).

Efficient translation requires both rapid binding of cognate aminoacyl-tRNAs to their respective codons and fast termination of protein synthesis at stop signals by RFs. In *E.coli*, for every 1000 to 10000 codons translated one amino acid misincorporation occurs. Since the average *E. coli* coding sequence is 335 codons long, 15% of all average-length protein molecules contain at least one misincorporated amino acid (Parker, 1989; Drummond & Wilke, 2009). In *S.cerevisiae*, average error frequency

varies between 10^{-4} - 10^{-5} per codon. Depending on the codon or the sequence under study, yeast error frequency is lower than that of *E. coli* (Stansfield et al., 1998; Farabaugh & Björk, 1999; Kramer et al., 2010).

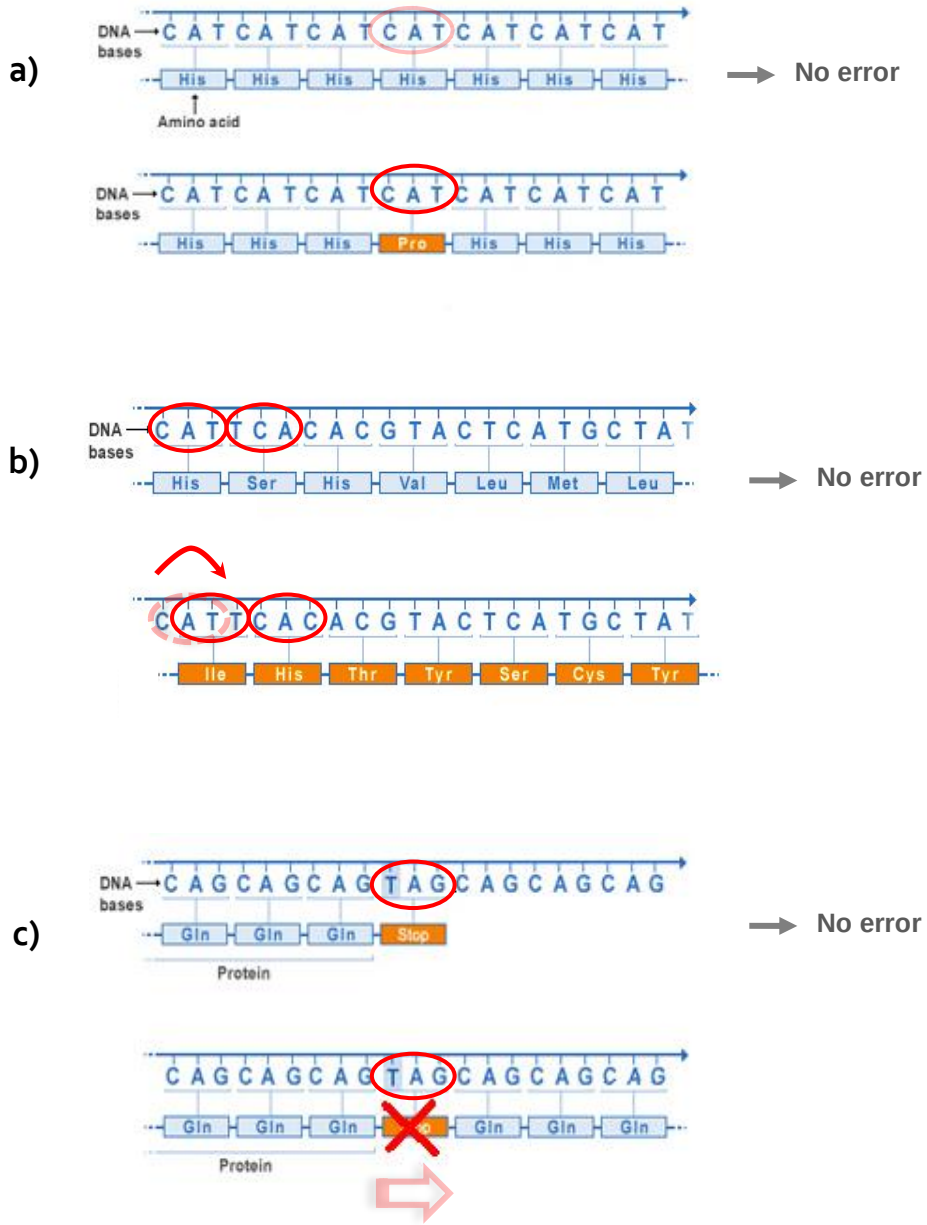

Figure 1.9 – Translational errors. a) Missense errors - the substitution of one amino acid for another b) Ribossome Frameshifting - Slipage of the ribossome either backward or forward in mRNA altering their reading frame (usually +1 or -1) c) Stop codon readthrough – False recognition of termination codons as sense codons.

Translation elongation is very complex and the potential for the process to go wrong is very high. Errors can arise from substitution of one amino acid for another (missense, or misreading of sense codons), mostly due to selection of the incorrect tRNA by the ribosome or erroneous aminoacylation of tRNAs by aaRSs (misacylation) (see Figure 1.9 a). Besides missense, protein synthesis accuracy can also be affected by premature termination or stop codon readthrough, which occur with predicted error rates in the order of 10^{-4} to 10^{-3} per elongation event (Parker, 1989; Keeling et al., 2004) (see Figure 1.9 c). Translational frameshifting affects processivity, resulting in synthesis of polypeptides sharing no homology with the normal product and many times truncated due to premature encounter of a termination codon in the shifted frame (Parker, 1989) (see Figure 1.9 b).

1.3.1. Missense errors (sense codon misreading)

The study of missense errors *in vivo* represents a major codon challenge. This is mainly related to the fact that aberrant proteins resulting from misreading have essentially the same size and amino acid composition as the native proteins (Parker, 1989). The few *in vivo* studies already carried out reported error frequencies ranging from 10^{-5} to 10^{-4} per codon in yeast, a value three times lower than in *E. coli*, alerting for the existence of additional mechanisms that reduce missense errors (Stansfield et al., 1998; Rakwalska & Rospert, 2004; Salas-Marco & Bedwell, 2005; Plant et al., 2007). However, these studies approach only a few codons, a limited number of contexts and a small range of all the amino acid changes that can occur at each codon. The most sensitive measurements generally rely on a reporter enzyme which is inactivated by a single point mutation. In such a system, a stimulation of enzymatic activity is assumed to reflect a decrease in the accuracy of the elongation process. Luciferase is many times chosen for these misincorporation reporter systems due to the availability of its crystal structure and the many genetic studies previously carried out with it (Salas-Marco & Bedwell, 2005; Kramer & Farabaugh, 2006).

Error rate is strongly influenced by competition between cognate and near-cognate tRNA and a major cause of missense is low availability of the cognate tRNA. This might help explain codon usage bias (nonrandom choices of synonymous codons) in *E. coli* and yeast genomes (Ikemura, 1981; Ikemura & Ozeki, 1983). Codons recognized by low-abundance cognate tRNAs are more error-prone than the ones recognized by high-abundance tRNAs. The exception to this rule is when misreading involves a wobble error and then an abundant cognate tRNA might not be enough to reduce error (Kramer & Farabaugh, 2006; Kramer et al., 2010). Missense errors are stimulated by amino acid starvation, due to changes in tRNA charging that alter the competition between cognate and non-cognate aminoacyl-tRNAs, further supporting this idea (Farabaugh & Björk, 1999).

1.3.2. Stop codon readthrough

tRNA suppression of stop codons results in extension of translation and synthesis of elongated proteins that can be functional or not, an event that is energetically very expensive for cells (Fearon et al., 1994).
Unlike peptide elongation, high termination fidelity is achieved without the help of a proofreading mechanism. The accuracy of termination arises from strong discrimination against sense codons in terms of release-factor binding efficiency (Sund et al., 2010; Freistroffer et al., 2000).

UAA is preferentially used both in *E.coli* and *S.cerevisiae* and UAG is rarely used. The available data show that in *E. coli*, readthrough of UGA (at least 10^{-2} to 10^{-3}) occurs at a higher frequency than that of UAG (7×10^{-3} to $1{,}1 \times 10^{-4}$) and that both occur at a significantly higher frequency than that of UAA (9×10^{-4} to less than 1×10^{-5}).
Although termination codons represent only ~ 4.7% of all codons, mutations that affect fidelity of translation termination usually have very prominent phenotypes, including sensitivity to osmotic stress, chromosome instability, respiratory deficiency, and cytoskeletal and cell-cycle defects (Valouev et al., 2002).

Since in eukaryotes eRF1 is the sole release factor for the three stop codons, its activity is critical for translation termination. In yeast, eRF1 levels directly correlate with termination efficiency. However, mutations in the yeast genes encoding both eRF1 (SUP45) and eRF3 (SUP35) are responsible for suppression of translation termination at all three stop codons. Another condition that reduces the efficiency of translation termination in yeast is the [PSI+] cellular state, characterized by the conversion of eRF3 to a nonfunctional prion form that associates in large aggregates within yeast cells (Serio & Lindquist, 1999). As a result, [PSI+] strains experience increased level of readthrough due to depletion of functional eRF3. In addition, mutations within the small subunit (18S) and large subunit (25S) of ribosomal RNAs have also been shown to cause an increased rate of translational readthrough in yeast (Liu & Liebman, 1996; Velichutina et al., 2000).

Codon context may also play an effect on the efficiency of translation termination in bacteria, yeast and mammals, and this is more striking in sub-groups of highly expressed genes (Brown et al., 1990; Mottagui-Tabar et al., 1994). The penultimate amino acid in the nascent peptide and the tRNA in the P-site exert regulatory influence on termination efficiency. Proximal sequences both upstream and downstream of the stop codon contribute to termination fine-tuning and can even act synergistically in *S.cerevisiae*. In yeast, the context influence on termination might extend as far as 3 - 6 nucleotides at the 3' side and signals that mediate efficient translation termination are used much more frequently than inefficient signals, as would be expected if selective pressure maintained this bias (Bonetti et al., 1995; Namy et al., 2001; Keeling et al., 2004).

The nucleotide context at the 3' side of the stop codon has a much distinct influence on termination efficiency. The identity of the tetranucleotide termination signal, containing the stop codon and the first downstream nucleotide (Brown et al., 1990; Bonetti et al., 1995; Poole et al., 1995), profoundly influences stop recognition by release factors. In accordance, during termination the bacterial release factor RF2 was

shown to directly interact with the first nucleotide following the stop codon (Poole et al., 1998).

1.3.2.1. Termination errors and cellular function

Translational readthrough can be highly deleterious, but on the other hand it might also regulate gene expression by permitting the differential production of more than one polypeptide from a single gene (Williams et al., 2004). Also, extending the C-termini of proteins by stop codon readthrough can markedly alter protein targeting, stability and activity, modulating the cellular proteome (Williams et al., 2004; Merritt et al., 2010).

For example, stop codon supression is essencial during the synthesis of many viral proteins like the Tobacco Mosaic Virus (TMV) RNA replicase domain and the gag–pol fusion protein from the Murine leukaemia virus (MuLV) (Skuzeski et al., 1991). Also, some genes were identified in budding yeast and Drosophila where the stop codon terminating the ORF is followed by a significantly long (>200 nt) downstream ORF (dORF) (Steneberg & Samakovlis, 2001; Namy et al., 2003).

The C-terminal of a protein can be an important determinant of targeting, stability and activity. Programmed stop codon readthrough results in proteins with additional amino acids at the C-termini and this has the potential to distinctly change the properties of the parent protein, ultimately imposing physiological changes for the cell. For example, the yeast PDE2 gene encoding a cAMP phosphodiesterase is readthrough between 2.2 and 8%, enlarging the Pde2p protein by 20 amino acids. This leads to modifications in cAMP concentrations, changing cell signaling and stress responses (Namy et al., 2002).

Alternatively, loss of translational accuracy could result in addition of even a small number of amino acids and end up completing a partial targeting signal already present at the C-terminus of a protein. This reprogramming event might represent a

gain of function that could potentially become genetically dominant and have phenotypic consequences for the cell (Williams et al., 2004). Therefore, by expanding the range of polypeptides encoded by a core set of genes, stop codon readthrough might be evolutionarily advantageous, potentially contributing to cell adaptation and survival under changing environments.

The chemical properties of the amino acid selenocysteine (Sec) make it functionally essential at the active centre of selenoproteins, mostly involved in anti-oxidant activity. The ability to recode UGA codons from a translation termination signal to a selenocysteine (Sec) codon is present in all domains of life. This occurs in organisms in which UGA is also known to function efficiently as a stop codon and is related with the presence of a Selenocysteine Insertion Sequence (SECIS) element in mRNA. The SECIS element is defined by characteristic nucleotide sequences and secondary structure base-pairing patterns (Hatfield & Gladyshev, 2002).

1.3.3. Frameshift

The reading frame is established during initiation and in normal conditions is maintained in translocation events until the stop codon is reached. Frameshifting errors arise usually from 2-base translocations, due to a 5′ slip by the ribosome, or 4-base translocations. A 2-base translocation is usually known as -1 frameshift and a 4-base frameshift as a +1 frameshift. Polypeptides resulting from a frameshifting event have little homology with the normal product. The protein will most likely be non-functional and shorter than the native protein, since stop codons are abundant in the alternative frames (Parker, 1989).

Frameshifting errors are not very frequent. Values for spontaneous frameshifting range from 10^{-4} to 10^{-3} in bacteria and in eukaryotic cells from 10^{-5} (yeast) to 10^{-4}- 10^{-3} (higher eukaryotes) (Curran & Yarus, 1986; Parker, 1989). Mutations in EF-Tu or in the eukaryotic cognate EF-1α might increase the frequency of codon-anticodon

mispairing, thereby intensifying the occurrence of spontaneous frameshifting errors (Tucker et al., 1989).

Frameshifting can be programmed to occur at rates from 1000- to 10000-fold higher than spontaneous frameshift. The expression of certain genes requires specific ribosomal frameshifting because the mRNA has coding information for protein in two different reading frames. In retroviruses, programmed frameshifting determines the synthesis of fusion peptides that function as structural elements. Such signals bypass the usual stop codon by shifting the ribosome out of frame by a single nucleotide, enabling the viral genome to increase its coding potential.
Frameshifting may also be responsible for autogenous control, namely, of the release factor 2 (RF2). The prfB gene of *E.coli*, which encodes release factor 2 (RF2), was one of the first +1 programmed frameshifting signals to be identified. When RF2 levels are high, termination is efficient, and synthesis of RF2 is downregulated. On the other hand, low RF2 levels result in inefficient recognition of the UGA codon, stimulating frameshifting and RF2 synthesis in the +1 frame (Craigen & Caskey, 1986).

There are general rules for programmed frameshifting. It generally occurs as a result of translational pausing, due to codon misreading or downstream secondary structures. The pause interferes with reading in the normal frame. During the pause, the tRNAs occupying the ribosomal decoding site briefly dissociate from the mRNA and rebind to a codon in a new reading frame (Parker, 1989; Farabaugh, 1996).
The most common form of programmed frameshifting is a –1 simultaneous slippage first found in eukaryotic viruses. The signal for -1 frameshift can be broken down into a slippery sequence of the form X-XXY-YYZ (where X = G, A, U, or C; Y = A or U; and Z is species specific), a linker region of variable length and composition, and a downstream region of secondary mRNA structure, typically an mRNA pseudoknot (Farabaugh, 1996).
Pseudoknots have several distinct folding topologies but are generally composed of two helical segments connected by single-stranded regions or loops. When the A- and P-sites of the ribosome are occupied by the slippery site sequence, the linker region

positions the pseudoknot on the surface of the ribosome, inducing elongating to pause. The slippery heptamer sequence has a repetitive nature that allows tRNAs decoding XXY-YYZ in the initial frame to shift to XXX-YYY in the –1 frame (Farabaugh, 1996; Dinman, 2006).

Starvation increases frameshifting, especially for certain amino acids like isoleucine, lysine, phenylalanine, proline, tryptophan or tyrosine. At first, a shortage of the cognate tRNA causes the ribosome to pause with an empty A-site. The suppressed codon is then read by an altered cognate tRNA or by a near-cognate tRNA, in those cases in which the mutated tRNA is unable to compete effectively for the A-site. Either way, a weak interaction is formed with the tRNA, and after normal nucleotide translocation the aberrant anticodon - codon interaction weakness prompts the peptidyl-tRNA to slip +1 in the P-site (Gallant & Lindsley, 1992). Ribosomes pausing at stop codons have a high propensity to frameshift, a situation analogous to frameshifting at hungry codons (Bertram et al., 2001).

Programmed frameshifts have now been found in a very wide spectrum of organisms, apparently involving paused ribosomes, specific shifty sequences and equally shifty tRNAs. The mechanisms are diverse and are likely adapted to the ribosomes of each organism (Farabaugh, 1996).

1.3.4 Ribosome Drop-off

Elongation might be delayed at rare codons or due to interactions between the nascent peptide and the ribosome within the peptide tunnel. This holdup can cause dissociation of tRNA from the mRNA and concomitant ribosome drop-off. This is often followed by decay of the mRNA through endonucleolytic attack and destruction of the incomplete polypeptide (Buchan & Stansfield, 2007).
In addition, the ribosome can also slide over hungry codons, resuming translation many nucleotides downstream, at an mRNA triplet complementary to the anticodon

of the peptidyl-tRNA. The resuming codon might not be in the original reading frame. Also, the efficiency of resuming declines with the length of the slide. There may be sequence contexts around or between the takeoff and landing sites that affect the frequency of sliding (Gallant & Lindsley, 1998). This tendency of ribosomes to ramble is greatly stimulated at hungry codons, but ribosomes in unstarved cells also stall or pause *in vivo*. *E.coli* ribosomes stalled at the rarely used arginine codon AGA do not resume under normal conditions, only when a tRNA that reads the codon is overproduced (Misra & Reeves, 1985).

1.4. Translational Quality Control

Gene expression represents a huge investment in energy, raw material and cellular resources. Selection for error minimization is a major driving force for genome evolution, constraining codon usage, codon context and major features of the translational machinery (Parker, 1989). A considerable effort is dedicated to optimizing the efficiency, responsiveness and accuracy of the translation process, since incorrectly synthesized proteins can critically interfere with processes essential to viability. Therefore, organisms developed mechanisms for reduction of error frequencies and also tolerance strategies that allow them to cope with the physiological consequences of protein-synthesis errors.

1.4.1. Reduction of error frequency

1.4.1.1. *Double – sieve* mechanism

During translation, aaRSs play a crucial role in maintaining a high accuracy (Schimmel & Soll, 1979; Carter, Jr., 1993). Each amino acid is specifically recognized out of twenty by its cognate aminoacyl-tRNA synthetase and esterified to the appropriate tRNA to form an aminoacyl-tRNA. tRNA molecules are large enough to provide a considerable number of specific interactions with synthetases, smoothing their recognition (Giege

et al., 1998) to error values in the order of 10^{-6} or less. Amino acids are much smaller than tRNAs and for many of them the side chains are structurally and chemically quite similar, and therefore their specific recognition could be a major problem, as in the case of valine, isoleucine and threonine. Surprisingly, experimentally determined error rate in amino acid selection is quite low, in the range of 10^{-4} to 10^{-5} (Sankaranarayanan & Moras, 2001). These values are explained by kinetic discrimination and proofreading (or editing) mechanisms occurring in two different catalytic sites of aaRSs, suggesting a *double-sieve* model of fidelity. This ensures that the correctly charged cognate tRNA is inserted into the A-site, contributing to the overall protein synthesis fidelity before peptide bond formation.

In a first stage, the synthetic site of aaRS shows some specificity by recognizing specific properties in each amino acid and sterically excluding amino acids with larger side chains than the cognate. However, amino acids having similar properties and a smaller size than the cognate amino acid can still be wrongly activated by adenylation and even misacylated at too high frequencies (Sankaranarayanan & and Moras, 2001; Cochella & Green, 2005b).

The solution for this discrimination problem became clear after the study of class I IleRS activity (Eldred & Schimmel, 1972). Valine is smaller than isoleucine by only a methylene group, being activated and charged on the $tRNA^{Ile}$ quite frequently. To prevent the eventual misincorporation of valine instead of isoleucine in nascent polypeptides, these enzymes have evolved a second active site, distinct from its synthetic aminoacylation active site - the editing site. Editing may occur through hydrolysis of the incorrectly formed aminoacyl adenylate (pre-transfer mechanism) or clearance of mischarged tRNAs (post-transfer mechanism) (Eldred & Schimmel, 1972; Sankaranarayanan & Moras, 2001) (Figure 1.10). Pre- and post-transfer editing activities are usually redundant and co-exist in tRNA synthetases. However, one of the mechanisms is frequently more prevalent and the other one is activated only if the first is compromised to prevent loss of protein synthesis accuracy (Martinis & Boniecki, 2010).

At first it was not clear how val-tRNA^{Ile} translocation occurs from the synthetic site to the editing site which is more than 25 Å away. There are now evidences that the tRNA molecule is directly involved in the translocation event (Schmidt & Schimmel, 1995). The CCA-end of the tRNA changes from a hairpin to a helical conformation in order to bend and shuttle the incorrectly added valine to the editing site, where it gets hydrolyzed. The mechanism of editing is very similar in a related class I enzyme, ValRS (Lin & Schimmel, 1996).

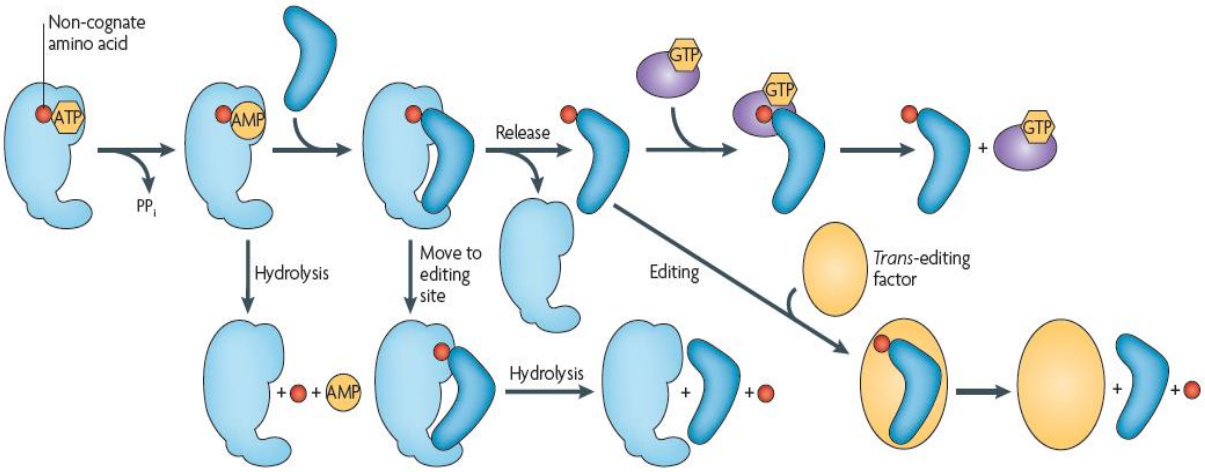

Figure 1.10 - *Double-sieve* mechanism for fidelity during tRNA aminoacylation. A non-cognate amino acid (red) might be activated at the synthetic site of aaRS and immediately hydrolysed and released. However, the reaction might proceed, resulting in the synthesis of a mischarged aminoacyl-tRNA that might then be translocated into the editing site of the aaRS for hydrolysis. However, the release of mischarged aminoacyl-tRNA from the aaRS without being edited is also possible, but usually culminates in editing by *trans*-editing factors or EF-Tu (purple) discrimination. Image adapted from Reynolds *et al.*, 2010.

Not much is known about how class II enzymes discriminate against closely related amino acids. The most studied is the editing mechanism of ThrRS. ThrRS must discriminate threonine from the isosteric valine and from serine, which is smaller but has a γ- hydroxyl group like threonine. It is thought that the CCA-end conformation of the tRNA changes in order to bend towards the editing site, but from helical to

hairpin, in symmetry with the mechanism for class I enzymes (Sankaranarayanan & Moras, 2001).

Some of the mischarged tRNA might dissociate from the aaRS instead of entering the editing site, escaping accuracy control. However, rather than being held directly by EF-Tu for protein synthesis, these released mischarged tRNAs can still rebind to the aaRS, allowing resampling by the editing site (Ling et al., 2009b). Trans editing also occurs through the action of autonomous factors like YbaK deacylase, which binds to ProRS and competes with EF-Tu for mischarged tRNAs, eventually hydrolyzing the non-cognate amino acid. In mammals, the trans-editing factor AlaX competes with EF-1α for Ser-tRNA^{Ala} in a process also dependent of AlaRS association, which plays a major role against neurodegeneration (Lee et al., 2006) (Figure 1.10).
After aminoacylation, quality control of aminoacyl-tRNA might also be complemented by EF-Tu binding specificity. Experimental evidences confirm that EF-Tu binds very weakly to misacylated tRNAs, such as Glu-tRNA^{Gln} and Asp-tRNA^{Asn}, therefore preventing delivery in the ribosome and misreading of the corresponding codons (Stanzel et al., 1994; Roy et al., 2007; Ling et al., 2009a).
Also, in higher eukaryotes aa-tRNA synthesis and proofreading takes place in multisynthetase complexes that also include translation elongation factors and associate with polysomal ribosomes. Some evidences suggest that this increases protein synthesis efficiency (Reynolds et al., 2010a).

1.4.1.2. Quality control by the ribosome

Missense errors might result in misfolded or non-functional proteins that must be refolded or destroyed after translation is finished. Remarkably, a new ribosome-centred mechanism characterized recently monitors the fidelity of protein synthesis after the formation of a peptide bond. The ribosome seems to recognize errors by evaluating the codon–anticodon helix in the P-site of the small subunit. Once an error occurs, the ribosome becomes much less efficient at adding amino acids; a general

loss of specificity in the A-site of the ribosome then results in several consecutive position mismatches in the P-site, until synthesis eventually stops and the polypeptide chain is released from the translational machinery prematurely. RF2 and RF3 are key players in the process by substantially accelerating the rate constant for peptide release activity, enhancing even more the overall accuracy. It had already been shown that RF3 stimulates release on certain ribosome complexes containing a near-cognate stop codon in the A-site (Zaher & Green, 2009). This post-peptidyl transfer process might contribute an order of magnitude to fidelity *in vivo*.

1.4.2. Increased tolerance – Proteostasis mechanisms

At an error rate of 10^{-4} (global error rate), 18% of proteins expressed from an average length (~400-codon) gene contain at least one misreading substitution. Around ~10–50% of random substitutions disrupt protein function but many more result in misfolding (Drummond & Wilke, 2008). Aberrant misfolded proteins expose natively buried hydrophobic residues and might bind to nonpolar exposed areas in other misfolded proteins, resulting in the formation of aggregates (Bucciantini et al., 2002). Protein aggregation has been linked to severe cytotoxic effects and to the pathogenesis of several neurodegenerative diseases. The buildup of protein aggregates is particularly deleterious to post-mitotic cells like neurons, presumably because they cannot dilute the toxic species during cell division (Ding et al., 2005; Lee et al., 2006).

Whether a polypeptide folds correctly or aggregates after synthesis depends on the kinetic competition between folding and aggregation (Kopito, 2000). Under stress, protein homeostasis mechanisms function as an integrated network that efficiently buffers the effects of decreased translational accuracy by acting on newly synthesized misfolded proteins before they can negatively impact cellular processes (Garcia-Mata et al., 2002). Efficient and correct folding *in vivo* is strongly dependent on molecular chaperones (Figure 1.11). Chaperones interact transiently with misfolded or partially

folded intermediates, stabilizing exposed hydrophobic residues and preventing incorrect molecular interactions. This mechanism eventually allows the protein to achieve proper folding.

The Hsp70 homolog Ssz1p and the Hsp40 homolog zuotin A compose a stable heterodimer, the ribosome-associated complex (RAC). Together with Ssb1/2p, another Hsp70 homolog, RAC are anchored to ribosomes and directly interact with nascent polypeptides, maintaining them in a folding-competent state and facilitating their transit through the ribosomal tunnel. Lack of functional RAC or Ssb1/2p causes severe problems in translational fidelity, which are strongly enhanced by paromomycin and correlated with growth inhibition (Rakwalska & Rospert, 2004).

Protein aggregation is however inevitable in cells and exacerbated because of intrinsic and environmental conditions such as oxidative stress, resulting in protein oxidation and carbonylation, and stress caused by heat, pH variation, changes in ionic strength and heavy metals. Aggregated proteins in the cytosol of *S.cerevisiae* are recovered by the coordinated action of the Hsp70 system (Ssa1/co-chaperone Ydj1) and the oligomeric ring-forming AAA+ chaperone Hsp104.

Hsp104 is a hexameric member of the HSP100/Clp family of ATPases and unlike other chaperones is not involved in preventing unspecific aggregation, but in repair functions after stress, by disaggregating misfolded proteins (Glover & Lindquist, 1998). Hsp104 is expressed at very low levels under normal conditions, but is induced under stress, enhancing cell survival from 100 to 1000-fold under extreme temperatures.

Hsp104 chaperones are not able to disaggregate substrates effectively on their own. Hsp70 restricts the access of proteases to the aggregates and assigns their transference to the substrate-processing pore of Hsp104, discriminating in favor of protein refolding (Zietkiewicz et al., 2004). The polypeptides are then present to Hsp104 and unfolded in a process mediated by ATP hydrolysis, which generates the necessary force to pull the substrate into the central translocation channel. The unfolded polypeptides are released following translocation and refold either

spontaneously or with the assistance of chaperones (Weibezahn et al., 2004; Lum et al., 2004).

The chaperone-mediated protein disaggregation process is also facilitated by direct interaction of small heat shock proteins (sHSPs) with protein aggregates (Haslbeck et al., 2005a). In the cytosol of *S. cerevisiae* two sHsps coexist, Hsp26 and Hsp42. The expression profiles of Hsp42 and Hsp26 are very similar. Both proteins are undetected during exponential growth and their synthesis is induced during diauxic shift and at heat shock temperatures (Haslbeck et al., 2004).
Small heat shock proteins (sHsps) selectively bind to misfolded proteins, preventing their irreversible aggregation by trapping them in a folding-competent state and inducing a more efficient disaggregation by the Hsp70 – Hsp104 system (Haslbeck et al., 1999; Haslbeck et al., 2005b). Therefore, the sHSP–substrate complexes function as a reservoir of misfolded proteins during stress conditions. sHSP in multicellular eukaryotes might potentially allow Hsp70 chaperones to act on aggregates even without the cooperation of an Hsp104-like AAA+ chaperone. It is remarkable that in higher eukaryotes Hsp104 homologues exist only in the mitochondria or chloroplasts. However, various studies showed that animal cells can solubilize aggregates, demonstrating the subsistence of a disaggregation activity in the absence of Hsp104 (Cohen et al., 2006; Tyedmers et al., 2010).

Cellular proteins that are unable to fold properly can also be targeted for degradation by the ubiquitin-proteasome system (UPS). The proteasome is a multisubunit complex located in the cytosol and nucleus that mediates degradation of cytosolic, nuclear, secretory and transmembrane proteins. Degradation of proteins via the UPS involves two distinct steps: targeting by covalent conjugation of multiple moieties of ubiquitin and degradation of the tagged substrate. Substrates of the UPS are marked with ubiquitin in a three-step ATP-consuming mechanism catalyzed by the enzymes E1 (ubiquitin-activating enzyme), E2 (ubiquitin-conjugating enzyme) and E3 (ubiquitin protein ligase). The first two enzymes are responsible for activation and transfer of ubiquitin to E3 that then catalyzes formation of a polyubiquitin chain anchored to the

targeted protein. Polyubiquitination of some proteins also requires E4 enzymes that cooperate with E3 ligases to extend the polyubiquitin chain. Finally, the polyubiquitin-tagged protein is degraded by the 26S proteasome, and free ubiquitin is released (Hershko & Ciechanover, 1998; Glickman & Ciechanover, 2002).

In vitro studies show that members of the 70-kDa family of molecular chaperones (Hsc70) are required for ubiquitin conjugation in mammals and subsequent degradation of certain proteolytic substrates. Molecular chaperones might act by unfolding the substrate to expose an ubiquitin ligase-binding site. Also, the chaperone can form a complex with the target substrate that serves as an intermediate in the proteolytic process. Hsc70 and E3 act together to generate the ubiquitinated substrates that are recognized by the 26 S proteasome (Bercovich et al., 1997).

Remarkably, protein aggregation directly impairs the function of the UPS, by saturating the capacity of molecular chaperones required for UPS function and causing accumulation of intracellular ubiquitin conjugates and UPS substrates (Bence et al., 2001). Therefore, in a positive feedback mechanism, protein aggregates can be simultaneously inhibitors of the pathway and the products that result from its inhibition, which results in an additional decline in UPS function.

In mammalian cells under stress and rapidly accumulating unfolded proteins the capacity of the quality-control systems might be exceeded. Protein aggregates are then transported via microtubules to organelles named aggresomes, localized to an indentation of the nuclear envelope at the microtubule-organizing centre (MToC). Recognition and transport to aggresomes is usually mediated by substrate ubiquitynation, but other signals might also be involved. In addition to protein aggregates, aggresomes are enriched in molecular chaperones, ubiquitination enzymes and both 19S and 26S proteasome subunits (Johnston et al., 1998; Kopito, 2000). Although prominent aggresomes are not normally seen in unstressed cells, this aggresome pathway might actually be a fundamental process that occurs

continuously to allow cells to deal with misfolded proteins that might escape other quality control mechanisms (Garcia-Mata et al., 2002). It is now known that clearance of aggregated protein sequestered in the aggresomes might be done by autophagy. How this process is regulated remains obscure (Pankiv et al., 2007; Rodriguez-Gonzalez et al., 2008). Aggresomes have also been detected in yeast, with a constitution closely similar to the mammalian counterparts (Wang et al., 2009) .

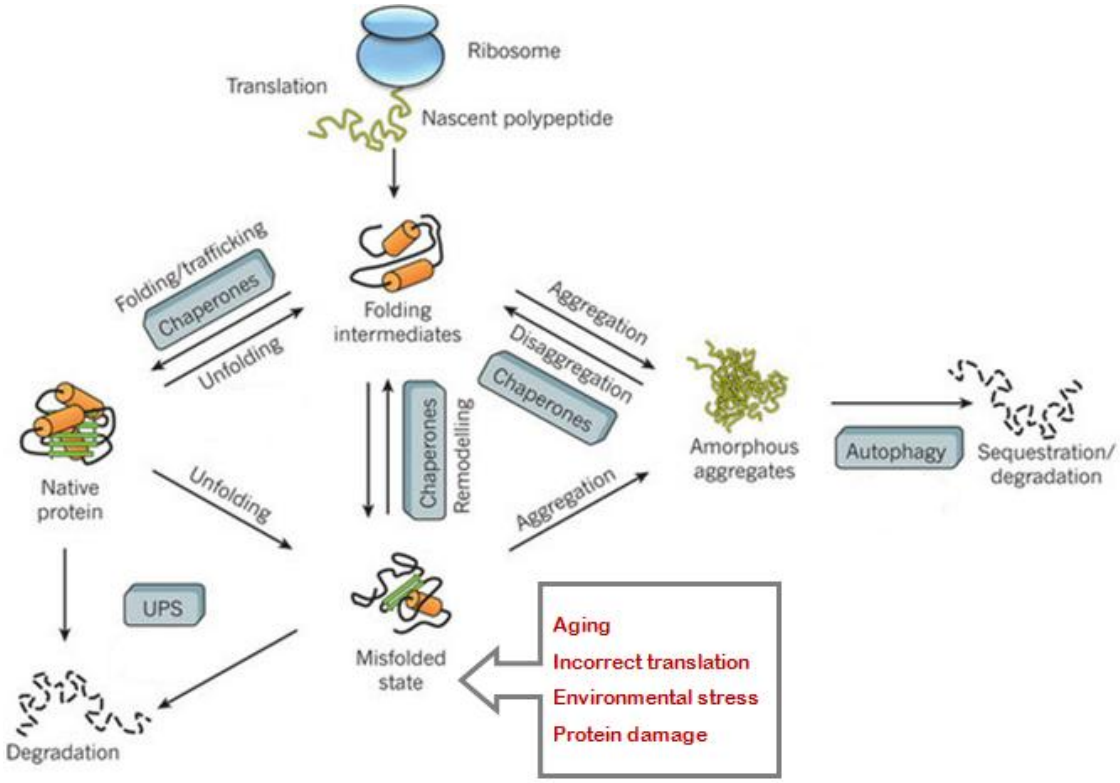

Figure 1.11 – Simplified schematic representation of the proteostasis network. Chaperones act at several levels, through the folding of newly synthesized proteins, remodelling of misfolded states and disaggregation. Protein degradation is mediated both by the UPS and autophagy pathways. Image adapted from Hartl et al., 2011.

Autophagy occurs at a basal level in normal growing conditions but certain types of environmental stress can result in a dramatic induction. Autophagy is responsible for bulk sequestration of cellular material into autophagosomes, double-membrane vesicular structures that in the end deliver these contents to the lysosome for degradation by hydrolytic enzymes and eventual recycling of the resulting

macromolecules (Yorimitsu & Klionsky, 2005). Autophagy is envolved in cellular homeostasis and also in processes such as cellular differentiation, cell defense and adaptation to adverse environments and metabolic changes within the cell (Cuervo, 2004). While UPS is essentially a fast degradation process, autophagy can therefore be a selective one (Kim et al., 2008) with a major role in removing excess or damaged organelles, parts of Golgi and endoplasmic reticulum, and even selective areas of the nucleus. Specific targeting mechanisms play a role in engulfment of mitochondria, peroxisomes, ribosomes and normally long-lived cytoplasmic substrates into autophagosomes.

There is close cooperation between UPS and autophagy in yeast cells. Several reports propose that some substrates are degraded by more than one protein degradation pathway. During acute nutrient starvation in yeast, amino acids for synthesis of new proteins are provided mainly by the UPS system, whereas during prolonged starvation autophagy becomes the major amino-acid-mobilizing pathway. Apparently, when proteasomal degradation is blocked the intracellular amino acid pool diminishes, which facilitates autophagy activation (Mizushima, 2007).

A buildup of cytosolic protein aggregates increases protein misfolding in the endoplasmic reticulum (ER), resulting is ER stress and induction of the unfolded protein response (UPR). The UPR involves upregulation of ER chaperones, promoting further degradation of misfolded polypeptides and might ultimately mediate apoptotic death, under conditions of extreme and prolonged ER stress (Rutkowski & Kaufman, 2004; Rochet, 2006).

1.5. Objectives of this work

Protein effectors are involved in nearly all cellular activities, conveying gene expression programs and managing all the physiological needs as well as adaptation to unfavorable environments. Translational errors represent a high energetic cost and are usually involved in deleterious phenotypes. Recent studies link mRNA mistranslation to cancer, neurodegeneration, aging and metabolic imbalances, especially under conditions that hamper protein control mechanisms. Interestingly, chromium toxicity was recently linked to decrease in protein synthesis fidelity (Holland S *et al.*, 2007), suggesting that environmental stressors may deregulate the translational machinery and disrupt protein homeostasis.

In line with previous studies, this work focuses mainly on the disclosure of a general link between environmental stress and the fidelity of eukaryotic protein synthesis, also exploring a potential correlation with evolution. Four main objectives are addressed along this thesis:

a) Quantify sense codon misreading and stop codon readthrough under environmental stress.
b) Characterize the cellular tolerance to mistranslation, under several specific environmental contexts.
c) Characterize mistranslation control mechanisms by exploring the effects of stress on key elements of the translational machinery.
d) Characterize a model of constitutive mistranslation depleted of key homeostasis regulators.

Chapter 2

The impact of environmental stress on protein synthesis fidelity

2.1. Introduction

2.1.1. mRNA mistranslation and proofreading

The maintenance of homeostasis is pivotal for cell survival. Environmental stress, including the response to environmental chemicals and radiation, as well as nutrient restrictions, plays a key role in degeneration and disease. Cells have evolved efficient mechanisms for gene expression regulation that swiftly guarantee survival and development under changing and sometimes particularly adverse environments. Accordingly, the flow of biological information from DNA to mRNA and then to protein must occur accurately and yet at a biologically significant rate, to cope with physiological and environmental needs without affecting the protein output.
To date, the effect of environmental stressors has been addressed mostly at the DNA mutagenesis level. Initially, mutagenesis was portrayed a random and stochastic process, blind to distinct environments. More recently, bacterial, yeast, and human cells were shown to possess mechanisms that stimulate mutagenesis rates specifically under the control of cellular stress responses. This stress-induced mutagenesis (SIM) allows cells to rapidly evolve and adapt to environmental changes (Galhardo et al., 2007; Shee et al., 2011).

During translation, both efficiency and accuracy conflicting demands are answered through the evolution of multiple accuracy mechanisms that block misincorporation events. Reducing translation error frequency to a minimum takes a huge but necessary kinetic price (Piepersberg et al., 1979). At least 95% of metabolic energy is consumed for protein synthesis in *E. coli* and *S.cerevisiae* (Jakubowski & Goldman, 1992). Protein synthesis errors occur at an average low frequency of around 1 misincorporated amino acid per 10^4 codons. This value reflects the cumulative fidelity of cognate tRNA aminoacylation and the decoding process performed by the ribosome. Remarkably, translational errors might in some cases represent the flexibility of alternative readings and became an advantage to organism evolution.

The spectrum of possible error types and mechanisms is quite diverse, however, not much is known about the effects of environmental stress on translation fidelity.

The occurrence of sense codon misreading (missense errors) brings coding ambiguity to the cell and is typically related to a single-base-pair mismatch between codon and anticodon or to the use of erroneously charged tRNAs (misacylation). The substitution of one amino acid for another has been previously detected in cells whose metabolism is unbalanced both by amino acid limitation or high-level production of a particular protein, occurring more frequently at the first or third position of the codon (Parker et al., 1983; Parker & Precup, 1986). In addition, in *E.coli*, the amount of amino acid misincorporation can also be increased by exposure to aminoglycoside antibiotics, such as streptomycin and neomycin (Parker, 1989). Finally, according to recent studies, high rates of tRNA misacylation with methionine might occur in mammalian cells, primarily as a defense mechanism against reactive oxygen species (ROS) (Netzer et al., 2009;). Also, *in vitro* data shows that methionyl-tRNA synthetase (MetRS) from *E.coli* is sufficient to mismethionylate several tRNA species (Jones et al., 2011). Methionine residues act as catalytic antioxidants, thereby protecting both the protein where they are located and other macromolecules (Luo & Levine, 2009).

Processivity errors such as premature termination and stop codon readthrough occur with a predicted error rate in the order of 10^{-4} to 10^{-3} per elongation event (Parker, 1989; Valente & Kinzy, 2003; Keeling et al., 2004). Translational frameshifting also affects processivity and occurs by tRNA shift of one or two bases in either 5′ or 3′ direction (Farabaugh & Björk, 1999). Processivity errors occur up to an order of magnitude more frequently than sense codon misreading errors (Parker, 1989; Stansfield et al., 1998) and usually result in the synthesis of non functional or even deleterious polypeptide sharing no homology with the expected product.
Efficient recognition of the standard genetic code is required for viability. However, in some viral genomes and several yeast genes, readthrough of stop codons is part of a regulated reprogramming mechanism, an important part of gene expression control (Namy et al., 2004). These events subvert the normal decoding rules by allowing the

synthesis of two related proteins from the same mRNA, sometimes with distinct biological functions, enhancing the coding potential of complex genomes (Namy et al., 2003). Reprogramming mechanisms might also lead to changes in both cell signaling and stress responses (Namy et al., 2002). Remarkably, increased levels of readthrough in [PSI+] yeast strains might under specific conditions confer a phenotypic advantage, namely by enhancing tolerance to environmental stress (Eaglestone et al., 1999).

2.1.2. Protein homeostasis mechanisms

Protein native and non-native conformations are separated by a surprisingly low energy barrier (Tyedmers et al., 2010). Both stress and defects in protein biogenesis greatly increase the risk of misfolding, with a concomitant loss of protein function. In order to better cope with costly protein-synthesis errors, organisms evolved strategies not only for improved accuracy but also for increased tolerance to unavoidable errors. Cells rely on molecular chaperones to capture and refold misfolded proteins. If refolding is unattainable, misfolded proteins are targeted for degradation. In cells with high degree of error-induced protein misfolding the buffering capacity of proteome quality control mechanisms is stimulated but might not be enough to prevent the buildup of protein aggregates (Garcia-Mata et al., 2002). This system overwhelm is linked to a number of disease states and might ultimately result in cell death (Dobson, 2004).

Small heat shock proteins (sHsps) like Hsp26 and Hsp24 are upregulated in response to conditions that increase protein unfolding and restrain the buildup of protein aggregates (Haslbeck et al., 2004). After heat shock, both Hsp26 and Hsp24 deletion mutants accumulate large amounts of cytosolic protein aggregates. In cells with the double deletion, an even higher increase of insoluble protein is observed (Liberek et al., 2008).

In *S. cerevisiae*, Hsp104 is induced under heat, ethanol, and sodium arsenite exposure (Sanchez et al., 1992). However, unlike other chaperones, Hsp104 is exclusively involved in repair functions after stress, by disaggregating misfolded proteins (Glover JR & Lindquist S, 1998). In this process, Hsp70 chaperones are first required to remove polypeptides from the aggregates, composed both of misfolded proteins and sHsps in stable complexes (Tyedmers et al., 2010).

In eukaryotic cells, the ubiquitin–proteasome system (UPS) is the central pathway for eliminating misfolded proteins (Hershko & Ciechanover, 1998; Wolf & Hilt, 2004). Rpn4p expression is induced under a variety of stress conditions and is required for normal levels of intracellular proteolysis, functioning as a positive transcriptional regulator of genes encoding proteasomal subunits (Xie & Varshavsky, 2001; Holland et al., 2007; Thorsen et al., 2009; Xie & Varshavsky, 2001). Autophagy can also be activated for clearance of aggregated proteins. Atg5p is essential for autophagosome formation and acts at a very initial stage of the autophagic process (Yorimitsu & Klionsky, 2005; Codogno & Meijer, 2006).

Changing environmental conditions often lead to a cellular adjustment in the number and quality of ribosomes. Under starvation, recent experimental evidences demonstrate the occurrence of ribophagy, a new form of autophagy by which the cell selectively degrades ribosomes. One of the proteins crucial for this process is Bre5p, identified as an ubiquitin protease cofactor (Kraft et al., 2008). Remarkably, this evidence strengthens the suggestion of a direct connection between the selective autophagy and the ubiquitin-proteasome pathway. Since both processes play an important role in many diseases such as Alzheimer's or Parkinson's, ribophagy is an important piece for a better understanding of many pathological mechanisms.

2.1.3. Environmental Stress Response and protein homeostasis

In yeast, many of the protein homeostasis mechanisms are induced as part of the Environmental Stress Response (ESR), a gene expression program strategically

activated for cellular adaptation and survival after a shift to an unfavorable environment (Gasch et al., 2000). The ESR is defined by transient growth arrest and an overall translation repression of housekeeping genes, coupled with the selective induction of transcripts critical for safeguarding adjustment and survival. Program initiation is tightly controlled in response to each distinct environment change. Therefore, regulation of these expression changes is gene-specific and condition-specific (Gasch AP, 2002). The magnitude of the changes in gene expression is directly linked to the extension of the environmental stress.

Coordinated changes in expression of numerous chaperone genes are a common feature in response to many unfavorable environments (Werner-Washburne et al., 1989; Kobayashi & McEntee, 1990; Susek & Lindquist, 1990). Among the most induced genes as part of the ESR are small heat shock proteins like HSP12 or HSP26, along with members of the Hsp70 family of chaperones (*SSA4*, *SSE2*) and *HSP104* (Gasch et al., 2000). Genes involved in both ubiquitin ligation and conjugation also participate in the ESR. Ubiquitination is essencial to target misfolded proteins for degradation in the proteasome (Glickman MH & Ciechanover A, 2002).

2.1.4. Cellular stress and the translational machinery

In *S. cerevisiae* the reprogramming of gene expression in response to stress is triggered by the highly coordinated and flexible action of several transcription factors, many of them acting in combination. The yeast activator protein (Yap) family of b-ZIP transcription factors includes eight members, each regulated in a specific and distinct manner. For example, Yap1p, Yap2p and Yap8p, are essential to guarantee homeostasis under exposure to oxidative stress (Fernandes et al., 1997; Temple et al., 2005). The transcriptional activity of Yap1p is usually regulated by a change in cellular localization. High cellular levels of ROS activate cellular pathways that culminate in formation of an intramolecular disulfide bond in Yap proteins. The resulting conformational change allows their transit from the cytoplasm to the nucleus and

concomitant transcription of anti-oxidant genes like TRX2 and GSH1 (Gulshan et al., 2005).

Excess of ROS can lead to oxidation of cellular macromolecules, such as nucleic acids, proteins, and lipids, resulting in impairment of important physiological functions. Oxidative stress impacts cells at least partially through targeting the translational machinery and the protein quality control machinery. For example, oxidation of mRNA does not necessarily suppress protein synthesis but results in a loss of translational efficiency by promoting premature termination and synthesis of modified full-length non functional proteins. In either case, potentially deleterious misfolded protein species can be generated and contribute to accumulation of protein aggregates, especially under conditions of saturated quality control capacity (Ding et al., 2005).

Chromate [Cr(VI)] is a highly toxic metal, classified as a carcinogen and a prevalent pollutant resulting from human activities.The major molecular mechanism of chromium toxicity was recently unveiled and linked to a decrease in translational accuracy. First, Cr exposure leads to sulfur starvation in yeast (Pereira et al., 2008) both by inhibiting sulfate uptake and by competition with the sulfate metabolism. This eventually results in depletion of the S-containing amino acids methionine (Met) and cysteine (Cys) (Pereira et al., 2008; Holland et al., 2010), altering the competition between cognate and non-cognate aminoacyl-tRNAs for codons and culminating in loss of translation accuracy (Farabaugh & Björk, 1999; Sørensen, 2001). Incorporation of erroneous amino acids originates misfolded proteins that might surpass protein homeostasis mechanisms and lead to the buildup of toxic protein aggregates (Holland et al., 2007).

The mechanism of Cr toxicity brings new light to the study of a dynamic connection between cellular homeostasis, stress response and components of the translational machinery. A number of cellular degenerative effects have been associated to mRNA mistranslation, namely through the buildup of misfolded protein aggregates, that can eventually be responsible for free radical formation, disruption of membrane integrity

and loss of crucial ionic balances (Stefani & Dobson, 2003; Stefani, 2007). Protein aggregation can culminate with apoptosis and cell death.

Common environmental contaminants might have an impact of unknown prevalence on translation machinery that seems important to reveal, for a better understanding of the tolerance mechanisms developed to prevent mistranslation induced cell degeneracy. Arsenic (As), cadmium (Cd), mercury (Hg), lithium (Li), ethanol, hydrogen peroxide and caffeine are well studied stressors associated with quite distinct tolerance and cellular responses in eukaryotes (Thorsen et al., 2009; Stanley et al., 2010; Valko et al., 2005; Dichtl et al., 1997; Kuranda et al., 2006). However, much information is still lacking on the complete mechanisms of action.

In this study we use the yeast model and bicistronic luciferase reporters to approach error quantification. Both wild-type cells and deletion mutants defective in protein homeostasis were tested under environmental stress conditions. Overall, our results demonstrate that the impact of the environmental stressors tested on the translational accuracy is quite low and concealed by the integrated activity of a number of protein homeostasis mechanisms, with a particular emphasis for proteasome activity. Hsp12, a stress protein with unique characteristics, is shown to assume an unexpected role in maintaining translational accuracy.

2.2. Material and Methods

2.2.1. Strains and growth conditions

The bacterial strains JM109 (endA1 glnV44 thi-1 relA1 gyrA96 recA1 mcrB$^+$ Δ(lac-proAB) e14- [F' traD36 proAB$^+$ lacI^q lacZΔM15] hsdR17($r_K^-m_K^+$)) and DH5α (F$^-$ endA1 glnV44 thi-1 recA1 relA1 gyrA96 deoR nupG Φ80d*lacZ*ΔM15 Δ(*lacZYA-argF*)U169, hsdR17(r_K^- m_K^+), λ–) were recurrently used in this study for plasmid amplification and grown at 37°C in Lysogeny Broth (LB) medium (Formedium) or LB 2% agar (Formedium), both supplemented with 50 µg/mL ampicillin when required.

The *S.cerevisiae* strains used in this study and their genotype are specified in Table 2.1.

Table 2.1 – *S.cerevisiae* strains used in the current error quantification study.

Strain	Genotype	Source
BY4743	*MATa/MATα his3Δ 0/his3Δ 0; leu2Δ /leu2Δ 0; met15Δ 0/MET15; LYS2/lys2Δ 0; ura3Δ 0/ura3Δ 0*	Euroscarf
Δatg5	BY4743 ; YPL149W::kanMX4/YPL149W::kanMX4	Euroscarf
Δrpn4	BY4743 ; YDL020C::kanMX4/YDL020C::kanMX4	Euroscarf
Δbre5	BY4743 ; YNR051C::kanMX4/YNR051C::kanMX4	Euroscarf
Δhsp26	BY4743 ; YBR072W::kanMX4/ YBR072W::kanMX4	Euroscarf
Δhsp42	BY4743 ; YDR171W::kanMX4/ YDR171W::kanMX4	Euroscarf
Δhsp104	BY4743 ; YLL026W::kanMX4/ YLL026W::kanMX4	Euroscarf
Δhsp12	BY4743 ; YFL014W::kanMX4/ YFL014W::kanMX4	Euroscarf
Δssb1Δssb2	BY4742 ; YDL229W::kanMX4/ YNL209W:: natMX	Dombek K. et al., 2004
Δtrm9	BY4743 ; YFL014W::kanMX4/ YML014W::kanMX4	Euroscarf
Δyap1Δyap2	BY4742 ; YML007W::kanMX4/ YDR423C::HIS3	(Azevedo et al., 2007)

Yeast cells were cultured at 30°C/180 rpm in rich YPD medium (1% yeast extract, 2% Peptone and 2% Glucose) or selective minimal medium (MM – 0.67% yeast nitrogen base, 2% glucose and 0.2% Drop-out mix, lacking the amino acids corresponding to the selection markers). Geneticin (G418) was used in deletion strains at a

concentration of 200mg/L. Solid media required agar up to 2%. All media were sterilized by heat at 120 ºC for 15 – 20 min.

2.2.2. Plasmids

The *S.cerevisiae* plasmids used in this study are specified in Table 2.2.

Table 2.2 – Luciferase plasmids used in the current study.

Plasmid	Description	Source
pDB688	Yeast PGK promoter and CYC2 transcription terminator.	Salas-Marco et al., 2005
pDB690	**CGA** at the readthrough cassette	Keeling K. et al., 2004
pDB691	**UGA** at the readthrough cassette	Keeling K. et al., 2004
pDB722	**CAA** at the readthrough cassette	Keeling K. et al., 2004
pDB723	**UAA** at the readthrough cassette	Keeling K. et al., 2004
pUA312	Wt AGA (Arg 218) from F-luc mutated to **AGC** (Ser)	This study

The vectors from the pDB series (Table 2.2) contain a URA marker and are derived from the pYEplac195 expression plasmid. The pDB series bears copies of luciferase genes derived from the sea pansy *Renilla reniformis* (R-luc) and the firefly *Photinus pyralis* (F-luc), merged into a single reading frame with a yeast *PGK* promoter and the *CYC1* transcription terminator. pDB pairs 690/691 and 722/723 express respectively either an in-frame stop codon or a cognate sense codon (control vector), positioned in a readthrough cassette between R-luc and F-luc genes, with the following sequence:

ATG TCG ACG TGC GAT **XXX N**CG TTC GGA TCC

where XXX is the sense / stop codon and N is a key position influencing termination efficiency. The plasmids used for this study hold a cytosine (C) at this position, favouring stop codon suppression (see Annexes 1 and 2).

pUA312 was built from pDB688 by Site-Directed Mutagenesis, using the QuikChange Kit (Stratagene) according to the manufacturer's instructions. For this purpose the

following oligonucleotides were designed and ordered from MWG-Biotech AG (Germany):

oUA - GAACTGCCTGCGTCAGCTTCTCGCATGCCAGAG
oUA - CTCTGGCATGCGAGAAGCTGACGCAGGCAGTTC

The resulting colonies were picked and grown for minipreps in 5ml LB + ampicillin (QIAprep Spin Miniprep Kit, used according to Qiagen's instructions). The mutation was then confirmed by DNA sequencing, using primers adjacent to the introduced mutation.

2.2.3. Yeast transformation

For efficient transformation of *S.cerevisiae* we adapted the LiAc/SS carrier DNA/PEG method (Gietz & Woods, 2006), with few modifications. Fresh yeast colonies were picked and grown overnight at 30ºC/180 rpm in YPD rich medium. Overnight cultures were then diluted 1:1000, grown to mid-log phase (OD_{600}~0,5) and harvested by centrifugation at 4000rpm. After washing with 5mL of sterile mQ water, the cell pellet was resuspended in 50µL of 0.1M LiAc solution and the following reagents were added in the designated order : 500µL 50% (w/w) PEG, 25µL single-stranded carrier DNA (2mg/mL) previously denatured for 5min. at 95ºC and 0.1 – 1µg of luciferase plasmids. Tubes were vortexed immediately until the mixture was homogeneous and then subjected to heat-shock at 42ºC for 45 min. Cells were then harvested by centrifugation at 5000rpm, the supernatant was discarded, the pellet resuspended in 100 µL of sterile mQ water and plated in selective minimal medium plates (MM – 0.67% yeast nitrogen base, 2% glucose, 0.2% Drop-out mix lacking uracil and 2% agar) that were then incubated at 30ºC until colonies were visible.

2.2.4. Preparation of cell extracts and dual luciferase assays

Individual yeast transformants carrying the dual luciferase vectors were picked and grown overnight at 30ºC/180 rpm to stationary phase in minimal medium lacking uracil (MM-Ura) and containing 200mg/L of geneticin (G418). Overnight cultures were then diluted 1:100 in MM-Ura, grown at 30ºC/180 rpm to mid – log phase (OD_{600} 0,5-0,6) and exposed for 4h to non lethal concentrations of the environmental stressors selected (see Table 2.3).

Table 2.3 - Environmental stressors used during the current study and respective concentrations.

Stressor	Concentration
As_2O_3	200 and 400µM
$CdCl_2$	125, 60 and 30µM
$HgCl_2$	25µM
H_2O_2	3mM
LiCl	40mM
Ethanol	5%
Caffeine	8mM

Cells were then recovered by centrifugation, washed twice and resuspended in 250µl ice cold PBS buffer. After addition of 2/3 volume of glass beads (0.5 mm diameter), cells were disrupted using a Precellys homogenizer (Bertin technologies) for 3 x 1 minutes with 2 min. incubation on ice between each disruption cycle. Cell lysates were then centrifuged at 5000 rpm for 15 minutes at 4ºC to remove intact cells and the supernatant transferred to a new tube. The Luciferase assay was performed using the Dual-Luciferase Reporter Assay System (Promega). Briefly, 50µl Luciferase assay reagent II were added to 5 - 20µl of each lysate in a 96 white opaque multiwell plate. Relative luminescence units (RLUs) produced by F-luc activity was measured for 10s using an available Synergy™ 2 Microplate luminometer module (BioTek). Stop&Glo buffer (50µl) was then added to each well to quench F-Luc activity and activate R-Luc

that is used as an internal normalization control for both mRNA abundance and the efficiency of translation initiation. Control constructs were assayed in each strain to determine the theoretical maximal level of expression for reporter systems.

Background measures were made with lysates of non-transformed BY4743 cells (lacking the Dual Luciferase Reporter Plasmid) and subtracted from test measurements. The ratio F-Luc/R-Luc is a measure of mistranslation and expressed in relative luminescence units (RLU).

2.2.5. Viability assay of yeast exposed to environmental stress

Yeast viability was accessed by the colony forming units (CFU) assay. Yeast cells harboring dual luciferase vectors (Table 2.2) were grown to mid-log phase (OD_{600} 0,5-0,6) and exposed for 4h to the indicated concentrations of environmental stressors (see Table 2.3). Cells were then collected by centrifugation and washed twice in PBS buffer. After counting, 100 cells were plated onto fresh MM-Ura plates. The number of colony forming units (CFU) was determined following incubation at 30ºC for 3 days, giving a measure of viability under toxic exposure.

2.2.6. Yeast growth under stress

For growth measurements, exponential phase cultures of yeast cells harboring dual luciferase vectors were exposed for 4h to the indicated concentrations of environmental stressors (see Table 2.3). The total number of cells in culture was monitored using a Vi-Cell (Beckman Coulter) before toxic exposure and after 4h incubation at 30ºC. Growth fold changes induced by stress were calculated by the ratio between cell number increase and the corresponding incubation time and are represented as percentage fold change relatively to control (cells not exposed to stress).

2.2.7. Statistics

Data is reported as mean±SEM. Significance was tested by one-way ANOVA and t-test (GraphPad Prism 5). Differences are considered significant when p<0,05.

2.3. Results

2.3.1. An assay system for measuring translation accuracy in yeast exposed to environmental stress

The search of a more extensive connection between stress exposure and accuracy of protein synthesis demanded a broader screening for potential toxic effectors, which we carried out in budding yeast. *S.cerevisiae* is one of the most widely used eukaryotic model organisms, being extremely easy to grow and manipulate genetically. It is thought that up to 30% of genes implicated in human disease have orthologs in the yeast proteome (Karathia et al., 2011), making it especially fitted to untangle the molecular mechanisms of stress and tolerance or accuracy strategies.

With this purpose, yeast cells were transformed with dual luciferase reporters specific for both stop codon suppression and sense codon misreading quantification. The basic features of the bicistronic dual luciferase reporter were originally described by Grentzmann et al. (1998) and since then suffered several adaptations. The readthrough reporter used here was developed by Keeling and Bedwell (2004) and consists of a translational fusion of the gene encoding *Renilla reniformis* luciferase (R-luc) with a downstream gene encoding the *Photinus pyralis* (firefly) luciferase (F-luc). The two consecutive luciferase genes are under the control of the PGK promoter and separated by an in-frame linker sequence.

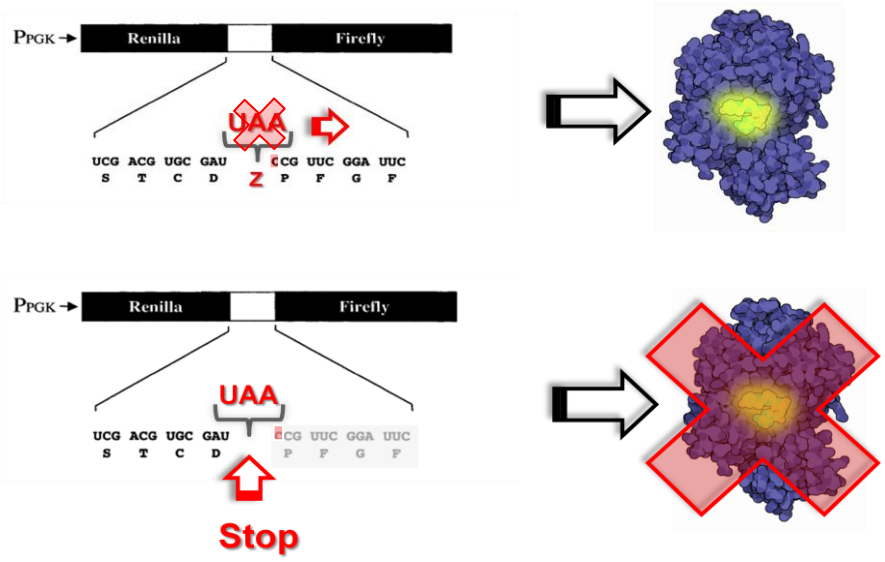

Figure 2.1 – Schematic representation of the dual luciferase Readthrough reporter system, initially described by Salas-Marco and Bedwell (2005). *Renilla* luciferase and firefly luciferase genes are under the transcriptional control of the *PGK* promoter. Supression of the stop codon, positioned in a cassette between the two genes, allows expression of both genes as a single polypeptide. Z represents any inserted amino acid. The activity from each luciferase can be measured independently in protein extracts, as they use different substrates. Rates of readthrough were calculated by dividing the ratio of firefly luciferase activity to *Renilla* luciferase activity from cells harbouring plasmids containing a premature stop codon by the ratio generated from cells with the plasmid having a sense codon between the two genes.

Both enzymes are then synthesized as a single polypeptide but their activities can be measured sequentially in the same sample with very different reaction conditions. R-luc serves as an internal normalization control for mRNA abundance and efficiency of translation initiation and so any differences accounted in the activity of F-luc relative to R-luc must be linked with changes in the activity of F-luc. In the particular case of the termination readthrought quantification reporter (Figure 2.1), a stop codon is placed in the linker sequence between the two luciferase genes. Stop codon suppression propels expression of F-luc and an increase in the ratio firefly/ *Renilla* luciferase activity.

S.cerevisiae BY4743 cells transformed with the readthrough reporter plasmid were grown to mid-log phase (OD_{600} 0,5-0,6) in MM lacking uracil and exposed to stressors for 4h. Concentrations of Arsenic (As), Cadmium (Cd), Ethanol, Caffeine and H_2O_2 induced a decrease in cell growth between 40-60% and a viability loss lower than 20%. Concentrations of lithium (Li) and mercury (Hg) were non-inhibitory (see Figure 2.2).

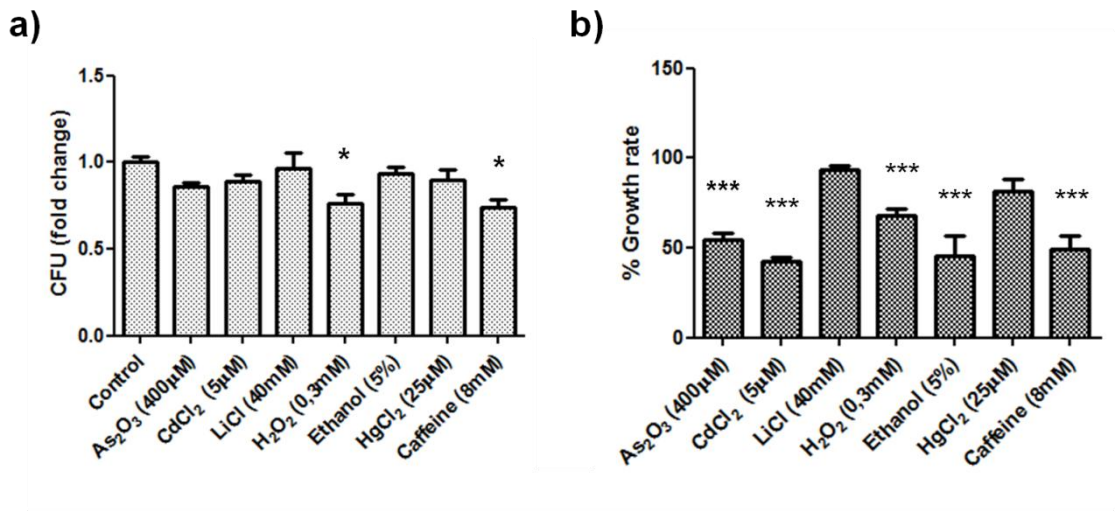

Figure 2.2 – Viability of *S.cerevisiae* BY4743 cells exposed to environmental stress. Exponentially growing yeast cells were exposed to stressors at the indicated concentrations for 4h. **a)** Colony forming units (CFU) assay – for each condition, the same number of cells was collected (100) and then plated onto fresh MM-Ura plates. The number CFU was determined after 3 days incubation at 30ºC and represented as a fold change relatively to control (plated cells not exposed to stress).**b)** Fold changes in yeast growth under stress - the total number of cells in culture was monitored using a Vi-Cell (Beckman Coulter) both before toxic exposure and after. Results are represented as percentage fold change relatively to control (cells not exposed to stress). * and *** represent values significantly different (P <0.05 and P<0.001, respectively; one-way ANOVA, Dunnett's post-test). Values are mean ± SEM of three biological replicates.

Control constructs harboring only in-frame near-cognate sense codons in the sequence between luciferase genes were assayed in each strain and under each stress condition. These allowed verifying the theoretical maximal level of expression (100% readthrough) for these reporter systems and also to proceed with final readthrough correction, excluding any pleiotropic effects of mutations or stress on luciferase

activity. Results were expressed in relative light units (RLU) (Keeling et al., 2004). Negative controls containing all the reaction components except the cell lysate were used to correct background noise for each luciferase reaction. In all cases, the background noise was negligible.

Although stop codon recognition by release factors is efficient, in certain circunstances stop codons are decoded instead by a near-cognate tRNA. Examples of tRNAs that decode stop codons include yeast $tRNA^{Gln}_{GUC}$ (decodes CAG and UAG), and $tRNA^{Gln}_{UUG}$ (decodes CAA and UAA). Two stop codons from *S.cerevisiae* were chosen for readthrough quantification in this work. UAA codon is the most efficient termination codon in yeast and also the most frequently used in highly expressed genes. On the other hand, UGA is the most error prone stop codon, and is rarely used in termination (Keeling et al., 2004; Liang et al., 2005). Context takes enormous importance in readthrough accuracy. A C residue located at the first position following the stop codon in each of the readthrough constructs in this study seems to reduce the efficiency of termination around 20-fold (Brown et al., 1990; Bonetti et al., 1995).

Previous studies with the dual luciferase reporter in yeast cells suggest that the UAG termination codon corresponds to a 2,5-fold increase in corrected readthrough relative to the UAA codon (Keeling et al., 2004). In our model, using however a distinct yeast background, we measured an increase of only 1,5-fold. The ribosome-targeting drug paromomycin was used as a positive control to confirm the reliability of our assay (Figure 2.3 c). Paromomycin is an aminoglycoside known to decrease translational accuracy in *E. coli* and yeast (Singh et al., 1979; Palmer et al., 1979). By binding to the small ribosomal subunit, paromomycin alters the kinetics of decoding, increasing the probability of near-cognate tRNA incorporation and blocking recognition of termination codons (Carter et al., 2000; Ogle et al., 2003). According to our results, paromomycin exposure increased stop codon readthrough approximately 1,7-fold, in accordance with the values already described in a similar system (Holland et al., 2007) (Figure 2.3 c).

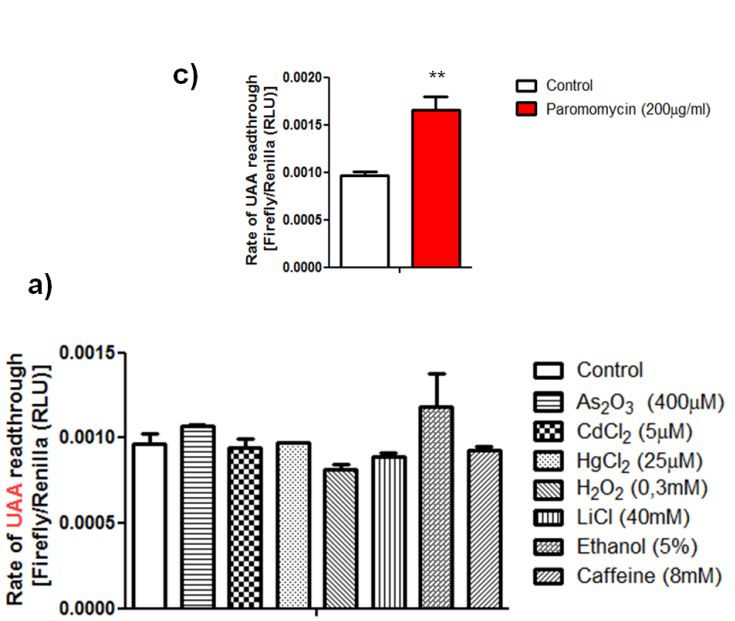

b)

	BY4743
As_2O_3 (400µM)	1.107 ± 0.015
$CdCl_2$ (5µM)	0.980 ± 0.053
$HgCl_2$ (25µM)	1.007 ± 0.046
H_2O_2 (0,3mM)	0.845 ± 0.036
LiCl (40mM)	0.923 ± 0.021
Ethanol 5%	1.226 ± 0.205
Caffeine (20mM)	0.960 ± 0.026

Figure 2.3 - UAA readthrough levels do not significantly increase upon exposure to environmental stress. BY4743 cells were transformed with dual luciferase reporters containing either a UAA stop codon or a sense codon between the two genes, grown to mid-log and exposed to stress for 4h. The ratio of firefly to renilla luciferase activity is a measure of UAA stop codon readthrough and is expressed in relative light units (RLU). Renilla luciferase activity was used as an internal standard. For each stress, values were normalized with the firefly to renilla luciferase activity ratio measured in construct carrying a sense codon in place of UAA. **a)** and **b)** readthrough values were calculated relative to control (cells not exposed to stress). **c)** Paromomycin was used as a positive control. * represents values significantly different ($P < 0.05$; unpaired Student's t-test) Values are mean ± SEM of at least four independent experiments done in triplicate.

Overall, our results demonstrate that the environmental stressors studied did not significantly impact UAA reading accuracy, suggesting that the eukaryotic translation machinery is very resistant to environmental stress (Figure 2.3 a and b). However, readthrough of a leaky UGA stop codon under the same downstream context was increased (1,360 ±0,140) by exposure to 5% ethanol (Figure 2.4 b and c).

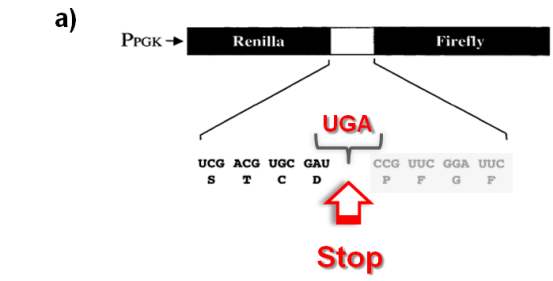

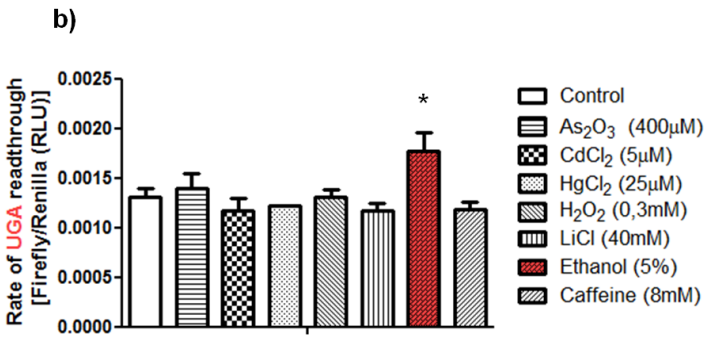

c)

	BY4743
As_2O_3 (400µM)	1,071 ± 0,117
$CdCl_2$ (5µM)	0,894 ± 0,104
$HgCl_2$ (25µM)	0,899 ± 0,110
H_2O_2 (0,3mM)	1,003 ± 0,052
LiCl (40mM)	0,901 ± 0,049
Ethanol 5%	* 1,360 ± 0,140
Caffeine (8mM)	0,910 ± 0,053

Figure 2.4 - UGA readthrough levels increase with exposure to ethanol. a) BY4743 cells were transformed with dual luciferase reporters containing either a UGA error prone stop codon or a sense codon between the two genes, grown to mid-log and exposed to stress for 4h. UGA stop codon readthrough is expressed in relative light units (RLU). Renilla luciferase activity was used as an internal standard. For each stress, readhtrought values were normalized with the firefly to renilla luciferase activity ratio measured in a strain that carried a sense codon in place of UGA. * represents a value significantly different from the control ($P < 0.05$; one-way ANOVA, Dunnett's test) **b)** and **c)** fold change in readthrough values relative to control (cells not exposed to stress). Values are mean ± SEM of at least four independent experiments.

Under the same stress conditions, an analogous bicistronic reporter was used to measure arginine misincorporation at mutant AGC codons. In Wt firefly luciferase, the amino acid residue at position 218 is part of the catalytic site and utterly determines enzymatic activity. Remarkably, beyond arginine no other amino acid is active at this site of firefly luciferase (Branchini et al., 2001; Plant et al., 2007). Serine has a polar side chain like arginine, but lacks the positive charge and for this reason cannot substitute its catalytic function. Therefore, this position is valid for highly specific

monitoring of AGC misreading, by eliminating the possibility of functional replacement by other amino acids during quantification of arginine misincorporation.

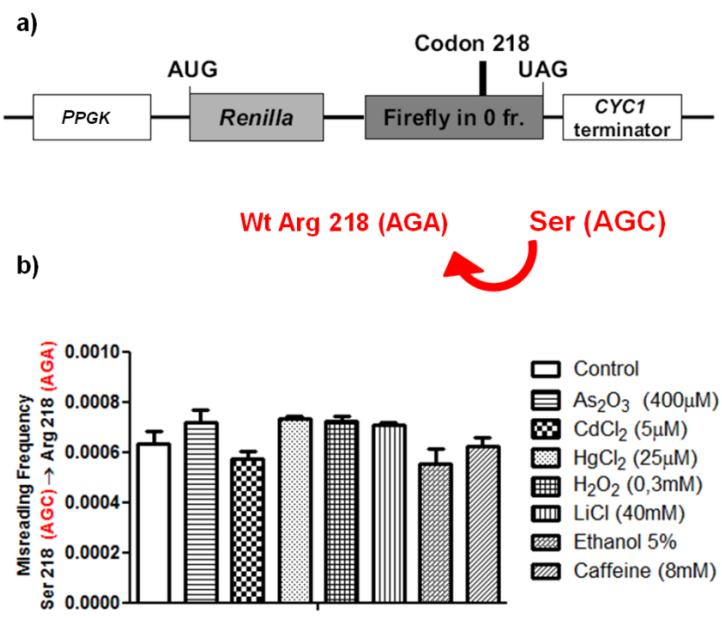

c)

	BY4743
As_2O_3 (400µM)	1,134 ± 0,080
$CdCl_2$ (5µM)	0,907 ± 0,044
$HgCl_2$ (25µM)	1,105 ± 0,020
H_2O_2 (0,3mM)	1,144 ± 0,026
LiCl (40mM)	1,116 ± 0,020
Ethanol 5%	0,875 ± 0,091
Caffeine (8mM)	0,982 ± 0,058

Figure 2.5 - AGC codon misreading is not significantly increased by exposure to environmental stress. a) Mutation of an arginine (AGA) to a serine (AGC) codon at the firefly luciferase active site ablates protein activity. AGC misreading might restore the enzymatic activity, allowing quantitative measurement of the error rate (adapted from Plant E. *et al.*, 2007). BY4743 cells were transformed with dual luciferase contructs containing either AGA wild-type codon or the AGC codon at position 218 of firefly luciferase, grown to mid-log and exposed to stress for 4h. AGC misreading is expressed in relative light units (RLU). Renilla luciferase activity was used as an internal standard. Rates of misreading were calculated by dividing the ratio of firefly luciferase activity to Renilla luciferase activity from cells harboring the plasmid with the mutant AGC codon by the ratio generated with the plasmid with the wild-type codon. **b)** and **c)** fold change in AGC misreading values relative to control (cells not exposed to stress). Values are mean ± SEM of at least four independent experiments.

Mutation of the wild-type AGA (Arg) codon to AGC (Ser) at position 218 represents a decrease of 4 orders of magnitude in the ratio of firefly to *Renilla* luciferase activities (Figure 2.5 b, Control). At low level, restoration of the enzymatic activity can occur

through AGC near-cognate misreading during protein synthesis, allowing reincorporation of an arginine at that location and providing an important tool to quantify translational error rates (Figure 2.5 a) (Rakwalska & Rospert, 2004; Plant et al., 2007). The measured increment in luminescence will be directly proportional to arginine misincorporation at the AGC codon. For each of the strains or stress conditions tested, rates of sense codon misreading were corrected by dividing the F-luc /R-luc activity ratio generated from cells harboring the missense construct by the ratio generated with the control non-inactivated construct (AGA wt codon at position 218 of firefly luciferase). Again, this allowed verifying the theoretical maximal level of expression for the reporter systems and also correction of the misreading values, excluding any pleiotropic effects of mutations or stress on luciferase activity. Results were expressed in relative light units (RLU) (Plant et al., 2007).

Sense codon misreading errors in both *E. coli* and in *S. cerevisiae* occur with an average frequency around 10^{-4} per codon (Stansfield et al., 1998; Salas-Marco & Bedwell, 2005; Kramer & Farabaugh, 2006). However, there is a wide variation in error frequencies between different codons (Kramer & Farabaugh, 2006; Kramer et al., 2010). As already mentioned, the missense reporter used in the current study allowed monitoring a specific near-cognate event responsible for erroneous amino acid incorporation. We observed that none of the stressors tested significantly impacted AGC codon misreading levels (Figure 2.5 b and c), suggesting that the cell has developed very efficient mechanisms to avert near-cognate incorporations.

Arginine misincorporation at AGC involves near-cognate decoding by the $tRNA^{Arg}_{UCU}$. This tRNA has a 5-methylcarbonylmethyluridine (mcm^5U) wobble base produced by the tRNA methyltransferase 9 (Trm9) and known to regulate specific codon-anticodon interactions, conspicuously restricting anticodon pairing (Begley et al., 2007). Nevertheless, $tRNA^{Arg}_{UCU}$ hypomidification by itself was not sufficient to cause a noticeable increment in AGC misreading relatively to the wt strain. Surprisingly, of all the stress conditions tested only exposure to a non-inhibitory lithium concentration significantly affected Δ*trm9* translational accuracy (Figure 2.6 a).

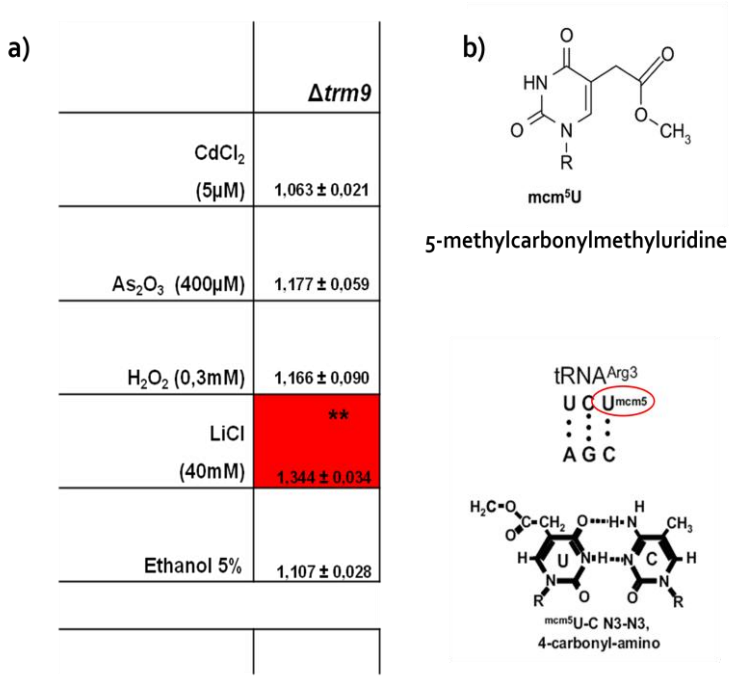

Figure 2.6 - Deficiency in tRNA methyltransferase 9 (Trm9) increases AGC codon misreading by Arg $tRNA_{UCU}$ in cells exposed to lithium. This effect is linked with loss of anticodon pairing restriction by 5-methylcarbonylmethyluridine (mcm^5U). *Δtrm9* cells were transformed with dual luciferase reporters containing either AGA wild-type codon or the AGC codon at position 218 of firefly luciferase, grown to mid-log and exposed to stress for 4h. AGC misreading is expressed in relative light units (RLU). Renilla luciferase activity was used as an internal standard. Rates of misreading were calculated by dividing the ratio of firefly luciferase activity to Renilla luciferase activity from cells harboring the plasmid with the mutant AGC codon by the ratio generated with the plasmid with the wild-type codon. **a)** fold change in AGC misreading values relative to control (cells not exposed to stress). ** represents values significantly different (P<0.01; one-way ANOVA, Dunnett's post-test). Values are mean ± SEM of at least four independent experiments.

2.3.2. Protein homeostasis (proteostasis) and translational accuracy

Evidence of unaltered translation accuracy in the presence of most of the environmental stressors tested drove us to a new approach. Accordingly, we tried to identify and characterize protein homeostasis mechanisms that disguise synthesis of aberrant proteins, potentiating the apparent resistance to stress. Strains harboring

deletions in key genes encoding protein chaperones, components of proteasome activity and autophagy activation were tested. This helped to understand the integrated role of these mechanisms in minimizing the effects of stress on the translational machinery, mostly by preventing the ensuing buildup of misfolded proteins.

Yeast Δ*atg5*, Δ*rpn4*, Δ*bre5*, Δ*hsp26*, Δ*hsp42*, Δ*hsp104*, Δ*hsp12* and Δ*ssb1/ssb2*, Δ*yap1/yap2* mutant cells transformed with the readthrough or with the sense codon misreading reporter plasmid were exposed to stressors as mentioned previously. Again, Arsenic (As), Cadmium (Cd), Ethanol, Caffeine and H_2O_2 induced a decrease in cell growth between 40 – 60% and a viability loss lower than 20%. Concentrations of lithium (Li) and mercury (Hg) produced no significant effect in viability or growth rate. The exceptions were Δ*bre5* and Δ*yap1/yap2* cells, which showed a higher susceptibility to environmental stress. H_2O_2 exposure caused a 70% growth and viability decrease in Δ*yap1/yap2* cells (see Figure A2 and A3, Annexes).

Table 2.4 - Proteome quality control impairment is associated with increased levels of UAA readthrough under environmental stress. Deletion mutant cells were transformed with dual luciferase reporter and exposed to stress for 4h. The ratio of firefly to renilla luciferase activity is a measure of UAA stop codon readthrough and is expressed in relative light units (RLU). For each stress condition, readhtrought values were normalized with the firefly to renilla luciferase activity ratio measured in a strain that carried a sense codon in place of UAA. The fold changes in readthrough under stress are calculated relative to the basal level of readthrough measured in the corresponding strain. *, ** and *** represent values significantly different from the control (P <0.05, P<0.01 and P<0.001, respectively; one-way ANOVA, Dunnett's post-test). Values are mean ± SEM of at least four independent experiments done in triplicate. ▶

Table 2.4 ▶

	Δatg5	*Δrpn4*	*Δbre5*	*Δhsp26*	*Δhsp42*	*Δhsp104*	*Δhsp12*
As_2O_3 (400µM)	1,334 ± 0,094 **	1,001 ± 0,219	1,375 ± 0,078 *	1.117 ± 0.179	1.092 ± 0.099	1,427 ± 0,163 **	1,273 ± 0,027 **
$CdCl_2$ (5µM)	1,025 ± 0,093	1,240 ± 0,040 *	1,007 ± 0,087	0.876 ± 0.051	0.819 ± 0.034	1,297 ± 0,030 **	1,154 ± 0,027
$HgCl_2$ (25µM)	1,076 ± 0,043	0,880 ± 0,052	1,163 ± 0,233	0,998 ± 0,067	1,010 ± 0,115	1,267 ± 0,146	1,446 ± 0,119 **
H_2O_2 (0,3mM)	0,965 ± 0,043	1,194 ± 0,025	0,998 ± 0,067	1.042 ± 0,029	0,920 ± 0,067	0,879 ± 0,030	1,071 ± 0,069
LiCl (40mM)	1,287 ± 0,030 **	1,074 ± 0,054	1,188 ± 0,025	1,011 ± 0,053	1,151 ± 0,042	1,420 ± 0,123 *	1,259 ± 0,061 *
Ethanol 5%	1,195 ± 0,044 *	1,340 ± 0,064 ***	1,425 ± 0,080 *	1.279 ± 0.056 *	1,225 ± 0.081	1,314 ± 0,030 *	1,238 ± 0,094 *
Caffeine (8mM)	0,982 ± 0,049	0,958 ± 0,067	0,916 ± 0,050	0.930 ± 0.065	0,913 ± 0,034	0,948 ± 0,044	1,081 ± 0,060

In deletion mutants, the amount of mistranslated proteins was not significantly increased over the levels measured in BY4743 cells. However, under stress conditions F-luc activity increases in Δ*rpn4*, Δ*hsp104* and mostly in Δ*hsp12* mutant cells, both due to readthrough and AGC misreading. Readthrough is specially related with ethanol, arsenic and lithium exposure but AGC misreading is particularly noticeable after growth in arsenic (Table 2.4 and 2.5). All the measured fold decreases in translational accuracy under stress were smaller than 1,5 - fold, which means that error rates are efficiently kept between the average general values already reported *in vivo* for *S.cerevisiae*, ranging from approximately 10^{-3} to 10^{-5} per codon (Stansfield et al., 1998; Rakwalska & Rospert, 2004; Salas-Marco & Bedwell, 2005; Plant et al., 2007; Kramer et al., 2010). Cells cope perfectly with this increase in error level and this tolerance is related with closely interconnected and many times redundant surveillance homeostatic mechanisms that buffer the effects of aberrant protein synthesis.

Ssb1/2p yeast chaperones are Hsp70 homologs that by direct interaction with the nascent polypeptide in the ribosome preserve a folding-competent state crucial for achieving translational accuracy (Rakwalska & Rospert, 2004).

Table 2.5 - Δ*hsp12* cells are prone to AGC codon misreading as shown by exposure to environmental stressors. Deletion mutant cells were transformed with the dual luciferase reporters containing either AGA wild-type codon or the AGC codon at position 218 of firefly luciferase, grown to mid-log and exposed to stress for 4h. AGC misreading is expressed in relative light units (RLU). Renilla luciferase activity was used as an internal standard. Rates of misreading were calculated by dividing the ratio of firefly luciferase activity to Renilla luciferase activity from cells harboring the plasmid with the mutant AGC codon by the ratio generated with the plasmid with the wild-type codon. *, ** and *** represent values significantly different from the control ($P < 0.05$, $P<0.01$ and $P<0.001$, respectively; one-way ANOVA, Dunnett's post-test). Values are mean ± SEM of at least four independent experiments done in triplicate. ▶

Table 2.5 ▶

	Δatg5	*Δrpn4*	*Δbre5*	*Δhsp26*	*Δhsp42*	*Δhsp104*	*Δhsp12*
As_2O_3 (400µM)	1,095 ± 0,074	0,937 ± 0,055	1,151 ± 0,044	0,970 ± 0,032	1,451 ± 0,146 *	1,243 ± 0,080 **	1,229 ± 0,034 *
$CdCl_2$ (5µM)	1,023 ± 0,054	1,068 ± 0,054	1,006 ± 0,031	1,108 ± 0,111	1,173 ± 0,043	1,064 ± 0,020	1,100 ± 0,051
$HgCl_2$ (25µM)	1,239 ± 0,110 *	0,994 ± 0,032	0,972 ± 0,030	0,974 ± 0,020	1,012 ± 0,052	0,999 ± 0,029	1,288 ± 0,085 **
H_2O_2 (0,3mM)	1,101 ± 0,084	1,064 ± 0,092	1,080 ± 0,034	0,929 ± 0,050	1,104 ± 0,043	1,033 ± 0,026	1,125 ± 0,042
LiCl (40mM)	1,076 ± 0,031	1,057 ± 0,013	1,267 ± 0,018 *	1,011 ± 0,030	1,173 ± 0,035	1,135 ± 0,059	1,366 ± 0,069 ***
Ethanol 5%	0,922 ± 0,023	0,884 ± 0,067	1,200 ± 0,024 *	1,029 ± 0,027	1,128 ± 0,099	0,871 ± 0,019	1,007 ± 0,024
Caffeine (8mM)	1,104 ± 0,041	1,142 ± 0,067	1,108 ± 0,063	0,892 ± 0,038	0,998 ±0,071	1,097 ± 0,033	1,127 ± 0,041

According to previous studies, Δ*ssb1*/Δ*ssb2* deletion mutants show a 1,2-fold increase in UAG readthrough, although no significant differences were detected in AGC misreading (Rakwalska & Rospert, 2004). Under the stress conditions tested here the synthesis of aberrant proteins in these cells is being further increased by non-lethal concentrations of lithium and mercury (Table 2.6). This observation may suggest a toxicity mechanism for lithium and mercury at least partly centered in the ribosome. Otherwise, it might be the result of changes in cation transport across the plasma membrane (Kim & Craig, 2005).

Table 2.6 - **UGA readthrough levels in measured in Δ*ssb1*/Δ*ssb2* cells under stress.** The fold changes in readthrough under stress are calculated relative to the basal level of readthrough measured in Δ*ssb1*/Δ*ssb2*cells at the corresponding stop codon.

	Δssb1/Δssb2
As_2O_3 (400µM)	1,147 ± 0,051
$CdCl_2$ (5µM)	0,847 ± 0,018
$HgCl_2$ (25µM)	*** 1,288 ± 0,019
H_2O_2 (0,3mM)	0,941 ± 0,024
LiCl (40mM)	* 1,151 ± 0,018
Ethanol 5%	0,871 ± 0,015

Yeast AP-1 (*YAP1*) and Yeast AP-2 (*YAP2*) genes are basic leucine zipper (bZIP) transcription factors, responsible for activation of anti-oxidant genes (Fernandes et al., 1997). Yap1 contributes to the arsenic stress response through the expression of a vacuolar detoxification pathway and by maintenance of the redox homeostasis disturbed by inorganic arsenic compounds (Menezes et al., 2008). Yap1p and Yap2p share high homology as well as some functional overlap, coordinating their gene target expression in order to provide the cell with the ability to cope with stress (Vilela et al., 1998; Rodrigues-Pousada et al., 2010).

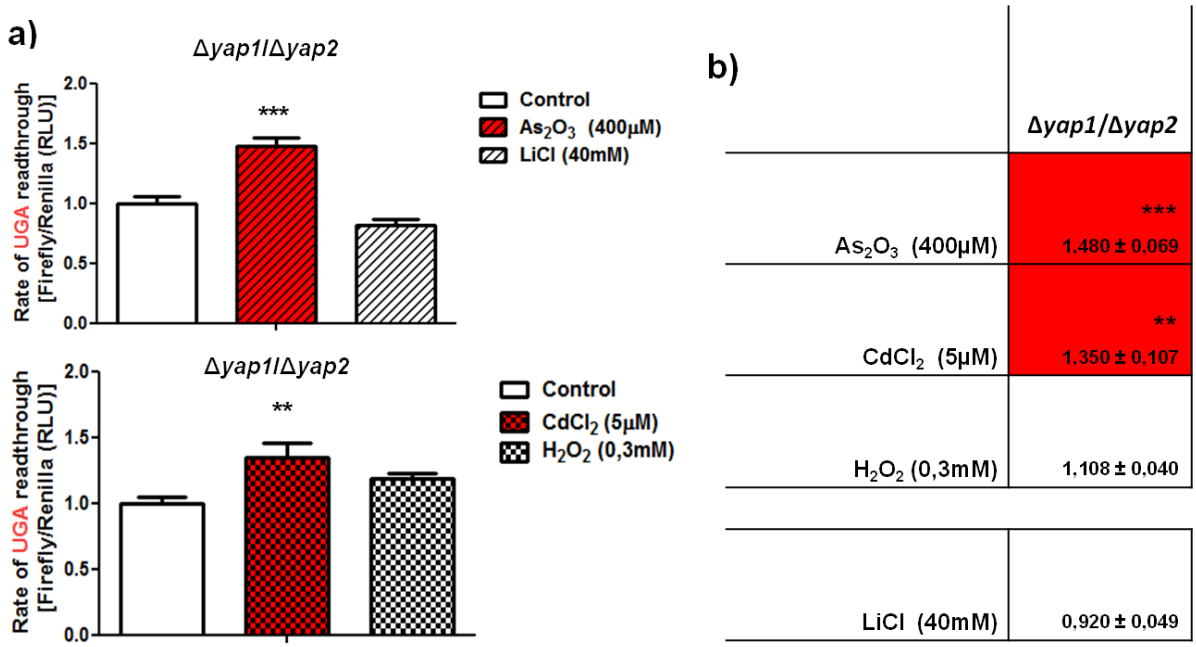

Figure 2.7 - Increased susceptibility to ROS makes cells more prone to UGA readthrough by exposure to environmental stressors. Cells transformed with the AGC misreading reporter or the UGA readthrough reporter were grown to mid-log phase (OD_{600} 0,5-0,6) in MM lacking uracil and exposed to stress for 4h. As depicted previously for these reporter systems the ratio of firefly to renilla luciferase activity is a measure of UGA stop codon readthrough or AGC misreading and is expressed in relative light units (RLU). ** and *** represent values significantly different from the control (P<0.01 and P<0.001, respectively; one-way ANOVA, Dunnett's post-test). Values are mean ± SEM of at least four independent experiments done in triplicate.

Yeast cells bearing disruptions in *YAP1* or *YAP2* genes are viable but show increased susceptibility to oxidative damage. Oxidative stress has the potential to modify the activity of translational machinery components (Avery, 2011) and an increase in reactive oxygen species (ROS) is known to occur in engineered mistranslating cells (Paredes J et al., in press). Prolonged exposure to high arsenic is known to induce severe oxidative damage in several *YAP* mutant cells (Menezes et al., 2008; Wysocki & Tamás, 2010). According to our report, Δ*yap1,2* cells are more prone to UGA readthrough under Cd (II) and As (III) exposure. However, no significant effect on error rates can be attributed to H_2O_2, a major oxidative toxicant (see Figure 2.7). These quite divergent results imply distinct mechanisms of action for each of the stressors, probably not exclusively related with oxidative damage.

2.4. Discussion

Protein synthesis fidelity is essential for life. Therefore, cells devote a considerable amount of time and energy in preserving translational accuracy through proofreading or editing mechanisms and regulation of protein homeostasis (proteostasis), minimizing the deleterious effects of aberrant protein accumulation. The demonstration of a direct link between mRNA mistranslation and chromium toxicity (Holland et al., 2007) prompted us to investigate the role of environmental stress on the accuracy of protein synthesis, both by direct influence on the translational machinery or through impairment of proteostasis mechanisms.

In the current work we examined mistranslation under assorted environmental stress conditions in the yeast model system using a dual luciferase reporter. We selected seven well studied chemicals that possess distinct toxicological effects : Arsenic oxide (As_2O_3), cadmium chloride ($CdCl_2$), ethanol (C_2H_5OH), hydrogen peroxide (H_2O_2), lithium chloride (LiCl), mercury chloride ($HgCl_2$) and caffeine ($C_8H_{10}N_4O_2$). According to the colony-forming unit (CFU) assays performed, the stress conditions tested were not causing significant cell death. This allowed us to abolish pleiotropic effects that

could arise due to viability loss. Concentrations of As (III), Cd (II), Ethanol, Caffeine and H_2O_2 induced a decrease in cell growth between 40 – 60% (see Figure 2.2 and A3 supplementary results). Such values imply a significant protein synthesis decrease and might probably cause an underestimation in error measurements Concentrations of Li^+ and mercury Hg (II) were non-inhibitory (less than 10%). Both the toxicity phenotypes and the transcriptional response of yeast exposure to each one of these toxics have already been broadly studied (Dichtl et al., 1997; Valko et al., 2005; Kuranda et al., 2006; Thorsen et al., 2009; Stanley et al., 2010), however much information is still lacking on their complete mechanisms of action.

2.4.1. Efficiency of dual luciferase reporters

The dual luciferase reporter system is composed of tandem *Renilla* and firefly luciferase genes encoding a single bifunctional protein. The relative abundance of these light-emitting proteins allows monitoring translational efficiency. The activity of the distal firefly luciferase provides a quantitative measure of error and the activity of *Renilla* luciferase serves as an internal control for mRNA abundance. For example, it was previously revealed that the recognition of a premature stop codon induces Nonsense-mediated decay (NMD) and results in a decrease in the rate of translation initiation (Muhlrad & Parker, 1999). However, in our system expression of both R-luc and F-luc is initiated from the same AUG codon and so this effect could not influence the corrected readthrough results.

Although a highly efficient and sensitive method for mistranslation quantification, dual luciferase reporters are codon specific and therefore average only a fraction of all potential translational errors. For these reason we carried our study using simultaneously three different reporters that allowed measuring both stop codon readthrough and sense codon misreading. Even so, many distinct mistranslating events have been excluded from this quantification analysis, underestimation global error rate and overlooking the specific effects of context or codon identity, limiting

the applicability of these conclusions to a limited and yet undetermined number of events in yeast.

Since this study was based on increasing enzymatic activity as an indication of error it is necessarily indirect and consequently our measurements could result from errors at different steps in gene expression. Therefore, enzyme activity can be the outcome of transcriptional errors or, specifically in the case of the misreading reporter, misacylation events. Transcriptional errors are estimated to occur around an order of magnitude below the translational observed frequency, making their detection virtually impossible by the dual luciferase enzymatic system. On the other hand, environmental oxidative stress conditions have been linked to changes in the activity of MetRS, resulting in tRNA misacylation and a concomitant increase in the methionine content of proteins (Netzer N et al., 2009). So far this phenomenon has not been attributed to any other aaRS and therefore, for example, the measured arginine misincorporation at an AGC codon is most probably related with near-cognate tRNA misreading in the ribosome.

2.4.2. Stop codon readthrough

Suppression of stop codons results in protein extension, an event that might lead to cellular toxicity or, on the other hand, act as a regulator of protein expression by expanding the range of polypeptides encoded and introducing new protein functions. In BY4743 cells UAA readthrough is not significantly increased under the stress conditions tested. UAA is the stop codon preferentially used in highly expressed genes of *E.coli* and yeast and this positive discrimination is probably related with its intrinsic low leakiness (Liang et al., 2005; Keeling et al., 2004). Indeed, the error prone UGA codon is the least frequent termination signal, probably due to the fact that it can be decoded by the near-cognate $tRNA^{Trp}$, as already confirmed *in vitro* (Parker, 1989).

Context is a key modulator of termination efficiency. In yeast, the identity of the tetranucleotide termination signal, containing the stop codon and the first

downstream nucleotide (Bonetti et al., 1995; Poole et al., 1998) is critical for stop recognition by release factors. UGA and UAA termination efficiency is influenced by the first downstream nucleotide in the order (from most efficient to least efficient) G > U > A > C. Therefore, the UAA C or a UGA C reporters used in this study allowed in principal to more easily disclose the potential influence of environmental stress on stop codon readthrough. Nevertheless, choosing a poorly efficient context was not enough to amplify UAA readthrough under stress, at least not to levels detectable with the dual luciferase system. However, UGA readthrough was increased in the presence of 5% ethanol (1,360±0,140) (Figure 2.4). Taking in consideration the pleiotropic effects of ethanol, a number of distinct mechanisms might be behind this outcome.

Ethanol is one of the major end products of yeast fermentation. Although *S. cerevisiae* is highly ethanol tolerant, high ethanol concentrations can have toxic effects, limiting cell growth and viability (Aguilera et al., 2006; Stanley et al., 2010). The predominant targets of ethanol are membrane structure and function (Stanley et al., 2010). Yeast exposure to ethanol results in increased membrane fluidity with a concomitant decrease in integrity (Mishra & Prased, 1989; Swan TM & Watson K, 1997). However, yeast cells have evolved several resistance mechanisms against ethanol. Yeast survival and growth under ethanol stress is achieved through complex signal transduction pathways that result in deep gene expression adjustments (Gasch AP, 2002). Ethanol exposure increases the expression of genes linked with energy production, namely genes associated with glycolysis and mitochondrial function, necessary to fuel a costly stress response. Also, vacuole function is of major importantance for ethanol tolerance, probably allowing protein turnover and maintenance of ion homoeostasis (Stanley et al., 2010).

Ethanol has previously been observed to reduce fidelity of poli (U) translation in rat brain cell-free extract and termination efficiency in cultured human amnion cells. In agreement to our results, this termination effect is more pronounced when the stop codon is UGA (Laughrea et al., 1984; Sogaard et al., 1999). This propensity for UGA

readthrough under the influence of ethanol is thought to reflect a greater tendency for the translational machinery to misread the third base of the stop codon. Some explanations can be presented for this fact. First, ethanol is less polar than water and therefore has a lower dielectric constant. This might stabilize the aa-tRNA-codon-ribosome complex, favoring misreading. Also, the low dielectric constants of ethanol can reduce the solvation of Mg^{2+} ions, resulting in a more effective neutralization of the phosphate backbones of the codon-anticodon complex. The repulsion between the phosphates would then decrease causing an additional stabilization of the codon-anticodon interaction and further increasing misreading (Glukhova et al., 1975; Laughrea et al., 1984).

Yeast strains overexpressing tryptophan biosynthesis genes showed enhanced tolerance to 5% ethanol. The addition of tryptophan to the culture medium had a similar effect. Furthermore, other studies have established a connection between amino acid biosynthesis, transport and ethanol stress tolerance. In fact, ethanol might be affecting the delivery of amino acids into the cell, probably by causing the disruption of membrane function (Pham & Wright, 2008; Yoshikawa et al., 2009). Ultimately, we can speculate that this might be causing depletion of specific amino acid pools, altering the competition between cognate and non-cognate aminoacyl-tRNAs during translation. As already described elsewhere this amino acid unbalance can result in loss of accuracy (Farabaugh & Björk, 1999; Sørensen, 2001). Further work is needed to test this hypothesis.

2.4.3. AGC codon misreading

AGC is in theory a particularly error-prone codon (Plant et al., 2007). Recent evidences in *E. coli* suggest that codon bias evolved in order to reduce the costs of both missense and nonsense errors, minimizing the deleterious effects of aberrant decoding (Najafabadi et al., 2007). Accordingly, AGC codons in highly expressed yeast genes correspond to less than 2% of the total Ser incorporated. Misreading error rate is also

influenced by competition between cognate and near-cognate tRNA species (Kramer & Farabaugh, 2006). In fact, codons with higher levels of misreading are decoded by lower abundance tRNAs while the more accurate codons are decoded by more abundant tRNAs. In yeast, tRNA abundance correlates closely with tRNA gene copy number. As expected from an error-prone codon, AGC is decoded by a low abundance $tRNA^{Ser}_{AGC}$ (4 copies).

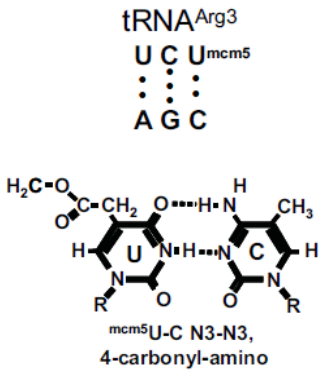

Figure 2.8 - Near-cognate codon-anticodon interactions between AGC codons and the highly abundant $tRNA^{Arg}_{AGA}$.

Finally, it is also essential to take in consideration the specific characteristics of the interaction between AGC codons and the highly abundant $tRNA^{Arg}_{AGA}$ that might promote near-cognate misreading. The first two bases of the AGC Ser codon can be recognized by the mcm^5UCU anticodon of this arginyl-tRNA. Quite remarkably, base pairing at the wobble positions is also possible through a N3-N3, 4- carbonyl-amino hydrogen bonding, providing the transient formation of a very stable mRNA:tRNA mini-helix (Lim et al., 2005; Plant et al., 2007) (Figure 2.8).

Efficiency of translation can be modulated by covalent modification of nucleosides in the anticodon of tRNAs, especially at position 34 (wobble position) and position 37. In yeast, 25% of the cytosolic tRNA species are covalently modified with either 5 - carbamoylmethyl (ncm^5) or 5 - methoxycarbonylmethyl (mcm^5) added to the 59

carbon of U34. tRNA species containing mcm^5 usually decode codon boxes containing pyrimidine and purine-ending codons that correspond to different amino acids, like in the case of $tRNA^{Arg}_{UCU}$. So far, presence of these covalent modifications at the wobble position is known to improve reading of A- or G-ending codons and restrict the remaining codon-anticodon interactions, thereby assuring the fidelity of translation (Huang et al., 2005; Johansson et al., 2008). Therefore, unmodified yeast $tRNA^{Arg}_{UCU}$ recognizes both AGA and AGG and has a higher chance of misreading codons ending with U or C, whereas the mcm^5U34 modification greatly restricts recognition to the AGA codon.

Synthesis of mcm^5U occurs by a complex mechanism that requires at first components the Elongator complex and culminates in methyl esterification of cm^5 by the Trm9p/Trm112p complex. Remarkably, the Elongator complex can also be found associated with RNA polymerase II and it is thought to be involved in the switch from transcription initiation to elongation (Krogan & Greenblatt, 2001).
Deletion of the *TRM9* gene results in complete loss of these modified wobble bases and increased sensitivity at 37°C to paromomycin. These results suggest a role for mcm^5U under stress (Kalhor & Clarke, 2003). Surprisingly, Δ*trm9* cells do not show a decrease in the level of tRNAs, suggesting that $tRNA^{Arg}_{UCU}$ is not degraded like most tRNAs undermodified at other positions (Jablonowski et al., 2006). Since AGC misreading rates in Δ*trm9* cells remain largely unchanged after stress exposure, it is likely that besides wobble modification additional mechanisms are tightly regulating AGC reading. A noticeable effect was however observed following growth under non-inhibitory concentrations of LiCl.

Lithium is not an essential element in nature and has low environmental toxicity. However, it is known to profoundly influence the development of various organisms. For example, it inhibits the formation of the dorsal–ventral axis in *Xenopus laevis* embryos and affects pattern formation in the unicellular ciliate *Tetrahymena thermophila*. It has been proposed that this effect of lithium on development is related to inhibition of RNA processing enzymes (RNA processing defects) (Dichtl et al., 1997).

Even at millimolar concentrations Li^{+} can also inhibit the activity of major phosphatases (Hal2 family) as well as sulphotransferases (Murguía et al., 1996). In fact, in a cellular environment, lithium interacts with sodium and potassium binding sites and affects the activity of Mg^{2+} containing enzymes by competitively displacing Mg^{2+} from its binding site (Csutora et al., 2005). Lithium may also interfere directly with the translation process. Divalent metal ions are vital for the functional integrity of RNAs, either structurally or by involvement in catalytic functions. Ribosome activity is also dependent on the presence of divalent metal ions and Mg^{2+} ions have functional significance for the translational machinery probably being involved in the catalysis of the peptidyl transfer reaction (Winter et al., 1997; Dorner et al., 2005). *In vitro* evidences also suggest that the binding of aminoacyl-tRNA to ribosomes is inhibited by relatively high concentrations of lithium (0,2 – 0,5M) (Suzuka & Kaji, 1968). Therefore, one might hypothesize that $tRNA^{Arg}_{UCU}$ wobble hipomodification in Δ*trm9* cells lowers the lithium concentration responsible for decoding interference in the ribosome to values as low as 40mM.

2.4.4. Mistranslation and protein homeostasis mechanisms

Translational errors are reported to occur at a lower rate in yeast than in *E.coli*, mostly in low-usage codons (Stansfield et al., 1998; Kramer et al., 2010). This strongly suggests that the eukaryotic translational machinery evolved for enhanced protein synthesis accuracy. In this work we report a remarkable resistance of the eukaryotic translational machinery to environmental stress. Notably, yeast has evolved highly efficient mechanisms that not only boost accuracy at the translational level but also operate in *trans* as an integrated network to reduce the cellular impact of aberrant protein synthesis. Therefore, our major goal was to untangle the complex integration of protein homeostasis mechanisms acting in the outcome of protein synthesis under stress conditions. This allowed a more precise quantification of the actual effects exerted by environmental stress on translational machinery.

In yeast, the Environmental Stress Response (ESR) is activated for protection against environmental stress. This program includes a very coordinated change in gene expression and the recruitment of protein homeostasis effectors as a strategy for adaptation after a shift to an unfavorable environment (Gasch et al., 2000). The protein homeostasis genes studied here (*ATG5*, *RPN4*, *BRE5*, *HSP26*, *HSP42*, *HSP104*, *HSP12* AND *SSB1, SSB2*, *YAP1, YAP2*) are quite frequently featured as part of the ESR under many different negative stimuli. In accordance with this observation, it is not surprising that deletion of each one of the mentioned genes results in reduced resistance to many of the stress conditions approached along this work. Under these conditions the function of the vacant chaperones and degradation mechanisms is more easily saturated.

Hsp70 homolog Ssb1/2p chaperones are anchored to ribosomes and interact directly with nascent polypeptides by helping in native stabilization of nascent chains under both physiological or stress conditions and allowing their passage through the ribosome. Ssa1 and 2 are constitutively expressed and share 98% amino acid identity. In addition, over half of the non identical residues are conservative substitutions (Nelson et al., 1992; Mayer & Bukau, 1998; Sharma & Masison, 2008). Strains lacking Ssb1/2p are viable but have a low number of translating ribosomes, growing very slowly, and present a cold-sensitive phenotype (Craig & Jacobsen, 1985).

Tanslational accuracy is decreased in Δ*ssb1*/Δ*ssb2* yeast mutants, an effect strongly enhanced by paromomycin (Rakwalska & Rospert, 2004). Although Ssb1/2p chaperones are associated with the ribosome their location is quite distant from the decoding center. Therefore, the influence exerted on protein synthesis accuracy must be due to an unknown indirect effect that probably decrease the functional availability of key proteins directly involved in translational fidelity and cellular integrity.
Our experimental observations are in agreement with these results and go further by showing that the amount of erroneously synthesized proteins is significantly increased in Δ*ssb1*/Δ*ssb2* yeast mutants under exposure to both lithium and mercury (Figure 2.6). As already mentioned, lithium influence on translation accuracy is

potentially related with interference in RNA processing and ribosome integrity as well as inhibition of Mg^{2+} containing enzymes. Mercury atoms are known to link covalently with a small number of ribosomal proteins but no correlation has ever been established with decoding efficiency. On the other hand, mercury has been linked with an increase in ROS by depleting free-radical scavengers such as glutathione (GSH) and protein-bound sulphydryl groups (Stohs & Bagchi, 1995; Ercal N et al., 2001). GSH depletion can then change the redox environment and impair the activities of GSH-dependent enzymes, such as glutathione peroxidases and glutathione S-transferases, affecting innumerous cellular processes. These conditions might potentiate protein misfolding and loss of function eventually affecting proteins involved the mechanisms of translation.

Due to the low number of translating ribosomes found in Δ*ssb1,2* cells and the inhibitory effect of stress on translation, the amount of protein synthesized during the 4h period of toxic exposure is probably low. Therefore, the error rates under stress might be underestimated.

Atg5p, Rpn4p and Hsp104p are not though to directly interact with the decoding center of the ribosome. Therefore, the influence that gene deletions exerted on protein synthesis accuracy is indirect, probably due to a decrease in the degradative and folding cellular capacity. Due to an existing intricate network of cooperative and redundant protein homeostasis mechanisms (Drummond & Wilke, 2009; Tyedmers et al., 2010; Gidalevitz et al., 2011), the lack of each of these proteins *per se* is not enough to influence global translational error rate. However, the exposure to stress is obviously increasing the cellular burden caused by misfolded protein accumulation and aggregation, eventually exceeding the already wekened buffering capacity of proteome quality control mechanisms. Over time, this will most likely free mistranslated protein into the cytoplasm and decrease the availability of functional key factors directly involved in maintaining protein synthesis fidelity. A deeper analysis of protein homeostasis regulation and functional redundancy influencing translational error would required the construction of double or triple gene deletion mutants, encompassing numerous of the processes highlighted above. However, due

to the essential nature of many of these connections, it is difficult to predict if many of these strains would be viable.

Surprisingly, Δ*hsp12* mutants stood-out in our measurements, showing decreased protein synthesis accuracy under various stress conditions. This susceptibility seems however hard to explain in light of the present knowledge on this chaperone. Hsp12p is only weakly expressed during exponential growth cultures but is induced 100-fold during entry into stationary phase and also by heat shock (Praekelt & Meacock, 1990). Interestingly, *HSP12* is one of the most upregulated Hsps in yeast, particularly in presence of high ethanol concentrations, glucose starvation or cell wall stress (Jamieson et al., 1994; Varela et al., 1995; Kandror et al., 2004). However, Hsp12p exhibits only limited sequence homology with other sHsps (Hsp42 and Hsp26) and is both structurally and functionally very different. Unlike all other Hsps, Hsp12 is a natively unfolded protein in the cytoplasm and becomes structured when it interacts with the plasma membrane, adopting a helical structure and making cells more resistant to breakage. However, its biochemical function is still largely unknown.
It is thought that its plasma membrane association might help in modulating membrane fluidity and stability under stress but without causing any detectable changes in the lipid composition of yeast cells (Welker et al., 2010). It is therefore possible to hypothesize that deletion of *HSP12* might influence the activity of plasma membrane proteins, namely ionic channels and amino acid transporters, also increasing the permeability to toxicants. For example, alterations in the relative concentration of the amino acid pools are known to increase tRNA mischarging levels and lessen the effectiveness of editing mechanisms in aaRSs (Ling & Söll, 2010). Hsp12 also has an important role as a Hog1 MAP kinase target. Besides the response to osmotic stress and activation of cell wall integrity pathways, Hog1 is also known to mediate the cellular response to late stage ER stress. Under extreme and persistent stress conditions, UPR activation is not sufficient to alleviate stress and unfolded proteins start to accumulate in the endoplasmic reticulum (ER). At this point, Hog1 MAP kinase becomes phosphorylated, translocates into the nucleus and regulates

gene expression in order to allow the ER to recover homeostasis (Bicknell et al., 2010). Among the induced genes are key autophagy components and *HSP12*.

In conclusion, environmental stress might influence accuracy by directly targeting the translational machinery, by simply shifting the protein homeostasis balance, or both. However, the available mechanistic details are still poorly understood.

Like Hg (II), Cd (II) is not a redox metal and has no participation in Fenton reactions (Stohs & Bagchi, 1995; Ercal N et al., 2001). However, even though Cd (II) cannot generate ROS directly, it might still induce oxidative damage by depleting free-radical scavengers such as glutathione (GSH) and protein-bound sulphydryl groups. Some evidences seem to argue against GSH depletion as a major Cd (II) toxicity mechanism in *S. cerevisiae*, since the metal concentrations necessary to significantly deplete cytosolic GSH are extremely high. Finally, Cd can also displace zinc from metalloproteins and cause the misfolding of Cu,Zn-superoxide dismutase (Sod1) protein, an abundant cytosolic enzyme that scavenges superoxide anions, altering its catalytic mechanism (Huang et al., 2006). Thereby, in cells particularly susceptible to oxidative damage, Cd (II) might be disturbing a number of vital cellular processes, causing a decrease in translational accuracy. In addition, the effects of Cd (II) - induced ROS might also target protein translation directly, by impacting the translation initiation factor eIF4E in human cell lines (Othumpangat et al., 2005).

Arsenic [As (III)] – the most toxic form of As – inhibits major enzymatic functions through sulfhydryl group binding (Bergquist et al., 2009). Arsenic exposure causes morphologic changes in mitochondrial integrity and a concomitant decline of mitochondrial membrane potential. These mitochondrial alterations can be somewhat responsible for the generation of reactive oxygen species (ROS), most specifically superoxide anion. This effect might however to be exacerbate by a decrease in glutathione production and by As (III) ability to mediate iron release from the iron storage protein ferritin (Salnikow & Zhitkovich, 2008). Free iron catalyses the decomposition of hydrogen peroxide via the Fenton reaction, causing formation of hydroxyl radical (Jomova et al., 2011). Remarkably, after a prolonged toxic exposure, As (III) is found preferentially associated with ribosomes of human bladder epithelium

cells. Therefore, it might be possible that protein synthesis machinery itself is targeted by As (III) (Dopp et al., 2008).

Chapter 3

Proteome quality control systems in the cellular response to mistranslation

3.1. Introduction

3.1.1. Physiological and evolutionary consequences of protein aggregation

Cell growth and adaptation are determined by the speed and accuracy of translation. Alterations in the primary structure of proteins caused by mutation or translational misincorporation are energetically expensive, leading to misfolding and to a subsequent loss of protein function (Buchberger A et al., 2010). At the basal error rate, protein quality control systems successfully maintain a stable proteome through the synthesis of chaperone and other cooperative systems that seize, refold, and degrade existing misfolded substrates before they can exert any negative impact on cellular processes (Parsell DA & Lindquist S, 1993). However, both internal and external stress factors might ultimately overwhelm the refolding or degradative capacity of a cell. This eventually culminates in development of protein aggregates, presented as highly toxic species that endanger cellular viability in a concentration-dependent manner (Drummond DA et al., 2005; Drummond DA & Wilke CO, 2008). For example, expression of aggregation-prone proteins in cell culture was shown to culminate in impairment of the ubiquitin proteasome pathway, leading to cellular dysfunction and death in response to aggregation (Bence et al., 2001).

The impact of protein aggregation can be particularly severe in membranes. Protein-membrane aggregation disturbs membrane integrity (Kourie & Henry, 2002; Stefani M & Dobson CM, 2003) probably through an initial electrostatic interaction, followed by structural changes that promote phospholipid insertion of exposed hydrophobic regions. This results in membrane permeability changes and is known to affect crucial ionic balances (e.g. Ca^{2+}), influencing mitochondrial functionality, redox balances or even apoptotic signaling mechanisms (Cecchi et al., 2005; Stefani M., 2007).
Misfolding leading to protein loss of function and aggregation has been linked to human disease. For example, mutations that affect the folding of the cystic fibrosis transmembrane conductance regulator (CFTR) impair the transport of this protein to

the plasma membrane, resulting in cystic fibrosis (Stefani M., 2004). Also, toxic deposits of fibrillar protein aggregates found as intracellular inclusions or extracellular plaques (amyloid) are a common trait in neurodegenerative diseases such as Alzheimer's disease (AD), Parkinson's disease (PD), Huntington's disease (HD) and amyotrophic lateral sclerosis (ALS) (Ross & Poirier, 2004). The onset of most amyloid diseases in humans is rather late, suggesting that the quality control machinery is very efficient in maintaining homeostatic balance throughout most of the life of the organism. However, factors like genetic mutations, stress, or the aging-induced decline in surveillance by the folding and degradation machineries, eventually yield catastrophic consequences for cell viability (McClellan et al., 2005).

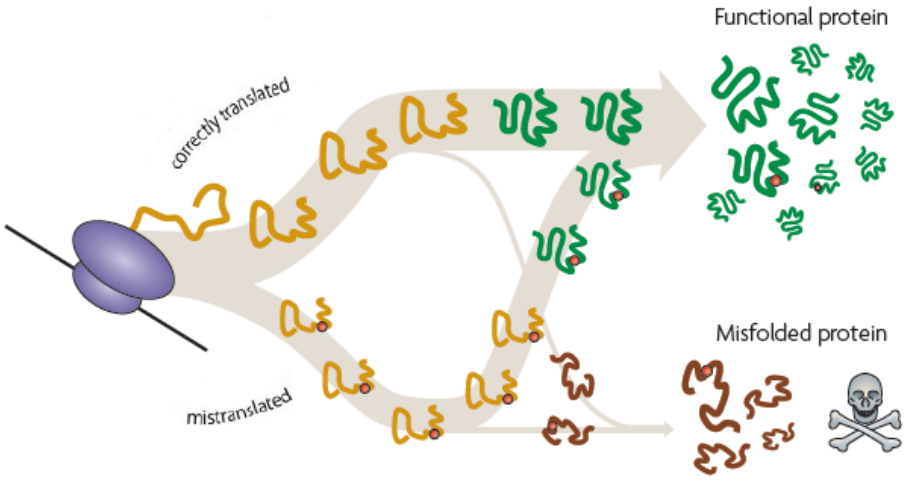

Figure 3.1 – Evolution favored protein robustness by discriminating against the huge cost of misfolded proteins. mRNA translated without errors produces mostly correctly folded protein. However, even under error-prone conditions highly expressed proteins can tolerate a broad range of amino acid substitutions (red dots) before losing their native folding and function (Adapted from Drummond, 2009).

Protein aggregation is inevitable in cells. At an error rate of 10^{-4} (global error rate), 4–12% of an average-length yeast protein is expected to misfold because of missense errors (Drummond DA & Wilke CO, 2008). Since the abundance of a protein ranges from fewer than 50 to more than 10^6 molecules per cell (Ghaemmaghami et al., 2003), the fitness impact of error-induced misfolding varies widely with the expression level.

Remarkably, highly expressed proteins evolve at rates fundamentally unrelated to their functions and by favoring robust sequences, termodinamically more stable, broadening the range of substitutions a protein can tolerate before misfolding (Bloom et al., 2005; Drummond DA et al., 2005) (see Figure 3.1). Eventually, this causes coding sequences to accumulate non synonymous (amino acid altering) substitutions at a slower rate than synonymous (amino acid preserving) substitutions.

3.1.2. Translational machinery and disease

Diseases can arise from mutations that hamper the function of essential translation machinery components, such tRNAs, amino-acyl-tRNA synthetases or ribosomes and also from alterations in the translation factors and cellular components that control them (Scheper et al., 2007). For example, mutations in the glycyl and tyrosyl -tRNA synthetase genes can trigger neurological disorders such as peripheral neuropathy (CMT), by affecting the activity and location of synthetases in granules within the cell bodies or neurite projections of neuronal cells (Jordanova et al., 2006; Antonellis et al., 2003). A mouse mutation in the editing site of alanyl-tRNA synthetase results in $tRNA^{Ala}$ charging with serine. Although all cells inherit the mutation, Purkinje cells show a degenerative phenotype, mostly due to unfolded protein buildup and formation of protein inclusions. This eventually culminates in apoptotic cell loss and ataxia, probably due to incapacity of Purkinje cells to dilute proteins by cell division (Lee et al., 2006).

Diamond–Blackfan anaemia (DBA) might be related with mutations in components of the 40S ribosomal subunit (ribosomal proteins S19 and S24), responsible for binding to eIF2 (Draptchinskaia et al., 1999; Scheper et al., 2007). Another bone marrow failure syndrome, dyskeratosis congenital (DC), can be linked to mutations in the gene encoding dyskerin (DKC1), a pseudouridine synthase that mediates posttranscriptional modification of ribosomal RNA. This eventually affects regions of the ribosome involved in tRNA and mRNA binding, causing an increase in tumour susceptibility and premature aging (Heiss et al., 1998; Pandolfi, 2004). Remarkably,

$tRNA_i^{Met}$ overexpression due to induction of the Brf1 transcription factor is able to stimulate cell transformation and tumor formation in mice (Marshall et al., 2008).

3.1.3. Environmental stress and the flow of biological information

After an insult, biological homeostasis is maintained through the activation of a large number of response pathways. The onset is driven by changes in secondary modification of multiple signaling effectors and results in adjustment of gene transcription and several metabolic pathways (Gasch AP et al., 2000). Environmental stress exerts a share of influence in the function of essential translation machinery components, with yet unknown effects on protein synthesis accuracy.

In general, tRNA modifications play a pivotal role in enhancing tRNA structure and function by modulating ribosome binding affinity and assuring translation fidelity (Bjork et al., 1999; Motorin & Helm, 2010). Recent findings suggest that individual tRNA modifications and their biosynthetic pathways work as modulators of cell proliferation and cell response to stress. In other words, dynamic reprogramming of tRNA modifications during cellular responses may work as part of a larger mechanism of translational control during the cellular stress response. Cells respond to stress exposure by modifying tRNA structure, enhancing the synthesis of proteins that are critical to cell survival (Agris, 2008; Chan et al., 2010). However, the impact of this biological reprogramming on translational accuracy under stress remains unknown, mostly due to the inherent complexity of the tRNA modification network.

3.1.3.1. Cellular targets for ROS

Reactive oxygen species are generated continuously during aerobic growth and are elevated by a range of different stress conditions, having the potential to cause oxidative deterioration of proteins, lipids, DNA and RNA. Oxidative damage is one of the major causes of aging and age-related diseases and organisms have evolved a

number of strategies to cope with this stress. Responses typically involve the up-regulation of antioxidant proteins, such as ROS-scavenging peroxidases and superoxide dismutases, or enzymes that reverse oxidative damage, such as methionine sulfoxide redutases (Imlay, 2008; Avery SV., 2011). Surprisingly, increased levels of reactive oxygen species result in methionine misincorporation due to tRNA misacylation by a yet unkown mechanism involving the activity of MetRS. Instead of deleterious this is an adaptive mechanism, since Met residues work as ROS scavengers and protect proteins from ROS-mediated damage (Netzer et al., 2009; Jones et al., 2011).

RNA is mostly single-stranded and its bases are scarcely protected by hydrogen bonding and proteins, making it much more susceptible to oxidative stress than DNA (Bregeon & Sarasin, 2005; Nunomura et al., 2006). The oxidation of rRNA, tRNA, and mRNA might impair the integrity of translational processes (Tanaka et al., 2007) resulting in synthesis of aberrant proteins, especially under conditions of saturated quality control (Ding Q et al., 2005), and was recently reported in post-mortem brains of patients with Alzheimer's disease (AD) and Parkinson's disease (PD) (Nunomura et al., 1999; Zhang et al., 1999). Remarkably, rRNA oxidation in neurons and glia is extensively promoted by low-level proteasome inhibition, dramatically altering RNA processing (Ding et al., 2004). Oxidative stress increases cellular dysfunction also by directly targeting proteins that regulate cell structure, cell signaling and various pivotal metabolic processes (Cecarini et al., 2007). Certain proteins are more susceptible to oxidative targeting due their relative content of sensitive amino acid residues, the presence of metal-binding sites, the specific molecular conformation or the rate of degradation. Remarkably, the group of oxidation-sensitive proteins includes mitochondrial proteins, chaperones, members of the ubiquitin-proteasome system and others associated with the energy metabolism (Avery SV., 2011).
Protein oxidation often occurs as an irreversible damage that might result from ROS mediated cleavage of peptide bonds or even from direct metal catalyzed oxidative (MCO) attack on the amino-acid side chains of proline, arginine, lysine and threonine (Nystrom, 2005; Cecarini et al., 2007). Metal-catalyzed oxidation (MCO) of proteins

requires the presence of ions such as Fe (III) or Cu (II) that bind to specific metal binding sites in the protein and react with H_2O_2. This results in generation of hydroxyl radicals that then attack nearby susceptible amino acid residues. Some amino acids might just be directly modified through side chain reactions with ROS, independently of metal ion presence. This group includes amino acids with aromatic or sulfhydryl side chains, which render them particularly susceptible to oxidative damage (Stadtman & Levine, 2003; Cecarini et al., 2007).

One of the major consequences of amino acid oxidation is the production of irreparable carbonyl groups. These carbonylated proteins can be marked for degradation by the proteasome, but many times avoid this destiny and end up forming high molecular weight aggregates that are usually age-related. Aggregation is promoted by carbonyl reactivity towards α- amino groups of lysine residues, which leads to extensive formation of intra- or inter-molecular cross-links (Sohal, 2002; Nystrom, 2005; Cecarini et al., 2007). Parkinson's disease, Alzheimer's disease, cancer, cataractogenesis and diabetes are diseases associated with increased protein carbonylation (Levine, 2002; Dalle-Donne et al., 2003).

The objective of this chapter was to evaluate the impact of misfolded proteins, generated through mistranslation and environmental stress, on components of the translational machinery.

We report that As_3O_2 triggers protein aggregation, with concomitant decrease in the cellular concentration of eRF1/eRF3 available for termination. This phenotype might lead to stop codon readthrough, but does not solely determine it. Deletion of *HSP12* produces a unique tRNA modification pattern under exposure to oxidative damaging concentrations of As_2O_3. Also, cells mistranslating constitutively misacylate various tRNAs with Met, by a yet unknown mechanism.

3.2. Material and methods

3.2.1. Strains and growth conditions

The bacterial strain JM109 (endA1 glnV44 thi-1 relA1 gyrA96 recA1 mcrB$^+$ Δ(lac-proAB) e14- [F' traD36 proAB$^+$ lacI^q lacZΔM15] hsdR17($r_K^-m_K^+$)) was used for plasmid amplification. It was grown at 37°C in Lysogeny Broth (LB) medium (Formedium) or LB 2% agar (Formedium), both supplemented with 50 µg/mL ampicillin (Sigma-Aldrich) when required.

The *S.cerevisiae* strains used in this study and their genotype are specified in Table 3.1.

Table 3.1 – *S.cerevisiae* strains used to study the cellular response to mistranslation.

Strain	Genotype	Source
BY4742	*MATα ; his3Δ 1; leu2Δ 0; lys2Δ 0; ura3Δ 0*	Euroscarf
Δ*rpn4*	BY4742 ; YDL020C::kanMX4/YDL020C::kanMX4	Euroscarf
Δ*hsp104*	BY4742 ; YLL026W::kanMX4/ YLL026W::kanMX4	Euroscarf
Δ*hsp12*	BY4742 ; YFL014W::kanMX4/ YFL014W::kanMX4	Euroscarf
Δ*yap1*	BY4742 ; YML007W::kanMX4	Euroscarf
HSP104 – GFP	BY4742; HSP104-GFP	(Huh WK et al., 2003)
HSP104-GFP- Δ*rpn4*	BY4742; YDL020C::kanMX4; *HSP104-GFP*	This thesis
HSP104-GFP- Δ*hsp12*	BY4742; YFL014W::kanMX4; *HSP104-GFP*	The thesis
HSP104-GFP- Δ*yap1*	BY4742; YML007W::kanMX4; *HSP104-GFP*	This thesis

Yeast cells were cultured at 30°C in rich YPD medium (1% yeast extract, 2% Peptone and 2% Glucose) or selective minimal medium (MM – 0.67% yeast nitrogen base, 2% glucose and 0.2% Drop-out mix, lacking only the amino acids corresponding to the selection markers). Geneticin (G418) (Formedium) was used in deletion strains at a concentration of 200µg/L. Solid media required agar up to 2%. All media were sterilized by autoclave at 120 °C for 15 – 20 min.

3.2.2. Plasmids

The *S.cerevisiae* plasmids used in this study are specified in Table 3.2.

Table 3.2 – Plasmids used to study the cellular response to mistranslation.

Plasmid	Description	Source
pFA6a–GFP–His3MX	Used as PCR template for C-terminal tagging of proteins by GFP at their chromosomal locations. Contains the *S. pombe his5*$^{+}$ gene and permits selection of transformed strains in histidine-free media.	(Wach A et al., 1997)
pUKC815	Single-copy URA3 vector containing *E.coli* lacZ gene under the control of the PGK1 promoter.	(Stansfield I et al., 1998)
pRS315	Single-copy LEU2 vector	(Santos MA et al., 1996)
pUKC715	Single-copy LEU2 vector containing the *C. albicans* G33 Ser-tRNA$_{CAG}$ gene.	(Santos MA et al., 1996)

3.2.3. Yeast transformation by the lithium acetate (LiAc) method

Fresh yeast colonies were picked and grown overnight at 30ºC in YPD rich medium. Overnight cultures were then diluted 1:1000, grown to mid-log phase (OD_{600} ~0,5) and harvested by centrifugation at 4000 rpm. After washing with 5mL of sterile mQ water, the cell pellet was resuspended in 50µL of 0,1M LiAc solution and the following reagents were added in the designated order : 500µL 50% (w/w) PEG, 25µL single-stranded carrier DNA (2mg/mL) previously denatured for 5 min. at 95ºC and 0,1 – 1µg of plasmid (Gietz RD & Woods RA, 2006). Tubes were vortexed immediately until the mixture was homogeneous and then subjected to heat-shock at 42ºC for 45 min. Cells were then harvested by centrifugation at 5000 rpm, supernatants were discarded, pellets resuspended in 100 µL of sterile mQ water and plated in selective media plates that were then incubated at 30ºC until colonies were visible.

3.2.4. Analysis of intracellular levels of cations

Overnight cultures of individual yeast transformants were diluted 100x in MM-Ura, grown at 30°C/180 rpm to mid-log phase (OD_{600} 0,5 – 0,6) and then incubated for 4h in the absence or presence of 400 µM As_2O_3, 125µM $CdCl_2$ and 40mM LiCl. Approximately 20 OD_{600} units of cells were then harvested for each condition, washed plentifully and resuspended in 500µl H_2O mQ. After addition of 1 ml 6M HNO_3, samples were digested for 20 min at 95°C, centrifuged to remove cellular debris and aliquots of the supernatant were analyzed using a flame atomic absorption spectrophotometer (Perkin Elmer AAnalyst 100).

3.2.5. Measurement of Hsp104 – GFP aggregates

3.2.5.1. HSP104 – GFP strain construction

Quantification of Hsp104 aggregates was performed as described previously (Erjavec et al., 2007). PFA6a–GFP (S65T)–His3MX plasmid was used as template to generate gene-specific cassettes containing a C-terminally positioned GFP tag and the *S.pombe* $his5^+$ gene that allows selection of transformed strains in histidine-free media (Wach A et al., 1997; Huh WK et al., 2003). Amplification of the cassette was done by standard PCR with reaction mixes containing 0.2mM dNTPs, 2.5mM of MgCl2, 100 ng of template DNA, 0.04U/µL of Taq polymerase (Fermentas), 1 x Taq buffer (Fermentas) and 1pmol/µL of each of the following primers, designed to share sequence complementarity with the C-terminal coding region of Hsp104 gene:

oUA2403

GACGATAATGAGGACAGTATGGAAATTGATGATGACCTAGATGGTGACGGTGCTGGTTTA

oUA2404

GATTCTTGTTCGAAAGTTTTTAAAAATCACACTATATTAAATCGATGAATTCGAGCTCG

The PCR program started with 2 min. at a temperature of 94°C, followed by 35 cycles with the following parameters: 95°C for 30 sec, 57°C (primers specific annealing

temperature - Tm) for 30 sec and 72ºC for 1 min. A single final incubation was done at 72ºC during 3 min.

The PCR products were purified using QIAquick PCR Purification Kit (according to Qiagen's instructions), quantified using the NanoDrop®1000 Spectrophotometer (Thermo Scientific) and at least 1 µg of DNA were then used for yeast transformation, carried out as described in 3.2.3. After selection of transformants in MM medium lacking histidine, insertion of the cassette by homologous recombination was verified by PCR of individual colonies with a GFP tag internal primer and an ORF-specific primer, designed to produce a product of approximately 500 bp (**0UA2405** - CTTGAACATAACCTTCTGGC and **0UA 2406** - GACTTCTTGGCCAAATATGG).

3.2.5.2. Microscopic imaging of Hsp104 – GFP aggregates

Overnight cultures of cells containing GFP tagged Hsp104p were diluted 1:100 in 5mL MM medium lacking histidine, grown at 30ºC to mid-log phase (OD_{600} 0,5-0,6) and then incubated for 4h in the absence or presence of several non lethal environmental stressors (200 or 400 µM As_3O_2; 5µM $CdCl_2$; 0,1 or 3 mM H_2O_2; 40mM LiCl; 5% ethanol) (Sigma-Aldrich). Cells were recovered by centrifugation, washed and resuspended in 1ml phosphate buffered saline (PBS). Fluorescence was visualized using an Axio Imager Z1 fluorescence microscope (Zeiss) equipped with GFP and brightfield filters, a 63x oil-immersion objective and a camera for image acquisition. Quantification of cells containing aggregates was done with ImageJ (NIH). For each condition, approximately 500 cells were analyzed in 6 different images per biological replicate.

3.2.6. Quantification of insoluble protein

The analysis of protein aggregation was performed as previously described (Rand & Grant, 2006), with several modifications. Equivalent cell numbers (10 A_{600} units) were harvested by centrifugation, washed, and resuspended in 450 µl of lysis buffer (50 mM

potassium phosphate buffer, pH 7, 1 mM EDTA, 5% (v/v) glycerol, 1 mM phenylmethylsulfonyl fluoride, and complete Mini protease inhibitor cocktail (Roche Diagnostics). After addition of 2/3 volume of glass beads (0.5 mm diameter), cells were disrupted using a Precellys homogenizer (Bertin technologies) for 3 × 1 min, with 2 min incubation on ice between each disruption cycle. Cell debris were removed by centrifugation of the crude extract at 5000 rpm at 4°C and for 15 min. 350µl of the resulting supernatant were then removed to a new tube. A 50 µl sample was immediately denatured for 5 min at 95°C in 6x gel loading buffer (50mM Tris-HCl pH 6.8, 100mM DTT, 2% SDS, 0.1% bromophenol blue, 10% glycerol). Aggregated insoluble proteins were isolated from the remaining total protein fraction by centrifugation at 13000 rpm for 20 min. Membrane proteins were removed by washing the resulting pellet with lysis buffer containing 2% Triton X-100. The final pellet was resuspended in 100µl lysis buffer and 6x gel loading buffer, just before denaturing for 5 min. at 95°C.

Total (6µl) and aggregated insoluble protein fractions (35µl) were analyzed under reducing conditions using 15% resolving SDS-polyacrylamide gels (PAGE). Resolving gels were made mixing water, 15% acrylamide/bisacrylamide mix, Tris/HCl pH 8, SDS and ammonium persulfate (APS) together with TEMED to start polymerization. Stacking gels are large pore gels (4% acrylamide) prepared using Tris/HCl pH 6,8 and cast over the resolving polymerized gels to increase the resolution of protein separation. Samples were fractionated in a Bio-Rad electrophoresis apparatus previously filled with running buffer (25mM Tris base, 250mM glycine pH 8.3, and 0.1% SDS) for approximately 2h and 120V. Gels were then removed from the apparatus, stained in a 0,1% coomassie brilliant blue R250 (Sigma-Aldrich) solution (40% ethanol and 15% acetic acid) for 30 min with agitation and immediately distained in a solution of 10% Ethanol / 7,5% Acetic Acid. Gels were visualized and scanned using the ODYSSEY Infrared Imaging System (Li-Cor Biosciences). The intensity of the bands was determined using the Odyssey® 3.0 Application Software. For each condition, the amount of aggregated insoluble protein was normalized with total protein values.

3.2.6.1. eRF1 and eRF3 western blot detection

Total (6µl) and aggregated protein (35µl) fractions were analyzed under reducing conditions by 15% SDS-PAGE and were blotted onto nitrocellulose membranes. The blots were run overnight at 30V, 4ºC in TGM buffer (25mM Tris base, 192mM glycine, 12% methanol) using a Bio-Rad wet transferring system (assembled according to manufacturer's instructions). Nitrocellulose membranes (GE Healthcare) were then blocked in TBS-T (20mM Tris-HCl; 127mM NaCl; 0,1% Tween) with 5% non-fat milk for 1h and incubated for 2h at room temperature with primary antibody diluted in TBS-T 1% non-fat milk (1:200 anti-eRF1 and 1:1000 anti-eRF3). After washing 3 x 10 minutes with TBS-T, bound primary antibody was visualized by incubating for 1 h in the dark with an IRDye680 goat anti-rabbit secondary antibody (Li-Cor Biosciences) at a 1:10000 dilution. Detection was performed using the ODYSSEY Infrared Imaging System (Li-Cor Biosciences). The amount of eRF1 and eRF3 in the insoluble fraction was normalized with the values present in the total fraction.

3.2.7. RNA extraction and tRNA isolation

Yeast cells carrying the pRS315 single-copy plasmid were grown at 30ºC to mid – log phase (OD_{600} ~0,5) in minimal medium (MM) lacking leucine and then incubated for 4h in the absence or presence of several selected non lethal environmental stressors (200 or 400 µM As_3O_2; 40mM LiCl; 5% ethanol) (Sigma-Aldrich). After harvesting, cells were frozen at -80ºC overnight and thawed by resuspending in a 1:1 mixture of lysis buffer (10 mM Tris pH 7,5; 10 mM EDTA; 0,5% SDS) and acid phenol chloroform 5:1 (pH 4,7) (Sigma-Aldrich), vortexing vigorously. Cells were then immediately incubated in a water bath at 65ºC, vortexing again every 10 min. After 1h, RNA aqueous phases were recovered by centrifugation at 8000xg for 30 min at 4ºC and then transferred to new tubes for additional re-extraction steps, first with 4ºC acid phenol chloroform 5:1 (pH 4,7) and then with chloroform Isoamyl Alcohol 24:1 (Fluka). RNA was then precipitated overnight at -30ºC with 3 vol. of ethanol and 0,1 vol. of 3M NaOAc/HOAc

pH 5,2. After harvesting by centrifugation (at 8000xg for 30 min, 4ºC) RNA was washed in 70% ethanol, resuspended in 2 ml of 0,1M NaOAc/HOAc pH 4,5 with 1mM EDTA and stored a -80ºC.

DEAE-cellulose columns equilibrated with the RNA ressuspension were used for tRNA isolation. Total RNA was added to the columns which were then washed with 10 vol. of 0,1 M NaOAc /0,3 M sodium chloride pH 4,5. tRNAs were eluted with 2 vol. of 0,1 M NaOAc /1M sodium chloride pH4,5 and precipitated in 2,5 vol. 100% ethanol overnight at -30ºC, harvested by centrifugation and finally resuspended in 10 mM NaOAc pH 4,5/1 mM EDTA and stored a -80ºC.

3.2.8. Quantification of tRNA modifications

Total tRNA preparations were enzymatically hydrolyzed so that individual modified ribonucleosides could be resolved by HPLC. Identification was then performed by high mass accuracy tandem mass spectrometry (MS/MS), through fragmentation patterns generated with collision-induced dissociation (CID) in a quadrupole time-of-flight mass spectrometer (QTOF – Agilent 6510) with an electrospray ionization source. Nucleosides were also identified by comparison with synthetic standards. For quantification of the previously identified tRNA modifications a HPLC column was coupled to an Agilent 6410 triple quadrupole mass spectrometer with an electrospray ionization source and operated in positive ion mode (LC-QQQ). The method allowed identification of 23 out of the 25 known ribonucleoside modifications of citoplasmic tRNAs from *S. cerevisiae*. Results are expressed as fold change of nucleoside level in cells exposed to stress relatively to levels in non-exposed cells.

These experiments were performed by collaborators in the laboratory of Prof. Peter C. Dedon at the Massachusetts Institute of Technology, Cambridge, Massachusetts, United States of America and according to the previously described protocol (Chan et al., 2010).

3.2.9. Quantification of intracellular reactive oxygen species

Approximately 10^6 yeast cells were harvested by centrifugation, washed and resuspended in PBS, pH 7,4. Cells were then labeled with 15µg/mL dihydrorhodamine 123 (DHR123) (Molecular Probes) (30ºC for 90 min in the dark) or 10µg/mL dihydroethidium (DHE) (Molecular Probes) (30ºC for 10 min in the dark). After washed in PBS, cells were analysed in a flow cytometer for ROS quantification as previously described (Almeida et al., 2007). Cells displaying higher values than a defined threshold of green fluorescence were considered as containing elevated intracellular ROS.

3.2.10. Yeast ^{35}S-Met pulse labeling to test for misacylation

Cells expressing pRS315 or pUKC715 (misreading tRNA) were grown overnight in MM lacking leucine. Overnight cultures were diluted to an initial 0,1 OD_{600} and grown at 30ºC to 0,4 OD_{600}. Approximately 12 OD_{600} units of cells were then harvested for each condition, resuspended in MM lacking leucine/ methionine and incubated for 1h at 30ºC/180rpm. Cells were again collected by centrifugation, resuspended in 300µl labeling medium [MM lacking leucine/ methionine plus 0.25 mCi ^{35}S-Met (PerkinElmer) per sample] and incubated at 30ºC for 1 minute. 300 µl of ice cold 0,3 M NaOAc/HOAc/10 mM EDTA pH 4.8 were then immediately added to the culture. Cells were washed 3 times and finally ressuspended in 300µl ice cold 0,3 M NaOAc/HOAc/10 mM EDTA pH 4,8.

For RNA extraction, cells were transferred to a tube containing 2.8 mm ceramic (zirconium oxide) beads (Precellys, Bertin technologies) and 1 vol. acid phenol chloroform 5:1 equilibrated with NaOAc/HOAc, pH4,8 (mix 1 volume of phenol/$CHCl_3$ with 1/10^{th} volume 5 M NaOAc/HOAc, pH 4.8). Cells were disrupted using a Precellys homogenizer (Bertin technologies) for 4× 1 min, with 2 min incubation on ice between each disruption cycle. The aqueous layer was collected by centrifugation (14,000 rpm, for 15 min. at 4ºC) and transferred again to a tube containing 300µl

phenol/$CHCl_3$/NaOAc/HOAc, pH4.8. The mixture was homogenized by vortexing for 60 seconds. The aqueous layer extraction procedure was then repeated two more times and RNA was finally precipitated in 1 vol isopropanol, at -30°C for 20min, followed by centrifugation (14000 rpm at 4° C for 15min). After resuspending in 100µl ice cold 0,3M NaOAc/HOAc/10 mM EDTA pH 4.8, RNA was again precipitated overnight in 2,7 volumes of 100% ethanol, at -30°C . Finally, RNA was harvested by centrifugation, resuspended in 50µl of 10mM NaOAc/HOAc pH 4.8/1mM EDTA and stored a -80°C. Quantification and RNA quality were accessed using the NanoDrop®1000 Spectrophotometer (Thermo Scientific).

3.2.10.1. tRNA microarray analysis

The procedure for tRNA microarray analysis using radioactive detection has been performed in the laboratory of Prof. Tao Pan at the University Of Chicago, United States Of America, as described in (Netzer et al., 2009; Jones et al., 2011).

A total of 4 arrays were hybridized for each of the selected conditions. In a regular array total RNA (20 µg) is hybridized directly. For a modification control array, total RNA is first deacylated at pH 9 (0.1 M Tris-HCl) for 45 min so that signals from aminoacyl- and peptidyl-tRNAs are eliminated. In a cross-hybridization control array, excess of DNA probes of cytosolic and mitochondrial $tRNA^{Met}$ are included in the hybridization mix. Finally, in a peptidyl-tRNA control array total RNA is treated with aminopeptidase-M at room temperature for 25 min, just before array hybridization, to remove signal from N-term peptidyl-tRNAs.

The array contains 40 nuclear-encoded yeast tRNA probes (orange) and 24 mitochondrial-encoded yeast tRNA probes (blue). In addition, the array includes 1 blank control (yellow) and 31 *E. coli* tRNA probes (green), which serve as negative controls. Each probe has 8 replicates (see Figure A5 in Annexes). For ^{35}S-labeled samples, essentially only *S. cerevisiae* spots showed signal, indicating that the array works well.

Total RNA was hybridized in 2xSSC (30mM tri-Sodium citrate, 0.3M NaCl) pH 4.8 at 60ºC for 50 min using a Hyb4 station (Genomic Solutions). After hybridization, arrays were washed twice in 2xSSC, pH 4.8, 0.1% SDS and then in 0.1xSSC, pH 4.8, dryed and exposed to phosphorimaging plates (FujiMedicals) for up to 14 days. Spot intensity was quantified using Fuji Imager software.

3.2.11. Statistics

Data is reported as mean ± SEM or SD. Significance was tested by one-way ANOVA and t-test (GraphPad Prism 5). Differences are considered significant when $p < 0,05$.

3.3. Results

3.3.1. Cation influx and stress sensitivity

Our previous results exposed translational accuracy defects in Δ*hsp104* but mostly in Δ*hsp12* cells under stress (see section 2.3.2). Both *HSP12* and *HSP104* are amongst the most upregulated genes normally included in the general stress response (Gasch AP et al., 2000). *HSP104* is central for ethanol, arsenite and heat-shock tolerance (Sanchez et al., 1992). *HSP12* is a plasma membrane protein that modulates membrane fluidity and stability under stress conditions (Welker S et al., 2010) and may influence the activity of numerous plasma membrane proteins, namely ionic channels and amino acid transporters.

On the other hand, the cellular toxicity of a metal or metalloid element depends on its uptake mechanism, on the oxidation state, the intracellular distribution and also on the interactions with various macromolecules (Valko M et al., 2005; Summers, 2009; Wysocki R & Tamás MJ, 2010). Due to charge and molecular similarity, toxic metals and metalloids can enter cells through membrane permeases and channels involved in the uptake of essential metals such as Fe, Mn, Zn, and nutrients such as phosphate or sulphate. There is quite limited information on how metal sensing occurs in each of the strains and how this information is translated into suitable cellular responses, by

ultimately influencing translational accuracy. As a first approach, we decided to investigate whether the sensitivity of Δ*hsp104* and Δ*hsp12* cells might be related with increased intracellular levels of cations due to altered plasma membrane transport. However, no differences were observed in intracellular levels of As^{3+}, Cd^{2+} or Li^{+} both in Δ*hsp12* and Δ*hsp104* cells, relatively to BY4742 control cells. Therefore, apparently, the environmental stress effects are not apparently linked with higher accumulation of toxic elements, but most probably with mechanisms more centered on translational machinery factors.

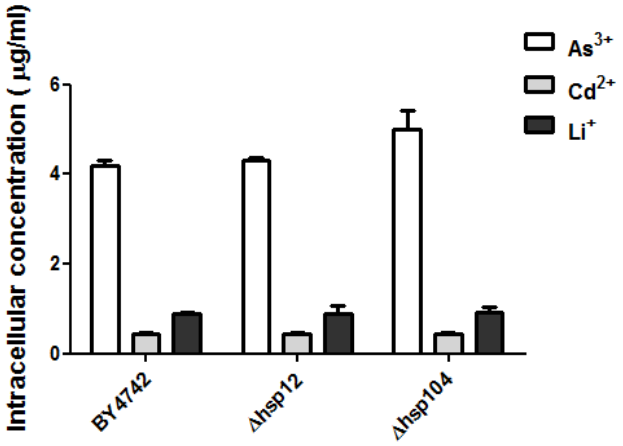

Figure3.2 - Intracellular As^{3+}, Cd^{2+} and Li^{+} concentration is not significantly increased in Δ*hsp12* or Δ*hsp104* cells relatively to wt (BY4742) cells, after 4h treatment of log-phase cultures with 400 µM As_2O_3, 125µM $CdCl_2$ and 40mM LiCl. Cells were washed and lysed as described in section 3.2.4. The concentrations of intracellular cations were measured by atomic absorption spectroscopy. Three independent experiments were performed.

3.3.2. Effects of environmental stress on protein aggregation

Protein aggregation is common in cells but can be exacerbated because of partial unfolding linked to intrinsic and environmental conditions that result in increased ROS production, thereby resulting in protein oxidation and carbonylation, and stress caused by heat, heavy metals and translational misincorporation (Buchberger A et al., 2010). Under these conditions, the accumulation of damaged proteins can perturb cellular homeostasis eventually affecting mechanisms involved in translational accuracy.

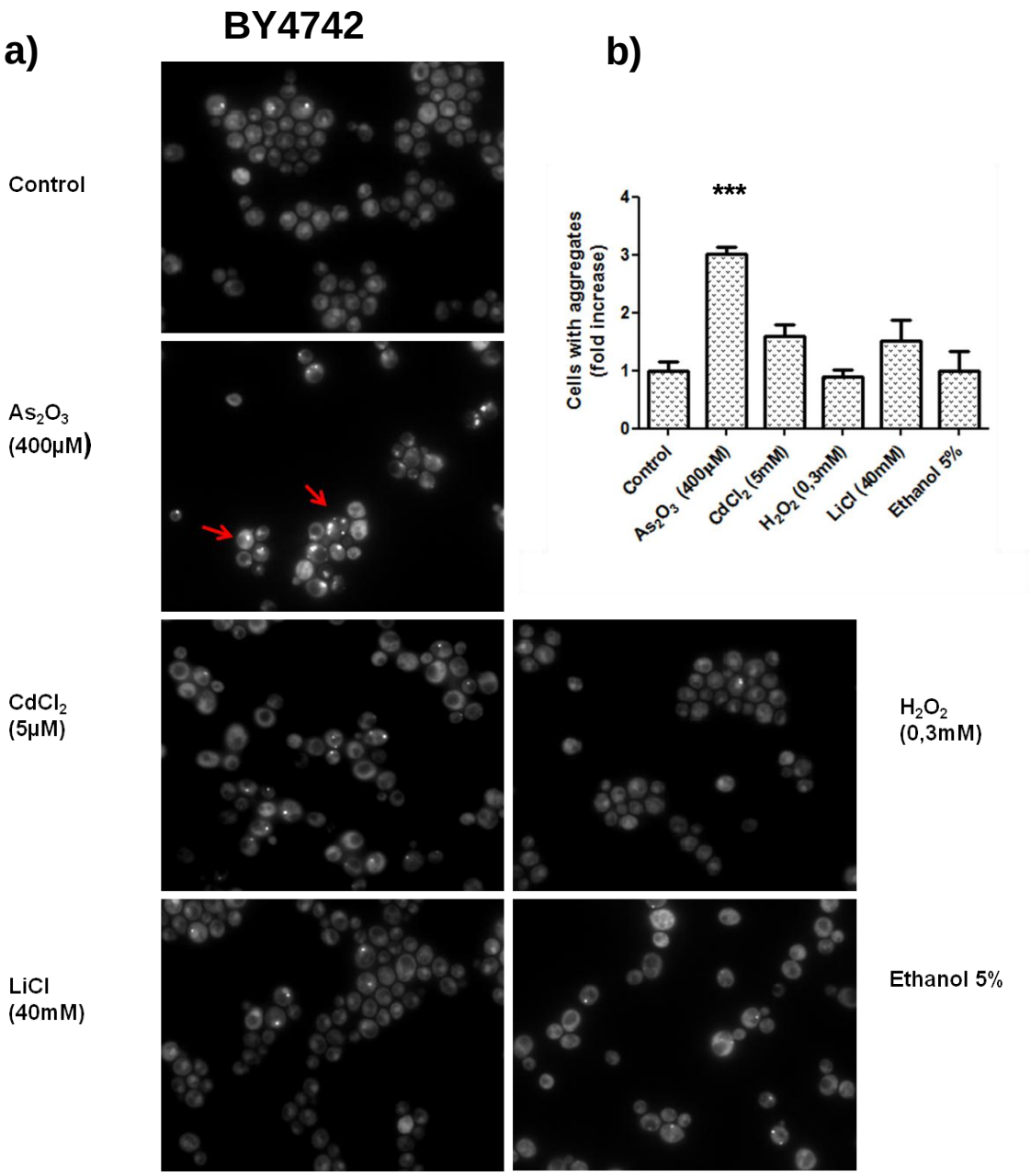

Figure 3.3 – Environmental oxidative stressors are linked to an increase in Hsp104-containing aggregates. BY4742 yeast cells labeled with an Hsp104 – GFP reporter were grown to mid-log and exposed to stress for 4h. a) Red arrows show the distribution of Hsp104-GFP agreggates in the cytoplasm as monitored by epifluorescence microscopy b) quantification of cells with Hsp104-GFP aggregates. *** ($P<0.001$) represents values significantly different from the control - cells not exposed to environmental stressors – (one-way ANOVA, Dunnett's post-test). Values are mean ± SEM. Approximately 500 cells were analyzed in 6 different images for each condition. Three independent experiments were performed.

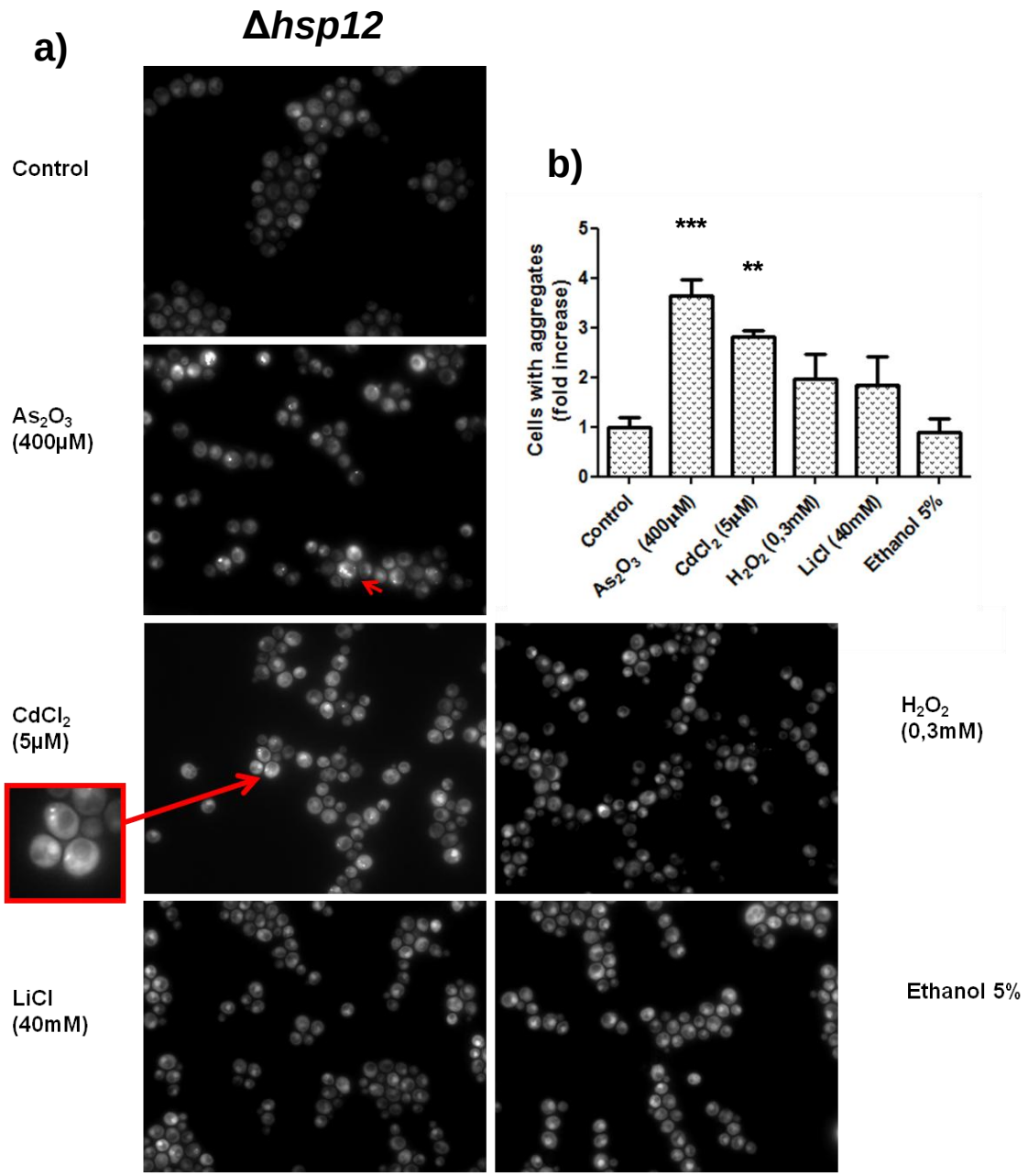

Figure 3.4 – Hsp104-containing aggregates increase in Δ*hsp12* cells after As and Cd exposure. Yeast cells labeled with an Hsp104 – GFP reporter were grown to mid-log and exposed to stress for 4h. a) Red arrows show the distribution of Hsp104-GFP agreggates in the cytoplasm as monitored by epifluorescence microscopy b) quantification of cells with Hsp104-GFP aggregates. ** (P<0.01) and *** (P<0.001) represent values significantly different from the control - cells not exposed to environmental stressors – (one-way ANOVA, Dunnett's post-test). Values are mean ± SEM. Approximately 500 cells were analyzed in 6 different images for each condition. Three independent experiments were performed.

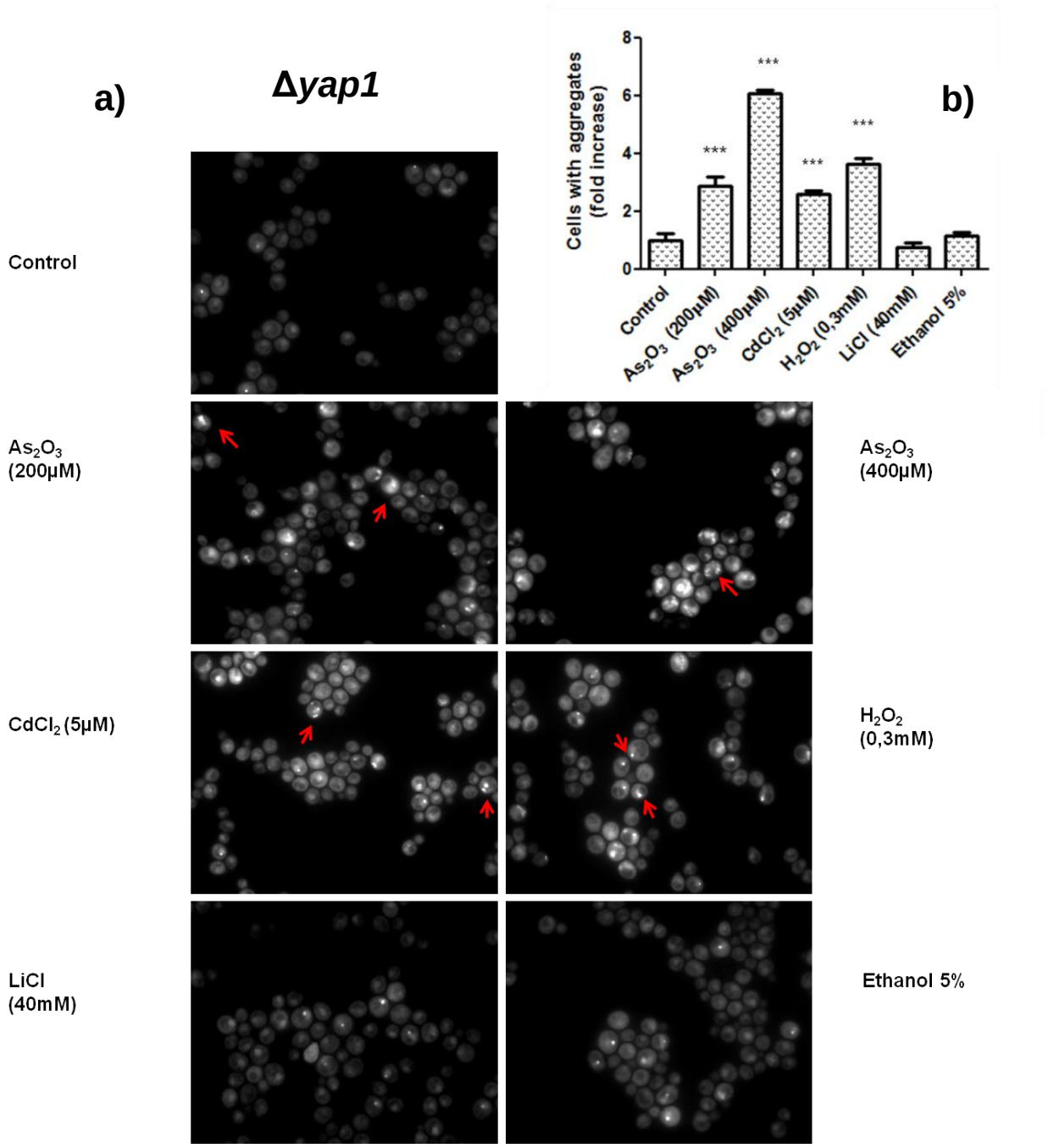

Figure 3.5 – Environmental oxidative stressors extensively increase Hsp104-containing aggregates in cells with low oxidative stress tolerance. Δ*yap1* cells labeled with an Hsp104 – GFP reporter were grown to mid-log and exposed to stress for 4h. a) Red arrows show the distribution of Hsp104-GFP agreggates in the cytoplasm as monitored by epifluorescence microscopy b) quantification of cells with Hsp104-GFP aggregates. *** (P<0.001) represent values significantly different from the control (one-way ANOVA, Dunnett's post-test). Values are mean ± SEM. Approximately 500 cells were analyzed in 6 different images for each condition. Three independent experiments were performed.

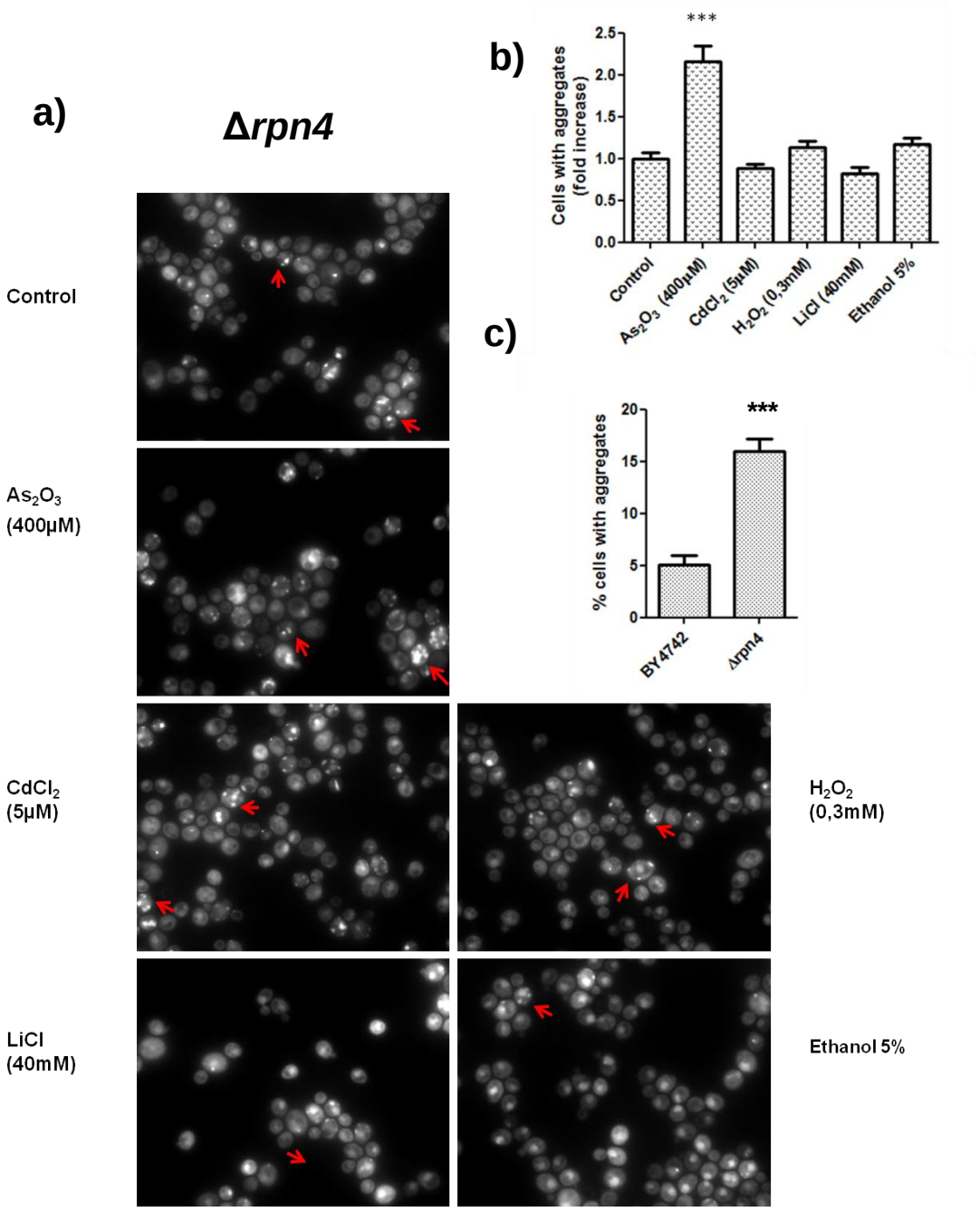

Figure 3.6 – Decreased proteasome activity leads to increase in Hsp104-containing aggregates in yeast. a) Red arrows show the distribution of Hsp104-GFP agreggates in the cytoplasm as monitored by epifluorescence microscopy b) quantification of cells with Hsp104-GFP aggregates c) Deletion of RPN4 promotes a 3x fold increase in *foci* of Hsp104 associated aggregates relatively to BY4742 cells, even in the absence of stress exposure. *** ($P<0.001$) represent values significantly different from the control (one-way ANOVA, Dunnett's post-test). Values are mean ± SEM. Approximately 500 cells were analyzed in 6 different images for each condition. Three independent experiments were performed.

As mentioned before, dissociation and reactivation of aggregated proteins in *S. cerevisiae* is mediated by Hsp104p, which in the process changes its intracellular distribution. Therefore, stress severity induces an increase in Hsp104p expression and an accompanying pattern change, from a weak diffuse distribution over the entire cell to a distinct accumulation surrounding the perimeter of protein aggregates.

Visualization and quantification of the Hsp104p associated aggregates can be done by epifluorescence microscopy in cells expressing a HSP104-GFP fusion reporter. This strategy allowed us to evaluate the involvement of some homeostasis genes in aggregate build-up, specifically under stress conditions previously associated with loss of translational accuracy. In all the strains tested, As_2O_3 exposure greatly contributed to the buildup of intense Hsp104-GFP foci spread throughout the entire cytoplasm (see Figure 3.3 - 3.6), explaining the crucial role of Hsp104p in arsenic resistance in yeast. The Yap1p transcription factor is pivotal in the response to oxidative stress. The effect of As in Δ*yap1* cells is concentration dependent and can increase Hsp104-containing aggregates 6-fold relatively to non exposed cells (figure 3.5). For that reason, the effect of As is most probably associated with oxidative damage to proteins (Wysocki R & Tamás MJ, 2010).

$CdCl_2$ also significantly increases the amount of Hsp104-containing aggregates in Δ*hsp12* and Δ*yap1* mutants, ~ 2 to 3 - fold (see figure 3.4 and 3.5). Indeed, Cd impact on proteins occurs by binding via thiol groups of cysteine residues, inhibiting chaperone-assisted folding and function (Sharma et al., 2008). On the other hand, the effect of H_2O_2 in the buildup of Hsp104-GFP aggregates is only relevant under low oxidative stress tolerance (figure 3.5) or upon exposure to high H_2O_2 concentrations (0,7mM; results not shown). This is probably due to the high efficiency of the peroxide detoxification enzyme catalase (Jamieson, 1998).

Deletion of *RPN4* results in inhibition of proteasome activity and increases Hsp104-GFP *foci* 3-fold relatively to BY4742 cells, even in the absence of stress exposure. Moreover, As_2O_3 exposure exacerbates protein aggregation in *Δrpn4* cells (2-fold increase, see Figure 3.6), although less pronouncedly than in other strains. Deletion of *RPN4* might increase Hsp104p expression, which is still slightly aggravated by stress exposure. This hyphothesis is consistent with previous studies which established a

correlation between exposure to a potent proteasome inhibitor (MG132) and a coordinated induction of many heat shock proteins (Lee & Goldberg, 1998). Taken together, our data suggests that deletion of *RPN4* and concomitant inhibition of the degradative function saturates intracellular folding capacities. Hsp104-GFP foci were scarcely visible upon ethanol and lithium exposure, even though these conditions have also been associated with UAA readthrough and AGC misreading in deletion mutants under defective protein homeostasis (Chapter 2, table 2.4 and 2.5). This suggests that ethanol or lithium may not impact mistranslation through protein aggregation.

In conclusion, stress or proteome quality control impairment might aggravate protein damage resulting in unfolding, followed by aggregation. Many of the aggregated proteins might be translation factors that regulate accuracy, like ribosomal proteins, elongation or release factors, resulting in synthesis of aberrant proteins that can further exacerbate cell degeneracy.

3.3.2.1. Effects of environmental stress on aggregation of release factors

Our previous results showed that environmental stress increases stop codon readthrough (Chapter 2, Figure 2.4 and Table 2.4) in the absence of homeostasis mechanisms. In eukaryotes, translation termination is mediated through the action of a single class I release factor (eRF1) that recognizes all three stop codons (UAG, UAA, and UGA) (Bertram G et al., 2001; Kisselev L et al., 2003). The eukaryotic class II release factor eRF3 facilitates eRF1 stop codon recognition and carries out GTP hydrolysis prior to polypeptide chain release (Salas-Marco J & Bedwell DM, 2005; Alkalaeva EZ et al., 2006), hence acting as an enhancing factor for the termination process. The efficiency of translation termination depends on competition between stop codon recognition by eRF1 and decoding of stop codons, by a near-cognate tRNAs. As a result, availability of eukaryotic release factors is determinant for termination accuracy (Stansfield et al., 1996) and any stress-induced damage on eRF1 or eRF3 proteins likely leads to stop codon suppression.

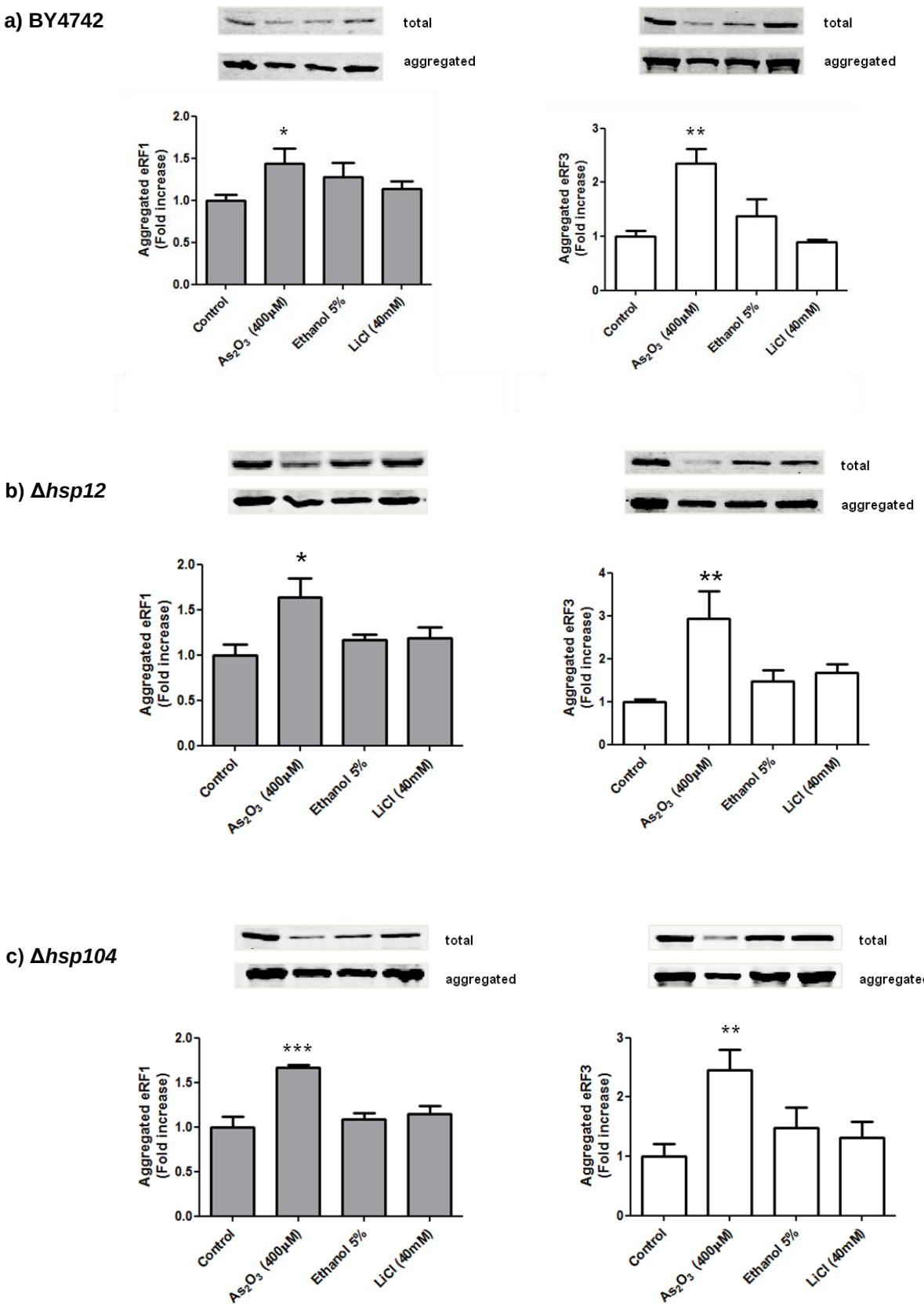
a) BY4742
total
aggregated
total
aggregated
Aggregated eRF1 (Fold increase)
2.0
1.5
1.0
0.5
0.0
*
Control
As2O3 (400µM)
Ethanol 5%
LiCl (40mM)
Aggregated eRF3 (Fold increase)
3
2
1
0
**
Control
As2O3 (400µM)
Ethanol 5%
LiCl (40mM)
b) Δhsp12
total
aggregated
total
aggregated
Aggregated eRF1 (Fold increase)
2.0
1.5
1.0
0.5
0.0
*
Control
As2O3 (400µM)
Ethanol 5%
LiCl (40mM)
Aggregated eRF3 (Fold increase)
4
3
2
1
0
**
Control
As2O3 (400µM)
Ethanol 5%
LiCl (40mM)
c) Δhsp104
total
aggregated
total
aggregated
Aggregated eRF1 (Fold increase)
2.0
1.5
1.0
0.5
0.0
***
Control
As2O3 (400µM)
Ethanol 5%
LiCl (40mM)
Aggregated eRF3 (Fold increase)
3
2
1
0
**
Control
As2O3 (400µM)
Ethanol 5%
LiCl (40mM)

Figure 3.7 ▶

Figure 3.7 – As_2O_3 increases eRF 1 and eRF3 in the insoluble protein fraction. Cells were grown to mid-log in Minimal Medium and exposed to stress for 4h. Equivalent cell numbers (10 A_{600} units) were harvested by centrifugation, washed and resuspended in PBS. Aggregated insoluble proteins were isolated from soluble and membrane proteins by centrifugation at 13,000 rpm for 20 min and by washing the pellet with lysis buffer containing Triton X-100, respectively. eRF1 and eRF3 were separated by SDS-PAGE and detected by immunoblotting. **a)** wild-type BY4742 cells, **b)** hsp12 null mutants, **c)** hsp104 null mutants. The amount of aggregated release factors was normalized with the values from the total protein fraction, * ($P < 0.05$), ** ($P<0.01$) and *** ($P<0.001$) represent values significantly different from the control (one-way ANOVA, Dunnett's post-test). Values are mean ± SEM of at least three independent experiments.

Therefore, we have investigated whether stress affects protein synthesis accuracy by limiting the access of release factors to stop codons. In order to do so, the aggregated protein fraction was first separated from the soluble fraction by a prolonged ultra speed centrifugation and then from membrane proteins by washing with a non-ionic surfactant. Immunodetection showed that exposure to As_2O_3 significantly increases the amount of both eRF1 and eRF3 in the insoluble fraction, potentially diminishing their availability for termination in BY4742, Δ*hsp12* and Δ*hsp104* cells. Remarkably, As_2O_3 does not affect translational accuracy in BY4742 (WT) cells (Chapter 2, Figure 2.3 and 2.4), suggesting that As_2O_3 induced aggregates do not exclusively result from decreased translational accuracy. On the other hand, eRF1/eRF3 solubility is not relevant to explain the effect of lithium or ethanol on protein synthesis, neither the differences observed in strain susceptibility.

3.3.3. Reprogramming of tRNA modifications

Modifications modulate tRNA binding affinity to ribosomes, thereby affecting the rate and fidelity of protein synthesis. In addition, tRNA modified mucleosides have also been strongly implicated in the cellular response to stress. Indeed, recent data indicates that deletion of *TRM1* and *TRM8* methyl transferase genes, involved in $m^2{}_2G$ and m^7G synthesis, respectively, cause severe heat and antibiotic sensitivity in yeast (Gustavsson & Ronne, 2008; Sinha et al., 2008).

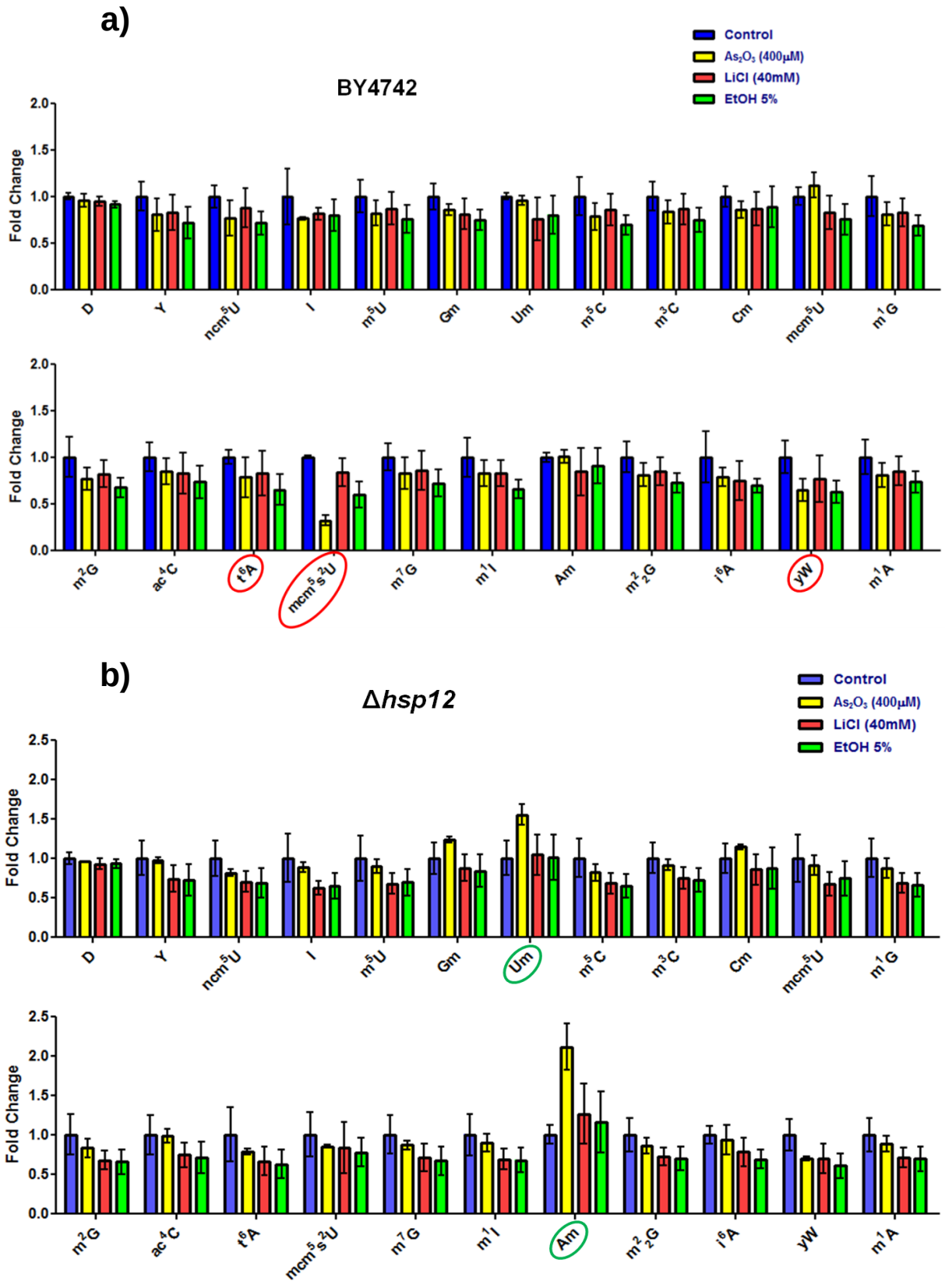
a)
BY4742
Control
As2O3 (400µM)
LiCl (40mM)
EtOH 5%
Fold Change
D
Y
ncm5U
I
m5U
Gm
Um
m5C
m3C
Cm
mcm5U
m1G
m2G
ac4C
t6A
mcm5s2U
m7G
m1I
Am
m22G
i6A
yW
m1A
b)
Δhsp12
Control
As2O3 (400µM)
LiCl (40mM)
EtOH 5%
Fold Change
D
Y
ncm5U
I
m5U
Gm
Um
m5C
m3C
Cm
mcm5U
m1G
m2G
ac4C
t6A
mcm5s2U
m7G
m1I
Am
m22G
i6A
yW
m1A

Figure 3.8 ▶

Figure 3.8 - Environmental stress affects tRNA modifications. Modified nucleoside levels after 4h exposure to non-iethal concentrations of As_2O_3 (400μM), LiCl (40mM) and ethanol 5%. Changes were quantified by liquid chromatography coupled electrospray-tripe quadrupole mass spectrometry (LC/QQQ). Mass spectrometer signals were normalized against the internal standard ([$^{15}N_5$]-29-deoxyriboadenosine). **a)** wild-type, BY4742 cells **b)** hsp12 null mutants. The red circles indicate the most significant decreases in modified nucleosides. The green circles indicate the most significant increases. Results are expressed as fold change of nucleoside level in cells exposed to stress relatively to levels in non-exposed cells. Values are mean ± SD of two biological replicates.

Newly discovered reprogramming of tRNA modifications under stress exposure is part of a translational control mechanism that assures cell survival responses (Chan et al., 2010). These data prompted us to evaluate possible changes in the level of tRNA modified nucleosides under environmental stress conditions. We hyphotezised that such changes could explain the low-level mistranslation measured in chapter 2. For this, we took advantage of a previously developed liquid chromatography – coupled mass spectrometric (LC-MS/MS) method (Chan et al., 2010) that allows robust separation, characterization and quantification of 23 distinct modified tRNA nucleosides. Two of the 25 known *S.cerevisiae* modifications were not detected, namely ncm^5Um and Ar(p). Signal intensities from each nucleoside were normalized by an internal standard ([$^{15}N_5$]-29-deoxyriboadenosine), allowing comparison across distinct samples. Cells were exposed to non – lethal concentrations of As_2O_3, LiCl and ethanol as previously described.

Our data show reduction in the levels of mcm^5S^2U in BY4742 cells exposed to arsenic and a less pronounced decrease in the level of yW. Ethanol also decreased yW and mcm^5S^2U modifications, although less intensively in the case of mcm^5S^2U. Additionally, ethanol reduced the levels of t^6A (see figure 3.8 a). On the other hand, *Δhsp12* cells under stress present a unique spectrum of modified nucleosides. yW levels were significantly diminished after treatment with As_2O_3 , similarly to BY4742 cells, while Um and Am levels varied in the opposite way (Figure 3.8 b). As_2O_3 exposure also leads to a decline in a considerable number of modifications in Δ*hsp104*

and Δ*yap1,2* cells. In Δ*hsp104*, levels of I, m^5U, mcm^5U, m^1G, t^6A, m^2_2G, i^6A, yW and m^1A were substantially decreased, as well as Gm, Um, Am, yW and m^1A in Δ*yap1,2* mutants (figure 3.9 a and b). Finally, exposure to non-inhibitory Li concentrations does not significantly alter the spectrum of tRNA modifications. Reprogramming is usually a dose-dependent response to more cytotoxic conditions (Chan et al., 2010).

a)

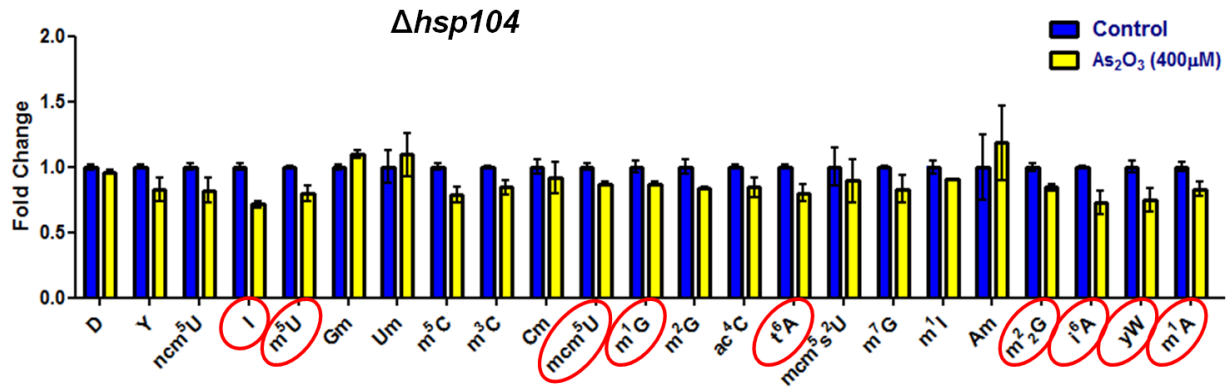

b)

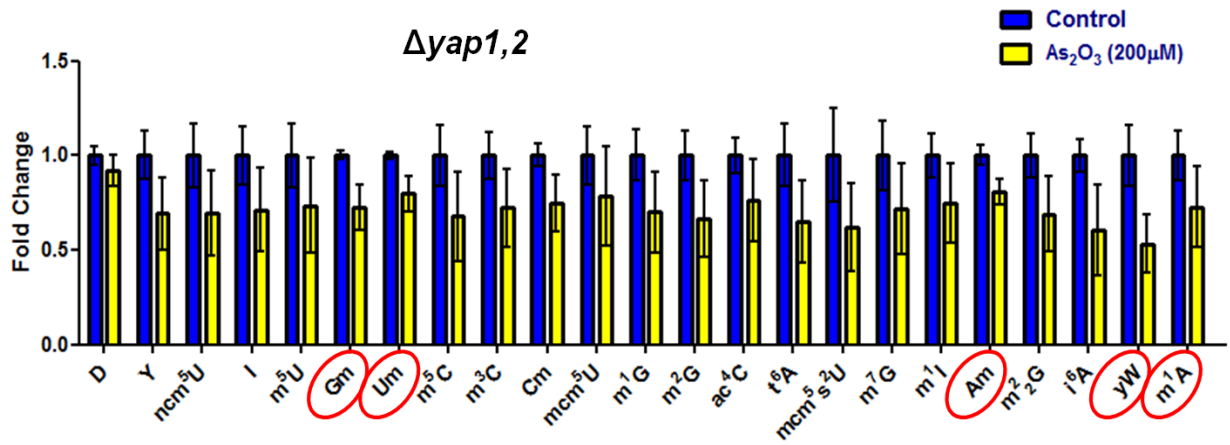

Figure 3.9 - Spectrum of tRNA modifications in Δ*hsp104* or Δ*yap1,2* cells exposed to As_2O_3. Changes were quantified by liquid chromatography coupled electrospray-tripe quadrupole mass spectrometry (LC/QQQ). Mass spectrometer signals were normalized against the internal standard ([$^{15}N_5$]-29-deoxyriboadenosine). a) Δ*hsp104* b) Δ*yap1,2*. The red circles indicate the most significant decreases in modified nucleosides. Results were expressed as fold change of nucleoside level in cells exposed to stress relatively to levels in non-exposed cells. Values are mean ± SD of two biological replicates.

3.3.4. Misacylation of specific non-methionyl-tRNAs

Previous studies have uncovered ununtecipated phenotypes associated with low-level mistranslation, namely increased ROS production and activation of oxidative stress response genes (Paredes et al., in press). Quantification of intracellular ROS levels in BY4742 and Δ*hsp12* cells illustrated a distinct response to constitutive mistranslation. Although there was a trend for increased ROS in both strains expressing misreading tRNAs, this increment was significant during stationary phase and mostly due to H_2O_2 build-up in the Δ*hsp12* cells (Figure 3.10), while mistranslating BY4742 cells showed a 4-fold increase both in H_2O_2 and superoxide during exponential phase.

Methionine misacylation recently emerged as an important cellular defense response to increased levels of ROS (Luo & Levine, 2009; Netzer et al., 2009). Indeed, methionine residues in proteins work as ROS scavengers, protecting the function of many macromolecules (Luo & Levine, 2009). In mammalian cells, Met-misacylation occurs at a basal level of ~1% and increases up to 10-fold under innate immune activation and after oxidative stress induction, representing a very significant but tolerated impact on translational fidelity (Netzer et al., 2009). We therefore explored misacylation in BY4742 and Δ*hsp12* cells expressing misreading tRNAs. For this, total tRNA from exponentially growing cells radiolabeled with ^{35}S-Met was hybridized to tRNA arrays, allowing detection of all the 40 chromosomal and 24 mitochondrial-encoded yeast tRNAs (see section 3.2.10 and Figure A5 in Annexes). ^{35}S-Met-tRNAs were then quantified by phosphorimaging analysis. As a control for ^{35}S labeling of tRNAs with thio-modifications, a sample of total RNA was deacylated and hybridized by the same procedure. In Figure 3.11 a), b) and c), deacylation resistant signals are represented in the left column (blue). Yeast tRNAs such as $tRNA^{Lys}_{UUU}$, $tRNA^{Glu}_{UUC}$, $tRNA^{Arg}_{UCU}$ and $tRNA^{Thr}_{IGU}$ were detected after deacylation due to thio-modifications at the wobble position of the anticodon. However, signals from other tRNAs that do not contain known thio-modifications were detectable even after deacylation, namely $tRNA^{Lys}_{CUU}$ and $tRNA^{Ile}_{IAG}$ (Figure 3.11).

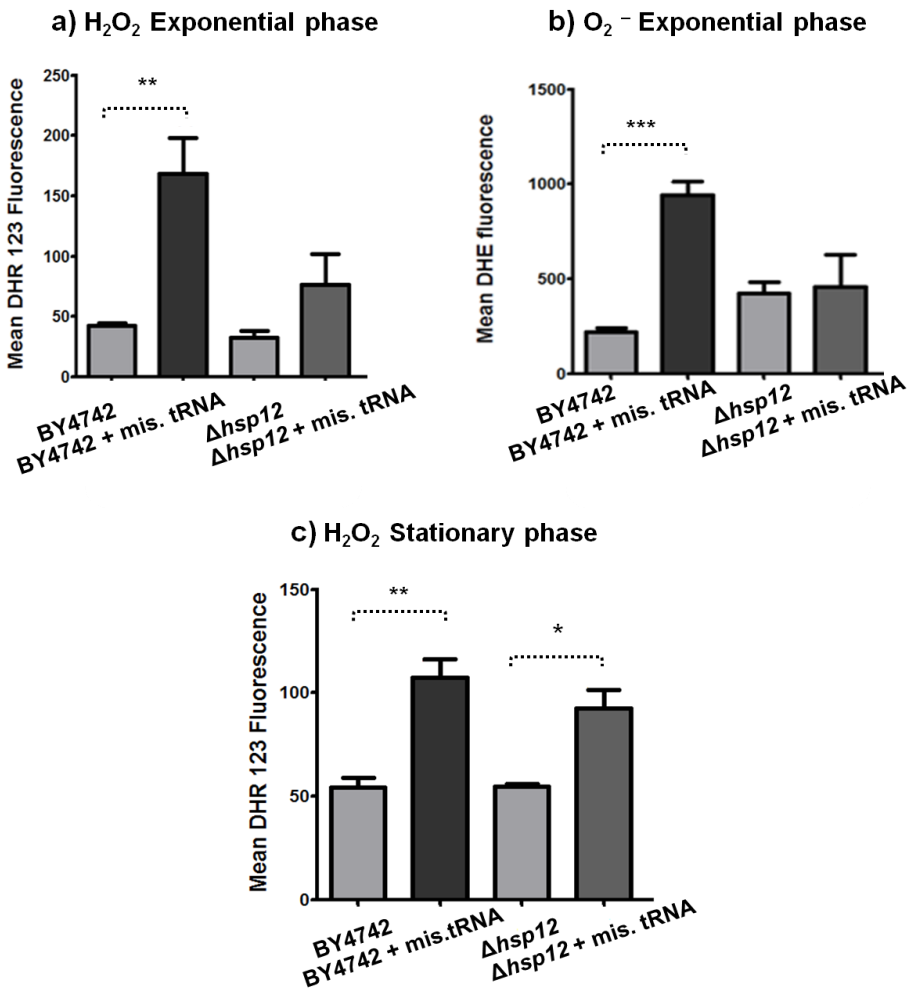

Figure 3.10 - Mistranslation increases ROS levels (H_2O_2 and superoxide anion) in By4742 and *Δhsp12* cells. The $tRNA^{Ser}_{CAG}$ from *C. albicans* was expressed in *S. cerevisiae* cells, resulting in a correctly processed and functional misreading tRNA (mis. tRNA), as accessed by a β-Gal assay (see Figure A4 in Annexes). This unique tRNA contains the body (long variable arm and discriminator base) of a serine tRNA and the anticodon of a leucine tRNA ($tRNA^{Ser}_{CAG}$), decoding the leucina CUG codon as serine (Santos MA et al., 1996). Therefore, both the seryl- and the leucyl-tRNA synthetases (SerRS and LeuRS) recognize this hybrid tRNA, generating CUG ambiguity (Santos MA et al., 1996; Suzuki et al., 1997). ROS were quantified by flow cytometry after labelling cells with dihydrorhodamine 123 (DHR123) and DHE (dihydroethidium), respectively. ROS tendencially increase in strains expressing misreading tRNAs. This increase is substantially higher in BY4742 (WT) cells and significant for Δ*hsp12* cells only during stationary phase. * ($P < 0.05$), ** ($P<0.01$) and *** ($P<0.001$) represent values significantly different from the control (non-mistranslating) cells (one-way ANOVA, Dunnett's post-test), as indicated by the dashed line. Results were expressed as mean ± SEM of three biological replicates.

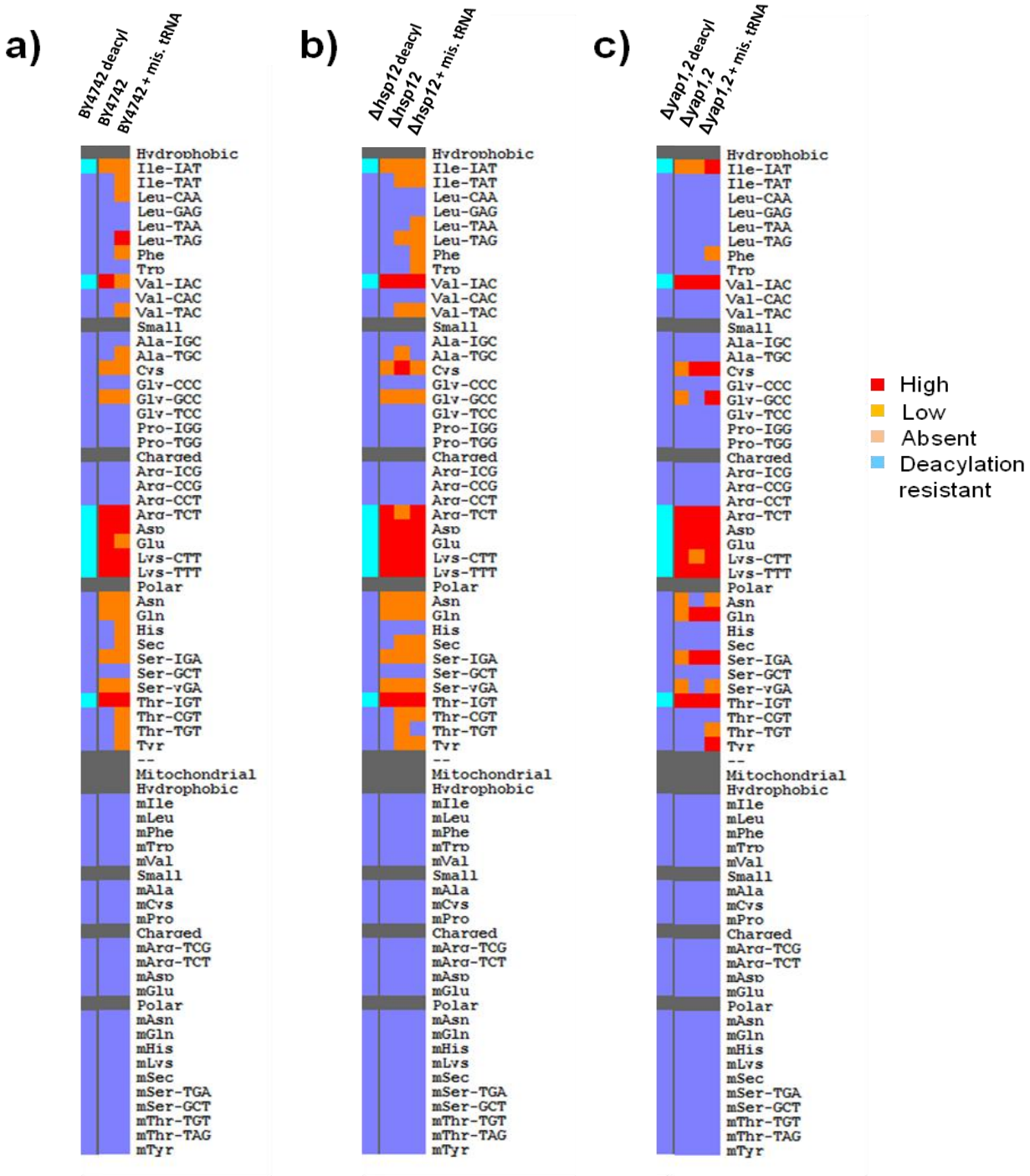
a)
BY4742 deacyl
BY4742
BY4742 + mis. tRNA
b)
Δhsp12 deacyl
Δhsp12
Δhsp12 + mis. tRNA
c)
Δyap1,2 deacyl
Δyap1,2
Δyap1,2 + mis. tRNA
Hydrophobic
Ile-IAT
Ile-TAT
Leu-CAA
Leu-GAG
Leu-TAA
Leu-TAG
Phe
Trp
Val-IAC
Val-CAC
Val-TAC
Small
Ala-IGC
Ala-TGC
Cys
Gly-CCC
Gly-GCC
Gly-TCC
Pro-IGG
Pro-TGG
Charged
Arg-ICG
Arg-CCG
Arg-CCT
Arg-TCT
Asp
Glu
Lys-CTT
Lys-TTT
Polar
Asn
Gln
His
Sec
Ser-IGA
Ser-GCT
Ser-yGA
Thr-IGT
Thr-CGT
Thr-TGT
Tyr
--
Mitochondrial
Hydrophobic
mIle
mLeu
mPhe
mTrp
mVal
Small
mAla
mCys
mPro
Charged
mArg-TCG
mArg-TCT
mAsp
mGlu
Polar
mAsn
mGln
mHis
mLys
mSec
mSer-TGA
mSer-GCT
mThr-TGT
mThr-TAG
mTyr
High
Low
Absent
Deacylation resistant

Figure 3.11 ▶

- **Figure 3.11 - Methionine misacylation occurs in wild-type cells and is elevated by mistranslation.** Cells expressing pRS315 or pUKC715 (misreading tRNA) were grown to exponential phase and labeled with ^{35}S-met. Total RNA was extracted and hybridized to yeast tRNA arrays. After hybridization, arrays were washed, dryed and exposed to phosphorimaging plates for up to 14 days (see Figure A5 and A6 in Annexes). Spot intensity was then quantified. Orange and red squares indicate tRNAs misacylated with Met. The ^{35}S-signal intensity is calculated relatively to tRNA^{Met}. Represented in the image are 40 nuclear-encoded and 24 mitochondrial-encoded yeast tRNAs, organized according to the nature of their cognate amino acid a) misreading tRNA (mis. tRNA) expression in wild-type (BY4742) cells increases Met-misacylation. Deacylation resistant signals are represented in the left column. The origin of these deacylation resistant signals is not known b) Δ*hsp12* increases Met-misacylation relative to wild-type basal levels, but no significant, additional increase is observed upon misreading tRNA expression. C) Δ*yap1,2* increases misacylation only upon misreading tRNA expression. Results were obtained from two biological replicates.

The origin of these deacylation resistant ^{35}S-signals remains unknown. Mistranslation induced by the misreading tRNA in BY4742 cells increased Met-misacylation (Figure 3.11 a). Nevertheless, except for tRNA$^{Leu}_{UAG}$, misacylation sinals were weak. Met-misacylation also increased in the Δ*hsp12* background, but remarkably, mistranslation did not result in an additional increment in these cells (Figure 3.11 b). As expected, misacylation also increased in *Δyap1,2* cells under mistranslation, but in this case misacylation sinals are much stronger than in BY4742 or Δ*hsp12* cells (Figure 3.11 c). No misacilation was detected in mitochondrial-coded tRNAs. The misacylated tRNAs varied much according to the nature of their cognate amino acid, with a particular prevalence of tRNAs encoding polar residues, especially in *Δyap1,2* cells.

3.4. Discussion

3.4.1. Impact of environmental stress on the plasma membrane

Hsp12p is not a common small heat shock protein (sHsp). It differs from sHsp in almost all structural and functional characteristics. During exponential phase, Hsp12p is present in low concentrations in the cytosol and as a soluble protein with no

noticeable secondary structure. Under stress, increased expression allows its integration in the plasma membrane, where it can modulate membrane fluidity and stability without requiring changes in the lipid composition of yeast cells. Interestingly, homologs of Hsp12p are only found in fungi. WH11 from *C.albicans* shares 47% homology to the amino-terminal region of Hsp12 and is involved in phenotypic switching and virulence (Park et al., 2004).
The role of Hsp12p in membrane integrity and organization was shown experimentally by the increased uptake of propidium iodide in Δ*hsp12* cells exposed to stress conditions (Welker S et al., 2010). The effect of Hsp12p on membrane organization may occur through interaction with protein components, including ion channels and transporters. With this in mind, we tested the influx of As, Cd and Li in Δ*hsp12* cells, in order to establish a potential connection with mistranslation.

Toxic metal and metalloid cellular influx occurs through permeases and channels used normally for the transport of essential nutrients. However, there are several defense mechanisms intended to reduce this toxic influx both by downregulating the expression of relevant transporters at the transcriptional and post-transcriptional levels or by inhibiting their activity. For example, the aquaglyceroporin Fps1p, normally involved in efflux of glycerol and in uptake of acetic acid, is the main entrance pathway of As(III) into yeast cells (Wysocki et al., 2001). The MAPK Hog1p is activated in response to As(III) and reduces transport through Fps1p, therefore mediating an essential tolerance mechanism (Wysocki R & Tamás MJ, 2010). In addition, As (III) detoxification in *S. cerevisiae* can also occur via the Acr3p uniporter, allowing export of the As anion $As(OH)_2O^-$ coupled to the membrane potential (Fu et al., 2009).

One of the major Cd influx pathways is through Zrt1p, normally involved in the uptake of Zn (Gomes et al., 2002; Gitan et al., 2003). In the presence of high Cd concentrations Zrt1p is removed from the cell surface by a tolerance mechanism triggered by Rsp5p dependent ubiquitylation, followed by endocytosis and degradation in the vacuole (Gitan & Eide, 2000). Another resistance mechanism is

associated to the intracellular distribution of this metal ion. In *S. cerevisiae*, the ATP-binding cassette (ABC) transporter Ycf1p, which is a YAP1 target, is involved in vacuolar sequestration of GSH-conjugated Cd and As.

Plasma membrane transport and cation tolerance are determined by the action of Pma1p H^+ pumping ATPases (Serrano et al., 1986) and Trk1/Trk2p K^+ transporters, both of which are pivotal in establishing the electrical membrane potential in *S. cerevisiae.* The negative-inside membrane potential allows lithium (Li) to enter yeast cells via NSC1 (non-specific cation channel) by a yet unclear mechanism (Bihler et al., 1998; Bihler et al., 2002). On the other hand, Li extrusion is dependent mainly on the ENA1-encoded efflux ATPase, which couples hydrolysis of ATP to the transport of cations against the electrochemical gradient.

Deletion of the ribosome-associated chaperones Ssb1/2p and Zuo1p renders cells hypersensitive to a wide range of cations, mostly due to an altered plasma membrane transport and concomitant influx rate increase of both Na^+ and Li^+. Remarkably, many pleiotropic effects have been recognized in Δ*ssb1/2* cells, including sensitivity to aminoglycosides and impairment of translational accuracy (Rakwalska M & Rospert S, 2004; Kim SY & Craig EA, 2005). Our results on the intracellular quantification of As, Cd and Li failed however to explain differential propensity for low-level mistranslation in BY4742, Δ*hsp104* or Δ*hsp12* cells. After a 4h exposure, *HSP12* and *HSP104* deletions do not visibly increase accumulation of stressors in the cytoplasm relative to WT cells. It is therefore likely that the differences in stress sensitivity are due to mechanisms targeting the translational machinery or even protein degradation.
However, cation influx or eflux defects cannot be completely excluded because intracellular ion quantification was carried out at a single point after prolonged stress exposure, disregarding the balance of ion movement across the plasma membrane. Future studies should focus on the time course of changes in intracellular ion concentration after addition and removal of stressors. It is also important to assess their distribution between cytoplasm and vacuole. This would allow evaluating the effectiveness of detoxification mechanisms in each of the strains. Finally, the

accumulation of As^{3+}, Cd^{2+} or Li^{+} might affect the intracellular ion pools of essential ions such as K^{+} or Cd^{2+} (Blackwell K & Jobin J, 1999), imposing modifications to the electrochemical membrane gradient or interfering with the activation of major intracellular signaling pathways. Hypothetically, these mechanisms might influence the cellular response to stress and deregulate the mechanisms that assure translational accuracy.

3.4.2. Impact of oxidative damage on protein aggregation and the translational machinery

Molecular chaperones and the ubiquitin-proteasome degradation pathway form a highly intricate network, representing the main protection responses against the buildup of misfolded protein and aggregates. However, under stress misfolded proteins may aggregate forming a large number of non-compartmentalized foci of different sizes, dispersed throughout the cytoplasm and associated with chaperones. Most of these aggregated proteins can be refolded to the native state by the Hsp104–Hsp70 bi-chaperone system.

Interestingly, even though Li and ethanol exposures were previously associated with low-level mistranslation (Chapter 2), protein aggregates were not detected in chaperone deletion mutants or WT cells (in the case of ethanol), suggesting that proteostasis mechanisms are efficient at preventing the buildup of misfolded proteins. In the case of Li, ethanol and low concentrations of Cd, misfolded proteins might be degradated by the proteasome. The lack of aggregates in Δ*rpn4* mutants suggests that autophagy may play a compensatory role in UPS defective cells (Ding et al., 2007). One possibility is that mistranslated proteins are removed by microautophagy, which involves direct uptake of cytoplasmic proteins at the vacuolar surface. Direct transport of misfolded proteins into yeast vacuoles has also been described in yeast by a mechanism related with Hsp70 (Horst et al., 1999). Interestingly, deletion in yeast genes related with protein targeting to vacuole has been implicated in decreased fitness defect under Li exposure (Hillenmeyer et al., 2008).

Under stress, damaged proteins can also be seized into several distinct quality-control compartments, namely, aggresomes, the the juxtanuclear quality-control compartment (JUNQ) adjacent to the nuclear membrane or the insoluble protein deposit (IPOD) adjacent to the vacuole. Spatial sequestration can protect the cellular environment from potentially deleterious protein species (Arrasate et al., 2004; Lansbury & Lashuel, 2006) and even facilitate clearance by alternative mechanisms such as autophagy (Rubinsztein, 2006). Aggresomes are microtubule-dependent cytoplasmic structures found both in mammalian and yeast cells. Aggregated proteins sequestered in the aggresomes are usually cleared by autophagy (Pankiv et al., 2007). The JUNQ transiently concentrates misfolded ubiquitylated proteins that can be degraded by the UPS or rapidly exchanged with the surrounding cytoplasm for refolding by chaperones. On the other hand, the IPOD contains terminally insoluble aggregated proteins, including yeast prions, and interacts with the autophagy associated Atg8p. Molecular chaperones are thought to contribute to the formation of JUNQ and IPOD and to the partition of substrate proteins between these compartments. Remarkably, the chaperone Hsp104 co-localizes with both JUNQ and IPOD, allowing fragmentation of aggregates and thereby keeping proteins soluble for either refolding or degradation (Kaganovich et al., 2008).

Cell exposure to As_3O_2, as well as deletion of *YAP1*, increase oxidative damage and formation of cytosolic Hsp104-GFP containing foci (Figure 3.3-3.6), dispersed throughout the cytoplasm or sequestered into quality-control compartments (Wysocki R & Tamás MJ, 2010), but additional experiments are required to confirm wheter mistranslation is relevant for such increment in protein aggregation. Nevertheless, in our study the buildup of protein aggregates is being underestimated in many of the tested conditions, since not all the insoluble proteins co-localize with Hsp104 in the cytoplasm or quality-control compartments such as JUNQ or IPOD. The aggregates sequestered in aggresomes are probably not visualized by epifluorescence microscopy.

As (III) toxicity is thought to be associated with its ability to covalently bind protein sulfhydryl groups. However, mechanisms linked to formation of ROS have also been

proposed (Valko M et al., 2005). Indeed, As (III) exposure impairs mitochondrial integrity by harming protein biosynthesis or even genome maintenance and targets cellular ROS detoxification mechanisms by decreasing the availability of glutathione. Also, As (III) mediates iron release from the storage protein ferritin (Salnikow & Zhitkovich, 2008), a process that culminates with hydrogen peroxide decomposition by the Fenton reaction and with synthesis of the highly damaging hydroxyl radical (Jomova et al., 2011). On the other hand, ROS are involved in the metal catalyzed introduction of carbonyl groups into the side chains of proline, arginine, lysine or threonine (Nystrom, 2005; Tyedmers J et al., 2010), which may happen under our experimental conditions.

Mistranslated proteins appear to be more susceptible to protein damage. Carbonylation has been reported to occur independently of ROS accumulation, under conditions that favor a boost in production of aberrant proteins available for oxidative attack (Dukan et al., 2000; Ballesteros et al., 2001). For example, carbonylation increases upon treatment with ribosome-targeting antibiotics even if superoxide production is unaltered (Dukan et al., 2000). Therefore, cellular protein oxidation is limited both by available reactive oxygen species and by the levels of aberrant proteins. These observations suggest an unexpected link between reduced translational accuracy and protein oxidation. If so, the mechanism of As (III) toxicity may involve mostly protein homeostasis, which should be explored in future experiments. Rapid carbonylation followed by aggregation guarantees that erroneous proteins promptly enter the degradation pathway and keep the cell free from mistranslated proteins (Dukan et al., 2000; Nystrom, 2005).

ROS generated by exposure to environmental stressors may also mediate permanent deleterious modifications of protein structure or function, by targeting mRNA translation. ROS may induce oxidation of the Cys182 residue in threonyl-tRNA synthetase, resulting in an impairment of aminoacylation editing activity, leading to Ser-tRNA^{Thr} formation and eventually to growth inhibition in *E.coli* (Ling J & Söll D, 2010).

Previously, a mass spectrometry analysis of metal - induced agresomes in mammalian cells revealed that approximately 26% of aggresome-enriched proteins are related to biosynthesis and protein translation, namely tRNA synthetases, translation initiation factors, and ribosomal proteins (Song et al., 2008). This establishes a connection between metal stress and the availability of translational factors. Our data on the impact of environmental stress on translational accuracy (Chapter 2) showed occurance of low-level mistranslation mostly at the expanse of stop codon readthrough. Therefore, we hypothesized that sequestration of eRFs into protein aggregates might shift the competition for stop codon recognition in favor of near-cognate tRNAs, leading to stop codon readthrough. We identified both eRF1 and eRF3 as components of the aggregate fraction that accumulate in As_2O_3 exposed cells. However, low-level stop codon readthrough also occurred under exposure to ethanol and lithium, where protein aggregation was not observed (Chapter 2, table 2.4 and 2.5). This suggests that As_2O_3, ethanol and Li may influence mistranslation in different ways.

3.4.3. Changes in the spectrum of tRNA modifications

Post-transcriptional modifications are essential to guarantee the structural and functional features of tRNAs. The lack of modified nucleosides can lead to serious translational defects, which might be linked to disease, particularly in mitochondria (Kirino et al., 2005). Tumor cells possess a significantly different tRNA modification pattern than those in normal cells (Dirheimer et al., 1995). However, the precise biological role of each modification is sometimes difficult to classify because of functional redundancy of some methyl-based modifications and the absense of strong phenotypes for some of the tRNA methytransferase-deletion strains. In fact, although many modifications or modification enzymes are conserved, only few modification enzymes are essential for viability.

A new biological function for ribonucleosides has recently begun to surface, mainly related with the cellular response to stress. Surprisingly, stress induces large changes

in the spectrum of ribonucleosides, as part of a dynamic translational control mechanism. This reprogramming is intended to enhance the synthesis of proteins that assure cell survival under unfavorable growth conditions (Chan et al., 2010). A recent example involves Trm9p – catalyzed modifications, known to modulate the cellular response to DNA damage. Trm9p is a methyltransferase that catalyzes the last step in the formation of mcm^5U and mcm^5s^2U in $tRNA^{Arg}_{UCU}$ and $tRNA^{Glu}_{UUC}$, respectively. Remarkably, many of the genes involved in DNA damage responses are enriched in AGA and GAA codons (Begley U et al., 2007). Therefore, an increase in Trm9 expression or a boost in the amount of cellular mcm^5U and mcm^5s^2U ribonucleosides prevents cell death under exposure to DNA damaging agents. This occurs through an enhancement in tRNA binding to AGA and GAA codons, with a concomitant increase in translational efficiency of defense genes (Begley U et al., 2007). Also, the human protein kinase B (Akt) and ribosomal s6 kinase (RSK) can phosphorylate and inactivate Trm8, required for m^7G modification of tRNA, corroborating a modification reprogramming occurring in the context of cellular regulatory responses (Cartlidge et al., 2005).

We approached the dynamics of tRNA modifications in the scope of environmental stress conditions already shown to induce low-level mistranslation (Chapter 2). We hypothesized that changes in the spectrum of ribonucleosides might decrease protein synthesis accuracy, thereby creating proteome diversity. Both BY4742 cells and the deletion mutants were exposed to As_3O_2, LiCl and ethanol as described in section 3.2.7. Remarkably, the pattern of stress-induced tRNA modification changes is distinct for each strain under study. Exposure of WT By4742 cells to As_3O_2 and ethanol results in an expressive decrease in the levels of mcm^5s^2U and yW (see figure 3.8 a), exclusively located respectively at position 34 and 37 in the anticodon region (see Table 3.3). Also t^6A, located exclusively at position 37 in *S.cerevisiae*, was quite decreased upon exposure to ethanol.

Most of the tRNA modifications are either located 3'-adjacent to the anticodon (position 37) or at the wobble position (position 34). These modifications enable

wobble base pairing and are a tool for efficient reading of degenerated codons. The wobble modifications at position 34 are pivotal for precise codon-anticodon decoding interactions, enabling wobble base pairing and efficient reading of degenerated codons. Modifications at position 37 have a large structural diversity. A total of 16 different modified nucleosides, including 12 adenosine derivatives, have been identified at position 37 in tRNAs of organisms from all domains of life. Position 37 of the *S.cerevisiae* tRNAs usually contains a hyper-modified purine nucleoside, namely t^6A, i^6A or yW, the last one found specifically in $tRNA^{Phe}$ (see table 3.3). yW consists of a tricyclic base with a bulky side chain and is one of the most complex of the modified guanosine residues. Although it does not have any major influence on the aminoacylation of $tRNA^{Phe}$ (Thiebe & Zachau, 1968), yW stabilizes the first base pair of the codon–anticodon duplex in the ribosomal A site by base stacking (Konevega et al., 2004) and contributes to maintain reading frame. Indeed, a change at position 37 of $tRNA^{Phe}$ from yW to a biosynthetic precursor such as m^1G, resulted in a 3-fold increase of -1 programmed ribosomal frameshifting (Waas et al., 2007).

We have observed a decrease in yW is also observed in Δ*hsp12* cells under ethanol and As_3O_2 exposure (see Figure 3.8 b) as well as in Δ*hsp104* and Δ*yap1,2* mutants, also in the presence of As_3O_2 (see Figure 3.9). Similar studies have identified an yW dose-dependent decrease in WT yeast cells exposed to concentrations of methylmethane sulfonate (MMS), H_2O_2, and NaOCl, producing 50% and 80% cytotoxicity (Chan et al., 2010). The fact that yW is only found in $tRNA^{Phe}$ (see table 3.3) makes the decrease effect more dramatic, because this variation change cannot be masked by an inverse change in the level of the modification in the remaining population of tRNA molecules. Therefore, the reduction in yW levels appears to be a general response to stress conditions, but no significant change in the levels of yW was identified upon exposure to Li.

Changes in the spectrum of tRNA modifications promote precise and coordinated biological responses to adverse conditions, by altering the expression of specific stress proteins. Hypothetically, -1 frameshifting events induced by yW decrease might direct translating ribosomes to premature stop codons, thereby regulating the expression of

specific stress response proteins through a nonsense-mediated decay mechanism (NMD) (Waas et al., 2007).

In yeast, a uridine at the wobble position is generally modified to ncm^5U, ncm^5Um, mcm^5U or mcm^5s^2U. A mcm^5s^2U34 wobble nucleoside is essential for the function of $tRNA^{Lys}$ and $tRNA^{Glu}$, both containing U34–U35 nucleosides in their anticodons and reading A/G-ending codons in split codon boxes. The unmodified U34–U35–U36 anticodon sequence from the $tRNA^{Lys}$ has a poor stacking capacity and does not even form a normal anticodon loop unless it contains mcm^5s^2U (Ashraf et al., 1999; Durant et al., 2005). However, this modified base allows counteracting the usually weak interaction with the A-rich codons, thereby increasing the efficiency of cognate codon reading. Remarkably, mcm^5s^2U also mediates aminoacylation activity in $tRNA^{Lys}$ and $tRNA^{Glu}$.

A decrease in mcm^5s^2U occurs quite specifically in WT BY4742 cells under As_3O_2 and ethanol exposure, but the cellular consequences of this phenotype are still unknown. The last step in the synthesis of both mcm^5s^2U and mcm^5U is catalized by the same enzyme but only one of the modifications is significantly reduced. Since their occurrence in tRNAs is distinct (see Table 3.3), this result indicates a specific degradation of $tRNA^{Lys}_{AAA}$ and $tRNA^{Glu}_{GAA}$ under stress exposure. Endonucleolytic cleavage of tRNAs is also known to occur as a conserved response to several stress conditions in yeast, most remarkably oxidative stress (Thompson et al., 2008) or by other quality control degradation pathways activated in response to reduced levels of specific tRNA modifications (Alexandrov et al., 2006; Chernyakov et al., 2008).

Both Δ*hsp104* and Δ*yap1,2* cells show a general decrease in the level of tRNA modification under As_3O_2 stress. Since quantification of tRNA modifications provides information mainly concerning population-level changes, the observed variations could result from changes in the activity and expression of modifying enzymes, tRNA degradation mechanisms or even changes in the number of tRNA copies. The distinct modification patterns observed for each strain under stress indicates differential cellular susceptibility and results from the activation of singular cytotoxicity or survival mechanisms, activated by each of the toxicants.

Table 3.3 - Identity and location of the tRNA modifications affected by the conditions tested in our study. Occurance is represented by the anticodon sequence.

tRNA modification	Position	Occurence in tRNAs Anticodon (5' – 3')	Gene responsible for modification
I (Inosine)	34	Ser (IGA), Thr (IGU), Val (IAC), Ala (IGC), Arg (ICG), Ile (IAU)	*TAD2, TAD3*
m^1A (1-methyladenosine)	58	Lys, (CUU), Lys (mcm^5s^2UUU), Met (CUA), Phe (GmAA), Pro (ncm^5UGG), Thr (IGU), Trp (CmCA), Tyr (GYA), Val (IAC), Val (CAC), Val (ncm^5UAC), Arg (ICG), Arg (mcm^5UCU), Asn (GUU), Cys (GCA), Ile (IAU), Ile (YAY), Leu, (UAG), Leu (ncm^5UmAA)	*TRM6, TRM61*
i^6A (N^6-isopentenyladenosine)	37	Ser (IGA), Ser (UGA), Ser (CGA), Tyr (GYA), Cys (CGA)	*Unknown*
t^6A (N^6-threonylcarbamoyladenosine)	37	Lys, (CUU), Lys (mcm^5s^2UUU), Met (CUA), Thr (IGU), Arg (mcm^5UCU), Asn (GUU), Ile (IAU), Ile (YAY),	*MOD5*
Am (2'-O-methyladenosine)	4	His (GUG)	*Unknown*
m^5C (5-methylcytidine)	34	Leu (m^5CAA)	*TRM4*
	40	Met (CUA)	
	48	Lys, (CUU), Lys (mcm^5s^2UUU), Met (CUA), Pro (ncm^5UGG), Ser (IGA), Ser (UGA), Ser (CGA), Trp (CmCA) Asn (GUU), Cys (GCA), Ile (IAU), Ile (YAY), Leu (m^5CAA), Leu,(UAG), Leu (ncm^5UmAA)	
	49	Lys (mcm^5s^2UUU), Met (CUA), Tyr (GYA), Val (IAC), Val (CAC), Val(ncm^5UAC), Arg (ICG), Asp (GUC), Glu (mcm^5s^2UUC), Gly (GCC), His (GUG)	
Cm (2'-O-methylcytidine)	32	Phe (GmAA), Trp (CmCA), Leu (ncm^5UmAA)	*TRM7*
	34	Trp (CmCA)	*TRM7*
	4	Pro (ncm^5UGG), Gly (GCC), Gly (UCC)	*Unknown*
$m^2{}_2G$ (N^2,N^2-dimethylguanosine)	26	Lys, (CUU), Lys (mcm^5s^2UUU), Met (CUA), Phe (GmAA), Ser (IGA), Ser (UGA), Ser (CGA), Thr (IGU), Tyr (GYA), Val (ncm^5UAC), Ala (IGC), Arg (ICG), Arg (mcm^5UCU), Asn (GUU), Leu (m^5CAA), Leu, (UAG), Leu (ncm^5UmAA)	*TRM1*
Gm (2'-O-methylguanosine)	18	Ser (IGA), Ser (UGA), Ser (CGA), Trp (CmCA), Tyr (GYA), His (GUG), Leu (m^5CAA), Leu(UAG), Leu (ncm^5UmAA)	*TRM3*
	34	Phe (GmAA)	*TRM7*
yW (Wybutosine)	37	Phe (GmAA)	*TRM5*
m^5U (5-methyluridine)	54	Lys, (CUU), Lys (mcm^5s^2UUU), Met (CUA), Phe (GmAA), Pro (ncm^5UGG), Ser (IGA), Ser (UGA), Ser (CGA), Thr (IGU), Trp (CmCA), Tyr (GYA), Val (IAC), Val (CAC), Val (ncm^5UAC), Ala (IGC), Arg (ICG), Arg (mcm^5UCU), Asn (GUU), Asp (GUC), Cys (GCA), Glu (mcm^5s^2UUC), Gly (GCC), Gly (UCC), His (GUG), Ile (IAU), Ile (YAY), Leu (m^5CAA), Leu, (UAG), Leu (ncm^5UmAA)	*TRM2*
Um (2'-O-methyluridine)	44	Ser (UGA), Ser (CGA), Thr (IGU)	*Unknown*
mcm^5U (5-methoxycarbonylmethyluridine)	34	Arg (mcm^5UCU)	*TRM9, ELP1 - 6, KTI11 - 13*
mcm^5s^2U (5-methoxycarbonylmethyl-2-Thiouridine)	34	Lys (mcm^5s^2UUU), Glu (mcm^5s^2UUC)	*TRM9, NFS1, ELP1 - 6, KTI11 - 13*

Most of the modifications outside the anticodon loop are simple methylations or thiolations, which play many important roles in tRNA folding or stability, also establishing major synergistic structural interactions. Under As_3O_2 exposure, Δ*hsp12* cells show a unique change in the level of 2'-O-methylation of the ribose sugar (see Figure 3.8 b), through an increase in Am and Um. These modifications are usually associated with a small number of long variable loop tRNAs , (see Table 3.3) and play a very important role in tRNA structure and stability (Kotelawala et al., 2008). Mature $tRNA^{Ser}_{CGA}$ and $tRNA^{Ser}_{UGA}$ from strains lacking Um and ac^4C are preferential targets for degradation by 5' – 3' exonucleases (Kotelawala et al., 2008), by a mechanism known as rapid tRNA decay (RTD) (Alexandrov et al., 2006).

3.4.4. Aminoacylation as a ROS target

The main cellular source of ROS is the mitochondria, where multiple one-electron transfer reactions take place. Mistranslation increases ROS production (superoxide and H_2O_2), suggesting that it disrupts mitochondrial function (Lima-Costa T et al., unpublished). A small number of transit electrons within the electron transport chain might be diverted to oxygen at intermediate points, namely at complexes I and III. This will eventually lead to generation of superoxide radical anions, which are later transformed into mitochondrial H_2O_2 and other ROS (Merry, 2004). Recent studies indicate that ROS may also be generated by soluble enzymes located at the mitochondrial matrix, such as pyruvate and α-ketoglutarate dehydrogenases (Starkov et al., 2004). Cells have acquired numerous defense mechanisms against ROS, such as superoxide dismutase and non-enzymatic reductant systems including glutathione (GSH) and thioredoxin (TRX), which can also work as cofactors for anti-oxidant enzymes. Permanent regeneration of reduced GSH or TRX is therefore essential and occurs through the action of NADPH-requiring GSH and TRX reductases (Jamieson, 1998). GSH and TRX are regenerated by NADPH-requiring GSH and TRX reductases, making NADPH pivotal for efficient cellular anti-oxidant defenses.

In the cytosol, the reduction of $NADP^+$ to NADPH is catalyzed by enzymes in the pentose phosphate pathway, including glucose-6-phosphate dehydrogenase and 6-phosphogluconate dehydrogenase (Pandolfi et al., 1995). The activity of Pos5p, a NADH kinase from the mitochondrial matrix, is one of the major NADPH sources in yeast (Outten & Culotta, 2003). Therefore, yeast mitochondria employ NADH preferentially over $NADP^+$ for the generation of NADPH and seem to exploit numerous overlapping pathways for NADH recycling.

Plasma membrane electron transport (PMET) is a ubiquitous property of living cells. The presence of a NADH-oxidizing pathway in *S. cerevisiae* in the form of PMET (Herst et al., 2008) might explain the lower accumulation of ROS in Δ*hsp12* mistranslating cells. Hypothetically, the role of Hsp12 in plasma membrane organization is somehow influencing the activity of the plasma membrane NADH – oxidizing pathway. *HSP12* deletion might therefore contribute to NADH accumulation and concomitantly to increased NADPH availability for defense mechanisms. Interestingly, a physical interaction between Hsp12p and Gnd2p was recently described (Tarassov et al., 2008). Gnd2p is a plasma membrane 6-phosphogluconate dehydrogenase that catalyzes a NADPH regenerating reaction in the pentose phosphate pathway and is therefore pivotal to protect yeast from oxidative damage (Izawa et al., 1998a). However, to confirm the above hypothesis it is necessary to quantificatify NAD^+/NADH and $NADP^+$/NADPH ratios in Δ*hsp12* mistranslating cells.

Many methionine residues in proteins are strategically placed to act as catalytic anti-oxidants, by readily reacting with a variety of ROS to form methionine sulfoxide and therefore protect both proteins and other macromolecules from permanent damage (Vogt, 1995; Luo & Levine, 2009). Cellular methionine sulfoxide reductases then catalyze the thioredoxin-dependent reduction of methionine sulfoxide back to methionine (Levine et al., 1996).

The role of methionine residues as endogenous antioxidants was known for a while, but only recent studies showed how this protection mechanism works. In eukaryotes, the elongation factor EF-1α is not known to discriminate misacylated tRNAs, consistent with mismethionylated tRNAs being used in translation. Met-misacylation

results in methionine substitution mostly at surface-exposed residues or near the active site of target proteins. In mammalian cells, Met-misacylation is actively regulated upon exposure to oxidative damaging stresses (Netzer N et al., 2009).This surprisingly demonstrated that a certain level of misacylation may be beneficial to the cell. In addition, our results showed that induced codon misreading increases Met misacylation in WT By4742 and Δ*yap1,2* cells, most probably due to an increase in ROS. Indeed, the stronger misacylation signals were observed in Δ*yap1,2* mistranslating mutants, which show a particular susceptibility to ROS, due to deficient anti-oxidant defense mechanisms.

The observed tRNA misacylation can most likely be explained by MetRS mischarging of non-methionyl-tRNAs. Hypothetically, MetRS may exist in two forms with distinct aminoacylation accuracy. The transition from one form to the other could be mediated by reversible post-translational modification triggered in response to increased ROS. Oxidation of Met residues in MetRS is an appealing possibility, but further studies are needed to confirm this hypothesis. Reprogramming of tRNA modifications due to increased ROS production might also promote non-methionyl-tRNAs acylation. Aditionally, subtle alterations in the amount of the individual misacylated tRNAs might occur due to stress-related degradation (Thompson et al., 2008). The number of Met mischarged tRNAs in Δ*hsp12* non-mistranslating cells increased significantly relative to WT BY4742. *HSP12* deletion might affect plasma membrane organization and therefore membrane permeability to amino acids, including ^{35}S-methionine. However, expression of Hsp12p is typically low at exponential phase and therefore no observable effects were expected of the deletion.

In conclusion, in this chapter we confirm that environmental stress impacts components of the translational machinery, both by triggering protein aggregation and by reprogramming of tRNA modifications. Future studies should focus on the link between these mechanisms and low-level mistranslation measured in chapter 2, mostly in Δ*hsp12* cells. On the other hand, constitutive mistranslation is linked with increased ROS in BY4742 cells and this promotes Met-misacylation, a protection mechanism that might determine adaptation to changing environmental conditions.

Chapter 4

Characterization of Δ*hsp12* mistranslating yeast

4.1. Introduction

The proteome quality control mechanisms are multilayered, involving a complex network of players that act both during protein synthesis and downstream, controlling the fate of cellular misfolded proteins. In this study we destabilize the yeast proteome using a misreading tRNA from *C. albicans* ($tRNA_{CAG}^{Ser}$) which misincorporates 1,4% serine at leucine CUG codons (Silva et al., 2007). Previous studies showed that such mistranslation activates the general stress response mediated by the transcription factors Msn2p and Msn4p. Amongst the most up-regulated genes were *HSP12*, *HSP26*, *HSP70* (*SSA4*), *HSP104* and drug-resistance as well as protein degradation genes. Mistranslation also decreased sporulation and mating efficiency and produced cell population heterogeneity (Silva et al., 2007).

Surprisingly, such translational errors are tolerated and may even be advantageous under adverse environments, by generating phenotypic and genetic diversity as well as promoting stress cross-protection (Santos et al., 1999; Silva et al., 2007). This might explain the deficient editing of non-cognate aminoacyl-tRNAs in pathogenic *Mycoplasma* spp. Similarly, substitutions in IleRS from *Acinetobacter baylyi* that favour mischarging of $tRNA^{Ile}$ with Val favour cell growth under conditions of limiting Ile. Supposedly, high Val incorporation in the proteome balances the limited availability of Ile (Bacher et al., 2007). *C.albicans,* for example, can tolerate up to 28% of leu misincorporation at specific Ser sites ans uses such ambiguity for stress adaptation. Finally, as described in the last chapter, Met misacylation is known to increase in response to growing levels of ROS, in order to protect cells from the effects of oxidative damage. Remarkably, this mechanism is conserved from fungal to mammalian cells (Netzer et al., 2009). Therefore, biological systems are not error free and errors may even be beneficial in certain physiological conditions, promoting phenotypic variation and thereby potential evolutional improvement (Kvitek et al., 2008; Lopez-Maury et al., 2008).

Activation of the environmental stress response (ESR) program results in modulation of gene expression, to assure cellular adaptation, cross-protection and survival after a

shift to an unfavourable environment (Gasch AP et al., 2000). To our surprise, the response of Δ*hsp12* cells to environmental stress includes a significant increase in the measured rate of mRNA mistranslation (Chapter 2, table 2.4 and 2.5). However, in the light of present knowledge on Hsp12p such observations cannot be explained. To go deep into this question, Δ*hsp12* cells were transformed with the misreading $tRNA_{CAG}^{Ser}$ to induce constitutive mistranslation. Phenotypic assays and DNA microarrays were used to obtain a global view of stress tolerance and gene expression responses. Surprisingly, more than an extensive response to stress, constitutive mistranslation induced a deep change in cellular metabolic networks involved in generation of energy and biosynthetic intermediates.

4.2. Material and Methods

4.2.1 Strains and growth conditions

The bacterial strain JM109 (endA1 glnV44 thi-1 relA1 gyrA96 recA1 $mcrB^+$ Δ(lac-proAB) e14- [F' traD36 $proAB^+$ $lacI^q$ lacZΔM15] hsdR17($r_K^-m_K^+$)) was recurrently used for plasmid amplification and grown at 37°C in Lysogeny Broth (LB) medium (Formedium) or LB 2% agar (Formedium), both supplemented with 50 µg/mL ampicillin (Sigma-Aldrich) when required.

Table 4.1 - *S.cerevisiae* strains used in the current study.

Strain	Genotype	Source
BY4742	*MATα ; his3Δ 1; leu2Δ 0; lys2Δ 0; ura3Δ 0*	Euroscarf
Δ*hsp104*	BY4742 ; YLL026W::kanMX4/ YLL026W::kanMX4	Euroscarf
Δ*hsp12*	BY4742 ; YFL014W::kanMX4/ YFL014W::kanMX4	Euroscarf
Δ*yap1*Δ*yap2*	BY4742 ; YML007W::kanMX4/ YDR423C::HIS3	(Azevedo D. et al., 2007)

Yeast cells were cultured at 30°C in rich YPD medium (1% yeast extract, 2% Peptone and 2% Glucose) or selective minimal medium (MM – 0.67% yeast nitrogen base, 2%

glucose and 0.2% Drop-out mix, lacking only the amino acids corresponding to the selection markers). Geneticin (G418) (Formedium) was used at a concentration of 200µg/L. Solid media required agar up to 2%. All media were sterilized by autoclave at 120 ºC for 15 – 20 min.

4.2.2. Plasmids

The *S.cerevisiae* plasmids used in this study are specified in Table 4.2.

Table 4.2 - Plasmids used in the current study.

Plasmid	Description	Source
pRS315	Single-copy LEU2 vector	(Santos MA et al., 1996)
pUKC715	Single-copy LEU2 vector containing the *C. albicans* G33 Ser-tRNA$_{CAG}$ gene.	(Santos MA et al., 1996)

4.2.3. Yeast transformation by the lithium acetate (LiAc) method

For efficient transformation of *S.cerevisiae* we adapted the LiAc/SS carrier DNA/PEG method (Gietz RD & Woods RA, 2006), with a few modifications. Fresh yeast colonies were picked and grown overnight at 30ºC/180 rpm in YPD rich medium. Overnight cultures were then diluted 1:1000, grown to mid-log (OD_{600} 0,5) and harvested by centrifugation at 4000rpm. After washing with 5mL of sterile mQ water, the pellet was resuspended in 50µL of 0,1M LiAc solution and the following reagents were added in the designated order : 500µL 50% (w/w) PEG, 25µL single-stranded carrier DNA (2mg/mL) previously denatured for 5min. at 95ºC and 0,1 – 1µg of the pRS315 or pUKC715 plasmids (Gietz RD & Woods RA, 2006). Tubes were vortexed immediately until the mixture was homogeneous and then subjected to heat-shock at 42ºC for 45 min. Cells were then harvested by centrifugation at 5000rpm, the supernatant was

discarded, the pellet resuspended in 100 µL of sterile mQ water and plated in selective media plates that were then incubated at 30ºC until visible colonies appeared.

4.2.4. Growth curves

Yeast cells transformed with the pRS315 or pUKC715 single-copy plasmids were grown overnight at 30ºC in selective MM lacking leucine, as described in section 4.2.1. Overnight cultures were then diluted to an initial 0,01 OD_{600} and their growth at 30ºC/180 rpm was followed until stationary phase by measuring OD_{600} at various time points. Growth rate was calculated in exponential phase as the slope of the log transformed ODs, according to (Toussaint & Conconi, 2006).

4.2.5. Phenotyping assay

Yeast cells carrying the pRS315 or the pUKC715 single-copy plasmids were grown at 30ºC to mid – log (OD_{600} 0,5). After harvesting, $1x10^7$ cells were collected and resuspended in PBS. Five ten-fold dilutions were then plated in MM lacking leucine and containing the appropriate stress (table 4.3) or a no-stress control, using a liquid handling station (Caliper LifeSciences). Cells were grown at 30ºC and photographed after 4 days. Colony size was determined using an ImageJ colony detector plug-in (Patch Detector Plus). As a growth measure, a percentual score was obtained adopting a method previously described (Homann et al., 2009). Briefly, the average colony size obtained from the three lowest dilutions was calculated and normalized with the corresponding undiluted size value, for each strain and stress condition. The viability of each strain under stress was calculated relative to the no-stress control for each strain. All experiments were done with three biological replicates.

Table 4.3 - Environmental stressors used during the current phenotyping assay.

Stressor	Concentration
As_2O_3	200 and 400μM
$CdCl_2$	125, 60 and 30μM
LiCl	40mM
Ethanol	5%

4.2.6. Statistics

Data is reported as mean ± SEM or SD. Differences are considered significant when p < 0,05. Significance was tested by one-way ANOVA post Dunnett's multiple comparison test or two-tailed unpaired Student's t-Test, with CI 95%. Most of the statistical tools are available in the GraphPad Prism 5.0 software.

4.2.7. RNA extraction

Yeast cells carrying the pRS315 or the pUKC715 single-copy plasmid were grown at 30ºC to mid – log (OD600 0,5) in minimal medium lacking leucine, quickly harvested by centrifugation at 4000 rpm and immediately frozen by immersion in liquid nitrogen, before storing at -80ºC. Pellets were thawed by resuspending them in a 1:1 mixture of lysis buffer (10 mM Tris pH 7,5; 10 mM EDTA; 0,5% SDS) and acid phenol chloroform 5:1 (pH 4,7) (Sigma-Aldrich) and vortexing vigorously. The cell suspensions were then immediately incubated in a water bath at 65ºC and vortexed every 10 min. After 1h, the RNA aqueous phase was recovered by centrifugation at 8000g for 30 min at 4ºC and then transferred to a new tube for new re-extraction, first with 4ºC acid phenol chloroform 5:1 (pH 4,7) and then with chloroform Isoamyl Alcohol 24:1 (Fluka). RNA was then precipitated overnight at -30ºC with 3 vol. of ethanol and 0,1 vol. of 3M NaOAc/HOAc pH 5,2. After harvesting by centrifugation (at 8000g for 30 min, 4ºC) RNA was washed in 70% ethanol and resuspended in mQ water to a final concentration of 1μg/μl.

4.2.8. One-Color Microarray-Based Gene Expression Analysis

Microarray analysis was carried out with Agilent whole *S.cerevisiae* genome oligonucleotide microarrays. Synthesis of Cy3-labeled cRNA was performed with the Agilent's Low Input Quick Amp Labelling Kit, according to the manufacturer's recommendations (see figure 4.1 for a general workflow). Briefly, 200 ng of total RNA were first used as template for cDNA synthesis, which was then incubated with T7 RNA polymerase for simultaneously amplification and cyanine 3-labeled CTP incorporation. The resulting cRNA was then mixed with ethanol 100% and purified on Qiagen's RNeasy mini spin columns, also according to the manufacturer's recommendations. The cleaned cRNA sample was eluted from the columns with RNase-free water and quantified using the NanoDrop®1000 Spectrophotometer (Thermo Scientific). After determining the yield (µg) and specific activity (pmol Cy3 per µg cRNA) of the labelling reactions, 600 ng of Cy3-lableled cRNA from each condition were prepared for hybridization.

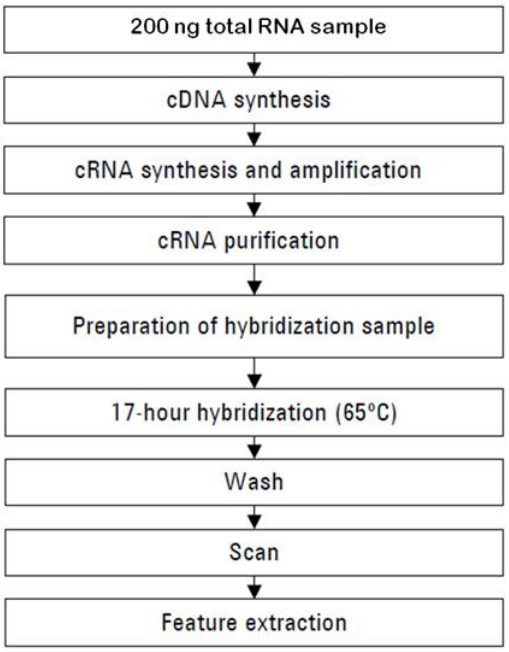

Figure 4.1 - Workflow for sample preparation, array hybridization and analysis.

cRNA fragmentation (30 min. at 60ºC), array hybridization (17 hours at 65ºC) and washing steps (0.005% triton X-102 wash buffer) were also carried out as recommended by the one-color microarray gene expression protocol supplied by the manufacturer (Agilent Technologies).

4.2.9. Microarray data analysis

Images from the hybridized microarrays were acquired by using the Agilent G2565AA scanner. Row data extraction was performed with Agilent's Feature Extraction software resorting to the recommended default extraction protocol file. Values were median normalized across arrays using BRB - ArrayTools v3.4.0, to correct the differences in labeling and hybridization efficiency. Data was then exported to MeV TM4.6.0 (TIGR, Rockville, MD) for calculation of $\log_2$ intensity ratios (M values) and discrimination of differentially expressed genes ($p<0.05$; fold change cut-off of 1.5). Functional annotation analysis of expression data was done using DAVID Bioinformatics Resources (Modified Fisher Exact test; Benjamini-Hochberg correcton for multiple testing, $p<0.05$) (Hosack et al., 2003; Huang et al., 2009) and the PRomoter Integration in Microarray Analysis (PRIMA) tool, included in the Expander 5.0 software (Fischer Exact test; Bonferroni correction for multiple testing, $p<0.05$) (Ulitsky et al., 2010). Results were presented as fold-enrichment for each GO term.

The fold-enrichment for a GO term is defined as a ratio of two proportions. It represents the ratio between the numbers of genes differentially expressed belonging to a specific GO term and the total number of genes differentially expressed, which have at least one GO annotation. This ratio is then compared to the ratio between the total number of genes in the GO term and the total number of genes in the *S.cerevisiae* genome with at least one GO annotation.

4.3. Results

4.3.1. Mistranslation and adaptation to environmental stress

As mentioned previously, yeast cells adapt to stress challenges by reprogramming gene expression (Gasch AP et al., 2000). Each environmental change imposes specific cellular demands, triggering a unique expression program. Nonetheless, a large number of genes have been implicated in a general yeast response to a wide variety of stressful conditions (Mager & De Kruijff, 1995; Ruis & Schuller, 1995; Gasch AP et al., 2000). *HSP12* is part of this specific gene expression program and is important for survival under high temperature, high ethanol concentrations, glucose starvation and cell wall stress, amongst others (Piper et al., 1994; Varela JC et al., 1995; Kandror O et al., 2004). Our previous results showed that Δ*hsp12* cells exposed to environmental stress are particularly susceptible to mRNA mistranslation (Chapter 2, table 2.4 and 2.5). No straight connection has yet been established between Hsp12p and the protein synthesis machinery and so, this effect on translational fidelity could be related with indirect changes in the function of proteins involved in translational fidelity. Cellular stress might contribute to this phenotype by wasting the degradative and folding machinery and probably even by a direct effect on the ribosome.

Here, we analyzed phenotypic variation in mistranslating cells under exposure to As_2O_3 , $CdCl_2$ and non-lethal concentrations of ethanol, LiCl and CrO_3, associated previously with an increase in the rates of stop codon readthrough and/or AGC misreading (Chapter 2, table 2.4 and 2.5) (Holland S et al., 2007). These conditions decreased stress tolerance both in WT, Δ*hsp12* and Δ*hsp104* mistranslating cells relatively to controls (empty plasmid) from the isogenic strain (see figure 4.3 a). Δ*hsp12* shows particular susceptibility to ethanol exposure. On the other hand, BY4742, Δ*hsp104* and Δ*yap1,2* mistranslating cells show increasing tolerance to highly inhibitory cadmium concentrations (Figure 4.3 a and b). A similar effect was observed in Δ*yap1,2* cells exposed to inhibitory amounts of As_2O_3 (400μM) (Figure 4.3 b). However, mistranslation in Δ*hsp12* cells did not produce visible selective advantages

under these conditions. Generally, our results indicate that mild stress decreases the viability of mistranslating cells. However, under more severe stress conditions mistranslation increases the chances of cell survival.

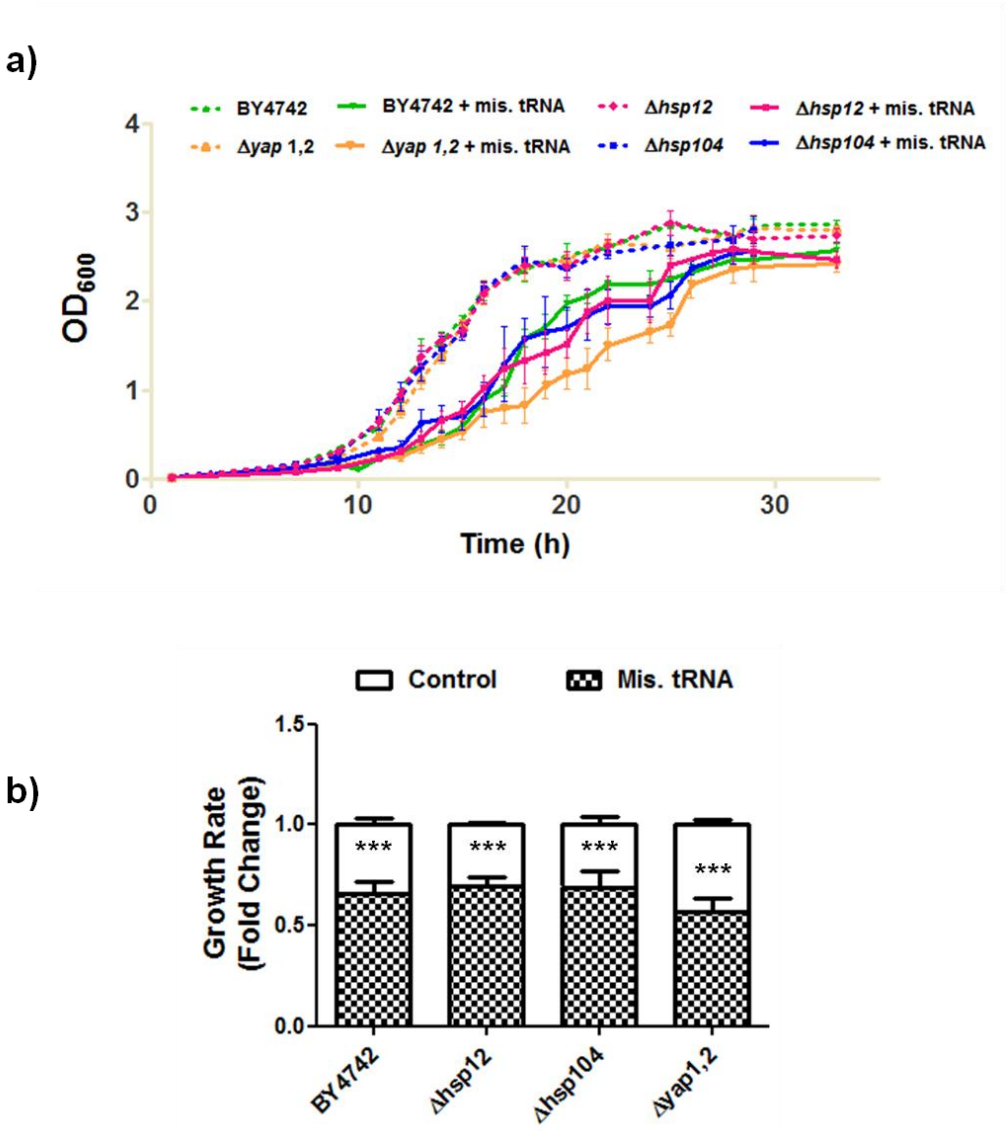

Figure 4.2 - Constitutive mistranslation slows yeast growth rate. a) growth of control cells with an empty plasmid (pRS315) or cells expressing the misreading $tRNA_{CAG}^{Ser}$ in MM lacking leucine was monitored by absorbance at 600 nm until stationary phase **b)** quantification of the fold change in growth rate under constitutive mistranslation. *** ($P<0.001$) represent values significantly different from cells harbouring an empty plasmid (two-tailed unpaired Student's t-Test). Values are mean ± SEM. The results correspond to three independent experiments.

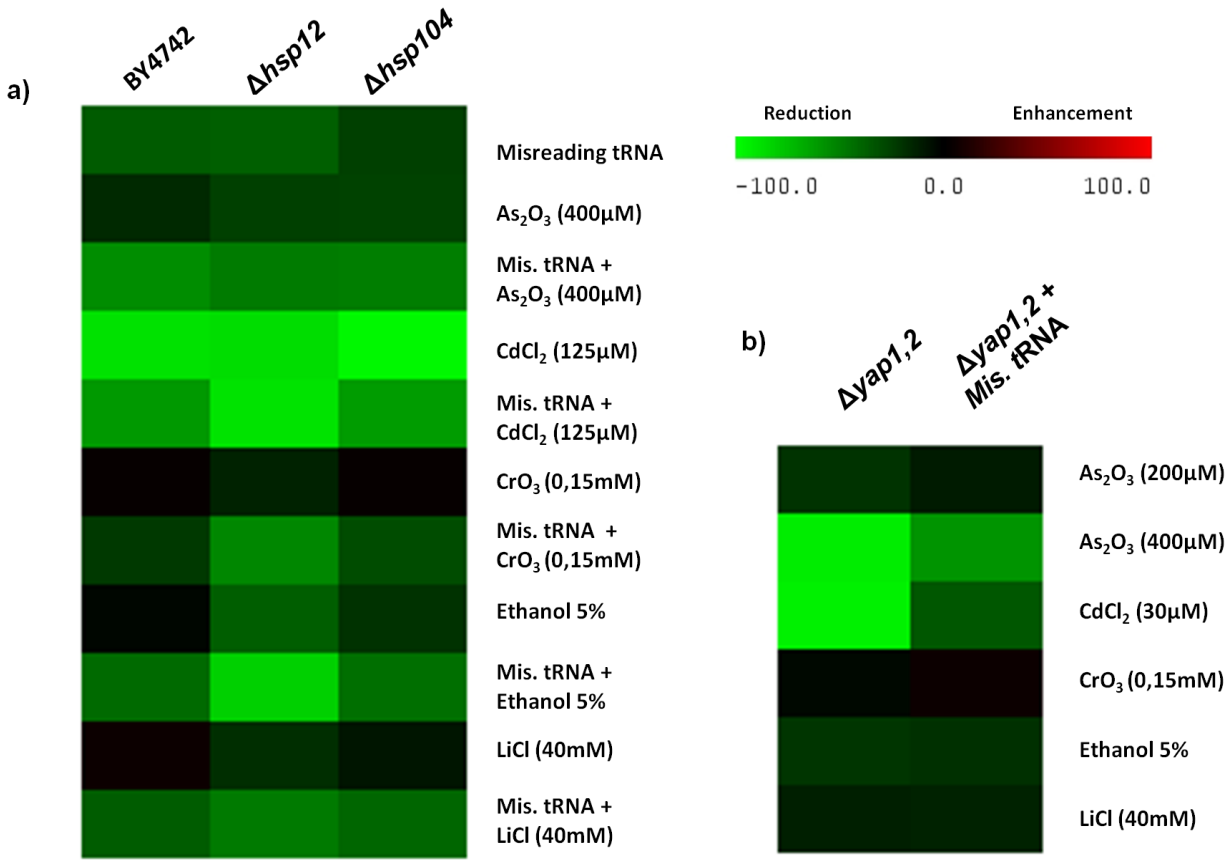

Figure 4.3 - **Phenotypic responses of mistranslating cells under environmental stress.** Mistranslation impacts stress tolerance in BY4742 WT and gene deletion cells **a)** and **b)** heat map representing the percentage of stress tolerance in exposed cells relative to that of the unexposed cells from the isogenic strain. Control cells (empty plasmid) or cells expressing the *C.albicans* $tRNA_{CAG}^{Ser}$ (misreading tRNA) were grown to mid-log (0,5 – 0,6 OD_{600}) in MM lacking leucine and suspended in PBS buffer. Serial dilutions (10^7 and 10^3 cells/ml) were then spotted onto solid minimal media supplemented with the toxics in the mentioned concentrations.

4.3.2. Transcriptomic analysis of Δ*hsp12* mistranslating cells

The Δ*hsp12* mistranslating cells (see Figure A4 in Annexes) were further characterized using DNA microarrays. Surprisingly, only 45 of the yeast genes (~6200) were repressed in Δ*hsp12* mistranslating cells. Functional enrichment identified genes corresponding to nucleolar proteins related with ribosome biogenesis and rRNA processing (see figure 4.4), such as *ESF1*, *RRP14*, *NOP13*, *UTP7*, *PXR1*, *FPR3*, *KRI1* or *NHP2*. Genes coding large ribosomal subunit proteins such as *RRP14*, *RPL36A*,

RPL18A, *RPL18B*, *RPL23A*, *RPL23B* and *RPL7A* and mitochondrial ribosomal protein genes (*VAR1*) were also repressed. Since the ribosome cellular content is proportional to growth rate (Rudra & Warner, 2004), this gene repression is in agreement with previously described results (see figure 4.2). In addition, the repression of ribosomal protein genes is linked with numerous stress responses (Warner, 1999), functioning as a vital mechanism for conservation of resources and energy.

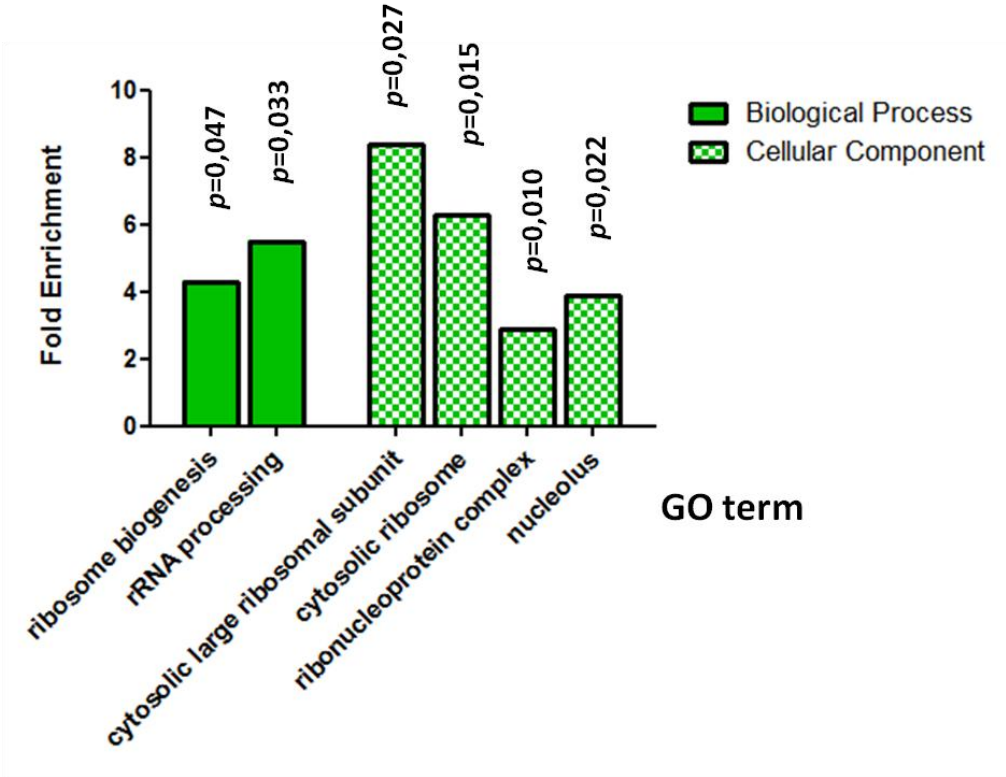

Figure 4.4 - Functional Enrichment Analysis of down-regulated genes in Δ*hsp12* mistranslating cells. Differentially expressed genes were calculated relative to BY4742 WT cells and analyzed for enriched functional classes using DAVID Bioinformatics Resources. Significant categories were determined based on a modified Fisher Exact Test with Benjamini-Hochberg multiple hypothesis correction (corrected p<0.05) (Hosack et al., 2003 and Huang D et al., 2009).

A large number of genes were up-regulated by mistranslation. Functional enrichment analysis of these genes allowed identification of classes mostly related with cellular metabolic networks involved in generation of energy or biosynthetic intermediates,

namely carbohydrate and vacuolar protein catabolic processes, sulfur compound metabolic processes, tricarboxylic acid cycle (TCA cycle) and amino acid biosynthesis. Also noteworthy was the induction of genes involved in cofactor metabolism, most specifically vitamin biosynthesis and utilization of acetyl-CoA or NADH (see figure 4.5). Facultative fermentative yeasts such as *S.cerevisiae* display a respiratory or fermentative metabolism depending on growth conditions, the type and concentration of sugars or oxygen availability. Under aerobic conditions and in the presence of high glucose concentrations, *S.cerevisiae* clearly diverges from other facultative fermentative yeasts by favouring alcoholic fermentation over an energetically more efficient respiratory dissimilation of glucose. This phenomenon is described as the Crabtree effect (Swanson & Clifton, 1948; Pronk et al., 1996), resulting from glucose transcriptional repression of respiratory enzymes synthesis and overflow of pyruvate into ethanol fermentation reactions (Kappeli, 1986). Glucose control of metabolic mechanisms might also occur by inhibition of enzyme activity. After uptake, each glucose molecule is broken through glycolysis into two molecules of pyruvate, with a net yield of two ATP. Pyruvate is located at a key metabolic branch-point between alcoholic fermentation, pulled by increasing glucose concentrations, and the respiratory breakdown of sugars, resulting in synthesis of acetyl-CoA. The tricarboxylic acid (TCA) cycle provides reducing equivalents to the respiratory chain through the oxidative decarboxylation of acetyl–CoA, but is glucose repressed in Crabtree-positive yeasts. Under these conditions, the TCA cycle operates in a branched fashion, functioning primarily to fulfil biosynthetic demands by providing the building blocks of essential molecules such as amino acids and nucleotide bases (Pronk et al., 1996; Gombert et al., 2001). Remarkably, our transcriptomic analysis portrays a distinct metabolic regulation.

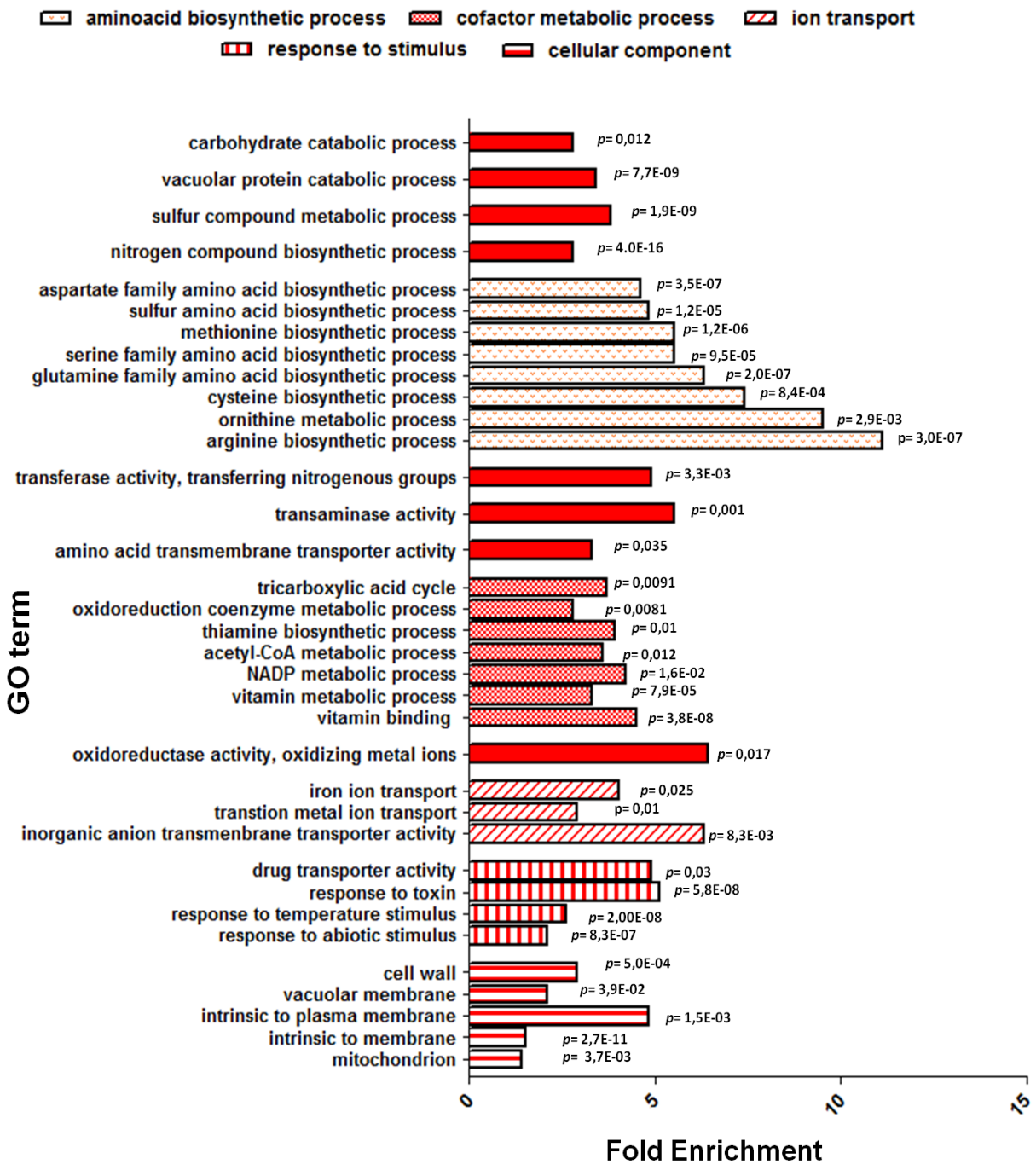

Figure 4.5 - Functional Enrichment Analysis of up-regulated genes in Δ*hsp12* mistranslating cells. Differentially expressed genes were calculated relative to BY4742 WT cells and analyzed for enriched functional classes using DAVID Bioinformatics Resources. Significant categories were determined based on a modified Fisher Exact Test with Benjamini-Hochberg multiple hypothesis correction (corrected p<0.05) (Hosack et al., 2003 and Huang D et al., 2009).

A significant up-regulation of *PKP2*, coding for mitochondrial protein kinase, might negatively regulate the activity of the pyruvate dehydrogenase complex, diverging pyruvate to acetaldehyde synthesis by decarboxylation. However, our mRNA profile offers evidences of alternate pyruvate dehydrogenase bypass pathways, involving up-regulation of minor isoforms of pyruvate decarboxylase (*PDC5* and *PDC6*) and acetyl-CoA synthetase (*ACS1*), tipically glucose regulated (Hohmann et al., 1991; de Jong-Gubbels et al., 1997), as well as of carnitine acetyltransferase (*YAT2*), responsible for acetyl-CoA transport into the mitochondria (see figure 4.6). Our data further suggests that pyruvate might first be decarboxylated to acetaldehyde in the cytosol and then converted to acetate by the mitochondrial acetaldehyde dehydrogenases (*ALD4* and *ALD5*), also significantly up-regulated. The acetate produced can be converted into acetyl-CoA in the cytosol or excreted in the culture medium (Boubekeur et al., 2001). *ALD4* is glucose repressed, while *ALD5*, encoding a minor isoform, is constitutively expressed (Wang et al., 1998; Tessier et al., 1998). Furthermore, the up-regulation of genes corresponding both to the pyruvate decarboxylase (*PYC1*) and mitochondrial oxaloacetate carrier (*OAC1*) indicates increased influx of oxaloacetate in the TCA cycle (see figure 4.6). Indeed, our data show significant enrichment in a number of TCA cycle catalytic components, such as members of the mitochondrial alpha-ketoglutarate dehydrogenase complex (*KGD1*), citrate synthase (*CIT3*) and isocitrate dehydrogenase (*IDP1*, *IDP2*) isoforms.

The pyruvate descarboxylase reaction depends on the cofactor thiamine pyrophosphate (TPP), derived from vitamin B_1. *S.cerevisiae* is able to synthesize thiamin pyrophosphate (TPP) *de novo* but can also efficiently uptake thiamin from the extracellular environment, using it to produce TPP (Wightman & Meacock, 2003). Indeed, our results indicate an up-regulation of *THI5*, *THI11*, *THI12* and THI13, which compose a subtelomeric gene family responsible for the synthesis of thiamine precursors.

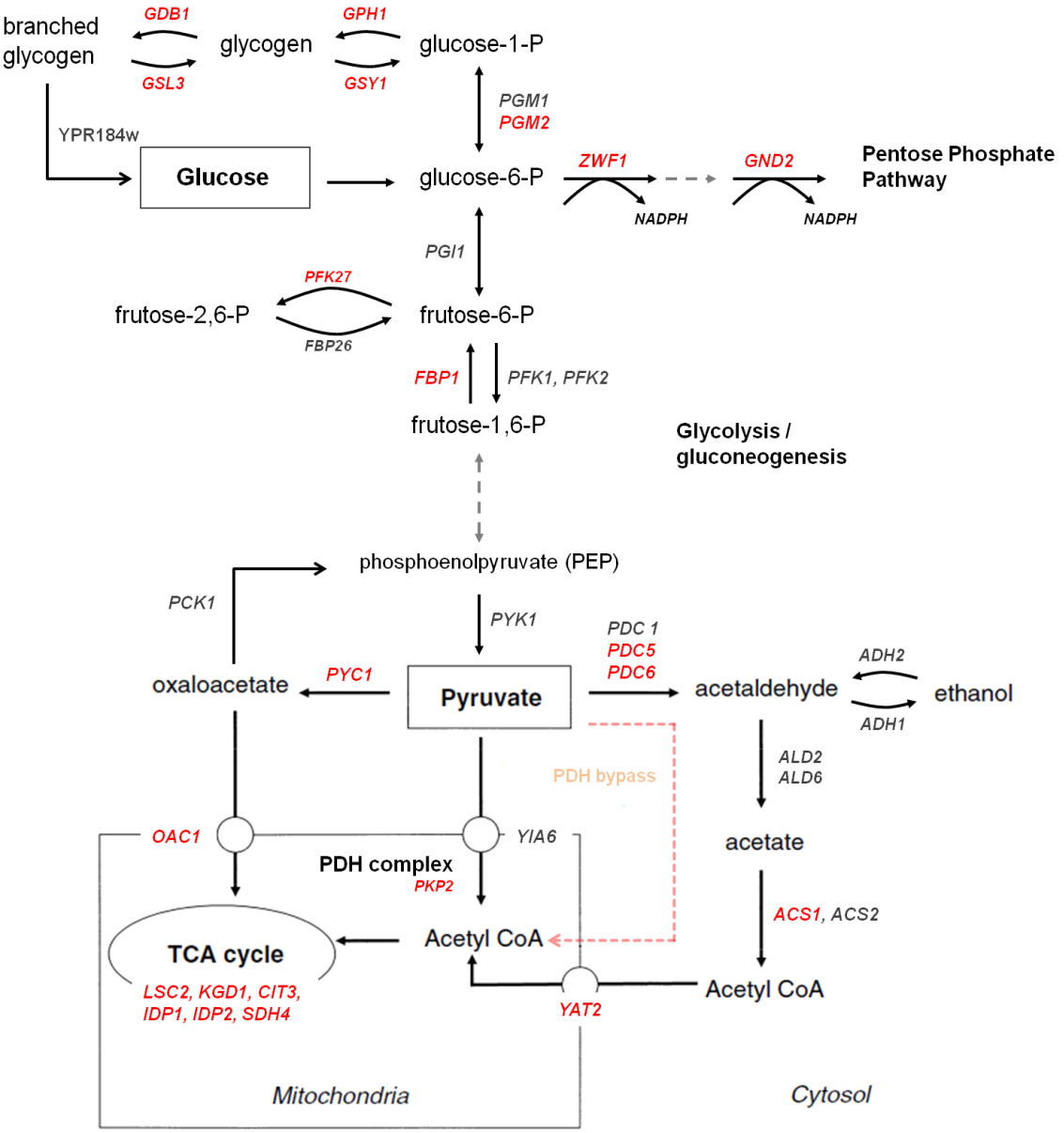

Figure 4.6 - Mistranslation induces metabolic reprogramming in Δ*hsp12* cells. Global analysis of gene expression allowed identification of induced genes involved in glycolysis, gluconeogenesis, the pentose phosphate pathway and the TCA cycle. The more relevant key metabolic intermediates are identified in the figure, together with the yeast genes encoding the enzymes that catalyze each metabolic step. All the significantly up-regulated genes are represented in red (adapted from Rodrigues et al., 2006).

Glucose can have additional catabolic fates besides the glycolytic breakdown to pyruvate. An alternative mode of glucose oxidation is the pentose phosphate

pathway, which in Crabtree positive yeasts such as *S. cerevisiae* is predominantly used for NADPH production (Blank & Sauer, 2004). Reducing equivalents in the form of NADPH are necessary for numerous biosynthetic enzymatic reactions such as production of amino acids and also to assure antioxidant mechanisms involving glutathione and thioredoxin (Juhnke et al., 1996; Izawa et al., 1998b). The first step in the pentose phosphate pathway is the irreversible dehydrogenation of glucose-6-phosphate, with concomitant generation of NADPH from $NADP^+$ through an oxidation/reduction reaction. *ZWF1*, corresponding to a cytoplasmic glucose-6-phosphate dehydrogenase, is up-regulated in Δ*hsp12* mistranslating cells, as well as *GND2*. Likewise, *GND2* encodes a key enzyme in the cytosolic oxidative branch of the pentose phosphate pathway, which catalyzes a second oxidative reduction of $NADP^+$ to NADPH (Sinha & Maitra, 1992; Maaheimo et al., 2001).

In mistranslating cells management of energy resources is of pivotal importance. Genes encoding glucose transporters, such as *HXT4*, *HXT6*, *HXT7* and *HXT10* are up-regulated to increase import of external glucose into the cell. Besides ATP synthesis through glycolysis or NADPH regeneration by the pentose phosphate pathway, glucose is also apparently directed to glycogen storage. Remarkably, genes encoding enzymes that promote both the synthesis (*GSY1, GLC3*) and degradation (*GPH1, GDB1*) of glycogen are induced by mistranslation, probably to allow a more precise modulation of glycogen levels. Storage of glucose in the form of glycogen is known to be critical in response to a wide variety of stress conditions, conferring survival and reproductive advantages through mobilization of energy resources (Parrou et al., 1997; Francois & Parrou, 2001).

Our data show significant up-regulation of *FBP1,* which encodes a regulatory enzyme (fructose-1,6-bisphosphatase) at a critical branch point in metabolism, important to determine allocation of metabolites to gluconeogenesis. Also up-regulated is *PFK27*, which is involved in the synthesis of fructose-2,6- bisphosphate, a positive allosteric effector of the enzyme phosphofructokinase that directs carbon flux towards glucose and glycogen. The activation of gluconeogenesis is further corroborated by the up-

regulation of *PGM2*, which is also pivotal for carbohydrate metabolism. *PGM2* encodes a major phosphoglucomutase isoform that catalyzes the interconversion of glucose-6-phosphate and glucose-1-phosphate (Boles et al., 1994). Aditionally, phosphoglucomutase is required for the synthesis of extracellular N-linked glycoproteins an is of major importance in stress adaptation (Dey et al., 1994; Masuda et al., 2001; Alexandre et al., 2001), also indirectly affecting cation uptake and calcium homeostasis (Fu et al., 2000; Mulet et al., 2004).

We have also observed up-regulation of amino acid biosynthesis genes in mistranslating Δ*hsp12* cells (see Figure 4.5), suggesting that mistranslation diverts a substrantial portion of the metabolic machinery to the synthesis of amino acids by increasing the influx of metabolites through the TCA cycle and also the available amount of NADPH reducing equivalents. On the other hand, increased expression of sulfur metabolism genes is mostly characterized by deregulation in *MET1* to *MET5*, *MET10*, *MET14*, *MET17*, *MET16*, *STR2* and *STR3*, involved in the biosynthesis of methionine and cysteine. Remarkably, cysteine is essential for synthesis of glutathione, a crucial antioxidant that protects cells against damage induced by oxidative stress (Grant et al., 1997; Grant, 2001).

Nitrogen-containing compounds such as amino acids can be synthesized from intermediates derived from glycolysis, the TCA cycle or the pentose phosphate pathway and ammonia. The nitrogen of ammonia is made available through incorporation into glutamate and glutamine, from which the other amino acids are synthesized. *GDH1* and *GDH3*, both up-regulated under mistranslation, code for isoforms of $NADP^+$-dependent glutamate dehydrogenase, which synthesizes glutamate from the condensation of ammonium and α – ketoglutarate, produced from the TCA cycle (Avendano et al., 1997; Deluna et al., 2001).

Amino acid biosynthesis mostly involves complex molecular rearrangements, such as transamination, which are usually promoted by enzymes containing pyridoxal phosphate, a vitamin B_6 derivative. Pyridoxal phosphate functions as an intermediate

carrier of amino groups at the active site of transaminases, and glutamate as the amino group donor for these biosynthetic pathways. Notably, mistranslation increased expression of both *SNO1* and *SNZ1* genes, involved in synthesis of the major vitamin B_6 forms. Vitamin B_6 is important for ROS resistance and essential in stationary phase, when cells are subjected to increased oxidative stress (Ehrenshaft et al., 1999).

Also interesting was the up-regulation of iron binding and import genes in mistranslating Δ*hsp12* cells. Iron is an essential cofactor for many of the enzymes involved in major cellular metabolic processes, from oxidation of acetyl-CoA via the tricarboxylic acid cycle to the biosynthesis of amino acids, mostly in the form of Fe-S clusters (Shakoury-Elizeh et al., 2010). Iron is also essential for *de novo* biosynthesis of NAD from tryptophan. *BNA1* and *BNA2*, both up-regulated by mistranslation, greatly contribute to this pathway (Bedalov et al., 2003). The first step in iron uptake involves reduction of ferric (Fe^{3+}) to ferrous ions (Fe^{2+}), which is followed by transport of the reduced ions through the plasma membrane (Stearman et al., 1996). Our data showed up-regulation of *FRE2*, *FRE3* and other homologous genes such as *FRE5, FRE6, FRE7* and *FRE8*, which are involved or predicted to be involved in ferric reduction prior to uptake by transporters. Together with *FRE1*, *FRE2* encodes a major plasma membrane metalloreductase that reduces extracellular oxidized forms of both iron and copper (Georgatsou & Alexandraki, 1994). *FRE5* and *FRE6,* respectively, encode mitochondrial and vacuolar membrane ferric redutases (Sickmann et al., 2003; Huh WK et al., 2003). *FET3*, encoding a multicopper ferroxidase which receives reduced iron from Fre1p or Fre2p and transfers it to Ftr1p, an iron permease ultimately responsible for cellular import, was also up-regulated (Stearman R et al., 1996).

Numerous transcription factors (TFs) are involved in regulating the expression of the up-regulated genes. The enrichment analysis of transcription factors showed a particular overrepresentation of genes under the control of transcriptional activator *GCN4* (see Figure 4.7). Gcn4p is known to bind the consensus sequence TGACTC, located upstream of several genes induced during amino acid starvation (Arndt &

Fink, 1986; Hinnebusch & Natarajan, 2002). In addition to the derepression of genes implicated in amino acid biosynthetic pathways, Gcn4p also appears to regulate the expression of genes related with purine biosynthesis, glycogen homeostasis, autophagy and multiple stress responses (Natarajan et al., 2001).

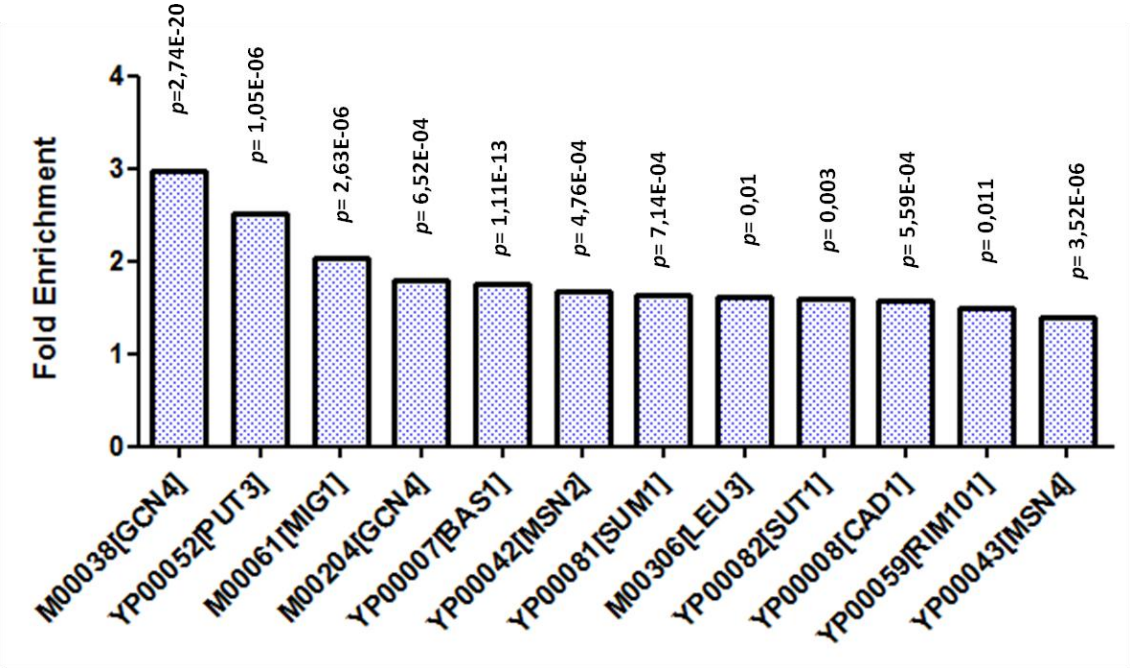

Figure 4.7 - Functional Enrichment Analysis of transcription factors corresponding to the up-regulated genes in Δ*hsp12* mistranslating cells. Differentially expressed genes were calculated relative to BY4742 WT cells and analyzed for enrichment in transcripton factors using the PRomoter Integration in Microarray Analysis (PRIMA) tool, included in the Expander 5.0 software (Fischer Exact test; Bonferroni correction for multiple testing, p<0.05) (Ulitsky I et al., 2010).

Another significantly enriched transcription factor in Δ*hsp12* mistranslating cells was encoded by *PUT3* (see figure 4.7). Put3p is a fungal specific transcriptional activator of the proline utilization pathway. Proline can serve as a nitrogen source in *S. cerevisiae*, in the absence of preferred nitrogen sources. Under nitrogen starvation, Put3p transcription of a set of genes encoding specific transporters and enzymes that convert proline to glutamate, a more usable nitrogen compound (des Etages et al., 1996; Huang & Brandriss, 2000). The *MIG1* encoded transcription factor, which is involved in glucose repression mechanisms (Lutfiyya et al., 1998) was also enriched.

LEU3 encodes a transcription factor that regulates genes involved in ammonia assimilation and branched-chain amino acid synthesis (Hu et al., 1995). Its expression is ultimately regulated by Gcn4p (Wang et al., 1999). Finally, Bas1p is involved in transcriptional regulation of genes implicated in the purine and histidine biosynthesis pathways (Daignan-Fornier and Fink, 1992).

Our gene enrichment analysis also highlighted *CAD1 (YAP2)*, *MSN2* and *MSN4* (see figure 4.7), which are normally activated in response to cellular stress. For example, Cad1p (Yap2p) is a transcriptional activator usually stimulated by aminotriazole and cadmium, being pivotal in metal and drug resistance (Fernandes L et al., 1997). However, increased expression of genes under the control of Cad1p does not seem to induce resistance to metals in Δ*hsp12* mistranslating cells (Figure 4.3 a). Some authors suggest an indirect influence of Cad1p on iron metabolism, through alterations of the cellular redox status (Lesuisse & Labbe, 1995).

Msn2p and Msn4p are mainly functional redundant and are generically activated in response to environmental insults, regulating a large number of genes (~200 genes) (Martinez-Pastor et al., 1996). For these reasons, these transcriptional factors are called general stress response transcriptional factors. Among the general stress response genes induced by mistranslation in Δ*hsp12* cells are *HSP26, HSP150, GRE1, HSP32, HSP33, SSA1, DDR2, HSP30, HSP31, SSA4, SSE2, UBC5* and *HSP104*, which encode mostly chaperones involved in unfolded protein binding, composing an important defence mechanism against proteome destabilization. Also significant is the deregulation of *GTT2* and *GTO3*, both encoding proteins with glutathione-S-transferase activity, involved in detoxification of electrophilic xenobiotics compounds by conjugation with the thiolate group of glutathione (GSH) (Collinson & Grant, 2003). In addition, glutathione transferase Gtt2p, seem to be pivotal in the response to H_2O_2 stress (Mariani et al., 2008). Some oxidative stress response genes were also up-regulated, namelly *GPX1*, *CTT1* and *PRX1*. Gpx1p is a phospholipid hydroperoxide glutathione peroxidase that protects cells from damaged phospholipids during oxidative stress (Avery & Avery, 2001). Ctt1p is a cytosolic catalase involved in

hydrogen peroxide detoxification and Prx1p is a mitochondrial peroxiredoxin responsible for hydroperoxide reduction (Jamieson, 1998; Grant, 2001).

4.4. Discussion

Yeast cells respond to stress by activating the so called environmental stress response (ESR), which involves a coordinated deregulation of up to ~14% of the *S.cerevisiae* genes (Gasch et al., 2000; Ball et al. 2000; Blandin et al. 2000). Indeed, these gene expression changes have already been described in cells exposed to heat shock, osmotic shock, extreme pH, oxidative and reductive stress, non-fermentable carbon sources, ethanol, cadmium, arsenic and nutrient (amino acid, nitrogen, phosphate) starvation, among others (Boy-Marcotte et al., 1998; Gasch AP et al., 2000; Ogawa et al., 2000; Alexandre et al., 2001; Momose & Iwahashi, 2001). Nevertheless, in addition to the stereotyped ESR, distinct environmental changes also induce specific and unique gene expression responses, highlightening the precision of yeast stress adaptation. The duration and amplitude of the transcriptional deregulation also varies with the extent of the environmental change. Cells experiencing larger doses of stress respond more intensily than cells experiencing milder environmental changes (Gasch et al. 2000).

Of the ~900 deregulated genes that compose the ESR in *S.cerevisiae*, ~600 genes are generally repressed and mostly encode proteins related with cell growth, DNA/RNA binding and translation mechanisms. Conversely, ~300 genes are upregulated and encode proteins involved in energy metabolism, transport, signaling, as well as protein protection, namely chaperones and DNA damage repair enzymes (Gasch et al., 2000). An important consequence of the general ESR is aqquisition of stress cross-protection. Indeed, cells exposed to a mild stress become resistant to deleterious doses of other unrelated stresses (Flattery-O'Brien et al., 1993; Lewis et al., 1995).

Mistranslation in *S.cerevisiae* induces changes in gene expression and triggers the general stress response, which may explain the increased resistence of mistranslating yeast to heat, heavy metals and drugs (Santos et al., 1996; Santos et al., 1999; Silva et

al., 2007). Among the genes most up-regulated by mistranslation were the molecular chaperones *HSP12*, *HSP26*, *HSP70 (SSA4)* and *HSP104* (Silva et al., 2007), all part of the ESR. We have also showed that *hsp12* and *hsp104* null mutants are translational error prone in presence of environmental stressors. Increased tolerance of BY4742, Δ*hsp104* and Δ*yap1,2* to highly inhibitory cadmium concentrations occurs by a cross-protection mechanism that involves induction of the general stress response. The same effect occurs in Δ*yap1,2* cells exposed to inhibitory amounts of As_2O_3 (400μM). On the other hand, As_2O_3, CrO_3, EtOH or LiCl exposure show synergistic effects with mistranslation on decreasing stress tolerance of Δ*hsp12* cells (see figure 4.3 a), which suggests the targeting of a common process in these cells. Our data further implies that mistranslation abrogates potential selective advantages in BY4742, Δ*hsp104* and Δ*yap1,2* exposed to non-lethal concentrations of stressors. Finally, genetic background and in particular molecular chaperones play a key role in stress adaptation of mistranslating cells.

Our mRNA profiling data did not show significant gene expression deregulation between Δ*hsp12* control cells relative to BY4742 WT cells. This is not surprising, since Hsp12p in only weakly expressed during exponential phase in the absence of stress and is non essential under these conditions (Welker S et al., 2010). Remarkably, the extensive gene expression reprogramming induced in mistranslating Δ*hsp12* cells relative to BY4742 WT cells is mostly characterized by gene up-regulation. Of the 652 significantly deregulated genes, only 45 were repressed and 587 up-regulated. The former are related to protein synthesis. This is probably connected with the decreased growth rate shown if figure 4.3 and may help to conserve energy (Warner, 1999; Gasch AP et al., 2000). Conversely, many of the genes induced in mistranslating Δ*hsp12* cells also integrate the ESR. These transcripts are involved in regulation of the carbohydrate metabolism, glycogen recycling and protein protection or stabilization. In addition, up-regulation of genes encoding cell wall proteins might intensify sensing of the surrounding environment and stimulate signaling transduction.

Analysis of the genes up-regulated by mistranslation in Δ*hsp12* cells allowed us to identify genes involved in amino acid biosynthetic processes, in line with enrichment of the *GCN4* transcriptional regulator, which regulates the general amino acid control (GAAC) (Hinnebusch, 1986; Mirande & Waller, 1988; Hinnebusch & Natarajan, 2002) and *GAP1*, *CAN1*, *BAP2* or *AGP1*, encoding plasma membrane amino acid permeases. Uncharged tRNAs accumulate in the cell under starvation conditions and stimulate activity of the Gcn2 kinase by binding to a regulatory domain structurally related to histidyl- tRNA synthetase (HisRS) (Wek et al., 1995). The sensor kinase Gcn2p then phosphorylates the translation initiation factor eIF2, resulting in efficient translation of *GCN4* (Hinnebusch & Natarajan, 2002) and, therefore, promoting Gcn4p binding at sequence-specific responsive elements (Oliphant et al., 1989). However, Gcn4p is also induced under conditions of stress besides amino acid deprivation, such as glucose limitation, high salinity, growth on ethanol and non-fermentable carbon sources and treatment with rapamycin (inhibitor Tor1p and Tor2p) or H_2O_2 (Yang et al., 2000; Goossens et al., 2001; Valenzuela et al., 2001; Hinnebusch, 2005; Mascarenhas et al., 2008). Thereby, Gcn4p controls the expression of a large set of genes from diverse functional categories and pathways, making up to 1/10 or more of the yeast genome (Jia et al., 2000; Natarajan et al., 2001). Most stress conditions impair synthesis of amino acids and interfere with their storage or uptake into the cells, increasing the concentration of uncharged tRNAs and the activity of Gcn2p kinase via the same conventional mechanism that takes place in amino acid-deprived cells (Yang et al., 2000; Natarajan et al., 2001; Goossens et al., 2001). Additionally, ROS may also oxidize free amino acids and amino acids in proteins, causing imbalances in amino acid pool sizes and eventually affecting the levels of uncharged tRNAs (Stadtman & Levine, 2003). Finally, *GCN4* can also be induced independently of Gcn2p, by a mechanism involving PKA activation (Engelberg et al., 1994), or due to defects in tRNA processing and nuclear export (Qiu et al., 2000; Hinnebusch & Natarajan, 2002).

Mistranslating Δ*hsp12* cells showed a distinct induction of vacuolar and plasma membrane transporters, which manage the uptake and storage of essential nutrients such as glucose, nitrogen, sulphur and phosphate. Quite remarkably, both *PHO89* -

coding for a Na+/ inorganic phosphate (Pi) co-transporter, and *PHO84* - a high-affinity Pi transporter, are among the most up-regulated genes in mistranslating Δ*hsp12* cells (20-fold and 100-fold, respectively). Conversely, we also reported a 10-fold induction of *PHO5*, coding for a periplasmic acid phosphatase that mediates extracellular phosphate scavenging. Inorganic phosphate is an essential nutrient required for energy metabolism and synthesis of major cellular constituents such as nucleic acids, proteins or phospholipids. The intracellular concentration of free phosphate is usually quite low but subjected to dynamic fluctuations when yeast cells switch from respiratory to fermentative metabolism. Most of the phosphate in yeast is in the form of polyphosphates (poly P), a linear polymer that consists of phosphoanhydride linked phosphate residues (Kornberg et al., 1999). Poly P is environmentally ubiquitous and has multiple roles, from phosphate storage to energy supply, enzyme activation, gene expression, translation fidelity or even stress adaptation (Kornberg et al., 1999; Ogawa et al., 2000). Indeed, Poly P is known to sequester $Cd^{2+}$and Hg^{2+}, therefore mediating cellular resistance to toxic metals (Brown & Kornberg, 2004). In *S.cerevisiae*, phosphate sensing mediates signalling through the protein kinase A (PKA) pathway. Changes in PKA activity might impact stress resistence, storage of glycogen and expression of ribosomal genes (Giots et al., 2003; Mouillon & Persson, 2006).

Phosphate has been depicted as a coupling factor in yeast mitochondria, crucial in maintaining the inner membrane integrity against proton leakage and preserving the membrane potential of respiring yeast mitochondria (Balcavage & Mattoon, 1968; Janssen et al., 2002). Although the transcriptomic analysis of Δ*hsp12* mistranslating cells seems to point to an increase in the TCA cycle flux, we did not identify a significant induction of genes involved in cellular respiration. This suggests that cellular ATP is still mostly synthesized through a fermentative metabolism, whereas the TCA cycle functions largely for biosynthesis, namely of amino acid precursors. Moreover, previous studies showed that mistranslating BY4742 WT cells are unable to grow in non-fermentable carbon sources such as glycerol and have strong alterations in mitochondrial morphology and network structure (Lima-Costa et al., unpublished).

This might be related to the fact that mitochondrial proteins normally show different turnover rates. Indeed, only 5% to 10% of the yeast mitochondrial proteome is subject to degradation within a generation time (Augustin et al., 2005). Even thought mitochondrial dysfunction is still unverified in Δ*hsp12* mistranslating cells, we can hypothesize that the induction of both *PHO89* and *PHO84* might simply represent a mitochondrial protection mechanism.

Our transcriptomic analysis revealed few differences in genetic deregulation between Δ*hsp12* and BY4742 mistranslating cells. However, functional enrichment analysis of BY4742 mistranslating cells allowed identifying genes involved in response to oxidative stress (Lima-Costa et al., unpublished). Amongst these genes are *GRX1* (encoding a disulfide oxidoreductase), *GPX1* (glutathione peroxidise), *TRX2* (cytoplasmic thioredoxin), *TSA1* (thioredoxin peroxidise), SRX1 (sulfiredoxin) and *CTT1* (cytosolic catalase). These observations are again consistent with data presented in the previous chapter (see figure3.10), showing a more expressive ROS increase in BY4742 cells than in Δ*hsp12* mistranslating cells.

Deregulation of gene expression in response to stress causes changes in mRNA transcripts that might not correlate with protein levels. Remarkably, the expression level of proteins encoded by similarly abundant mRNAs can vary as much as 30-fold (Gygi et al., 1999).The discrepancies between mRNA and protein expression might occur due to post-transcriptional mechanisms controlling translation rates, variation in mRNA and protein half-lives (Varshavsky, 1996; Urlinger et al., 1997; Gygi et al., 1999), differential recruitment of mRNAs to translating ribosomes (Halbeisen & Gerber, 2009) and even intracellular location of the proteins (Urlinger et al., 1997). Indeed, localizations such as the nucleolus typically present a high correlation between mRNA and protein levels, while other locations such as mitochondria present a lower correlation (Greenbaum et al., 2003). Interestingly, a considerable proportion of the induced genes in Δ*hsp12* mistranslating cells encode mitochondrial proteins (see figure 4.6). Remarkably, correlation between transcriptome and translatome is higher after a severe stress but decreases under milder stresses that do not affect cell

growth (Halbeisen & Gerber, 2009). Conversely, highly expressed genes result in more correlated level of protein than lower expressed ones (Greenbaum et al., 2003).

Since proteins are the true cellular effectors, complementary measurements of relative mRNA and protein levels are pivotal for a complete understanding of how the cell works. Also, this analysis might be the key to understand which post-transcriptional mechanisms determine the phenotypes of Δ*hsp12* and BY4742 cells under constitutive mistranslation and the specificity of their stress responses. A quantitative method such as real-time PCR should be used to confirm the mRNA levels of some key genes. In addition, a proteome analysis could be implemented by the combination of two-dimensional gel electrophoresis (2DE) - which allows separation, visualization, and quantification of proteins - with analytical methods for their large-scale identification, such as mass spectrometry.

Chapter 5

General Discussion

5.1. General Discussion

5.1.1. Strategies for protein synthesis accuracy

The evolution of efficient proofreading and repair processes ensure DNA replication average error rates in the order of 10^{-8} to 10^{-11} nucleotide exchanges per base pair per replication cycle (Drake, 1991; Drake et al., 1998). The correlation between DNA mutation rate and genome size is strongly negative, but the mutation rates per genome differ only by a factor of two, for most of the organisms tested so far (Drake et al., 1998). On the other hand, translational errors (protein mutation) are 6 orders of magnitude more frequent than genetic mutations, ranging from 10^{-3} to 10^{-5} per codon in *S.cerevisiae* (Stansfield et al. 1998; Rakwalska & Rospert 2004; Salas-Marco and Bedwell 2005; Plant et al. 2007). An explanation for such difference in error rates is that DNA mutations are fixed and transmitted, while protein mutations introduced during mRNA decoding are not.

In order to preserve cellular viability, translation must efficiently balance speed and accuracy (Parker 1989). There are several events determining fidelity of translation, including synthesis of cognate amino acid-tRNA pairs by aminoacyl-tRNA synthetases (aaRSs), binding and delivery of aminoacyl-tRNAs (aa-tRNAs) to the ribosome by elongation factors and selection of aa-tRNAs by the ribosome. Multiple substrate recognition and proofreading mechanisms are involved in these processes, to minimize error rate without negatively affecting the total protein output and optimal growth. For example, editing during aminoacylation lowers the error rate of this mechanism to 10^{-6} (Schulman, 1991). On the other hand, mRNA decoding accuracy at the ribosomal A-site is surveyed by the rate of EF-Tu GTPase activation (Rodnina et al., 2005). Also, in eukaryotic cells, mRNAs failing to accurately encode the original gene sequence are recognized and degraded rapidly by a nonsense-mediated mRNA decay (NMD) mechanism, before deleterious accumulation of aberrant protein products (Jaillon et al., 2008; Drummond & Wilke, 2009). Despite this, if we consider

an error rate of 5×10^{-4} and the average length of yeast proteins to be ~400 amino acids, around 18% of the synthesized molecules contain at least one misincorporated amino acid (Burger et al., 2006; Drummond et al., 2005). In addition, 10 - 50% of the overall random substitutions might result in protein misfolding and concomitant loss of function (Markiewicz et al., 1994; Guo et al., 2004), with deleterious effects in 4–12% of the average-length yeast proteins (Drummond et al., 2005).

Misfolded proteins are generally cytotoxic due to wasting of cellular metabolic resources and formation of aggregates (Bucciantini et al., 2002), known to ultimately promote senescence, neurodegeneration and cancer (Ballesteros et al., 2001; Lee et al., 2006; Brulliard et al., 2007). Remarkably, gene expression levels are negatively correlated with the protein aggregation rate measured *in vitro*. This seems to suggest that the most expressed proteins have evolved to fold properly and resist aggregation, functioning efficiently even under conditions that induce translational errors and misfolding (Drummond DA et al., 2005; Drummond DA & Wilke CO, 2008). In other words, selection optimizes codon usage in such a manner that highly expressed genes use preferred codons that are less prone to error. It also acts on protein robustness, favoring thermodynamically stable protein sequences that tolerate amino acid substitutions without imposing an unbearable fitness cost (Bloom et al., 2005; Drummond DA et al., 2005).

Interestingly, loss of translational accuracy increases frequency of spontaneous mutations in *E.coli*, by promoting synthesis of mutant DNA polymerase molecules (Boe, 1992; Ninio, 1991), which replicate DNA inaccurately. Conversely, similar mechanisms might also explain the high DNA mutation rates associated with prolonged amino acid starvation (Hall, 1990; Boe, 1990), editing defects in translation (Bacher & Schimmel, 2007) or mutations in tRNA genes (Al Mamun et al., 2002). Remarkably, an editing defect in a single tRNA synthetase (isoleucyl-tRNA synthetase) increases mutation rate in aging bacteria, due to deficient DNA repair by the bacterial SOS response (Bacher & Schimmel, 2007). The activity of SOS-induced

enzymes is affected by accumulation of translational errors, potentially resulting in occurrence of free DNA ends (Kowalczykowski, 2000; Bacher & Schimmel, 2007).
The *E.coli* mutator mutA and mutC alleles often result in expression of a tRNA that inserts glycine at approximately 1-2% of the aspartic acid codons. This also increases mutation frequency by promoting amino acid substitutions in DNA pol III that hamper the editing function of the enzyme (Slupska et al., 1996; Al Mamun et al., 2002). These data are in line with the controversial hypothesis that aging is mostly related with the buildup of random amino acid misincorporations. Such phenotype would then inevitably result in an exponential decrease in the accuracy of information flow from DNA to protein, by introducing errors in the sequence of proteins involved in translation and DNA replication (ORGEL, 1963). However, this hypothesis neglected the role of cellular homeostasis mechanisms, which recognize misfolded proteins resulting from mistranslation and target them for degradation or recovery. Nevertheless, mistranslation can potentially saturate protein quality control mechanisms, leading to disease and promoting aging.

The demands on the quality control machinery diverge according to different growth conditions and are in some cases organelle or cell-specific. For example, besides the cytoplasmic PheRS, eukaryotes maintain a quite distinct mitochondrial form of the enzyme (mtPheRS), which lacks an editing domain and maintains the fidelity of aminoacylation through higher level of amino acid specificity (Roy et al., 2005; Reynolds et al., 2010b). Reducing the specificity of the mtPheRS blocked mitochondrial biogenesis. Nevertheless, this error-prone mtPheRS still supported cytoplasmic protein synthesis and normal growth when tested in the yeast cytoplasm, revealing distinct requirements for accuracy according to the cellular compartment (Reynolds et al., 2010b). In addition, also cellular physiology arises as an important determinant of translational quality control. For example, a missense mutation in the editing site of mouse AlaRS results in the accumulation of misfolded proteins and cell death exclusively in the non-dividing Purkinje neuronal cells, although all cells inherited the mutation (Lee et al., 2006). Previous studies with bacteria indicated that frameshifting increases transiently 3- to 10-fold upon entrance into the stationary

phase (Wenthzel et al., 1998). Altogether, an opposite effect was found in *S.cerevisiae*. There is not a general change in translational accuracy, but programmed frameshifting at particular sites decreases with a change from a fermentative to a respiratory metabolism (change from exponential to stationary phase). These mechanisms allow cells to coordinate the expression of a protein product with variations in cellular growth and physiology (Stahl et al., 2004).

External factors might also modulate translational fidelity and cellular tolerance to protein synthesis errors. In *E.coli*, an increasing level of ROS reduces translational fidelity by oxidizing a critical Cys residue in the editing site of ThrRS, resulting in Ser-tRNA^{Thr} formation and accumulation of misfolded proteins (Ling & Söll, 2010). On the other hand, starvation for particular amino acids stimulates missense errors, due to shortage of cognate tRNAs and competition with non-cognate aminoacyl-tRNAs (Farabaugh & Björk, 1999). These conditions lead the ribosome to frequently pause with an empty A-site, which eventually forces the peptidyl-tRNA to slip +1 in the P-site or even slide extensively over other hungry codons, resuming translation at a cognate codon many nucleotides downstream, in the same or in a distinct reading frame (Gallant & Lindsley, 1992; Gallant & Lindsley, 1998). In addition, exposure to chromium, a human carcinogen and widespread pollutant, results in mistranslation and concomitant buildup of toxic protein aggregates (Holland et al., 2007).

Our study focused on the vulnerability of the eukaryotic translational machinery to environmental stress, encompassing a wide range of chemicals that possess distinct toxicological effects. We took advantage of distinct bicistronic luciferase reporters to quantify both stop codon readthrough and misreading in *S.cerevisiae* cells under non-lethal conditions. Our results suggest that the eukaryotic translation machinery is generally very resistant to environmental stress. Cells do not harbor perfectly synthesized proteomes, but mistranslation is limited to a tolerable level that allows optimal growth under specific environmental conditions. This is not exclusively achieved by the mitigation of error frequencies, but by a conjugation of mechanisms that effectively reduce the costs of all unavoidable errors and the cellular impact of

aberrant protein synthesis. For example, both *S.cerevisiae* and *E.coli* cope with amino acid misincorporation by triggering the expression of protein chaperones and proteases, guaranteeing the presence of sufficient functional proteins (Silva et al., 2007; Ruan et al., 2008). On the other hand, proteasomal activity is of crucial importance for cellular chromium (Cr) resistance, by attenuating the effects of protein aggregate accumulation (Holland et al., 2007). Therefore, for a precise quantification of the actual effects exerted by environmental stress on the translational machinery it is necessary to untangle the complex integration of protein homeostasis mechanisms acting on aberrantly synthezised products.

5.1.2. Cellular strategies to preserve protein homeostasis

The translational machinery is a potential target of common environmental or metabolic stressors, which might directly or indirectly decrease the accuracy of protein synthesis, resulting in protein misfolding and aggregation (Holland et al., 2007; Balch et al., 2008; Haigis & Yankner, 2010). This phenotype is most particularly evident in cells missing key ribosome-associated molecular chaperones (Rakwalska M & Rospert S, 2004; Kim SY & Craig EA, 2005). In order to preserve the integrity of the proteome, cells must maintain the balance between the intrinsic and extrinsic factors that interfere with proper protein folding by adapting to an unfavorable environment. To face these challenges cells activate the environmental stress response (ESR), thereby increasing the expression of chaperones and other protective cellular components, which can actively promote protein refolding or determine their degradation by the ubiquitin-proteasome pathway (Gasch et al., 2000; McClellan et al., 2005; Tyedmers et al., 2010). Interestingly, the high mutation rate in cancer cells also results in accumulation of misfolded proteins and overexpression of chaperones, also inducing an ESR-like response (Whitesell & Lindquist, 2005).

With the assistance of molecular chaperones, misfolded or aggregated proteins might be sequestered into specialized quality control compartments, such as juxtanuclear quality-control compartments (JUNQ), perivacuolar insoluble protein deposits (IPOD)

or aggresomes (Bagola and Sommer 2008; Kaganovich et al. 2008), thereby enhancing refolding or degradation and preventing a further build-up of toxic species. Compartmentalization also regulates the inheritance of toxic protein aggregates (Tyedmers J et al., 2010). Remarkably, aggregates distribute asymmetrically during cell division, being largely retained in the mother cell by a mechanism involving the participation of the actin cytoskeleton and the chaperone Hsp104. This occurrence has major implications in cellular ageing, freeing daughter cells of damaged proteins and favoring their rejuvenation (Aguilaniu et al., 2003; Erjavec et al., 2007). Aggregated proteins sequestered in the aggresomes are targeted for degradation by autophagy (Pankiv et al., 2007). On the other hand, the IPOD co-localize with the autophagy associated protein Atg8 (Kaganovich et al., 2008). Autophagy is mainly activated under persistent stress, when the capacity of immediate quality-control systems is exceeded, and consists of a bulk degradation pathway that ultimately delivers protein aggregates in the lysosome (Klionsky et al., 2010). Importantly, there are evidences of a functional relationship between proteasomal and autophagic degradation of misfolded proteins (Hara et al., 2006; Pandey et al., 2007).

The buildup of protein aggregates in the cytosol might also induce protein misfolding in the endoplasmic reticulum (ER), thereby triggering ER stress and induction of the unfolded protein response (UPR), to avoid the exit of misfolded secretory and membrane proteins from the ER. The unfolded protein response (UPR) initiates a vast transcriptional program in a Hac1-dependent manner (Cox et al., 1993; Cox & Walter, 1996; Mori et al., 1996). UPR target genes encompass protein translocation, folding (ER-resident molecular chaperones), components of the protein degradation machinery (ER-associated degradation) and autophagy (Spear et al., 2001). ER-associated degradation (ERAD) substrates might be either misfolded domains in the lumen of the ER, membrane proteins with lesions in a membrane span or a cytosolic domain and misfolded cytosolic proteins unable to enter the secretory pathway (Taxis et al., 2003; Vashist & Ng, 2004; Carvalho et al., 2006). The UPR is also activated by mistranslation (Paredes et al., in press). Our transcriptomic analysis (chapter 4) identified up-regulation of *IRE1*, the ER endoribonuclease which splices the pre-mRNA of *HAC1*, the activator of UPR.

Under control of the ESR, both *HSP12*, *HSP104* and *RPN4* are among the most up-regulated genes in mistranslating cells (Silva et al., 2007). In agreement with these results, our data show that deletion of these genes results in a significant decrease in translational accuracy. Indeed, both UAA/UGA stop codon readthrough and AGC misreading were increased between 20 – 40% relatively to the isogenic WT strain, mostly under ethanol, As_2O_3 and LiCl exposure (see table 2.4 and 2.5). *Per se*, none of the gene deletions tested contributed to a significant loss of translational accuracy. Therefore, saturation of protein homeostasis mechanisms under stress has a direct impact on protein synthesis fidelity, most likely by freeing mistranslated protein into the cytoplasm and decreasing the functional availability of key proteins directly involved in translational fidelity and cellular integrity. If so, our data suggests that the real rate of mistranslation is normally underestimated and should be determined under stress or homeostasis inhibitors. Hsp12p associates with the plasma membrane under stress, which may contribute to modulate both membrane fluidity and stability. Importantly, this may suggest that key membrane components are targets of protein synthesis errors.

Remarkably, increased susceptibility to ROS further contributes to the buildup of protein aggregates in the presence of stress (see Figure 3.5). Indeed, conditions that favor oxidation of rRNA, tRNA, and mRNA, typically impair the integrity of translational processes (Tanaka et al., 2007), resulting in the synthesis of aberrant proteins under conditions of saturated quality control (Ding Q et al., 2005). Amino acid oxidation can lead to the production of aggregation-prone carbonyl groups, but several reports show that carbonylation can also occur independently of ROS, under conditions that favor production of mistranslated proteins (Dukan et al., 2000; Ballesteros et al., 2001). For example, carbonylation increases upon treatment with ribosome-targeting antibiotics even if superoxide production is unaltered (Dukan et al., 2000). Remarkably, the buildup of protein aggregates in our study is being underestimated, since not all the insoluble proteins co-localize with Hsp104 in the

cytoplasm. Some are probably sequestered in aggresomes, which are not known to co-localize with hsp104, and not visualized by epifluorescence microscopy.
Carbonylated proteins accumulate mostly in the cytoplasm of aged yeast cells (Erjavec et al., 2007). This suggests a reduced capacity of ageing cells to manage protein quality control and eliminate misfolded proteins, a phenotype probably associated with the late age onset of Alzheimer's and Parkinson's disease (Tyedmers et al., 2010). Remarkably, the activity of the proteasome decreases during aging in human tissues as well as in senescent primary cultures due to accumulation of protease-resistant aggregates, which bind to it (Grune et al., 2004; Nystrom, 2005). Therefore, protein aggregates can inhibit the UPS and the products that buildup because of its inhibition, a positive feedback mechanism that results in additional cellular decline.

5.1.3. The benefits of protein synthesis errors in stress resistance

Surprisingly, in some organisms loss of quality control mechanisms and substantial decreased protein synthesis accuracy do not produced visible changes in grow rate. In specific conditions translational errors can even produce direct benefits and increase fitness. For example, stop codon readthrough contributes to cellular adaptation and survival under changing environments (Williams et al., 2004). Indeed, the yeast [PSI+] prion is associated with increased stop codon readthrough and variability. Prion induction increases several times in cells exposed to oxidative stress (H_2O_2) or high salt concentrations. The severity of stress and the frequency of [PSI+] induction are highly correlated (Tyedmers et al., 2008). Moreover, point mutations in the editing domains of LeuRS and PheRS genes from *Mycoplasma* parasites impair the ability of these enzymes to edit non-cognate amino acids. The resulting increase in the levels of mistranslation likely contributes to antigen diversity, allowing these organisms to escape host defense systems (Li et al., 2011). A unique $tRNA_{CAG}^{Ser}$ found in *Candida* spp can be aminoacylated with both Ser and Leu, leading to ambiguous decoding of CUG codons. Leu misincorporation creates a statistical proteome and enhances

resistance to cadmium, arsenate and hydrogen peroxide exposure through a cross-protection associated to the general stress response (Santos et al., 1996 and 1999; Miranda et al., 2006). In addition, amino acid substitutions in a TEM1-β-lactamase enzyme confer bacterial resistance to the antibiotic cephalosporin (Wang et al., 2002). Remarkably, our results demonstrate that Met-misacylation has a very significant impact in *S.cerevisiae* cells expressing misreading tRNAs (see Figure 3.11) , nevertheless preserving levels of translational fidelity that ensure cell viability. This event represents an adaptive benefit, since Met residues are ROS scavengers. Yeast MetRS is now known to be responsible for such extensive misacylation of non-methionyl tRNAs, however, changes in tRNA modifications may also be involved in regulating this process.

Large changes in the spectrum of ribonucleosides in cells exposed to environmental stress (Figure 3.8 and 3.9), are known to occur as part of a dynamic translational control mechanism that enhances the synthesis of proteins involved in cell survival and adaptation to unfavorable growth conditions (Chan et al., 2010). The degree of tRNA modification is most probably determined by changes in the activity and expression of modifying enzymes or by tRNA degradation mechanisms, as endonucleolytic cleavage of tRNAs is a conserved response to several stress conditions in yeast, including increased ROS (Thompson et al., 2008). Post-transcriptional modifications are essential to guarantee the structural and functional features of tRNAs and by this means regulate gene expression and translational fidelity. However, no evidence point to the involvement of mistranslation in this cell defense mechanism.

5.2. Conclusions and future studies

Environmental stress puts significant constraints on the components of the translational machinery to enssure accurate synthesis of proteins under suboptimal growth conditions. Our study took advantage of distinct bicistronic luciferase reporters to quantify both stop codon readthrough and misreading in *S.cerevisiae* under non-lethal concentrations of distinct environmental stressors. Our results imply that the eukaryotic translation machinery is in general very resistant to environmental stress. Error rates under stress are maintained at a tolerable level by a conjugation of homeostasis mechanisms that effectively reduce the cellular impact of aberrant protein synthesis.

Protein homeostasis under environmental stress is guaranteed by a complex network of mechanisms, which can actively promote protein refolding and determine their degradation by the ubiquitin-proteasome pathway. Many of these defense pathways are determined by the expression of a comprehensive set of redundant genes under the control of the environmental stress response (ESR). Our quantitative approach allowed us to identify genes that are essential to counteract the negative impact of environmental stress on the translational machinery, namely *HSP12*, *HSP104* and *RPN4*, which limit the accumulation of mistranslated protein into the cytoplasm and maintain the functional key factors directly involved in accuracy. Additionally, environmental stressors induced changes in the spectrum of tRNA ribonucleosides, which improve synthesis of cell survival and adaptation proteins, confirming that the translational machinery is a potential target of suboptimal environmental conditions.

This study also allowed us to unravel some benefits of protein synthesis errors in resistance to stress. The ESR is activated in mistranslating cells and increased tolerance of BY4742, Δ*hsp104* and Δ*yap1,2* cells to high stressor concentrations by a cross-protection mechanism. Besides a wide response to stress, constitutive mistranslation also promoted a shift in cellular metabolism, which might have a role in energy management and cell adaptation. Finally, Met-misacylation increases in

mistranslating *S.cerevisiae* cells expressing misreading tRNAs (see Figure 3.11), providing protection for cellular proteins against ROS produced by dysfunctional mitochondria.

Our data left innumerous unanswered biological questions, which can be the ground to future studies. First, quantification of sense codon misreading should be extended to a larger number of codons, both rare and abundant. Since the current reporter allows only a low number of possible substitutions in the active center of firefly luciferase, a more flexible reporter should be chosen. As an alternative, several endogenous proteins could be purified cells exposed to stress and analyzed by mass spectrometry.

Since mitochondria are particularly susceptible to mistranslation, it would be interesting to focus on protein homeostasis mechanisms in this organelle. One of the hypotheses is the deletion of Hsp78p or Ssc3p, both chaperones involved in protein folding and refolding in the mitochondria.

Δ*hsp12* cells show unique phenotypes under environmental stress and mistranslation which remain unexplained. Since this chaperone is a membrane protein, we suggest an evaluation of cellular permeability to amino acids, which is mediated by permeases and ion channels.

Finally, further work is necessary to understand the influence of the tRNA modification profile on translational accuracy. A full characterization of deletion mutants for modification enzymes would allow us to reconstruct the link between accuracy, gene expression and survival mechanisms.

References

Reference List

1. Abelson, J., Trotta, C. R., & Li, H. (1998). tRNA splicing. *J Biol Chem, 273,* 12685-12688.

2. Agris, P. F. (2004). Decoding the genome: a modified view. *Nucleic Acids Research*.

3. Agris, P. F. (2008). Bringing order to translation: the contributions of transfer RNA anticodon-domain modifications. *EMBO Rep., 9,* 629-635.

4. Agris, P. F., Soll, D., & Seno, T. (1973). Biological function of 2-thiouridine in Escherichia coli glutamic acid transfer ribonucleic acid. *Biochemistry, 12,* 4331-4337.

5. Aguilaniu, H., Gustafsson, L., Rigoulet, M., & Nystrom, T. (2003). Asymmetric inheritance of oxidatively damaged proteins during cytokinesis. *Science, 299,* 1751-1753.

6. Aguilera, F., Peinado, R., Millán, C., Ortega, J., & Mauricio, J. (2006). Relationship between ethanol tolerance, H+ -ATPase activity and the lipid composition of the plasma membrane in different wine yeast strains. *Int J Food Microbiol, 110 (1),* 34-42.

7. Al Mamun, A. A., Marians, K. J., & Humayun, M. Z. (2002). DNA polymerase III from Escherichia coli cells expressing mutA mistranslator tRNA is error-prone. *J Biol Chem, 277,* 46319-46327.

8. Alexandre, H., nsanay-Galeote, V., Dequin, S., & Blondin, B. (2001). Global gene expression during short-term ethanol stress in Saccharomyces cerevisiae. *FEBS Lett., 498,* 98-103.

9. Alexandrov, A., Chernyakov, I., Gu, W., Hiley, S. L., Hughes, T. R., Grayhack, E. J. et al. (2006). Rapid tRNA decay can result from lack of nonessential modifications. *Mol Cell, 21,* 87-96.

10. Alkalaeva EZ, Pisarev AV, Frolova LY, Kisselev LL, & Pestova TV (2006). In vitro reconstitution of eukaryotic translation reveals cooperativity between release factors eRF1 and eRF3. *Cell, 25,* 1125-1136.

11. Alkalaeva, E., Pisarev, A., Frolova, L., Kisselev, L., & Pestova, T. (2006). In vitro reconstitution of eukaryotic translation reveals cooperativity between release factors eRF1 and eRF3. *Cell, 25,* 1125-1136.

12. Almeida, B., Buttner, S., Ohlmeier, S., Silva, A., Mesquita, A., Sampaio-Marques, B. et al. (2007). NO-mediated apoptosis in yeast. *J Cell Sci, 120,* 3279-3288.

13. Antonellis, A., Ellsworth, R. E., Sambuughin, N., Puls, I., Abel, A., Lee-Lin, S. Q. et al. (2003). Glycyl tRNA synthetase mutations in Charcot-Marie-Tooth disease type 2D and distal spinal muscular atrophy type V. *Am J Hum.Genet, 72,* 1293-1299.

14. Arndt, K. & Fink, G. R. (1986). GCN4 protein, a positive transcription factor in yeast, binds general control promoters at all 5' TGACTC 3' sequences. *Proc Natl Acad Sci U S A, 83,* 8516-8520.

15. Arnez, J. G. & Moras, D. (1997). Structural and functional considerations of the aminoacylation reaction. *Trends Biochem Sci, 22,* 211-216.

16. Arrasate, M., Mitra, S., Schweitzer, E. S., Segal, M. R., & Finkbeiner, S. (2004). Inclusion body formation reduces levels of mutant huntingtin and the risk of neuronal death. *Nature, 431,* 805-810.

17. Ashraf, S. S., Sochacka, E., Cain, R., Guenther, R., Malkiewicz, A., & Agris, P. F. (1999). Single atom modification (O-->S) of tRNA confers ribosome binding. *RNA, 5,* 188-194.

18. Augustin, S., Nolden, M., Muller, S., Hardt, O., Arnold, I., & Langer, T. (2005). Characterization of peptides released from mitochondria: evidence for constant proteolysis and peptide efflux. *J Biol Chem, 280,* 2691-2699.

19. Avendano, A., Deluna, A., Olivera, H., Valenzuela, L., & Gonzalez, A. (1997). GDH3 encodes a glutamate dehydrogenase isozyme, a previously unrecognized route for glutamate biosynthesis in Saccharomyces cerevisiae. *J Bacteriol, 179,* 5594-5597.

20. Avery SV. (2011). Molecular targets of oxidative stress. *Biochem J, 434 (2),* 201-210.

21. Avery, A. M. & Avery, S. V. (2001). Saccharomyces cerevisiae expresses three phospholipid hydroperoxide glutathione peroxidases. *J Biol Chem, 276,* 33730-33735.

22. Avery, SV. (2011). Molecular targets of oxidative stress. *Biochem J, 434 (2),* 201-210.

23. Azevedo D., Nascimento L., Labarre J., & Rodrigues-Pousada C (2007). The S. cerevisiae Yap1 and Yap2 transcription factors share a common cadmium-sensing domain. *FEBS Lett., 581(2),* 187-195.

24. Azevedo, D., Nascimento, L., Labarre, J., & Rodrigues-Pousada, C. (2007). The S. cerevisiae Yap1 and Yap2 transcription factors share a common cadmium-sensing domain. *FEBS Lett., 581(2),* 187-195.

25. Bacher, J. M. & Schimmel, P. (2007). An editing-defective aminoacyl-tRNA synthetase is mutagenic in aging bacteria via the SOS response. *Proc Natl Acad Sci U S A, 104,* 1907-1912.

26. Bacher, J. M., Waas, W. F., Metzgar, D., de Crecy-Lagard, V., & Schimmel, P. (2007). Genetic code ambiguity confers a selective advantage on Acinetobacter baylyi. *J Bacteriol, 189,* 6494-6496.

27. Balcavage, W. X. & Mattoon, J. R. (1968). Properties of Saccharomyces cerevisiae mitochondria prepared by a mechanical method. *Biochim Biophys Acta, 153,* 521-530.

28. Balch, W. E., Morimoto, R. I., Dillin, A., & Kelly, J. W. (2008). Adapting proteostasis for disease intervention. *Science, 319,* 916-919.

29. Baldwin, A. N. & Berg, P. (1966). Transfer ribonucleic acid-induced hydrolysis of valyladenylate bound to isoleucyl ribonucleic acid synthetase. *J Biol Chem, 241,* 839-845.

30. Ballesteros, M., Fredriksson, A., Henriksson, J., & Nystrom, T. (2001). Bacterial senescence: protein oxidation in non-proliferating cells is dictated by the accuracy of the ribosomes. *EMBO J, 20,* 5280-5289.

31. Bedalov, A., Hirao, M., Posakony, J., Nelson, M., & Simon, J. A. (2003). NAD+-dependent deacetylase Hst1p controls biosynthesis and cellular NAD+ levels in Saccharomyces cerevisiae. *Mol Cell Biol, 23,* 7044-7054.

32. Begley U, Dyavaiah M, Patil A, Rooney JP, DiRenzo D, Young CM et al. (2007). Trm9-catalyzed tRNA modifications link translation to the DNA damage response. *Mol Cell, 28 (5),* 860-870.

33. Begley, U., Dyavaiah, M., Patil, A., Rooney, J., DiRenzo, D., Young, C. et al. (2007). Trm9-catalyzed tRNA modifications link translation to the DNA damage response. *Mol Cell, 28 (5),* 860-870.

34. Bence, N. F., Sampat, R. M., & Kopito, R. R. (2001). Impairment of the ubiquitin-proteasome system by protein aggregation. *Science, 292,* 1552-1555.

35. Bercovich, B., Stancovski, I., Mayer, A., Blumenfeld, N., Laszlo, A., Schwartz, A. L. et al. (1997). Ubiquitin-dependent degradation of certain protein substrates in vitro requires the molecular chaperone Hsc70. *J Biol Chem, 272,* 9002-9010.

36. Bergquist, E. R., Fischer, R. J., Sugden, K. D., & Martin, B. D. (2009). Inhibition by methylated organo-arsenicals of the respiratory 2-oxo-acid dehydrogenases. *J Organomet.Chem, 694,* 973-980.

37. Bertram G, Innes S, Minella O, Richardson J, & Stansfield I (2001). Endless possibilities: translation termination and stop codon recognition. *Microbiology, 147,* 255-269.

38. Bertram, G., Innes, S., Minella, O., Richardson, J., & Stansfield, I. (2001). Endless possibilities: translation termination and stop codon recognition. *Microbiology, 147,* 255-269.

39. Bicknell, A., Tourtellotte, J., & Niwa, M. (2010). Late phase of the endoplasmic reticulum stress response pathway is regulated by Hog1 MAP kinase. *J Biol Chem, 285 (23),* 17545-17555.

40. Bihler, H., Slayman, C. L., & Bertl, A. (1998). NSC1: a novel high-current inward rectifier for cations in the plasma membrane of Saccharomyces cerevisiae. *FEBS Lett., 432,* 59-64.

41. Bihler, H., Slayman, C. L., & Bertl, A. (2002). Low-affinity potassium uptake by Saccharomyces cerevisiae is mediated by NSC1, a calcium-blocked non-specific cation channel. *Biochim Biophys Acta, 1558,* 109-118.

42. Biniszkiewicz, D., Cesnaviciene, E., & Shub, D. A. (1994). Self-splicing group I intron in cyanobacterial initiator methionine tRNA: evidence for lateral transfer of introns in bacteria. *EMBO J, 13,* 4629-4635.

43. Bjork, G. R., Durand, J. M., Hagervall, T. G., Leipuviene, R., Lundgren, H. K., Nilsson, K. et al. (1999). Transfer RNA modification: influence on translational frameshifting and metabolism. *FEBS Lett., 452,* 47-51.

44. Blackwell K & Jobin J (1999). Cadmium accumulation and its effects on intracellular ion pools in a brewing strain of *Saccharomyces cerevisiae*. *J Ind Microbiol Biotechnol, 23 (3),* 204-208.

45. Blank, L. M. & Sauer, U. (2004). TCA cycle activity in Saccharomyces cerevisiae is a function of the environmentally determined specific growth and glucose uptake rates. *Microbiology, 150,* 1085-1093.

46. Blattner, F. R., Plunkett, G. 3., Bloch, C. A., Perna, N. T., Burland, V., Riley, M. et al. (1997). The complete genome sequence of Escherichia coli K-12. *Science, 277,* 1453-1462.

47. Bloom, J. D., Silberg, J. J., Wilke, C. O., Drummond, D. A., Adami, C., & Arnold, F. H. (2005). Thermodynamic prediction of protein neutrality. *Proc Natl Acad Sci U S A, 102,* 606-611.

48. Boe, L. (1990). Mechanism for induction of adaptive mutations in Escherichia coli. *Mol Microbiol, 4,* 597-601.

49. Boe, L. (1992). Translational errors as the cause of mutations in Escherichia coli. *Mol Gen Genet, 231,* 469-471.

50. Boles, E., Liebetrau, W., Hofmann, M., & Zimmermann, F. K. (1994). A family of hexosephosphate mutases in Saccharomyces cerevisiae. *Eur J Biochem, 220,* 83-96.

51. Bonetti, B., Fu, L., Moon, J., & Bedwell, D. (1995). The efficiency of translation termination is determined by a synergistic interplay between upstream and downstream sequences in Saccharomyces cerevisiae. *J Mol Biol, 251,* 334-345.

52. Boy-Marcotte, E., Perrot, M., Bussereau, F., Boucherie, H., & Jacquet, M. (1998). Msn2p and Msn4p control a large number of genes induced at the diauxic transition which are repressed by cyclic AMP in Saccharomyces cerevisiae. *J Bacteriol, 180,* 1044-1052.

53. Branchini, B. R., Magyar, R. A., Murtiashaw, M. H., & Portier, N. C. (2001). The role of active site residue arginine 218 in firefly luciferase bioluminescence. *Biochemistry, 40,* 2410-2418.

54. Bregeon, D. & Sarasin, A. (2005). Hypothetical role of RNA damage avoidance in preventing human disease. *Mutat.Res, 577,* 293-302.

55. Brennan, T. & Sundaralingam, M. (1976). Structlre of transfer RNA molecules containing the long variable loop. *Nucleic Acids Res, 3,* 3235-3250.

56. Brown, C. M., Stockwell, P. A., Trotman, C. N., & Tate, W. P. (1990). Sequence analysis suggests that tetra-nucleotides signal the termination of protein synthesis in eukaryotes. *Nucleic Acids Res, 18,* 6339-6345.

57. Brown, M. R. & Kornberg, A. (2004). Inorganic polyphosphate in the origin and survival of species. *Proc Natl Acad Sci U S A, 101,* 16085-16087.

58. Brulliard, M., Lorphelin, D., Collignon, O., Lorphelin, W., Thouvenot, B., Gothie, E. et al. (2007). Nonrandom variations in human cancer ESTs indicate that mRNA heterogeneity increases during carcinogenesis. *Proc Natl Acad Sci U S A, 104,* 7522-7527.

59. Bucciantini, M., Giannoni, E., Chiti, F., Baroni, F., Formigli, L., Zurdo, J. et al. (2002). Inherent toxicity of aggregates implies a common mechanism for protein misfolding diseases. *Nature, 416,* 507-511.

60. Buchan, J. R. & Stansfield, I. (2007). Halting a cellular production line: responses to ribosomal pausing during translation. *Biol Cell, 99,* 475-487.

61. Buchberger A, Bukau B, & Sommer T (2010). Protein quality control in the cytosol and the endoplasmic reticulum: brothers in arms. *Mol Cell, 40 (2),* 238-252.

62. Burger, R., Willensdorfer, M., & Nowak, M. A. (2006). Why are phenotypic mutation rates much higher than genotypic mutation rates? *Genetics, 172,* 197-206.

63. Carter, A. P., Clemons, W. M., Brodersen, D. E., Morgan-Warren, R. J., Wimberly, B. T., & Ramakrishnan, V. (2000). Functional insights from the structure of the 30S ribosomal subunit and its interactions with antibiotics. *Nature, 407(6802),* 340-348.

64. Carter, C. W., Jr. (1993). Cognition, mechanism, and evolutionary relationships in aminoacyl-tRNA synthetases. *Annu Rev Biochem, 62,* 715-748.

65. Cartlidge, R. A., Knebel, A., Peggie, M., Alexandrov, A., Phizicky, E. M., & Cohen, P. (2005). The tRNA methylase METTL1 is phosphorylated and inactivated by PKB and RSK in vitro and in cells. *EMBO J, 24,* 1696-1705.

66. Carvalho, P., Goder, V., & Rapoport, T. A. (2006). Distinct ubiquitin-ligase complexes define convergent pathways for the degradation of ER proteins. *Cell, 126,* 361-373.

67. Cavaille, J., Chetouani, F., & Bachellerie, J. P. (1999). The yeast Saccharomyces cerevisiae YDL112w ORF encodes the putative 2'-O-ribose methyltransferase catalyzing the formation of Gm18 in tRNAs. *RNA, 5,* 66-81.

68. Cavarelli, J. & Moras, D. (1993). Recognition of tRNAs by aminoacyl-tRNA synthetases. *FASEB J, 7,* 79-86.

69. Cecarini, V., Gee, J., Fioretti, E., Amici, M., Angeletti, M., Eleuteri, A. M. et al. (2007). Protein oxidation and cellular homeostasis: Emphasis on metabolism. *Biochim Biophys Acta, 1773,* 93-104.

70. Cecchi, C., Baglioni, S., Fiorillo, C., Pensalfini, A., Liguri, G., Nosi, D. et al. (2005). Insights into the molecular basis of the differing susceptibility of varying cell types to the toxicity of amyloid aggregates. *J Cell Sci, 118,* 3459-3470.

71. Chan, C. T., Dyavaiah, M., DeMott, M. S., Taghizadeh, K., Dedon, P. C., & Begley, T. J. (2010). A quantitative systems approach reveals dynamic control of tRNA modifications during cellular stress. *PLoS Genet, 6,* e1001247.

72. Chaudhuri, J., Chowdhury, D., & Maitra, U. (1999). Distinct functions of eukaryotic translation initiation factors eIF1A and eIF3 in the formation of the 40 S ribosomal preinitiation complex. *J Biol Chem, 274,* 17975-17980.

73. Chen, J. Y., Kirchner, G., Aebi, M., & Martin, N. C. (1990). Purification and properties of yeast ATP (CTP):tRNA nucleotidyltransferase from wild type and overproducing cells. *J Biol Chem, 265,* 16221-16224.

74. Cheng, Z., Saito, K., Pisarev, A. V., Wada, M., Pisareva, V. P., Pestova, T. V. et al. (2009). Structural insights into eRF3 and stop codon recognition by eRF1. *Genes Dev, 23,* 1106-1118.

75. Chernyakov, I., Whipple, J. M., Kotelawala, L., Grayhack, E. J., & Phizicky, E. M. (2008). Degradation of several hypomodified mature tRNA species in Saccharomyces cerevisiae is mediated by Met22 and the 5'-3' exonucleases Rat1 and Xrn1. *Genes Dev, 22,* 1369-1380.

76. Ciesla, M., Towpik, J., Graczyk, D., Oficjalska-Pham, D., Harismendy, O., Suleau, A. et al. (2007). Maf1 is involved in coupling carbon metabolism to RNA polymerase III transcription. *Mol Cell Biol, 27,* 7693-7702.

77. Cochella, L. & Green, R. (2005a). An active role for tRNA in decoding beyond codon:anticodon pairing. *Science, 308,* 1178-1180.

78. Cochella, L. & Green, R. (2005b). Fidelity in protein synthesis. *Curr Biol, 15,* R536-R540.

79. Codogno, P. & Meijer, A. J. (2006). Atg5: more than an autophagy factor. *Nat Cell Biol, 8 (10),* 1045-1047.

80. Cohen, E., Bieschke, J., Perciavalle, R. M., Kelly, J. W., & Dillin, A. (2006). Opposing activities protect against age-onset proteotoxicity. *Science, 313,* 1604-1610.

81. Collinson, E. J. & Grant, C. M. (2003). Role of yeast glutaredoxins as glutathione S-transferases. *J Biol Chem, 278,* 22492-22497.

82. Cox, J. S., Shamu, C. E., & Walter, P. (1993). Transcriptional induction of genes encoding endoplasmic reticulum resident proteins requires a transmembrane protein kinase. *Cell, 73,* 1197-1206.

83. Cox, J. S. & Walter, P. (1996). A novel mechanism for regulating activity of a transcription factor that controls the unfolded protein response. *Cell, 87,* 391-404.

84. Craig, E. A. & Jacobsen, K. (1985). Mutations in cognate genes of Saccharomyces cerevisiae hsp70 result in reduced growth rates at low temperatures. *Mol Cell Biol, 5 (12),* 3517-3524.

85. Craigen, W. J. & Caskey, C. T. (1986). Expression of peptide chain release factor 2 requires high-efficiency frameshift. *Nature, 322,* 273-275.

86. Csutora, P., Strassz, A., Boldizsár, F., Németh, P., Sipos, K., Aiello, D. P. et al. (2005). Inhibition of phosphoglucomutase activity by lithium alters cellular calcium homeostasis and signaling in Saccharomyces cerevisiae. *Am J Physiol Cell Physiol, 289 (1),* C58-C67.

87. Cuervo, AM. (2004). Autophagy: in sickness and in health. *Trends Cell Biol, 14,* 70-77.

88. Curran, J. F. & Yarus, M. (1986). Base substitutions in the tRNA anticodon arm do not degrade the accuracy of reading frame maintenance. *Proc Natl Acad Sci U S A, 83,* 6538-6542.

89. Cusack, S., Berthet-Colominas, C., Hartlein, M., Nassar, N., & Leberman, R. (1990). A second class of synthetase structure revealed by X-ray analysis of Escherichia coli seryl-tRNA synthetase at 2.5 A. *Nature, 347,* 249-255.

90. Dalle-Donne, I., Giustarini, D., Colombo, R., Rossi, R., & Milzani, A. (2003). Protein carbonylation in human diseases. *Trends Mol Med, 9,* 169-176.

91. Deluna, A., Avendano, A., Riego, L., & Gonzalez, A. (2001). NADP-glutamate dehydrogenase isoenzymes of Saccharomyces cerevisiae. Purification, kinetic properties, and physiological roles. *J Biol Chem, 276,* 43775-43783.

92. des Etages, S. A., Falvey, D. A., Reece, R. J., & Brandriss, M. C. (1996). Functional analysis of the PUT3 transcriptional activator of the proline utilization pathway in Saccharomyces cerevisiae. *Genetics, 142,* 1069-1082.

93. Dey, N. B., Bounelis, P., Fritz, T. A., Bedwell, D. M., & Marchase, R. B. (1994). The glycosylation of phosphoglucomutase is modulated by carbon source and heat shock in Saccharomyces cerevisiae. *J Biol Chem, 269,* 27143-27148.

94. Dichtl, B., Stevens, A., & Tollervey, D. (1997). Lithium toxicity in yeast is due to the inhibition of RNA processing enzymes. *EMBO J, 16 (23),* 7184-7195.

95. Ding Q, Markesbery WR, Chen Q, Li F, & Keller JN (2005). Ribosome dysfunction is an early event in Alzheimer's disease. *J Neurosci, 25 (40),* 9171-9175.

96. Ding, Q., Markesbery, W. R., Chen, Q., Li, F., & Keller, J. N. (2005). Ribosome dysfunction is an early event in Alzheimer's disease. *J Neurosci, 25 (40),* 9171-9175.

97. Ding, Q., Dimayuga, E., Markesbery, W. R., & Keller, J. N. (2004). Proteasome inhibition increases DNA and RNA oxidation in astrocyte and neuron cultures. *J Neurochem., 91,* 1211-1218.

98. Ding, W. X., Ni, H. M., Gao, W., Yoshimori, T., Stolz, D. B., Ron, D. et al. (2007). Linking of autophagy to ubiquitin-proteasome system is important for the regulation of endoplasmic reticulum stress and cell viability. *Am J Pathol., 171,* 513-524.

99. Dinman, J. D. (2006). Programmed Ribosomal Frameshifting Goes Beyond Viruses: Organisms from all three kingdoms use frameshifting to regulate gene expression, perhaps signaling a paradigm shift. *Microbe Wash.DC., 1,* 521-527.

100. Dirheimer, G., Baranowski, W., & Keith, G. (1995). Variations in tRNA modifications, particularly of their queuine content in higher eukaryotes. Its relation to malignancy grading. *Biochimie, 77,* 99-103.

101. Dobson, C. M. (2004). Principles of protein folding, misfolding and aggregation. *Semin.Cell Dev Biol, 15,* 3-16.

102. Dopp, E., von, R. U., Hartmann, L. M., Stueckradt, I., Pollok, I., Rabieh, S. et al. (2008). Subcellular distribution of inorganic and methylated arsenic compounds in human urothelial cells and human hepatocytes. *Drug Metab Dispos., 36,* 971-979.

103. Dorner, S., Schmid, W., & Barta, A. (2005). Activity of 3'-thioAMP derivatives as ribosomal P-site substrates. *Nucleic Acids Res, 33 (9),* 3065-3071.

104. Drake, J. W. (1991). A constant rate of spontaneous mutation in DNA-based microbes. *Proc Natl Acad Sci U S A, 88,* 7160-7164.

105. Drake, J. W., Charlesworth, B., Charlesworth, D., & Crow, J. F. (1998). Rates of spontaneous mutation. *Genetics, 148,* 1667-1686.

106. Draptchinskaia, N., Gustavsson, P., Andersson, B., Pettersson, M., Willig, T. N., Dianzani, I. et al. (1999). The gene encoding ribosomal protein S19 is mutated in Diamond-Blackfan anaemia. *Nat Genet, 21,* 169-175.

107. Drummond DA, Bloom JD, Adami C, Wilke CO, & Arnold FH (2005). Why highly expressed proteins evolve slowly. *Proc Natl Acad Sci U S A, 102 (40),* 14338-43.

108. Drummond DA & Wilke CO (2008). Mistranslation-induced protein misfolding as a dominant constraint on coding-sequence evolution. *Cell, 134,* 341-352.

109. Drummond, D. A., Bloom, J. D., Adami, C., Wilke, C. O., & Arnold, F. H. (2005). Why highly expressed proteins evolve slowly. *Proc Natl Acad Sci U S A, 102 (40),* 14338-43.

110. Drummond, D. A. & Wilke, C. O. (2008). Mistranslation-induced protein misfolding as a dominant constraint on coding-sequence evolution. *Cell, 134,* 341-352.

111. Drummond, D. A. & Wilke, C. O. (2009). The evolutionary consequences of erroneous protein synthesis. *Nat Rev Genet, 10,* 715-724.

112. Dukan, S., Farewell, A., Ballesteros, M., Taddei, F., Radman, M., & Nystrom, T. (2000). Protein oxidation in response to increased transcriptional or translational errors. *Proc Natl Acad Sci U S A, 97,* 5746-5749.

113. Durant, P. C., Bajji, A. C., Sundaram, M., Kumar, R. K., & Davis, D. R. (2005). Structural effects of hypermodified nucleosides in the Escherichia coli and human tRNALys anticodon loop: the effect of nucleosides s2U, mcm5U, mcm5s2U, mnm5s2U, t6A, and ms2t6A. *Biochemistry, 44,* 8078-8089.

114. Eaglestone, S. S., Cox, B. S., & Tuite, M. F. (1999). Translation termination efficiency can be regulated in Saccharomyces cerevisiae by environmental stress through a prion-mediated mechanism. *EMBO J, 18,* 1974-1981.

115. Ehrenshaft, M., Bilski, P., Li, M. Y., Chignell, C. F., & Daub, M. E. (1999). A highly conserved sequence is a novel gene involved in de novo vitamin B6 biosynthesis. *Proc Natl Acad Sci U S A, 96,* 9374-9378.

116. Eldred, E. W. & Schimmel, P. R. (1972). Rapid deacylation by isoleucyl transfer ribonucleic acid synthetase of isoleucine-specific transfer ribonucleic acid aminoacylated with valine. *J Biol Chem, 247,* 2961-2964.

117. Engelberg, D., Klein, C., Martinetto, H., Struhl, K., & Karin, M. (1994). The UV response involving the Ras signaling pathway and AP-1 transcription factors is conserved between yeast and mammals. *Cell, 77,* 381-390.

118. Ercal N, Gurer-Orhan H, & Aykin-Burns N (2001). Toxic metals and oxidative stress part I: mechanisms involved in metal-induced oxidative damage. *Curr Top Med Chem, 1 (6),* 529-539.

119. Eriani, G., Delarue, M., Poch, O., Gangloff, J., & Moras, D. (1990). Partition of tRNA synthetases into two classes based on mutually exclusive sets of sequence motifs. *Nature, 347,* 203-206.

120. Erjavec, N., Larsson, L., Grantham, J., & Nystrom, T. (2007). Accelerated aging and failure to segregate damaged proteins in Sir2 mutants can be suppressed by overproducing the protein aggregation-remodeling factor Hsp104p. *Genes Dev, 21,* 2410-2421.

121. Eswara, M. B., McGuire, A. T., Pierce, J. B., & Mangroo, D. (2009). Utp9p facilitates Msn5p-mediated nuclear reexport of retrograded tRNAs in Saccharomyces cerevisiae. *Mol Biol Cell, 20,* 5007-5025.

122. Eurwilaichitr, L., Graves, F. M., Stansfield, I., & Tuite, M. F. (1999). The C-terminus of eRF1 defines a functionally important domain for translation termination in Saccharomyces cerevisiae. *Mol Microbiol, 32,* 485-496.

123. Farabaugh, P. J. & Björk, G. R. (1999). How translational accuracy influences reading frame maintenance. *EMBO J., 18,* 1427-1434.

124. Farabaugh, P. J. (1996). Programmed translational frameshifting. *Microbiol Rev, 60,* 103-134.

125. Fearon, K., McClendon, V., Bonetti, B., & Bedwell, D. M. (1994). Premature translation termination mutations are efficiently suppressed in a highly conserved region of yeast Ste6p, a member of the ATP-binding cassette (ABC) transporter family. *J Biol Chem, 269,* 17802-17808.

126. Fernandes L, Rodrigues-Pousada C, & Struhl K (1997). Yap, a novel family of eight bZIP proteins in Saccharomyces cerevisiae with distinct biological functions. *Mol Cell Biol, 17 (12),* 6982-6993.

127. Fernandes, L., Rodrigues-Pousada, C., & Struhl, K. (1997). Yap, a novel family of eight bZIP proteins in Saccharomyces cerevisiae with distinct biological functions. *Mol Cell Biol, 17 (12),* 6982-6993.

128. Flattery-O'Brien, J., Collinson, L. P., & Dawes, I. W. (1993). Saccharomyces cerevisiae has an inducible response to menadione which differs from that to hydrogen peroxide. *J Gen Microbiol, 139,* 501-507.

129. Francois, J. & Parrou, J. L. (2001). Reserve carbohydrates metabolism in the yeast Saccharomyces cerevisiae. *FEMS Microbiol Rev, 25,* 125-145.

130. Fraser, C. S., Berry, K. E., Hershey, J. W., & Doudna, J. A. (2007). eIF3j is located in the decoding center of the human 40S ribosomal subunit. *Mol Cell, 26,* 811-819.

131. Freistroffer, D. V., Kwiatkowski, M., Buckingham, R. H., & Ehrenberg, M. (2000). The accuracy of codon recognition by polypeptide release factors. *Proc Natl Acad Sci U S A, 97,* 2046-2051.

132. Freistroffer, D. V., Pavlov, M. Y., MacDougall, J., Buckingham, R. H., & Ehrenberg, M. (1997). Release factor RF3 in E.coli accelerates the dissociation of release factors RF1 and RF2 from the ribosome in a GTP-dependent manner. *EMBO J, 16,* 4126-4133.

133. Frolova, L., Seit-Nebi, A., & Kisselev, L. (2002). Highly conserved NIKS tetrapeptide is functionally essential in eukaryotic translation termination factor eRF1. *RNA, 8,* 129-136.

134. Frolova, L. Y., Tsivkovskii, R. Y., Sivolobova, G. F., Oparina, N. Y., Serpinsky, O. I., Blinov, V. M. et al. (1999). Mutations in the highly conserved GGQ motif of class 1 polypeptide release factors abolish ability of human eRF1 to trigger peptidyl-tRNA hydrolysis. *RNA, 5,* 1014-1020.

135. Fu, H. L., Meng, Y., Ordonez, E., Villadangos, A. F., Bhattacharjee, H., Gil, J. A. et al. (2009). Properties of arsenite efflux permeases (Acr3) from Alkaliphilus metalliredigens and Corynebacterium glutamicum. *J Biol Chem, 284,* 19887-19895.

136. Fu, L., Miseta, A., Hunton, D., Marchase, R. B., & Bedwell, D. M. (2000). Loss of the major isoform of phosphoglucomutase results in altered calcium homeostasis in Saccharomyces cerevisiae. *J Biol Chem, 275,* 5431-5440.

137. Galhardo, R. S., Hastings, P. J., & Rosenberg, S. M. (2007). Mutation as a stress response and the regulation of evolvability. *Crit Rev Biochem Mol Biol, 42,* 399-435.

138. Gallant, J. A. & Lindsley, D. (1992). Leftward ribosome frameshifting at a hungry codon. *J Mol Biol, 223,* 31-40.

139. Gallant, J. A. & Lindsley, D. (1998). Ribosomes can slide over and beyond "hungry" codons, resuming protein chain elongation many nucleotides downstream. *Proc Natl Acad Sci U S A, 95,* 13771-13776.

140. Garcia-Mata, R., Gao, Y., & Sztul, E. (2002). Hassles with taking out the garbage: aggravating aggresomes. *Traffic, 3,* 388-396.

141. Gasch AP (2002). The environmental stress response: a common yeast response to diverse environmental stresses. *Topics in Current Genetics, eds.Hohmann S & Mager P (Springer, Heidelberg), Vol. 1,* 11-70.

142. Gasch AP, Spellman PT, Kao CM, Carmel-Harel O, Eisen MB, Storz G et al. (2000). Genomic expression programs in the response of yeast cells to environmental changes. *Mol Biol Cell, 11 (12),* 4241-4257.

143. Gasch, A. P., Spellman, P. T., Kao, C. M., Carmel-Harel, O., Eisen, M. B., Storz, G. et al. (2000). Genomic expression programs in the response of yeast cells to environmental changes. *Mol Biol Cell, 11 (12),* 4241-4257.

144. Georgatsou, E. & Alexandraki, D. (1994). Two distinctly regulated genes are required for ferric reduction, the first step of iron uptake in Saccharomyces cerevisiae. *Mol Cell Biol, 14,* 3065-3073.

145. Ghaemmaghami, S., Huh, W. K., Bower, K., Howson, R. W., Belle, A., Dephoure, N. et al. (2003). Global analysis of protein expression in yeast. *Nature, 425,* 737-741.

146. Gidalevitz, T., Prahlad, V., & Morimoto, R. I. (2011). The stress of protein misfolding: from single cells to multicellular organisms. *Cold Spring Harb Perspect Biol, 3 (6)*.

147. Giege, R., Sissler, M., & Florentz, C. (1998). Universal rules and idiosyncratic features in tRNA identity. *Nucleic Acids Res, 26,* 5017-5035.

148. Gietz RD & Woods RA (2006). Yeast transformation by the LiAc/SS Carrier DNA/PEG method. *Methods Mol Biol, 313,* 107-120.

149. Gietz, R. D. & Woods, R. A. (2006). Yeast transformation by the LiAc/SS Carrier DNA/PEG method. *Methods Mol Biol, 313,* 107-120.

150. Giots, F., Donaton, M. C., & Thevelein, J. M. (2003). Inorganic phosphate is sensed by specific phosphate carriers and acts in concert with glucose as a nutrient signal for activation of the protein kinase A pathway in the yeast Saccharomyces cerevisiae. *Mol Microbiol, 47,* 1163-1181.

151. Gitan, R. S. & Eide, D. J. (2000). Zinc-regulated ubiquitin conjugation signals endocytosis of the yeast ZRT1 zinc transporter. *Biochem J, 346 Pt 2,* 329-336.

152. Gitan, R. S., Shababi, M., Kramer, M., & Eide, D. J. (2003). A cytosolic domain of the yeast Zrt1 zinc transporter is required for its post-translational inactivation in response to zinc and cadmium. *J Biol Chem, 278,* 39558-39564.

153. Glickman MH & Ciechanover A. (2002). The ubiquitin-proteasome proteolytic pathway: destruction for the sake of construction. Physiol Rev 82 (2), 373-428.
Ref Type: Generic

154. Glickman, M. H. & Ciechanover, A. (2002). The ubiquitin-proteasome proteolytic pathway: destruction for the sake of construction. *Physiol Rev., 82 (2),* 373-428.

155. Glover JR & Lindquist S. (1998). Hsp104, Hsp70, and Hsp40: a novel chaperone system that rescues previously aggregated proteins. Cell 94, 73-82.
Ref Type: Generic

156. Glover, J. R. & Lindquist, S. (1998). Hsp104, Hsp70, and Hsp40: a novel chaperone system that rescues previously aggregated proteins. *Cell, 94,* 73-82.

157. Glukhova, M. A., Spirin, A. S., & Spirin, A. S. (1975). A study of codon-dependent binding of aminoacyl-tRNA with the ribosomal 30-S subparticle of Escherichia coli. Determination of the active-particle fraction and binding constants in different media. *Eur J Biochem, 52 (1),* 197-202.

158. Goldsmith, M. & Tawfik, D. (2009). Potential role of phenotypic mutations in the evolution of protein expression and stability. *Proc.Natl.Acad.Sci, 106,* 6197-6202.

159. Gombert, A. K., Moreira dos, S. M., Christensen, B., & Nielsen, J. (2001). Network identification and flux quantification in the central metabolism of Saccharomyces cerevisiae under different conditions of glucose repression. *J Bacteriol, 183,* 1441-1451.

160. Gomes, D. S., Fragoso, L. C., Riger, C. J., Panek, A. D., & Eleutherio, E. C. (2002). Regulation of cadmium uptake by Saccharomyces cerevisiae. *Biochim Biophys Acta, 1573,* 21-25.

161. Goossens, A., Dever, T. E., Pascual-Ahuir, A., & Serrano, R. (2001). The protein kinase Gcn2p mediates sodium toxicity in yeast. *J Biol Chem, 276,* 30753-30760.

162. Grant, C. M. (2001). Role of the glutathione/glutaredoxin and thioredoxin systems in yeast growth and response to stress conditions. *Mol Microbiol, 39,* 533-541.

163. Grant, C. M., MacIver, F. H., & Dawes, I. W. (1997). Glutathione synthetase is dispensable for growth under both normal and oxidative stress conditions in the yeast Saccharomyces cerevisiae due to an accumulation of the dipeptide gamma-glutamylcysteine. *Mol Biol Cell, 8,* 1699-1707.

164. Green, R. & Noller, H. F. (1997). Ribosomes and translation. *Annu Rev Biochem, 66,* 679-716.

165. Greenbaum, D., Colangelo, C., Williams, K., & Gerstein, M. (2003). Comparing protein abundance and mRNA expression levels on a genomic scale. *Genome Biol, 4,* 117.

166. Grosjean, H. (2009). Nucleic Acids Are Not Boring Long Polymers of Only Four Types of Nucleotides: A Guided Tour. In *DNA and RNA Modification Enzymes: Structure, Mechanism, Function and Evolution* (Austin (TX): Landes Bioscience.

167. Grosjean, H., Szweykowska-Kulinska, Z., Motorin, Y., Fasiolo, F., & Simos, G. (1997). Intron-dependent enzymatic formation of modified nucleosides in eukaryotic tRNAs: a review. *Biochimie, 79,* 293-302.

168. Grune, T., Jung, T., Merker, K., & Davies, K. J. (2004). Decreased proteolysis caused by protein aggregates, inclusion bodies, plaques, lipofuscin, ceroid, and 'aggresomes' during oxidative stress, aging, and disease. *Int J Biochem Cell Biol, 36,* 2519-2530.

169. Gulshan, K., Rovinsky, S. A., Coleman, S. T., & Moye-Rowley, W. S. (2005). Oxidant-specific folding of Yap1p regulates both transcriptional activation and nuclear localization. *J Biol Chem, 280 (49),* 40524-40533.

170. Guo, H. H., Choe, J., & Loeb, L. A. (2004). Protein tolerance to random amino acid change. *Proc Natl Acad Sci U S A, 101,* 9205-9210.

171. Gustavsson, M. & Ronne, H. (2008). Evidence that tRNA modifying enzymes are important in vivo targets for 5-fluorouracil in yeast. *RNA, 14,* 666-674.

172. Gygi, S. P., Rochon, Y., Franza, B. R., & Aebersold, R. (1999). Correlation between protein and mRNA abundance in yeast. *Mol Cell Biol, 19,* 1720-1730.

173. Haigis, M. C. & Yankner, B. A. (2010). The aging stress response. *Mol Cell, 40,* 333-344.

174. Halbeisen, R. E. & Gerber, A. P. (2009). Stress-Dependent Coordination of Transcriptome and Translatome in Yeast. *PLoS Biol, 7,* e105.

175. Hall, B. G. (1990). Spontaneous point mutations that occur more often when advantageous than when neutral. *Genetics, 126,* 5-16.

176. Hara, T., Nakamura, K., Matsui, M., Yamamoto, A., Nakahara, Y., Suzuki-Migishima, R. et al. (2006). Suppression of basal autophagy in neural cells causes neurodegenerative disease in mice. *Nature, 441,* 885-889.

177. Hartmann, E. & Hartmann, R. K. (2003). The enigma of ribonuclease P evolution. *Trends Genet, 19,* 561-569.

178. Haslbeck, M., Braun, N., Stromer, T., Richter, B., Model, N., Weinkauf, S. et al. (2004). Hsp42 is the general small heat shock protein in the cytosol of Saccharomyces cerevisiae. *EMBO J., 23 (3),* 638-649.

179. Haslbeck, M., Franzmann, T., Weinfurtner, D., & Buchner, J. (2005a). Some like it hot: the structure and function of small heat-shock proteins. *Nat Struct.Mol Biol, 12,* 842-846.

180. Haslbeck, M., Miess, A., Stromer, T., Walter, S., & Buchner, J. (2005b). Disassembling protein aggregates in the yeast cytosol. The cooperation of Hsp26 with Ssa1 and Hsp104. *J Biol Chem, 280,* 23861-23868.

181. Haslbeck, M., Walke, S., Stromer, T., Ehrnsperger, M., White, H. E., Chen, S. et al. (1999). Hsp26: a temperature-regulated chaperone. *EMBO J, 18,* 6744-6751.

182. Hatfield, D. L. & Gladyshev, V. N. (2002). How selenium has altered our understanding of the genetic code. *Mol Cell Biol, 22,* 3565-3576.

183. Heiss, N. S., Knight, S. W., Vulliamy, T. J., Klauck, S. M., Wiemann, S., Mason, P. J. et al. (1998). X-linked dyskeratosis congenita is caused by mutations in a highly conserved gene with putative nucleolar functions. *Nat Genet, 19,* 32-38.

184. Hershko, A. & Ciechanover, A. (1998). The ubiquitin system. *Annu Rev Biochem, 67,* 425-479.

185. Herst, P. M., Perrone, G. G., Dawes, I. W., Bircham, P. W., & Berridge, M. V. (2008). Plasma membrane electron transport in Saccharomyces cerevisiae depends on the presence of mitochondrial respiratory subunits. *FEMS Yeast Res, 8,* 897-905.

186. Hillenmeyer, M. E., Fung, E., Wildenhain, J., Pierce, S. E., Hoon, S., Lee, W. et al. (2008). The chemical genomic portrait of yeast: uncovering a phenotype for all genes. *Science, 320,* 362-365.

187. Hinnebusch, A. G. (1986). The general control of amino acid biosynthetic genes in the yeast Saccharomyces cerevisiae. *CRC Crit Rev Biochem, 21,* 277-317.

188. Hinnebusch, A. G. (2005). Translational regulation of GCN4 and the general amino acid control of yeast. *Annu Rev Microbiol, 59,* 407-450.

189. Hinnebusch, A. G. & Natarajan, K. (2002). Gcn4p, a master regulator of gene expression, is controlled at multiple levels by diverse signals of starvation and stress. *Eukaryot Cell, 1,* 22-32.

190. Holland S, Lodwig E, Sideri T, Reader T, Clarke I, Gkargkas K et al. (2007). Application of the comprehensive set of heterozygous yeast deletion mutants to elucidate the molecular basis of cellular chromium toxicity. *Genome Biol, 8,* R268.

191. Holland, S., Ghosh, E., & Avery, S. V. (2010). Chromate-induced sulfur starvation and mRNA mistranslation in yeast are linked in a common mechanism of Cr toxicity. *Toxicol In Vitro, 24,* 1764-1767.

192. Holland, S., Lodwig, E., Sideri, T., Reader, T., Clarke, I., Gkargkas, K. et al. (2007). Application of the comprehensive set of heterozygous yeast deletion mutants to elucidate the molecular basis of cellular chromium toxicity. *Genome Biol, 8,* R268.

193. Holley, R. W. (1965). Structure of an alanine transfer ribonucleic acid. *JAMA, 194,* 868-871.

194. Homann, O. R., Dea, J., Noble, S. M., & Johnson, A. D. (2009). A phenotypic profile of the Candida albicans regulatory network. *PLoS Genet, 5,* e1000783.

195. Hopfield, J. J. (1974). Kinetic proofreading: a new mechanism for reducing errors in biosynthetic processes requiring high specificity. *Proc.Natl.Acad.Sci, 71,* 4135-4139.

196. Horst, M., Knecht, E. C., & Schu, P. V. (1999). Import into and degradation of cytosolic proteins by isolated yeast vacuoles. *Mol Biol Cell, 10,* 2879-2889.

197. Hosack, D. A., Dennis, G., Jr., Sherman, B. T., Lane, H. C., & Lempicki, R. A. (2003). Identifying biological themes within lists of genes with EASE. *Genome Biol, 4,* R70.

198. Hu, Y., Cooper, T. G., & Kohlhaw, G. B. (1995). The Saccharomyces cerevisiae Leu3 protein activates expression of GDH1, a key gene in nitrogen assimilation. *Mol Cell Biol, 15,* 52-57.

199. Huang, B., Johansson, M. J., & Byström, A. S. (2005). An early step in wobble uridine tRNA modification requires the Elongator complex. *RNA, 11 (4),* 424-436.

200. Huang, d. W., Sherman, B. T., & Lempicki, R. A. (2009). Bioinformatics enrichment tools: paths toward the comprehensive functional analysis of large gene lists. *Nucleic Acids Res, 37,* 1-13.

201. Huang, H. L. & Brandriss, M. C. (2000). The regulator of the yeast proline utilization pathway is differentially phosphorylated in response to the quality of the nitrogen source. *Mol Cell Biol, 20,* 892-899.

202. Huang, Y. H., Shih, C. M., Huang, C. J., Lin, C. M., Chou, C. M., Tsai, M. L. et al. (2006). Effects of cadmium on structure and enzymatic activity of Cu,Zn-SOD and oxidative status in neural cells. *J Cell Biochem, 98,* 577-589.

203. Huh WK, Falvo JV, Gerke LC, Carroll AS, Howson RW, Weissman JS et al. (2003). Global analysis of protein localization in budding yeast. Nature 425, 686-691.
Ref Type: Generic

204. Hurto, R. L., Tong, A. H., Boone, C., & Hopper, A. K. (2007). Inorganic phosphate deprivation causes tRNA nuclear accumulation via retrograde transport in Saccharomyces cerevisiae. *Genetics, 176,* 841-852.

205. Ikemura, T. (1981). Correlation between the abundance of Escherichia coli transfer RNAs and the occurrence of the respective codons in its protein genes. *J Mol Biol, 146,* 1-21.

206. Ikemura, T. & Ozeki, H. (1983). Codon usage and transfer RNA contents: organism-specific codon-choice patterns in reference to the isoacceptor contents. *Cold Spring Harb Symp Quant Biol, 47 Pt 2,* 1087-1097.

207. Imlay, J. A. (2008). Cellular defenses against superoxide and hydrogen peroxide. *Annu Rev Biochem, 77,* 755-776.

208. Inagaki, Y., Blouin, C., Doolittle, W. F., & Roger, A. J. (2002). Convergence and constraint in eukaryotic release factor 1 (eRF1) domain 1: the evolution of stop codon specificity. *Nucleic Acids Res, 30,* 532-544.

209. Isken, O. & Maquat, L. E. (2007). Quality control of eukaryotic mRNA: safeguarding cells from abnormal mRNA function. *Genes Dev, 21,* 1833-1856.

210. Ito, K., Uno, M., & Nakamura, Y. (2001). A tripeptide 'anticodon' deciphers stop codons in messenger RNA. *Nature, 403,* 680-684.

211. Ito, K., Ebihara, K., & Nakamura, Y. (1998). The stretch of C-terminal acidic amino acids of translational release factor eRF1 is a primary binding site for eRF3 of fission yeast. *RNA, 4,* 958-972.

212. Ito, K., Ebihara, K., Uno, M., & Nakamura, Y. (1996). Conserved motifs in prokaryotic and eukaryotic polypeptide release factors: tRNA-protein mimicry hypothesis. *Proc Natl Acad Sci U S A, 93,* 5443-5448.

213. Izawa, S., Maeda, K., Miki, T., Mano, J., Inoue, Y., & Kimura, A. (1998a). Importance of glucose-6-phosphate dehydrogenase in the adaptive response to hydrogen peroxide in Saccharomyces cerevisiae. *Biochem J, 330 (Pt 2),* 811-817.

214. Izawa, S., Maeda, K., Miki, T., Mano, J., Inoue, Y., & Kimura, A. (1998b). Importance of glucose-6-phosphate dehydrogenase in the adaptive response to hydrogen peroxide in Saccharomyces cerevisiae. *Biochem J, 330 (Pt 2),* 811-817.

215. Jablonowski, D., Zink, S., Mehlgarten, C., Daum, G., & Schaffrath, R. (2006). tRNAGlu wobble uridine methylation by Trm9 identifies Elongator's key role for zymocin-induced cell death in yeast. *Mol Microbiol,* 677-688.

216. Jackson, R. J., Hellen, C. U., & Pestova, T. V. (2010). The mechanism of eukaryotic translation initiation and principles of its regulation. *Nat Rev Mol Cell Biol, 11,* 113-127.

217. Jaillon, O., Bouhouche, K., Gout, J. F., Aury, J. M., Noel, B., Saudemont, B. et al. (2008). Translational control of intron splicing in eukaryotes. *Nature, 451,* 359-362.

218. Jakubowski, H. & Goldman, E. (1992). Editing of Errors in Selection of Amino Acids for Protein Synthesis. *Microbiol Rev, 56 (3),* 412-429.

219. Jamieson, D. J., Rivers, S. L., & Stephen, D. W. (1994). Analysis of Saccharomyces cerevisiae proteins induced by peroxide and superoxide stress. *Microbiology, 140 (Pt 2),* 3277-3283.

220. Jamieson, D. J. (1998). Oxidative stress responses of the yeast Saccharomyces cerevisiae. *Yeast, 14,* 1511-1527.

221. Janssen, M. J., de, K. B., & de Kroon, A. I. (2002). Phosphate is required to maintain the outer membrane integrity and membrane potential of respiring yeast mitochondria. *Anal.Biochem, 300,* 27-33.

222. Johansson, M., Bouakaz, E., Lovmar, M., & Ehrenberg, M. (2008). The kinetics of ribosomal peptidyl transfer revisited. *Mol Cell, 30 (5),* 598.

223. Johnston, J. A., Ward, C. L., & Kopito, R. R. (1998). Aggresomes: a cellular response to misfolded proteins. *J Cell Biol, 143,* 1883-1898.

224. Jomova, K., Jenisova, Z., Feszterova, M., Baros, S., Liska, J., Hudecova, D. et al. (2011). Arsenic: toxicity, oxidative stress and human disease. *J Appl Toxicol, 31,* 95-107.

225. Jones, T. E., Alexander, R. W., & Pan, T. (2011). Misacylation of specific nonmethionyl tRNAs by a bacterial methionyl-tRNA synthetase. *Proc Natl Acad Sci U S A, 108,* 6933-6938.

226. Jordanova, A., Irobi, J., Thomas, F. P., Van, D. P., Meerschaert, K., Dewil, M. et al. (2006). Disrupted function and axonal distribution of mutant tyrosyl-tRNA synthetase in dominant intermediate Charcot-Marie-Tooth neuropathy. *Nat Genet, 38,* 197-202.

227. Juhnke, H., Krems, B., Kotter, P., & Entian, K. D. (1996). Mutants that show increased sensitivity to hydrogen peroxide reveal an important role for the pentose phosphate pathway in protection of yeast against oxidative stress. *Mol Gen Genet, 252,* 456-464.

228. Kadaba, S., Krueger, A., Trice, T., Krecic, A. M., Hinnebusch, A. G., & Anderson, J. (2004). Nuclear surveillance and degradation of hypomodified initiator tRNAMet in S. cerevisiae. *Genes Dev, 18,* 1227-1240.

229. Kaganovich, D., Kopito, R., & Frydman, J. (2008). Misfolded proteins partition between two distinct quality control compartments. *Nature, 454,* 1088-1095.

230. Kalhor, H. R. & Clarke, S. (2003). Novel methyltransferase for modified uridine residues at the wobble position of tRNA. *Mol Cell Bio, 23 (24),* 9283-9292.

231. Kandror O, Bretschneider N, Kreydin E, Cavalieri D, & Goldberg AL (2004). Yeast adapt to near-freezing temperatures by STRE/Msn2,4-dependent induction of trehalose synthesis and certain molecular chaperones. *Mol Cell, 13 (6),* 771-781.

232. Kandror, O., Bretschneider, N., Kreydin, E., Cavalieri, D., & Goldberg, A. L. (2004). Yeast adapt to near-freezing temperatures by STRE/Msn2,4-dependent induction of trehalose synthesis and certain molecular chaperones. *Mol Cell, 13 (6),* 771-781.

233. Kapp, L. & Lorsch JR (2004). The molecular mechanics of eukaryotic translation. *Annu Rev Biochem, 73,* 657-704.

234. Kappeli, O. (1986). Regulation of carbon metabolism in Saccharomyces cerevisiae and related yeasts. *Adv.Microb.Physiol, 28,* 181-209.

235. Karathia, H., Vilaprinyo, E., Sorribas, A., & Alves, R. (2011). Saccharomyces cerevisiae as a model organism: a comparative study. *PLoS One, 6,* e16015.

236. Karimi, R., Pavlov, M. Y., Buckingham, R. H., & Ehrenberg, M. (1999). Novel roles for classical factors at the interface between translation termination and initiation. *Mol Cell, 3,* 601-609.

237. Keeling, K., Lanier, J., Du, M., Salas-Marco, J., Gao, L., Kaenjak-Angeletti, A. et al. (2004). Leaky termination at premature stop codons antagonizes nonsense-mediated mRNA decay in S. cerevisiae. *RNA, 10,* 691-703.

238. Kim SY & Craig EA (2005). Broad sensitivity of Saccharomyces cerevisiae lacking ribosome-associated chaperone ssb or zuo1 to cations, including aminoglycosides. *Eukaryot Cell, 4 (1),* 82-89.

239. Kim, P. K., Hailey, D. W., Mullen, R. T., & Lippincott-Schwartz, J. (2008). Ubiquitin signals autophagic degradation of cytosolic proteins and peroxisomes. *Proc Natl Acad Sci U S A, 105,* 20567-20574.

240. Kim, S. Y. & Craig, E. A. (2005). Broad sensitivity of Saccharomyces cerevisiae lacking ribosome-associated chaperone ssb or zuo1 to cations, including aminoglycosides. *Eukaryot Cell, 4 (1),* 82-89.

241. Kirino, Y., Goto, Y., Campos, Y., Arenas, J., & Suzuki, T. (2005). Specific correlation between the wobble modification deficiency in mutant tRNAs and the clinical features of a human mitochondrial disease. *Proc Natl Acad Sci U S A, 102,* 7127-7132.

242. Kisselev L, Ehrenberg M, & Frolova L. (2003). Termination of translation: interplay of mRNA, rRNAs and release factors? EMBO J. 22, 175-182.
Ref Type: Generic

243. Kisselev, L., Ehrenberg, M., & Frolova, L. (2003). Termination of translation: interplay of mRNA, rRNAs and release factors? *EMBO J., 22,* 175-182.

244. Klionsky, D. J., Codogno, P., Cuervo, A. M., Deretic, V., Elazar, Z., Fueyo-Margareto, J. et al. (2010). A comprehensive glossary of autophagy-related molecules and processes. *Autophagy., 6*.

245. Kobayashi, N. & McEntee, K. (1990). Evidence for a heat shock transcription factor-independent mechanism for heat shock induction of transcription in Saccharomyces cerevisiae. *Proc Natl Acad Sci U S A, 87 (17),* 6550-6554.

246. Konevega, A. L., Soboleva, N. G., Makhno, V. I., Semenkov, Y. P., Wintermeyer, W., Rodnina, M. V. et al. (2004). Purine bases at position 37 of tRNA stabilize codon-anticodon interaction in the ribosomal A site by stacking and Mg2+-dependent interactions. *RNA, 10,* 90-101.

247. Kopito, R. R. (2000). Aggresomes, inclusion bodies and protein aggregation. *Trends Cell Biol, 10,* 524-530.

248. Kornberg, A., Rao, N. N., & ult-Riche, D. (1999). Inorganic polyphosphate: a molecule of many functions. *Annu Rev Biochem, 68,* 89-125.

249. Kotelawala, L., Grayhack, E. J., & Phizicky, E. M. (2008). Identification of yeast tRNA Um(44) 2'-O-methyltransferase (Trm44) and demonstration of a Trm44 role in sustaining levels of specific tRNA(Ser) species. *RNA, 14,* 158-169.

250. Kourie, J. I. & Henry, C. L. (2002). Ion channel formation and membrane-linked pathologies of misfolded hydrophobic proteins: the role of dangerous unchaperoned molecules. *Clin.Exp.Pharmacol Physiol, 29,* 741-753.

251. Kowalczykowski, S. C. (2000). Initiation of genetic recombination and recombination-dependent replication. *Trends Biochem Sci, 25,* 156-165.

252. Kozak, M. (1999). Initiation of translation in prokaryotes and eukaryotes. *Gene, 234,* 187-208.

253. Kozak, M. (2002). Pushing the limits of the scanning mechanism for initiation of translation. *Gene, 299,* 1-34.

254. Kraft, C., Deplazes, A., Sohrmann, M., & Peter, M. (2008). Mature ribosomes are selectively degraded upon starvation by an autophagy pathway requiring the Ubp3p/Bre5p ubiquitin protease. *Nat Cell Biol, 10 (5),* 602-610.

255. Kramer, E. & Farabaugh, P. (2006). The frequency of translational misreading errors in E. coli is largely determined by tRNA competition. *RNA, 13,* 87-96.

256. Kramer, E., Vallabhaneni, H., Mayer, L., & Farabaugh, P. (2010). A comprehensive analysis of translational missense errors in the yeast Saccharomyces cerevisiae. *RNA, 16,* 1797-1808.

257. Krogan, N. J. & Greenblatt, J. F. (2001). Characterization of a six-subunit holo-elongator complex required for the regulated expression of a group of genes in Saccharomyces cerevisiae. *Mol Cell Biol., 21 (23),* 8203-8212.

258. Kunkel, T. A. & Bebenek, K. (2000). DNA replication fidelity. *Annu Rev Biochem, 69,* 497-529.

259. Kuranda, K., Leberre, V., Sokol, S., Palamarczyk, G., & François, J. (2006). Investigating the caffeine effects in the yeast Saccharomyces cerevisiae brings new insights into the connection between TOR, PKC and Ras/cAMP signalling pathways. *Mol Microbiol, 61 (5),* 1147-1166.

260. Kvitek, D. J., Will, J. L., & Gasch, A. P. (2008). Variations in stress sensitivity and genomic expression in diverse S. cerevisiae isolates. *PLoS Genet, 4,* e1000223.

261. Lancaster, L., Kiel, M. C., Kaji, A., & Noller, H. F. (2002). Orientation of ribosome recycling factor in the ribosome from directed hydroxyl radical probing. *Cell, 111,* 129-140.

262. Lansbury, P. T. & Lashuel, H. A. (2006). A century-old debate on protein aggregation and neurodegeneration enters the clinic. *Nature, 443,* 774-779.

263. Laughrea, M., Latulippe, J., & Filion, A. M. (1984). Effect of ethanol, phenol, formamide, dimethyl sulfoxide, paromomycin, and deuterium oxide on the fidelity of translation in a brain cell-free system. *Biochemistry, 23 (4),* 753-758.

264. Lee, D. H. & Goldberg, A. L. (1998). Proteasome inhibitors cause induction of heat shock proteins and trehalose, which together confer thermotolerance in Saccharomyces cerevisiae. *Mol Cell Biol, 18,* 30-38.

265. Lee, J. W., Beebe, K., Nangle, L. A., Jang, J., Longo-Guess, C. M., Cook, S. A. et al. (2006). Editing-defective tRNA synthetase causes protein misfolding and neurodegeneration. *Nature, 443,* 50-55.

266. Lesuisse, E. & Labbe, P. (1995). Effects of cadmium and of YAP1 and CAD1/YAP2 genes on iron metabolism in the yeast Saccharomyces cerevisiae. *Microbiology, 141 (Pt 11),* 2937-2943.

267. Levine, R. L. (2002). Carbonyl modified proteins in cellular regulation, aging, and disease. *Free Radic Biol Med, 32,* 790-796.

268. Levine, R. L., Mosoni, L., Berlett, B. S., & Stadtman, E. R. (1996). Methionine residues as endogenous antioxidants in proteins. *Proc Natl Acad Sci U S A, 93,* 15036-15040.

269. Lewis, J. G., Learmonth, R. P., & Watson, K. (1995). Induction of heat, freezing and salt tolerance by heat and salt shock in Saccharomyces cerevisiae. *Microbiology, 141 (Pt 3),* 687-694.

270. Li, L., Boniecki, M. T., Jaffe, J. D., Imai, B. S., Yau, P. M., Luthey-Schulten, Z. A. et al. (2011). Naturally occurring aminoacyl-tRNA synthetases editing-domain mutations that cause mistranslation in Mycoplasma parasites. *Proc Natl Acad Sci U S A, 108,* 9378-9383.

271. Liang, H., Cavalcanti, A. R., & Landweber, L. F. (2005). Conservation of tandem stop codons in yeasts. *Genome Biol, 6 (4),* R31.

272. Liberek, K., Lewandowska, A., & Zietkiewicz, S. (2008). Chaperones in control of protein disaggregation. *EMBO J., 27,* 328-335.

273. Lim, V. I., Curran, J. F., & Garber, M. B. (2005). Ribosomal elongation cycle: energetic, kinetic and stereochemical aspects. *J Mol Biol, 351 (3),* 470-480.

274. Lin, L. & Schimmel, P. (1996). Mutational analysis suggests the same design for editing activities of two tRNA synthetases. *Biochemistry, 35,* 5596-5601.

275. Ling J & Söll D. (2010). Severe oxidative stress induces protein mistranslation through impairment of an aminoacyl-tRNA synthetase editing site. Proc Natl Acad Sci U S A 107 (9), 4028-4033.
Ref Type: Generic

276. Ling, J. & Söll, D. (2010). Severe oxidative stress induces protein mistranslation through impairment of an aminoacyl-tRNA synthetase editing site. *Proc Natl Acad Sci U S A, 107 (9),* 4028-4033.

277. Ling, J., Reynolds, N., & Ibba, M. (2009a). Aminoacyl-tRNA synthesis and translational quality control. *Annu Rev Microbiol, 63,* 61-78.

278. Ling, J., So, B. R., Yadavalli, S. S., Roy, H., Shoji, S., Fredrick, K. et al. (2009b). Resampling and editing of mischarged tRNA prior to translation elongation. *Mol Cell, 33,* 654-660.

279. Liu, R. & Liebman, S. W. (1996). A translational fidelity mutation in the universally conserved sarcin/ricin domain of 25S yeast ribosomal RNA. *RNA, 2,* 254-263.

280. Lodish, H., Berk, A., Zipursky, S., Matsudaira, P., Baltimore, D., & Darnell, J. (2000). *Molecular Cell Biology*. (4th ed.) New York: W.H.Freeman and Company.

281. Lopez-Maury, L., Marguerat, S., & Bahler, J. (2008). Tuning gene expression to changing environments: from rapid responses to evolutionary adaptation. *Nat Rev Genet, 9,* 583-593.

282. Ludmerer, S. W. & Schimmel, P. (1987). Gene for yeast glutamine tRNA synthetase encodes a large amino-terminal extension and provides a strong confirmation of the signature sequence for a group of the aminoacyl-tRNA synthetases. *J Biol Chem, 262,* 10801-10806.

283. Lum, R., Tkach, J. M., Vierling, E., & Glover, J. R. (2004). Evidence for an unfolding/threading mechanism for protein disaggregation by Saccharomyces cerevisiae Hsp104. *J Biol Chem, 279,* 29139-29146.

284. Lund, E. & Dahlberg, J. E. (1998). Proofreading and aminoacylation of tRNAs before export from the nucleus. *Science, 282,* 2082-2085.

285. Luo, S. & Levine, R. L. (2009). Methionine in proteins defends against oxidative stress. *FASEB J, 23,* 464-472.

286. Lustig, F., Elias, P., Axberg, T., Samuelsson, T., Tittawella, I., & Lagerkvist, U. (1981). Codon reading and translational error. Reading of the glutamine and lysine codons during protein synthesis in vitro. *J Biol Chem, 256,* 2635-2643.

287. Lutfiyya, L. L., Iyer, V. R., DeRisi, J., DeVit, M. J., Brown, P. O., & Johnston, M. (1998). Characterization of three related glucose repressors and genes they regulate in Saccharomyces cerevisiae. *Genetics, 150,* 1377-1391.

288. Maaheimo, H., Fiaux, J., Cakar, Z. P., Bailey, J. E., Sauer, U., & Szyperski, T. (2001). Central carbon metabolism of Saccharomyces cerevisiae explored by biosynthetic fractional (13)C labeling of common amino acids. *Eur J Biochem, 268,* 2464-2479.

289. Mager, W. H. & De Kruijff, A. J. (1995). Stress-induced transcriptional activation. *Microbiol Rev, 59,* 506-531.

290. Mamane, Y., Petroulakis, E., Rong, L., Yoshida, K., Ler, L. W., & Sonenberg, N. (2004). eIF4E--from translation to transformation. *Oncogene, 23,* 3172-3179.

291. Mann, H., Ben-Asouli, Y., Schein, A., Moussa, S., & Jarrous, N. (2003). Eukaryotic RNase P: role of RNA and protein subunits of a primordial catalytic ribonucleoprotein in RNA-based catalysis. *Mol Cell, 12,* 925-935.

292. Marechal-Drouard, L., Weil, J. H., & Guillemaut, P. (1988). Import of several tRNAs from the cytoplasm into the mitochondria in bean Phaseolus vulgaris. *Nucleic Acids Res, 16,* 4777-4788.

293. Mariani, D., Mathias, C. J., da Silva, C. G., Herdeiro, R. S., Pereira, R., Panek, A. D. et al. (2008). Involvement of glutathione transferases, Gtt1and Gtt2, with oxidative stress response generated by H2O2 during growth of Saccharomyces cerevisiae. *Redox Rep., 13,* 246-254.

294. Markiewicz, P., Kleina, L. G., Cruz, C., Ehret, S., & Miller, J. H. (1994). Genetic studies of the lac repressor. XIV. Analysis of 4000 altered Escherichia coli lac repressors reveals essential and non-essential residues, as well as "spacers" which do not require a specific sequence. *J Mol Biol, 240,* 421-433.

295. Marshall, L., Kenneth, N. S., & White, R. J. (2008). Elevated tRNA(iMet) synthesis can drive cell proliferation and oncogenic transformation. *Cell, 133,* 78-89.

296. Martinez-Pastor, M. T., Marchler, G., Schuller, C., Marchler-Bauer, A., Ruis, H., & Estruch, F. (1996). The Saccharomyces cerevisiae zinc finger proteins Msn2p and Msn4p are required for transcriptional induction through the stress response element (STRE). *EMBO J, 15,* 2227-2235.

297. Martinis, S. A. & Boniecki, M. T. (2010). The balance between pre- and post-transfer editing in tRNA synthetases. *FEBS Lett., 584,* 455-459.

298. Mascarenhas, C., Edwards-Ingram, L. C., Zeef, L., Shenton, D., Ashe, M. P., & Grant, C. M. (2008). Gcn4 is required for the response to peroxide stress in the yeast Saccharomyces cerevisiae. *Mol Biol Cell, 19,* 2995-3007.

299. Masuda, C. A., Xavier, M. A., Mattos, K. A., Galina, A., & Montero-Lomeli, M. (2001). Phosphoglucomutase is an in vivo lithium target in yeast. *J Biol Chem, 276,* 37794-37801.

300. Mayer, M. P. & Bukau, B. (1998). Hsp70 chaperone systems: diversity of cellular functions and mechanism of action. *Biol Chem, 379 (3),* 261-268.

301. McClellan, A. J., Tam, S., Kaganovich, D., & Frydman, J. (2005). Protein quality control: chaperones culling corrupt conformations. *Nat Cell Biol, 7,* 736-741.

302. McCraith, S. M. & Phizicky, E. M. (1991). An enzyme from Saccharomyces cerevisiae uses NAD+ to transfer the splice junction 2'-phosphate from ligated tRNA to an acceptor molecule. *J Biol Chem, 266,* 11986-11992.

303. Menezes, R. A., Amaral, C., Batista-Nascimento, L., Santos, C., Ferreira, R. B., Devaux, F. et al. (2008). Contribution of Yap1 towards Saccharomyces cerevisiae adaptation to arsenic-mediated oxidative stress. *Biochem J, 414(2),* 301-311.

304. Merritt, G. H., Naemi, W. R., Mugnier, P., Webb, H. M., Tuite, M. F., & von der, H. T. (2010). Decoding accuracy in eRF1 mutants and its correlation with pleiotropic quantitative traits in yeast. *Nucleic Acids Res, 38,* 5479-5492.

305. Merry, B. J. (2004). Oxidative stress and mitochondrial function with aging--the effects of calorie restriction. *Aging Cell, 3,* 7-12.

306. Mirande, M. & Waller, J. P. (1988). The yeast lysyl-tRNA synthetase gene. Evidence for general amino acid control of its expression and domain structure of the encoded protein. *J Biol Chem, 263,* 18443-18451.

307. Mishra, P. & Prased, R. (1989). Relationship between ethanol tolerance and fatty acyl composition of *S. cerevisiae*. *Appl Microbiol Biotechnol, 30,* 294-298.

308. Misra, R. & Reeves, P. (1985). Intermediates in the synthesis of TolC protein include an incomplete peptide stalled at a rare Arg codon. *Eur J Biochem, 152,* 151-155.

309. Mizushima, N. (2007). Collaboration of proteolytic systems. *Autophagy., 3,* 179-180.

310. Moazed, D. & Noller, H. F. (1989). Intermediate states in the movement of transfer RNA in the ribosome. *Nature, 342,* 142-148.

311. Momose, Y. & Iwahashi, H. (2001). Bioassay of cadmium using a DNA microarray: genome-wide expression patterns of Saccharomyces cerevisiae response to cadmium. *Environ.Toxicol Chem, 20,* 2353-2360.

312. Moore, P. B. & Steitz, T. A. (2003). After the ribosome structures: how does peptidyl transferase work? *RNA, 9,* 155-159.

313. Moore, P. B. & Steitz, T. A. (2011). The roles of RNA in the synthesis of protein. *Cold Spring Harb Perspect Biol, 3,* a003780.

314. Mori, K., Kawahara, T., Yoshida, H., Yanagi, H., & Yura, T. (1996). Signalling from endoplasmic reticulum to nucleus: transcription factor with a basic-leucine zipper motif is required for the unfolded protein-response pathway. *Genes Cells, 1,* 803-817.

315. Motorin, Y. & Helm, M. (2010). tRNA stabilization by modified nucleotides. *Biochemistry, 49,* 4934-4944.

316. Mottagui-Tabar, S., Bjornsson, A., & Isaksson, L. A. (1994). The second to last amino acid in the nascent peptide as a codon context determinant. *EMBO J, 13,* 249-257.

317. Mouillon, J. M. & Persson, B. L. (2006). New aspects on phosphate sensing and signalling in Saccharomyces cerevisiae. *FEMS Yeast Res, 6,* 171-176.

318. Muhlrad, D. & Parker, R. (1999). Recognition of yeast mRNAs as "nonsense containing" leads to both inhibition of mRNA translation and mRNA degradation: implications for the control of mRNA decapping. *Mol Biol Cell, 10 (11),* 3971-3978.

319. Mulet, J. M., Alejandro, S., Romero, C., & Serrano, R. (2004). The trehalose pathway and intracellular glucose phosphates as modulators of potassium transport and general cation homeostasis in yeast. *Yeast, 21,* 569-582.

320. Muramatsu, T., Nishikawa, K., Nemoto, F., Kuchino, Y., Nishimura, S., Miyazawa, T. et al. (1988). Codon and amino-acid specificities of a transfer RNA are both converted by a single post-transcriptional modification. *Nature, 336,* 179-181.

321. Murao, K., Hasegawa, T., & Ishikura, H. (1982). Nucleotide sequence of valine tRNA mo5UAC from bacillus subtilis. *Nucleic Acids Res, 10,* 715-718.

322. Murguía, J. R., Bellés, J. M., & Serrano, R. (1996). The yeast HAL2 nucleotidase is an in vivo target of salt toxicity. *J Biol Chem, 271 (46),* 29029-29033.

323. Murthi, A., Shaheen, H. H., Huang, H. Y., Preston, M. A., Lai, T. P., Phizicky, E. M. et al. (2010). Regulation of tRNA bidirectional nuclear-cytoplasmic trafficking in Saccharomyces cerevisiae. *Mol Biol Cell, 21,* 639-649.

324. Najafabadi, H. S., Lehmann, J., & Omidi, M. (2007). Error minimization explains the codon usage of highly expressed genes in Escherichia coli. *Gene, 387 (1 - 2),* 150-155.

325. Namy, O., Duchateau-Nguyen, G., Hatin, I., Hermann-Le Denmat, S., Termier, M., & Rousset, J. P. (2003). Identification of stop codon readthrough genes in Saccharomyces cerevisiae. *Nucleic Acids Res, 31 (9),* 2289-2296.

326. Namy, O., Rousset, J. P., Napthine, S., & Brierley, I. (2004). Reprogrammed genetic decoding in cellular gene expression. *Mol Cell, 13 (2),* 157-168.

327. Namy, O., Duchateau-Nguyen, G., & Rousset, J. P. (2002). Translational readthrough of the PDE2 stop codon modulates cAMP levels in Saccharomyces cerevisiae. *Mol Microbiol, 43,* 641-652.

328. Namy, O., Hatin, I., & Rousset, J. P. (2001). Impact of the six nucleotides downstream of the stop codon on translation termination. *EMBO Rep., 2,* 787-793.

329. Natarajan, K., Meyer, M. R., Jackson, B. M., Slade, D., Roberts, C., Hinnebusch, A. G. et al. (2001). Transcriptional profiling shows that Gcn4p is a master regulator of gene expression during amino acid starvation in yeast. *Mol Cell Biol, 21,* 4347-4368.

330. Nelson, R. J., Ziegelhoffer, T., Nicolet, C., Werner-Washburne, M., & Craig, E. A. (1992). The translation machinery and 70 kd heat shock protein cooperate in protein synthesis. *Cell, 71 (1),* 97-105.

331. Netzer N, Goodenbour JM, David A, Dittmar KA, Jones RB, Schneider JR et al. (2009). Innate immune and chemically triggered oxidative stress modifies translational fidelity. Nature 462(7272), 522-526.
Ref Type: Generic

332. Netzer, N., Goodenbour, J. M., David, A., Dittmar, K. A., Jones, R. B., Schneider, J. R. et al. (2009). Innate immune and chemically triggered oxidative stress modifies translational fidelity. *Nature, 462,* 522-526.

333. Nierhaus, K. H. (2006). Decoding errors and the involvement of the E-site. *Biochimie, 88,* 1013-1019.

334. Ninio, J. (1975). Kinetic amplification of enzyme discrimination. *Biochimie, 57,* 587-595.

335. Ninio, J. (1991). Transient mutators: a semiquantitative analysis of the influence of translation and transcription errors on mutation rates. *Genetics, 129,* 957-962.

336. Nunomura, A., Honda, K., Takeda, A., Hirai, K., Zhu, X., Smith, M. A. et al. (2006). Oxidative damage to RNA in neurodegenerative diseases. *J Biomed.Biotechnol, 2006,* 82323.

337. Nunomura, A., Perry, G., Pappolla, M. A., Wade, R., Hirai, K., Chiba, S. et al. (1999). RNA oxidation is a prominent feature of vulnerable neurons in Alzheimer's disease. *J Neurosci, 19,* 1959-1964.

338. Nystrom, T. (2005). Role of oxidative carbonylation in protein quality control and senescence. *EMBO J, 24,* 1311-1317.

339. Ogawa, N., DeRisi, J., & Brown, P. O. (2000). New components of a system for phosphate accumulation and polyphosphate metabolism in Saccharomyces cerevisiae revealed by genomic expression analysis. *Mol Biol Cell, 11,* 4309-4321.

340. Ogle, J. M., Carter, A. P., & Ramakrishnan, V. (2003). Insights into the decoding mechanism from recent ribosome structures. *Trends Biochem Sci, 28 (5),* 259-266.

341. Ogle, J. M., Brodersen, D. E., Clemons, W. M., Jr., Tarry, M. J., Carter, A. P., & Ramakrishnan, V. (2001). Recognition of cognate transfer RNA by the 30S ribosomal subunit. *Science, 292,* 897-902.

342. Ogle, J. M., Murphy, F. V., Tarry, M. J., & Ramakrishnan, V. (2002). Selection of tRNA by the ribosome requires a transition from an open to a closed form. *Cell, 111,* 721-732.

343. Ogle, J. M. & Ramakrishnan, V. (2005). Structural insights into translational fidelity. *Annu Rev Biochem, 74,* 129-177.

344. Oliphant, A. R., Brandl, C. J., & Struhl, K. (1989). Defining the sequence specificity of DNA-binding proteins by selecting binding sites from random-sequence oligonucleotides: analysis of yeast GCN4 protein. *Mol Cell Biol, 9,* 2944-2949.

345. ORGEL, L. E. (1963). The maintenance of the accuracy of protein synthesis and its relevance to ageing. *Proc Natl Acad Sci U S A, 49,* 517-521.

346. Othumpangat, S., Kashon, M., & Joseph, P. (2005). Eukaryotic translation initiation factor 4E is a cellular target for toxicity and death due to exposure to cadmium chloride. *J Biol Chem, 280 (26),* 25162-25169.

347. Outten, C. E. & Culotta, V. C. (2003). A novel NADH kinase is the mitochondrial source of NADPH in Saccharomyces cerevisiae. *EMBO J, 22,* 2015-2024.

348. Palmer, E., Wilhelm, J. M., & Sherman, F. (1979). Phenotypic suppression of nonsense mutants in yeast by aminoglycoside antibiotics. *Nature, 277 (5692),* 148-150.

349. Pandey, U. B., Nie, Z., Batlevi, Y., McCray, B. A., Ritson, G. P., Nedelsky, N. B. et al. (2007). HDAC6 rescues neurodegeneration and provides an essential link between autophagy and the UPS. *Nature, 447,* 859-863.

350. Pandolfi, P. P. (2004). Aberrant mRNA translation in cancer pathogenesis: an old concept revisited comes finally of age. *Oncogene, 23,* 3134-3137.

351. Pandolfi, P. P., Sonati, F., Rivi, R., Mason, P., Grosveld, F., & Luzzatto, L. (1995). Targeted disruption of the housekeeping gene encoding glucose 6-phosphate dehydrogenase (G6PD): G6PD is dispensable for pentose synthesis but essential for defense against oxidative stress. *EMBO J, 14,* 5209-5215.

352. Pankiv, S., Clausen, T. H., Lamark, T., Brech, A., Bruun, J. A., Outzen, H. et al. (2007). p62/SQSTM1 binds directly to Atg8/LC3 to facilitate degradation of ubiquitinated protein aggregates by autophagy. *J Biol Chem, 282,* 24131-24145.

353. Pape, T., Wintermeyer, W., & Rodnina, M. (1999). Induced fit in initial selection and proofreading of aminoacyl-tRNA on the ribosome. *EMBO J, 18,* 3800-3807.

354. Pape, T., Wintermeyer, W., & Rodnina, M. V. (1998). Complete kinetic mechanism of elongation factor Tu-dependent binding of aminoacyl-tRNA to the A site of the E. coli ribosome. *EMBO J, 17,* 7490-7497.

355. Park, Y. N., Strauss, A., & Morschhauser, J. (2004). The white-phase-specific gene WH11 is not required for white-opaque switching in Candida albicans. *Mol Genet Genomics, 272,* 88-97.

356. Parker, J. (1989). Errors and alternatives in reading the universal genetic code. *Microbiol Rev, 53,* 273-298.

357. Parker, J., Johnston, T. C., Borgia, P. T., Holtz, G., Remaut, E., & Fiers, W. (1983). Codon usage and mistranslation. In vivo basal level misreading of the MS2 coat protein message. *J Biol Chem, 258,* 10007-10012.

358. Parker, J. & Precup, J. (1986). Mistranslation during phenylalanine starvation. *Mol Gen Genet, 204,* 70-74.

359. Parrou, J. L., Teste, M. A., & Francois, J. (1997). Effects of various types of stress on the metabolism of reserve carbohydrates in Saccharomyces cerevisiae: genetic evidence for a stress-induced recycling of glycogen and trehalose. *Microbiology, 143 (Pt 6),* 1891-1900.

360. Parsell DA & Lindquist S. (1993). The function of heat-shock proteins in stress tolerance: degradation and reactivation of damaged proteins. Annu Rev Genet 27, 437-496. Ref Type: Generic

361. Pereira, Y., Lagniel, G., Godat, E., Baudouin-Cornu, P., Junot, C., & Labarre, J. (2008). Chromate causes sulfur starvation in yeast. *Toxicol Sci, 106,* 400-412.

362. Perret, V., Garcia, A., Puglisi, J., Grosjean, H., Ebel, J. P., Florentz, C. et al. (1990). Conformation in solution of yeast tRNA(Asp) transcripts deprived of modified nucleotides. *Biochimie, 72,* 735-743.

363. Pestova, T. V., Borukhov, S. I., & Hellen, C. U. (1998). Eukaryotic ribosomes require initiation factors 1 and 1A to locate initiation codons. *Nature, 394,* 854-859.

364. Pestova, T. V., Kolupaeva, V. G., Lomakin, I. B., Pilipenko, E. V., Shatsky, I. N., Agol, V. I. et al. (2001). Molecular mechanisms of translation initiation in eukaryotes. *Proc Natl Acad Sci U S A, 98,* 7029-7036.

365. Pestova, T. V., Lomakin, I. B., Lee, J. H., Choi, S. K., Dever, T. E., & Hellen, C. U. (2000). The joining of ribosomal subunits in eukaryotes requires eIF5B. *Nature, 403,* 332-335.

366. Pham, T. K. & Wright, P. C. (2008). The proteomic response of Saccharomyces cerevisiae in very high glucose conditions with amino acid supplementation. *J Proteome Res, 7 (11),* 4766-4774.

367. Phizicky, E. M. (2005). Have tRNA, will travel. *Proc Natl Acad Sci U S A, 102,* 11127-11128.

368. Phizicky, E. M. & Hopper, A. K. (2010). tRNA biology charges to the front. *Genes Dev, 24,* 1832-1860.

369. Phizicky, E. M., Schwartz, R. C., & Abelson, J. (1986). Saccharomyces cerevisiae tRNA ligase. Purification of the protein and isolation of the structural gene. *J Biol Chem, 261,* 2978-2986.

370. Piepersberg, W., Noseda, V., & Böck, A. (1979). Bacterial ribosomes with two ambiguity mutations: effects of translational fidelity, on the response to aminoglycosides and on the rate of protein synthesis. *Mol Gen Genet, 171 (1),* 23-34.

371. Piper, P. W., Talreja, K., Panaretou, B., Moradas-Ferreira, P., Byrne, K., Praekelt, U. M. et al. (1994). Induction of major heat-shock proteins of Saccharomyces cerevisiae,

including plasma membrane Hsp30, by ethanol levels above a critical threshold. *Microbiology, 140 (Pt 11),* 3031-3038.

372. Pisareva, V. P., Pisarev, A. V., Hellen, C. U., Rodnina, M. V., & Pestova, T. V. (2006). Kinetic analysis of interaction of eukaryotic release factor 3 with guanine nucleotides. *J Biol Chem, 281,* 40224-40235.

373. Plant, E., Nguyen, P., Russ, J., Pittman, Y., Nguyen, T., Quesinberry, J. et al. (2007). Differentiating between near- and non-cognate codons in Saccharomyces cerevisiae. *PLoS One, 2,* e517.

374. Polacek, N. & Mankin, A. S. (2005). The ribosomal peptidyl transferase center: structure, function, evolution, inhibition. *Crit Rev Biochem Mol Biol, 40,* 285-311.

375. Poole, E. S., Major, L. L., Mannering, S. A., & Tate, W. (1998). Translational termination in Escherichia coli: three bases following the stop codon crosslink to release factor 2 and affect the decoding efficiency of UGA-containing signals. *Nucleic Acids Res, 26 (4),* 954-960.

376. Poole, E. S., Brown, C. M., & Tate, W. P. (1995). The identity of the base following the stop codon determines the efficiency of in vivo translational termination in Escherichia coli. *EMBO J, 14,* 151-158.

377. Praekelt, U. & Meacock, P. (1990). HSP12, a new small heat shock gene of Saccharomyces cerevisiae: analysis of structure, regulation and function. *Mol Gen Genet, 223 (1),* 97-106.

378. Preiss, T. & Hentze, W. (2003). Starting the protein synthesis machine: eukaryotic translation initiation. *Bioessays, 25,* 1201-1211.

379. Pronk, J. T., Yde, S. H., & van Dijken, J. P. (1996). Pyruvate metabolism in Saccharomyces cerevisiae. *Yeast, 12,* 1607-1633.

380. Qiu, H., Hu, C., Anderson, J., Bjork, G. R., Sarkar, S., Hopper, A. K. et al. (2000). Defects in tRNA processing and nuclear export induce GCN4 translation independently of phosphorylation of the alpha subunit of eukaryotic translation initiation factor 2. *Mol Cell Biol, 20,* 2505-2516.

381. Rakwalska M & Rospert S (2004). The ribosome-bound chaperones RAC and Ssb1/2p are required for accurate translation in Saccharomyces cerevisiae. *Mol Cell Biol, 24,* 9186-9197.

382. Rakwalska, M. & Rospert, S. (2004). The ribosome-bound chaperones RAC and Ssb1/2p are required for accurate translation in Saccharomyces cerevisiae. *Mol Cell Biol, 24,* 9186-9197.

383. Ramakrishnan, V. (2002). Ribosome structure and the mechanism of translation. *Cell, 108,* 557-572.

384. Rand, J. D. & Grant, C. M. (2006). The thioredoxin system protects ribosomes against stress-induced aggregation. *Mol Biol Cell, 17,* 387-401.

385. Reynolds, N. M., Lazazzera, B. A., & Ibba, M. (2010a). Cellular mechanisms that control mistranslation. *Nat Rev Microbiol, 8,* 849-856.

386. Reynolds, N. M., Ling, J., Roy, H., Banerjee, R., Repasky, S. E., Hamel, P. et al. (2010b). Cell-specific differences in the requirements for translation quality control. *Proc Natl Acad Sci U S A, 107,* 4063-4068.

387. Rochet, J. C. (2006). Errors in translation cause selective neurodegeneration. *ACS Chem Biol, 1 (9),* 562-566.

388. Rodnina, M. V., Pape, T., Fricke, R., Kuhn, L., & Wintermeyer, W. (1996). Initial binding of the elongation factor Tu.GTP.aminoacyl-tRNA complex preceding codon recognition on the ribosome. *J Biol Chem, 271,* 646-652.

389. Rodnina, M. V. & Wintermeyer, W. (2001). Ribosome fidelity: tRNA discrimination, proofreading and induced fit. *Trends Biochem Sci, 26,* 124-130.

390. Rodrigues-Pousada, C., Menezes, R. A., & Pimentel, C. (2010). The Yap family and its role in stress response. *Yeast, 27 (5),* 245-258.

391. Rodriguez-Gonzalez, A., Lin, T., Ikeda, A. K., Simms-Waldrip, T., Fu, C., & Sakamoto, K. M. (2008). Role of the aggresome pathway in cancer: targeting histone deacetylase 6-dependent protein degradation. *Cancer Res, 68,* 2557-2560.

392. Roe, B., Michael, M., & Dudock, B. (1973). Function of N2 methylguanine in phenylalanine transfer RNA. *Nat New Biol, 246,* 135-138.

393. Ross, C. A. & Poirier, M. A. (2004). Protein aggregation and neurodegenerative disease. *Nat Med, 10 Suppl,* S10-S17.

394. Roy, H., Becker, H. D., Mazauric, M. H., & Kern, D. (2007). Structural elements defining elongation factor Tu mediated suppression of codon ambiguity. *Nucleic Acids Res, 35,* 3420-3430.

395. Roy, H., Ling, J., Alfonzo, J., & Ibba, M. (2005). Loss of editing activity during the evolution of mitochondrial phenylalanyl-tRNA synthetase. *J Biol Chem, 280,* 38186-38192.

396. Ruan, B., Palioura, S., Sabina, J., Marvin-Guy, L., Kochhar, S., Larossa, R. A. et al. (2008). Quality control despite mistranslation caused by an ambiguous genetic code. *Proc.Natl.Acad.Sci, 105,* 16502-16507.

397. Rubinsztein, D. C. (2006). The roles of intracellular protein-degradation pathways in neurodegeneration. *Nature, 443,* 780-786.

398. Rudra, D. & Warner, J. R. (2004). What better measure than ribosome synthesis? *Genes Dev, 18,* 2431-2436.

399. Ruis, H. & Schuller, C. (1995). Stress signaling in yeast. *Bioessays, 17,* 959-965.

400. Rutkowski, D. T. & Kaufman, R. J. (2004). A trip to the ER: coping with stress. *Trends Cell Biol, 14 (1),* 20-28.

401. Salas-Marco J & Bedwell DM. (2005). Discrimination between defects in elongation fidelity and termination efficiency provides mechanistic insights into translational readthrough. J.Mol.Biol. 348, 801-815.
Ref Type: Generic

402. Salas-Marco, J. & Bedwell, D. (2005). Discrimination between defects in elongation fidelity and termination efficiency provides mechanistic insights into translational readthrough. *J.Mol.Biol., 348,* 801-815.

403. Salnikow, K. & Zhitkovich, A. (2008). Genetic and epigenetic mechanisms in metal carcinogenesis and cocarcinogenesis: nickel, arsenic, and chromium. *Chem Res Toxicol, 21,* 28-44.

404. Sanbonmatsu, K. Y., Joseph, S., & Tung, C. S. (2005). Simulating movement of tRNA into the ribosome during decoding. *Proc Natl Acad Sci U S A, 102,* 15854-15859.

405. Sanchez, Y., Taulien, J., Borkovich, K. A., & Lindquist, S. (1992). Hsp104 is required for tolerance to many forms of stress. *EMBO J, 11,* 2357-2364.

406. Sankaranarayanan, R. & and Moras, D. (2001). The fidelity of the translation of the genetic code. *Acta Biochim Pol., 48 (2),* 323-335.

407. Santos MA, Perreau VM, & Tuite MF (1996). Transfer RNA structural change is a key element in the reassignment of the CUG codon in Candida albicans. *EMBO J., 15,* 5060-5068.

408. Santos, M. A., Cheesman, C., Costa, V., Moradas-Ferreira, P., & Tuite, M. F. (1999). Selective advantages created by codon ambiguity allowed for the evolution of an alternative genetic code in Candida spp. *Mol Microbiol, 31,* 937-947.

409. Scheper, G. C., van der Knaap, M. S., & Proud, C. G. (2007). Translation matters: protein synthesis defects in inherited disease. *Nat Rev Genet, 8,* 711-723.

410. Schimmel, P. (1991). RNA minihelices and the decoding of genetic information. *FASEB J, 5,* 2180-2187.

411. Schimmel, P. (2008). Development of tRNA synthetases and connection to genetic code and disease. *Protein Sci, 17,* 1643-1652.

412. Schimmel, P. & Ribas de, P. L. (1995). Transfer RNA: from minihelix to genetic code. *Cell, 81,* 983-986.

413. Schimmel, P. & Ribas de, P. L. (2000). Footprints of aminoacyl-tRNA synthetases are everywhere. *Trends Biochem Sci, 25,* 207-209.

414. Schimmel, P. R. & Soll, D. (1979). Aminoacyl-tRNA synthetases: general features and recognition of transfer RNAs. *Annu Rev Biochem, 48,* 601-648.

415. Schmeing, T. M., Huang, K. S., Kitchen, D. E., Strobel, S. A., & Steitz, T. A. (2005). Structural insights into the roles of water and the 2' hydroxyl of the P site tRNA in the peptidyl transferase reaction. *Mol Cell, 20,* 437-448.

416. Schmidt, E. & Schimmel, P. (1995). Residues in a class I tRNA synthetase which determine selectivity of amino acid recognition in the context of tRNA. *Biochemistry, 34,* 11204-11210.

417. Schulman, L. H. (1991). Recognition of tRNAs by aminoacyl-tRNA synthetases. *Prog.Nucleic Acid Res Mol Biol, 41,* 23-87.

418. Scolnick, E., Tompkins, R., Caskey, T., & Nirenberg, M. (1968). Release factors differing in specificity for terminator codons. *Proc Natl Acad Sci U S A, 61,* 768-774.

419. Seit-Nebi, A., Frolova, L., Justesen, J., & Kisselev, L. (2001). Class-1 translation termination factors: invariant GGQ minidomain is essential for release activity and ribosome binding but not for stop codon recognition. *Nucleic Acids Res, 29,* 3982-3987.

420. Serio, T. R. & Lindquist, S. L. (1999). [PSI+]: an epigenetic modulator of translation termination efficiency. *Annu Rev Cell Dev Biol, 15,* 661-703.

421. Serrano, R., Kielland-Brandt, M. C., & Fink, G. R. (1986). Yeast plasma membrane ATPase is essential for growth and has homology with (Na+ + K+), K+- and Ca2+-ATPases. *Nature, 319,* 689-693.

422. Shaheen, H. H. & Hopper, A. K. (2005). Retrograde movement of tRNAs from the cytoplasm to the nucleus in Saccharomyces cerevisiae. *Proc Natl Acad Sci U S A, 102,* 11290-11295.

423. Shakoury-Elizeh, M., Protchenko, O., Berger, A., Cox, J., Gable, K., Dunn, T. M. et al. (2010). Metabolic response to iron deficiency in Saccharomyces cerevisiae. *J Biol Chem, 285,* 14823-14833.

424. Sharma, D. & Masison, D. C. (2008). Functionally redundant isoforms of a yeast Hsp70 chaperone subfamily have different antiprion effects. *Genetics, 179 (3),* 1301-1311.

425. Sharma, S. K., Goloubinoff, P., & Christen, P. (2008). Heavy metal ions are potent inhibitors of protein folding. *Biochem Biophys Res Commun., 372,* 341-345.

426. Shee, C., Gibson, J. L., Darrow, M. C., Gonzalez, C., & Rosenberg, S. M. (2011). Impact of a stress-inducible switch to mutagenic repair of DNA breaks on mutation in Escherichia coli. *Proc Natl Acad Sci U S A, 108,* 13659-13664.

427. Sickmann, A., Reinders, J., Wagner, Y., Joppich, C., Zahedi, R., Meyer, H. E. et al. (2003). The proteome of Saccharomyces cerevisiae mitochondria. *Proc Natl Acad Sci U S A, 100,* 13207-13212.

428. Silva, R. M., Paredes, J. A., Moura, G. R., Manadas, B., Lima-Costa, T., Rocha, R. et al. (2007). Critical roles for a genetic code alteration in the evolution of the genus Candida. *EMBO J, 26,* 4555-4565.

429. Singh, A., Ursic, D., & Davies, J. (1979). Phenotypic suppression and misreading Saccharomyces cerevisiae. *Nature, 277 (5692),* 146-148.

430. Sinha, A. & Maitra, P. K. (1992). Induction of specific enzymes of the oxidative pentose phosphate pathway by glucono-delta-lactone in Saccharomyces cerevisiae. *J Gen Microbiol, 138,* 1865-1873.

431. Sinha, H., David, L., Pascon, R. C., Clauder-Munster, S., Krishnakumar, S., Nguyen, M. et al. (2008). Sequential elimination of major-effect contributors identifies additional quantitative trait loci conditioning high-temperature growth in yeast. *Genetics, 180,* 1661-1670.

432. Skuzeski, J. M., Nichols, L. M., Gesteland, R. F., & Atkins, J. F. (1991). The signal for a leaky UAG stop codon in several plant viruses includes the two downstream codons. *J Mol Biol, 218,* 365-373.

433. Slupska, M. M., Baikalov, C., Lloyd, R., & Miller, J. H. (1996). Mutator tRNAs are encoded by the Escherichia coli mutator genes mutA and mutC: a novel pathway for mutagenesis. *Proc Natl Acad Sci U S A, 93,* 4380-4385.

434. Sogaard, T. M., Jakobsen, C. G., & Justesen, J. (1999). A sensitive assay of translational fidelity (readthrough and termination) in eukaryotic cells. *Biochemistry (Mosc), 64 (12),* 1408-1417.

435. Sohal, R. S. (2002). Role of oxidative stress and protein oxidation in the aging process. *Free Radic Biol Med, 33,* 37-44.

436. Sonenberg, N. & Hinnebusch, A. G. (2009). Regulation of translation initiation in eukaryotes: mechanisms and biological targets. *Cell, 136,* 731-745.

437. Song, C., Xiao, Z., Nagashima, K., Li, C. C., Lockett, S. J., Dai, R. M. et al. (2008). The heavy metal cadmium induces valosin-containing protein (VCP)-mediated aggresome formation. *Toxicol Appl Pharmacol, 228,* 351-363.

438. Song, H., Mugnier, P., Das, A. K., Webb, H. M., Evans, D. R., Tuite, M. F. et al. (2000). The crystal structure of human eukaryotic release factor eRF1--mechanism of stop codon recognition and peptidyl-tRNA hydrolysis. *Cell, 100,* 311-321.

439. Sørensen, M. A. (2001). Charging levels of four tRNA species in Escherichia coli Rel(+) and Rel(-) strains during amino acid starvation: a simple model for the effect of ppGpp on translational accuracy. *J Mol Biol, 307 (3),* 785-798.

440. Spiegel, P. C., Ermolenko, D. N., & Noller, H. F. (2007). Elongation factor G stabilizes the hybrid-state conformation of the 70S ribosome. *RNA, 13,* 1473-1482.

441. Sprinzl, M. & Vassilenko, K. S. (2005). Compilation of tRNA sequences and sequences of tRNA genes. *Nucleic Acids Res, 33,* D139-D140.

442. Stadtman, E. R. & Levine, R. L. (2003). Free radical-mediated oxidation of free amino acids and amino acid residues in proteins. *Amino.Acids, 25,* 207-218.

443. Stahl, G., Salem, S. N., Chen, L., Zhao, B., & Farabaugh, P. J. (2004). Translational accuracy during exponential, postdiauxic, and stationary growth phases in Saccharomyces cerevisiae. *Eukaryot Cell, 3,* 331-338.

444. Stanley, D., Bandara, A., Fraser, S., Chambers, P. J., & Stanley, G. A. (2010). The ethanol stress response and ethanol tolerance of Saccharomyces cerevisiae. *J Appl Microbiol, 109 (1),* 13-24.

445. Stansfield I, Jones KM, Herbert P, Lewendon A, Shaw WV, & Tuite MF. (1998). Missense translation errors in Saccharomyces cerevisiae. J Mol Biol 282, 13-24.
Ref Type: Generic

446. Stansfield, I., Jones, K., Herbert, P., Lewendon, A., Shaw, W., & Tuite, M. (1998). Missense translation errors in Saccharomyces cerevisiae. *J Mol Biol, 282,* 13-24.

447. Stansfield, I., Eurwilaichitr, L., Akhmaloka, & Tuite, M. F. (1996). Depletion in the levels of the release factor eRF1 causes a reduction in the efficiency of translation termination in yeast. *Mol Microbiol, 20,* 1135-1143.

448. Stansfield, I., Jones, K. M., Kushnirov, V. V., Dagkesamanskaya, A. R., Poznyakovski, A. I., Paushkin, S. V. et al. (1995). The products of the SUP45 (eRF1) and SUP35 genes interact to mediate translation termination in Saccharomyces cerevisiae. *EMBO J, 14,* 4365-4373.

449. Stanzel, M., Schon, A., & Sprinzl, M. (1994). Discrimination against misacylated tRNA by chloroplast elongation factor Tu. *Eur J Biochem, 219,* 435-439.

450. Starkov, A. A., Fiskum, G., Chinopoulos, C., Lorenzo, B. J., Browne, S. E., Patel, M. S. et al. (2004). Mitochondrial alpha-ketoglutarate dehydrogenase complex generates reactive oxygen species. *J Neurosci, 24,* 7779-7788.

451. Stearman, R., Yuan, D. S., Yamaguchi-Iwai, Y., Klausner, R. D., & Dancis, A. (1996). A permease-oxidase complex involved in high-affinity iron uptake in yeast. *Science, 271,* 1552-1557.

452. Stefani M & Dobson CM. (2003). Protein aggregation and aggregate toxicity: new insights into protein folding, misfolding diseases and biological evolution. J Mol Med 81, 678-699.
Ref Type: Generic

453. Stefani M. (2004). Protein misfolding and aggregation: new examples in medicine and biology of the dark side of the protein world. Biochim Biophys Acta 1739, 5-25.
Ref Type: Generic

454. Stefani M. (2007). Generic cell dysfunction in neurodegenerative disorders: role of surfaces in early protein misfolding, aggregation, and aggregate cytotoxicity. Neuroscientist 13, 519-531.
Ref Type: Generic

455. Stefani, M. & Dobson, C. M. (2003). Protein aggregation and aggregate toxicity: new insights into protein folding, misfolding diseases and biological evolution. *J Mol Med, 81,* 678-699.

456. Stefani, M. (2007). Generic cell dysfunction in neurodegenerative disorders: role of surfaces in early protein misfolding, aggregation, and aggregate cytotoxicity. *Neuroscientist, 13,* 519-531.

457. Steitz, T. A. (2008). A structural understanding of the dynamic ribosome machine. *Nat Rev Mol Cell Biol, 9,* 242-253.

458. Steitz, T. A. & Moore, P. B. (2003). RNA, the first macromolecular catalyst: the ribosome is a ribozyme. *Trends Biochem Sci, 28,* 411-418.

459. Steneberg, P. & Samakovlis, C. (2001). A novel stop codon readthrough mechanism produces functional Headcase protein in Drosophila trachea. *EMBO Rep., 2,* 593-597.

460. Stohs, S. J. & Bagchi, D. (1995). Oxidative mechanisms in the toxicity of metal ions. *Free Radic Biol Med, 18 (2),* 321-336.

461. Summers, A. O. (2009). Damage control: regulating defenses against toxic metals and metalloids. *Curr Opin.Microbiol, 12,* 138-144.

462. Sund, J., Andér, M., & Aqvist, J. (2010). Principles of stop-codon reading on the ribosome. Nature 465, 947-950.
Ref Type: Generic

463. Susek, R. E. & Lindquist, S. (1990). Transcriptional derepression of the Saccharomyces cerevisiae HSP26 gene during heat shock. *Mol Cell Biol, 10 (12),* 6362-6373.

464. Suzuka, I. & Kaji, A. (1968). Reversible effect of lithium chloride on ribosomes. *J Biol Chem, 243 (11),* 3136-3141.

465. Suzuki, T., Ueda, T., & Watanabe, K. (1997). The 'polysemous' codon--a codon with multiple amino acid assignment caused by dual specificity of tRNA identity. *EMBO J, 16,* 1122-1134.

466. Swan TM & Watson K. (1997). Membrane fatty acid composition and membrane fluidity as parameters of stress tolerance in yeast. Can J Microbiol 43 (1), 70-77.
Ref Type: Generic

467. Swanson, W. H. & Clifton, C. E. (1948). Growth and Assimilation in Cultures of Saccharomyces cerevisiae. *J Bacteriol, 56,* 115-124.

468. Takano, A., Endo, T., & Yoshihisa, T. (2005). tRNA actively shuttles between the nucleus and cytosol in yeast. *Science, 309,* 140-142.

469. Tanaka, M., Chock, P. B., & Stadtman, E. R. (2007). Oxidized messenger RNA induces translation errors. *Proc Natl Acad Sci U S A, 104,* 66-71.

470. Tarassov, K., Messier, V., Landry, C. R., Radinovic, S., Serna Molina, M. M., Shames, I. et al. (2008). An in vivo map of the yeast protein interactome. *Science, 320,* 1465-1470.

471. Taxis, C., Hitt, R., Park, S. H., Deak, P. M., Kostova, Z., & Wolf, D. H. (2003). Use of modular substrates demonstrates mechanistic diversity and reveals differences in chaperone requirement of ERAD. *J Biol Chem, 278,* 35903-35913.

472. Temple, M. D., Perrone, G. G., & Dawes, I. W. (2005). Complex cellular responses to reactive oxygen species. *Trends Cell Biol, 16 (6),* 319-326.

473. Tessier, W. D., Meaden, P. G., Dickinson, F. M., & Midgley, M. (1998). Identification and disruption of the gene encoding the K(+)-activated acetaldehyde dehydrogenase of Saccharomyces cerevisiae. *FEMS Microbiol Lett., 164,* 29-34.

474. Thiebe, R. & Zachau, H. G. (1968). A specific modification next to the anticodon of phenylalanine transfer ribonucleic acid. *Eur J Biochem, 5,* 546-555.

475. Thompson, D. M., Lu, C., Green, P. J., & Parker, R. (2008). tRNA cleavage is a conserved response to oxidative stress in eukaryotes. *RNA, 14,* 2095-2103.

476. Thompson, R. C. & Stone, P. J. (1977). Proofreading of the codon-anticodon interaction on ribosomes. *Proc Natl Acad Sci U S A, 74,* 198-202.

477. Thorsen, M., Perrone, G. G., Kristiansson, E., Traini, M., Ye, T., Dawes, I. W. et al. (2009). Genetic basis of arsenite and cadmium tolerance in Saccharomyces cerevisiae. *BMC Genomics, 10,* 105.

478. Toussaint, M. & Conconi, A. (2006). High-throughput and sensitive assay to measure yeast cell growth: a bench protocol for testing genotoxic agents. *Nat Protoc., 1,* 1922-1928.

479. Trobro, S. & Aqvist, J. (2005). Mechanism of peptide bond synthesis on the ribosome. *Proc Natl Acad Sci U S A, 102,* 12395-12400.

480. Tucker, S. D., Murgola, E. J., & Pagel, F. T. (1989). Missense and nonsense suppressors can correct frameshift mutations. *Biochimie, 71,* 729-739.

481. Tyedmers J, Mogk A, & Bukau B. (2010). Cellular strategies for controlling protein aggregation. Nat Rev Mol Cell Biol 11 (11), 777-788.
Ref Type: Generic

482. Tyedmers, J., Mogk, A., & Bukau, B. (2010). Cellular strategies for controlling protein aggregation. *Nat Rev Mol Cell Biol, 11 (11),* 777-788.

483. Tyedmers, J., Madariaga, M. L., & Lindquist, S. (2008). Prion switching in response to environmental stress. *PLoS Biol, 6,* e294.

484. Uhlenbeck, O. C., Martin, F. H., & Doty, P. (1971). Self-complementary oligoribonucleotides: effects of helix defects and guanylic acid-cytidylic acid base pairs. *J Mol Biol, 57,* 217-229.

485. Ulitsky, I., Maron-Katz, A., Shavit, S., Sagir, D., Linhart, C., Elkon, R. et al. (2010). Expander: from expression microarrays to networks and functions. *Nat Protoc., 5,* 303-322.

486. Unbehaun, A., Borukhov, S. I., Hellen, C. U., & Pestova, T. V. (2004). Release of initiation factors from 48S complexes during ribosomal subunit joining and the link between establishment of codon-anticodon base-pairing and hydrolysis of eIF2-bound GTP. *Genes Dev, 18,* 3078-3093.

487. Urlinger, S., Kuchler, K., Meyer, T. H., Uebel, S., & Tampe, R. (1997). Intracellular location, complex formation, and function of the transporter associated with antigen processing in yeast. *Eur J Biochem, 245,* 266-272.

488. Valente, L. & Kinzy, T. G. (2003). Yeast as a sensor of factors affecting the accuracy of protein synthesis. *Cell Mol Life Sci, 60 (10),* 2115-2130.

489. Valenzuela, L., Aranda, C., & Gonzalez, A. (2001). TOR modulates GCN4-dependent expression of genes turned on by nitrogen limitation. *J Bacteriol, 183,* 2331-2334.

490. Valko M, Morris H, & Cronin MT. (2005). Metals, toxicity and oxidative stress. Curr Med Chem 12, 1161-1208.
Ref Type: Generic

491. Valko, M., Morris, H., & Cronin, M. T. (2005). Metals, toxicity and oxidative stress. *Curr Med Chem, 12,* 1161-1208.

492. Valouev, I. A., Kushnirov, V. V., & Ter-Avanesyan, M. D. (2002). Yeast polypeptide chain release factors eRF1 and eRF3 are involved in cytoskeleton organization and cell cycle regulation. *Cell Motil.Cytoskeleton, 52,* 161-173.

493. Varela JC, Praekelt UM, Meacock PA, Planta RJ, & Mager WH. (1995). The Saccharomyces cerevisiae HSP12 gene is activated by the high-osmolarity glycerol pathway and negatively regulated by protein kinase A. Mol Cell Biol 15 (11), 6232-6245.
Ref Type: Generic

494. Varela, J. C., Praekelt, U. M., Meacock, P. A., Planta, R. J., & Mager, W. H. (1995). The Saccharomyces cerevisiae HSP12 gene is activated by the high-osmolarity glycerol pathway and negatively regulated by protein kinase A. *Mol Cell Biol, 15 (11),* 6232-6245.

495. Varshavsky, A. (1996). The N-end rule: functions, mysteries, uses. *Proc Natl Acad Sci U S A, 93,* 12142-12149.

496. Vashist, S. & Ng, D. T. (2004). Misfolded proteins are sorted by a sequential checkpoint mechanism of ER quality control. *J Cell Biol, 165,* 41-52.

497. Velichutina, I. V., Dresios, J., Hong, J. Y., Li, C., Mankin, A., Synetos, D. et al. (2000). Mutations in helix 27 of the yeast Saccharomyces cerevisiae 18S rRNA affect the function of the decoding center of the ribosome. *RNA, 6,* 1174-1184.

498. Vilela, C., Linz, B., Rodrigues-Pousada, C., & McCarthy, J. E. (1998). The yeast transcription factor genes YAP1 and YAP2 are subject to differential control at the levels of both translation and mRNA stability. *Nucleic Acids Res, 26 (5),* 1150-1159.

499. Vogt, W. (1995). Oxidation of methionyl residues in proteins: tools, targets, and reversal. *Free Radic Biol Med, 18,* 93-105.

500. Waas, W. F., Druzina, Z., Hanan, M., & Schimmel, P. (2007). Role of a tRNA base modification and its precursors in frameshifting in eukaryotes. *J Biol Chem, 282,* 26026-26034.

501. Wach A, Brachat A, Alberti-Segui C, Rebischung C, & Philippsen P. (1997). Heterologous HIS3 marker and GFP reporter modules for PCR-targeting in Saccharomyces cerevisiae. Yeast 13, 1065-1075.
Ref Type: Generic

502. Wang, D., Zheng, F., Holmberg, S., & Kohlhaw, G. B. (1999). Yeast transcriptional regulator Leu3p. Self-masking, specificity of masking, and evidence for regulation by the intracellular level of Leu3p. *J Biol Chem, 274,* 19017-19024.

503. Wang, X., Mann, C. J., Bai, Y., Ni, L., & Weiner, H. (1998). Molecular cloning, characterization, and potential roles of cytosolic and mitochondrial aldehyde dehydrogenases in ethanol metabolism in Saccharomyces cerevisiae. *J Bacteriol, 180,* 822-830.

504. Wang, X., Minasov, G., & Shoichet, B. K. (2002). Evolution of an antibiotic resistance enzyme constrained by stability and activity trade-offs. *J Mol Biol, 320,* 85-95.

505. Wang, Y., Meriin, A. B., Zaarur, N., Romanova, N. V., Chernoff, Y. O., Costello, C. E. et al. (2009). Abnormal proteins can form aggresome in yeast: aggresome-targeting signals and components of the machinery. *FASEB J, 23,* 451-463.

506. Warner, J. R. (1999). The economics of ribosome biosynthesis in yeast. *Trends Biochem Sci, 24,* 437-440.

507. Weibezahn, J., Tessarz, P., Schlieker, C., Zahn, R., Maglica, Z., Lee, S. et al. (2004). Thermotolerance requires refolding of aggregated proteins by substrate translocation through the central pore of ClpB. *Cell, 119,* 653-665.

508. Weinger, J. S., Parnell, K. M., Dorner, S., Green, R., & Strobel, S. A. (2004). Substrate-assisted catalysis of peptide bond formation by the ribosome. *Nat Struct.Mol Biol, 11,* 1101-1106.

509. Wek, S. A., Zhu, S., & Wek, R. C. (1995). The histidyl-tRNA synthetase-related sequence in the eIF-2 alpha protein kinase GCN2 interacts with tRNA and is required for activation in response to starvation for different amino acids. *Mol Cell Biol, 15,* 4497-4506.

510. Welker S, Rudolph B, Frenzel E, Haslbeck M, Kessler H, & Buchner J. (2010). Hsp12 is an intrinsically unstructured stress protein that folds upon membrane association and

modulates membrane function. Mol Cell 39 (4), 507-520.
Ref Type: Generic

511. Welker, S., Rudolph, B., Frenzel, E., Haslbeck, M., Kessler, H., & Buchner, J. (2010). Hsp12 is an intrinsically unstructured stress protein that folds upon membrane association and modulates membrane function. *Mol Cell, 39 (4),* 507-520.

512. Wenthzel, A. M., Stancek, M., & Isaksson, L. A. (1998). Growth phase dependent stop codon readthrough and shift of translation reading frame in Escherichia coli. *FEBS Lett., 421,* 237-242.

513. Werner-Washburne, M., Becker, J., Kosic-Smithers, J., & Craig, E. A. (1989). Yeast Hsp70 RNA levels vary in response to the physiological status of the cell. *J Bacteriol, 171 (5),* 2680-2688.

514. Whitesell, L. & Lindquist, S. L. (2005). HSP90 and the chaperoning of cancer. *Nat Rev Cancer, 5,* 761-772.

515. Whitney, M. L., Hurto, R. L., Shaheen, H. H., & Hopper, A. K. (2007). Rapid and reversible nuclear accumulation of cytoplasmic tRNA in response to nutrient availability. *Mol Biol Cell, 18,* 2678-2686.

516. Wightman, R. & Meacock, P. A. (2003). The THI5 gene family of Saccharomyces cerevisiae: distribution of homologues among the hemiascomycetes and functional redundancy in the aerobic biosynthesis of thiamin from pyridoxine. *Microbiology, 149,* 1447-1460.

517. Williams, I., Richardson, J., Starkey, A., & Stansfield, I. (2004). Genome-wide prediction of stop codon readthrough during translation in the yeast Saccharomyces cerevisiae. *Nucleic Acids Res, 32,* 6605-6616.

518. Winter, D., Polacek, N., Halama, I., Streicher, B., & Barta, A. (1997). Lead-catalysed specific cleavage of ribosomal RNAs. *Nucleic Acids Res, 25 (9),* 1817-1824.

519. Wohlgemuth, I., Brenner, S., Beringer, M., & Rodnina, M. V. (2008). Modulation of the rate of peptidyl transfer on the ribosome by the nature of substrates. *J Biol Chem, 283,* 32229-32235.

520. Wolf, D. H. & Hilt, W. (2004). The proteasome: a proteolytic nanomachine of cell regulation and waste disposal. *Biochim Biophys Acta, 1695,* 19-31.

521. Wolin, S. L. & Matera, A. G. (1999). The trials and travels of tRNA. *Genes Dev, 13,* 1-10.

522. Wysocki R & Tamás MJ. (2010). How Saccharomyces cerevisiae copes with toxic metals and metalloids. FEMS Microbiol Rev 34 (6), 925-951.
Ref Type: Generic

523. Wysocki, R. & Tamás, M. J. (2010). How Saccharomyces cerevisiae copes with toxic metals and metalloids. *FEMS Microbiol Rev, 34 (6),* 925-951.

524. Wysocki, R., Chery, C. C., Wawrzycka, D., Van, H. M., Cornelis, R., Thevelein, J. M. et al. (2001). The glycerol channel Fps1p mediates the uptake of arsenite and antimonite in Saccharomyces cerevisiae. *Mol Microbiol, 40,* 1391-1401.

525. Xie, Y. & Varshavsky, A. (2001). RPN4 is a ligand, substrate, and transcriptional regulator of the 26S proteasome: a negative feedback circuit. *Proc Natl Acad Sci U S A, 98(6),* 3056-3061.

526. Yang, R., Wek, S. A., & Wek, R. C. (2000). Glucose limitation induces GCN4 translation by activation of Gcn2 protein kinase. *Mol Cell Biol, 20,* 2706-2717.

527. Yorimitsu, T. & Klionsky, D. J. (2005). Autophagy: molecular machinery for self-eating. *Cell Death Differ, 12,* 1542-1552.

528. Yoshihisa, T., Yunoki-Esaki, K., Ohshima, C., Tanaka, N., & Endo, T. (2003). Possibility of cytoplasmic pre-tRNA splicing: the yeast tRNA splicing endonuclease mainly localizes on the mitochondria. *Mol Biol Cell, 14,* 3266-3279.

529. Yoshikawa, K., Tanaka, T., Furusawa, C., Nagahisa, K., Hirasawa, T., & Shimizu, H. (2009). Comprehensive phenotypic analysis for identification of genes affecting growth under ethanol stress in Saccharomyces cerevisiae. *FEMS Yeast Res, 9 (1),* 32-44.

530. Zaher, H. S. & Green, R. (2009). Quality control by the ribosome following peptide bond formation. *Nature, 457,* 161-166.

531. Zavialov, A., Buckingham, R., & Ehrenberg, M. (2001). A posttermination ribosomal complex is the guanine nucleotide exchange factor for peptide release factor RF3. *Cell, 107,* 115-124.

532. Zhang, J., Perry, G., Smith, M. A., Robertson, D., Olson, S. J., Graham, D. G. et al. (1999). Parkinson's disease is associated with oxidative damage to cytoplasmic DNA and RNA in substantia nigra neurons. *Am J Pathol., 154,* 1423-1429.

533. Zietkiewicz, S., Krzewska, J., & Liberek, K. (2004). Successive and synergistic action of the Hsp70 and Hsp100 chaperones in protein disaggregation. *J Biol Chem, 279,* 44376-44383.

Annexes

Annexe 1 – Map of the dual luciferase reporter plasmids

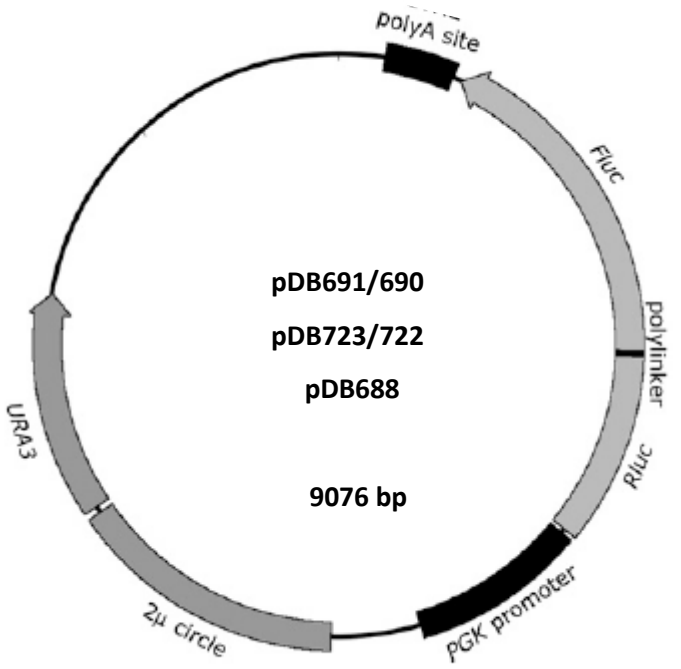

Figure A1 - Plasmids pDB691/690, pDB723/722 and pDB688 expressing the dual luciferase reporter. Both *Renilla* and Firefly genes were subcloned from p2luc (Grentzmann G et al., 1998) and fused into a single open reading frame. A polylinker (readthrough cassette) was introduced between the two genes as a SalI/BamHI fragment. The reporter is flanked by the promoter of the constitutively expressed *PGK* gene and by the *CYC1* transcriptional terminator. A segment of the 2 µ circle confers the plasmid autonomous replication in *S. cerevisiae* and $URA3^+$ was used as the selectable marker (adapted from Kramer E et al., 2010).

Annexe 2 - Sequence of the R-luc – F-luc gene fusion

ATGACTTCGAAAGTTTATGATCCAGAACAAAGGAAACGGATGATAACTGGTCCGCAGTGGTGGG
CCAGATGTAAACAAATGAATGTTCTTGATTCATTTATTAATTATTATGATTCAGAAAAACATGC
AGAAAATGCTGTTATTTTTTTACATGGTAACGCGGCCTCTTCTTATTTATGGCGACATGTTGTG
CCACATATTGAGCCAGTAGCGCGGTGTATTATACCAGACCTTATTGGTATGGGCAAATCAGGCA
AATCTGGTAATGGTTCTTATAGGTTACTTGATCATTACAAATATCTTACTGCATGGTTTGAACT
TCTTAATTTACCAAAGAAGATCATTTTTGTCGGCCATGATTGGGGTGCTTGTTTGGCATTTCAT
TATAGCTATGAGCATCAAGATAAGATCAAAGCAATAGTTCACGCTGAAAGTGTAGTAGATGTGA
TTGAATCATGGGATGAATGGCCTGATATTGAAGAAGATATTGCGTTGATCAAATCTGAAGAAGG
AGAAAAAATGGTTTTGGAGAATAACTTCTTCGTGGAAACCATGTTGCCATCAAAAATCATGAGA
AAGTTAGAACCAGAAGAATTTGCAGCATATCTTGAACCATTCAAAGAGAAAGGTGAAGTTCGTC
GTCCAACATTATCATGGCCTCGTGAAATCCCGTTAGTAAAAGGTGGTAAACCTGACGTTGTACA
AATTGTTAGGAATTATAATGCTTATCTACGTGCAAGTGATGATTTACCAAAAATGTTTATTGAA
TCGGACCCAGGATTCTTTTCCAATGCTATTGTTGAAGGTGCCAAGAAGTTTCCTAATACTGAAT
TTGTCAAAGTAAAAGGTCTTCATTTTTCGCAAGAAGATGCACCTGATGAAATGGGAAAATATAT
CAAATCGTTCGTTGAGCGAGTTCTCAAAAATGAACAA**ATGTCGACGTGCGATXXXNCGTTCGGA**
TCCTTCAACTTCCCTGAGCTCGAAGACGCCAAAAACATAAAGAAAGGCCCGGCGCCATTCTATC
CTCTAGAGGATGGAACCGCTGGAGAGCAACTGCATAAGGCTATGAAGAGATACGCCCTGGTTCC
TGGAACAATTGCTTTTACAGATGCACATATCGAGGTGAACATCACGTACGCGGAATACTTCGAA
ATGTCCGTTCGGTTGGCAGAAGCTATGAAACGATATGGGCTGAATACAAATCACAGAATCGTCG
TATGCAGTGAAAACTCTCTTCAATTCTTTATGCCGGTGTTGGGCGCGTTATTTATCGGAGTTGC
AGTTGCGCCCGCGAACGACATTTATAATGAACGTGAATTGCTCAACAGTATGAACATTTCGCAG
CCTACCGTAGTGTTTGTTTCCAAAAAGGGGTTGCAAAAAATTTTGAACGTGCAAAAAAAATTAC
CAATAATCCAGAAAATTATTATCATGGATTCTAAAACGGATTACCAGGGATTTCAGTCGATGTA
CACGTTCGTCACATCTCATCTACCTCCCGGTTTTAATGAATACGATTTTGTACCAGAGTCCTTT
GATCGTGACAAAACAATTGCACTGATAATGAATTCCTCTGGATCTACTGGGTTACCTAAGGGTG
TGGCCCTTCCGCATAGAACTGCCTGCGTC**AGA**TTCTCGCATGCCAGAGATCCTATTTTTGGCAA
TCAAATCATTCCGGATACTGCGATTTTAAGTGTTGTTCCATTCCATCACGGTTTTGGAATGTTT
ACTACACTCGGATATTTGATATGTGGATTTCGAGTCGTCTTAATGTATAGATTTGAAGAAGAGC
TGTTTTTACGATCCCTTCAGGATTACAAAATTCAAAGTGCGTTGCTAGTACCAACCCTATTTTC
ATTCTTCGCCAAAAGCACTCTGATTGACAAATACGATTTATCTAATTTACACGAAATTGCTTCT
GGGGGCGCACCTCTTTCGAAAGAAGTCGGGGAAGCGGTTGCAAAACGCTTCCATCTTCCAGGGA
TACGACAAGGATATGGGCTCACTGAGACTACATCAGCTATTCTGATTACACCCGAGGGGGATGA
TAAACCGGGCGCGGTCGGTAAAGTTGTTCCATTTTTTGAAGCGAAGGTTGTGGATCTGGATACC
GGGAAAACGCTGGGCGTTAATCAGAGAGGCGAATTATGTGTCAGAGGACCTATGATTATGTCCG
GTTATGTAAACAATCCGGAAGCGACCAACGCCTTGATTGACAAGGATGGATGGCTACATTCTGG
AGACATAGCTTACTGGGACGAAGACGAACACTTCTTCATAGTTGACCGCTTGAAGTCTTTAATT
AAATACAAAGGATATCAGGTGGCCCCCGCTGAATTGGAATCGATATTGTTACAACACCCCAACA
TCTTCGACGCGGGCGTGGCAGGTCTTCCCGACGATGACGCCGGTGAACTTCCCGCCGCCGTTGT
TGTTTTGGAGCACGGAAAGACGATGACGGAAAAAGAGATCGTGGATTACGTCGCCAGTCAAGTA
ACAACCGCGAAAAAGTTGCGCGGAGGAGTTGTGTTTGTGGACGAAGTACCGAAAGGTCTTACCG
GAAAACTCGACGCAAGAAAAATCAGAGAGATCCTCATAAAGGCCAAGAAGGGCGGAAAGTCCAA
ATTGTAA

The polylinker region (readthrough cassette) is represented in grey. The sequence in red is variable between pDB plasmids, according to table A1. In the pDB pairs 690/691 and 722/723 XXX is the sense / stop codon and N is a key 3' position influencing termination efficiency.

Table A1 - Polylinker variable region in pDB plasmids.

pDB plasmid	Variable codon and 3' context
690	CGA C
691	UGA C
722	CAA C
723	UAA C
688	CAA A

The codon in yellow was mutated to AGC in pDB688, giving origin to pUA312.

Annexe 3 – Supplementary methods and results

A3.1. – Viability assay of yeast exposed to environmental stress

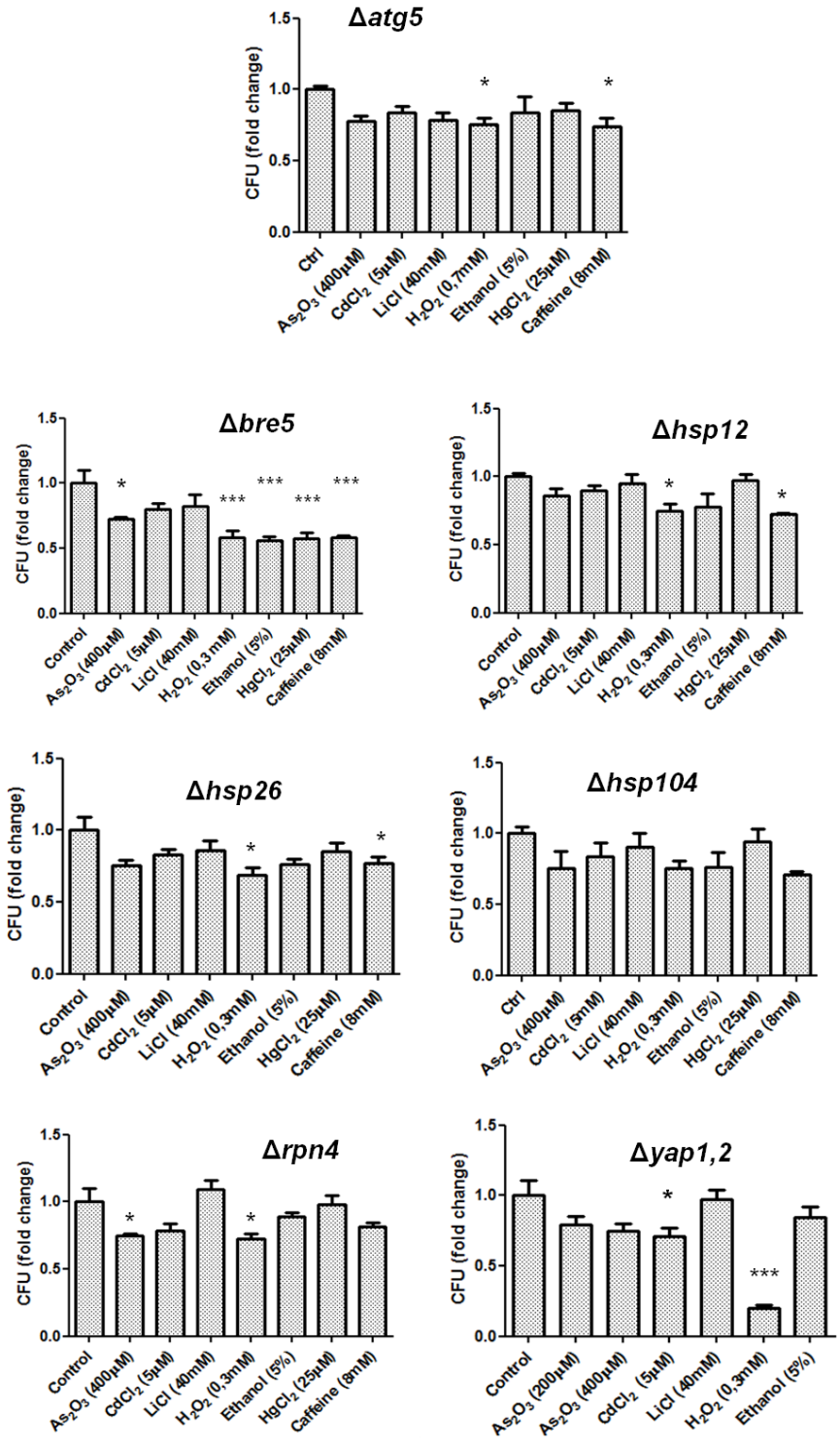

Figure A2 ▶

Figure A2 - Viability of yeast exposed to environmental stress by the colony forming units (CFU) assay (as described in section 2.2.5). Exponentially growing yeast cells were exposed to stressors at the indicated concentrations for 4h. Cells then collected and washed in PBS. The same number of cells (100) was then plated onto fresh plates. The number of colony forming units (CFU) was determined after 3 days incubation at 30ºC and represented as a fold change relatively to control (plated cells not exposed to stress). * and *** represent values significantly different ($P < 0.05$ and $P < 0.001$, respectively; one-way ANOVA, Dunnett's post-test). Values are mean ± SEM of three biological replicates.

A3.2. – Yeast growth under stress

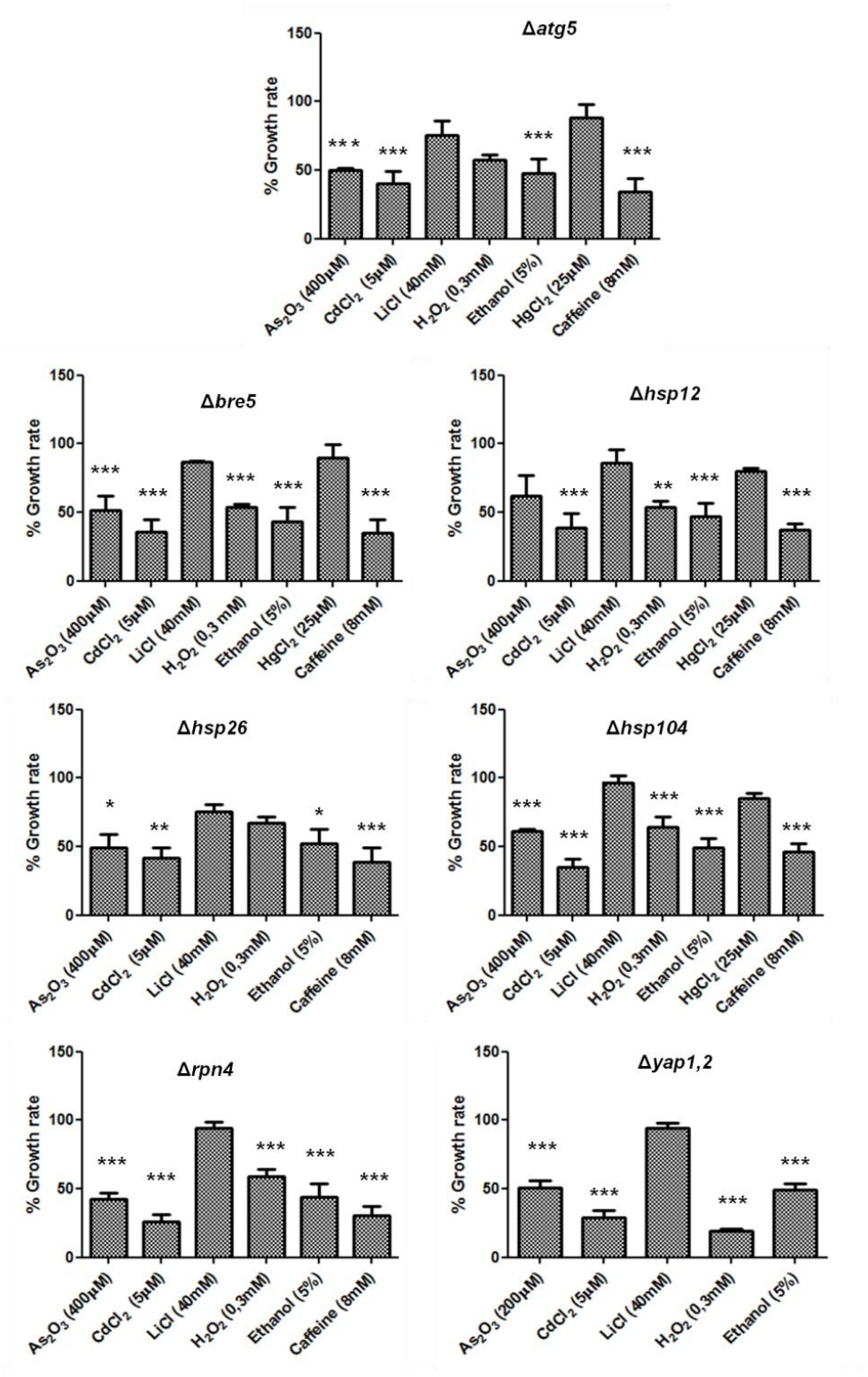

Figure A3 ▶

Figure A3 - Fold changes in yeast growth under stress. Exponentially growing yeast cells were exposed to stressors at the indicated concentrations for 4h. The total number of cells in culture was monitored using the Vi-Cell (Beckman Coulter) just before toxic exposure and after 4h incubation at 30ºC (as described in section 2.2.6). Results are represented as percentage fold change relatively to control (cells not exposed to stress). * and *** represent values significantly different (P <0.05 and P<0.001, respectively; one-way ANOVA, Dunnett's post-test). Values are mean ± SEM of three biological replicates.

A3.3. β-Galactosidase Activity Assay

To monitor serine misincorporation caused by expression of the G33 tRNACAGSer, the *E. coli LacZ* gene was co-expressed in *S.cerevisiae* wt and deletions strains. *LacZ* gene contains 54 CUG codons and serine insertion has severe costs for β-Gal thermal stability. In the cell β-gal catalyzes the cleavage of lactose to glucose. However, the synthetic compound o-nitrophenyl-β-D-galactoside (ONPG) is also recognized as a substrate and cleaved into galactose and o-nitrophenol, which has a yellow color. When ONPG is in excess over the enzyme in a reaction, the production of o-nitrophenol per unit time is proportional to the concentration of active β-Gal. The enzyme fraction that remains functional after denaturation provides an indirect measure of misincorporation.

Cells co-expressing pUKC815 and pRS315/pUKC715 were grown at 30ºC to mid – log (OD_{600} ~ 0,5 – 0,6) in 5ml MM lacking uracil and leucine. Cells were then collected and immediately washed, resuspended and disrupted as described in section **2.2.4** and **3.2.6**. Total protein from crude cell extracts was quantified using the BCA Protein Assay kit (Thermo Scientific), according to the manufacturer's instructions. 10µl crude extracts were mixed (vortex) in 990 µl of Z-buffer (60mM Na_2HPO_4, 40mM $NaH_2PO_4.2H2O$, 10mM KCl, 1mM $MgSO_4.7H_2O$, 50mM 2-mercaptoethanol, pH 7.0) and incubated at 52ºC for 30 min. to promote β-Gal unfolding. Immediately after, samples were kept on ice for 30 min for protein refolding. β-Gal activity was quantified at 37ºC. The assay tubes were incubated for 5min. at 37ºC and then 200µl of 4mg/mL o-nitrophenyl-β-D-galactopyranoside (ONPG) (Calbiochem) substrate were added to each tube. Reactions were allowed to proceed for 10 min approximately, until a pale yellow color appeared, and stopped by the addition of 400 µl of 1M Na_2CO_3. β-gal specific activity was determined by monitoring *o*-nitrophenol synthesis at 420nm, using the following formula: OD_{420} X 1.7 / 0.0045 x protein concentration x extract volume x time, where OD_{420} is

the optical density of the product, *o*-nitrophenol, at 420 nm. The factor 1.7 corrects for the reaction volume. The factor 0.0045 is the optical density of a 1 nmole/ml solution of *o*-nitrophenol. Protein concentration is expressed as mg/ml. Extract volume is the volume assayed in ml. Time is in minutes. Specific activity is expressed as nmoles/minute/mg protein.

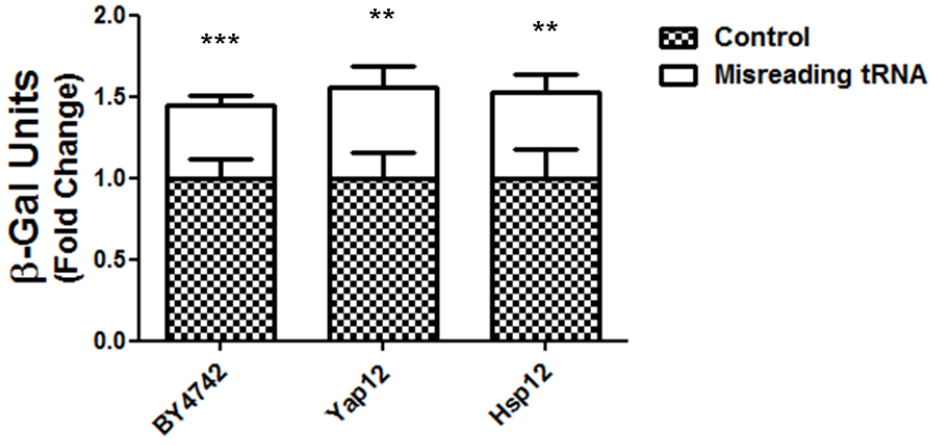

Figure A4 - $tRNA_{CAG}^{Ser}$ is expressed in wild-type and null deletion strains and has decoding activity, as assessed by a β-galactosidase thermal stability assay. The activity of the β-galactosidase fraction that remained functional after 30 min at 47ºC was determined by incubating cells at 37ºC in presence of ONPG and monitoring o-nitrophenol synthesis at 420nm.** and *** represent values significantly different from the control ($P < 0.01$ and $P<0.001$, respectively; one-way ANOVA, Dunnett's post-test). Values are mean ± SEM of at least four independent experiments done in triplicate.

A3.4. Methionine Misacylation of tRNA in *S. cerevisiae*

The array contains 40 nuclear-encoded yeast tRNA probes (orange) and 24 mitochondrial-encoded yeast tRNA probes (blue). In addition, the array includes 1 blank control (yellow) and 31 E. coli tRNA probes (green), which serve as negative controls (see Figure A5). Each probe has 8 replicates. The *S.cerevisiae* nuclear-encoded tRNA microarray probes are depicted in Table A2.

Yeast nuclear	Orange
Yeast michondrial	Blue
Ecoli	Green
Control	Yellow

Yeast/coli array layout

upper left

myHis	Val-3	Met-5	myHis	Val-3	Met-5	tm-2	myThr1	Met-3	tm-2	myThr1	Met-3	Gly-8	myArg-2	Glu-3	Gly-8	myArg-2	Glu-3	myVal	Thr-5	mycys	myVal	Thr-5	mycys
Lys-2	myleu	Leu-10	Lys-2	myleu	Leu-10	mygln	myPhe	Asn-3	mygln	myPhe	Asn-3	Ser-7	Lys-4	Thr-6	Ser-7	Lys-4	Thr-6	myThr1	Asp-3	Gly-5	myThr1	Asp-3	Gly-5
Met-5	myHis	Val-3	Met-5	myHis	Val-3	Met-3	tm-2	myThr1	Met-3	tm-2	myThr1	Glu-3	Gly-8	myArg-2	Glu-3	Gly-8	myArg-2	mycys	myVal	Thr-5	mycys	myVal	Thr-5
Leu-10	Lys-2	myleu	Leu-10	Lys-2	myleu	Asn-3	mygln	myPhe	Asn-3	mygln	myPhe	Thr-6	Ser-7	Lys-4	Thr-6	Ser-7	Lys-4	Gly-5	myThr1	Asp-3	Gly-5	myThr1	Asp-3
Pro-5	Gly-3	Trp-2	Pro-5	Gly-3	Trp-2	Ser-8	Val-5	Pro-6	Ser-8	Val-5	Pro-6	Ser-11	myAsn	myTrp	Ser-11	myAsn	myTrp	Gln-4	myMeti	Cys-2	Gln-4	myMeti	Cys-2
Arg-12	Val-7	Met-4	Arg-12	Val-7	Met-4	Met-5	mySer2	mypro	Met-5	mySer2	mypro	Cys-3	myAsp	myAsp	Cys-3	myAsp	myAsp	myIle	Glu-3	Lys-4	myIle	Glu-3	Lys-4
Trp-2	Pro-5	Gly-3	Trp-2	Pro-5	Gly-3	Pro-6	Ser-8	Val-5	Pro-6	Ser-8	Val-5	myTrp	Ser-11	myAsn	myTrp	Ser-11	myAsn	Cys-2	Gln-4	myMeti	Cys-2	Gln-4	myMeti
Met-4	Arg-12	Val-7	Met-4	Arg-12	Val-7	mypro	Met-5	mySer2	mypro	Met-5	mySer2	myAsp	Cys-3	myAsp	myAsp	Cys-3	myAsp	Lys-4	myIle	Glu-3	Lys-4	myIle	Glu-3
mycys	mypro	myAla	mycys	mypro	myAla	Lys-2	Cys-2	myHis	Lys-2	Cys-2	myHis	Asn-2	blank	Leu-9	Asn-2	blank	Leu-9	Thr-3	Arg-7	Pro-5	Thr-3	Arg-7	Pro-5
Leu-11	Leu-12	Pro-6	Leu-11	Leu-12	Pro-6	Val-5	Ala-5	Ile-3	Val-5	Ala-5	Ile-3	Pro-2	Sec-1	myPhe	Pro-2	Sec-1	myPhe	Leu-12	Trp-3	blank	Leu-12	Trp-3	blank
myAla	mycys	mypro	myAla	mycys	mypro	myHis	Lys-2	Cys-2	myHis	Lys-2	Cys-2	Leu-9	Asn-2	blank	Leu-9	Asn-2	blank	Pro-5	Thr-3	Arg-7	Pro-5	Thr-3	Arg-7
Pro-6	Leu-11	Leu-12	Pro-6	Leu-11	Leu-12	Ile-3	Val-5	Ala-5	Ile-3	Val-5	Ala-5	myPhe	Pro-2	Sec-1	myPhe	Pro-2	Sec-1	blank	Leu-12	Trp-3	blank	Leu-12	Trp-3
myArg-1	Phe-3	Thr-6	myArg-1	Phe-3	Thr-6	Arg-9	Ile-3	Thr-5	Arg-9	Ile-3	Thr-5	Gly-7	myTyr	Arg-12	Gly-7	myTyr	Arg-12	myArg-2	Ile-4	Ala-3	myArg-2	Ile-4	Ala-3
Ser-11	Sec-2	Val-6	Ser-11	Sec-2	Val-6	mySer2	myVal	Glu-2	mySer2	myVal	Glu-2	Ile-4	Tyr-3	mySer	Ile-4	Tyr-3	mySer	Sec-1	Arg-9	Lys-3	Sec-1	Arg-9	Lys-3
Thr-6	myArg-1	Phe-3	Thr-6	myArg-1	Phe-3	Thr-5	Arg-9	Ile-3	Thr-5	Arg-9	Ile-3	Arg-12	Gly-7	myTyr	Arg-12	Gly-7	myTyr	Ala-3	myArg-2	Ile-4	Ala-3	myArg-2	Ile-4
Val-6	Ser-11	Sec-2	Val-6	Ser-11	Sec-2	Glu-2	mySer2	myVal	Glu-2	mySer2	myVal	mySer	Ile-4	Tyr-3	mySer	Ile-4	Tyr-3	Lys-3	Sec-1	Arg-9	Lys-3	Sec-1	Arg-9
myIle	Val-8	Ser-4	myIle	Val-8	Ser-4	Met-6	Ala-6	Ile-5	Met-6	Ala-6	Ile-5	Leu-14	Ser-10	myArg-1	Leu-14	Ser-10	myArg-1	Gln-2	Asp-2	Ser-10	Gln-2	Asp-2	Ser-10
Gly-7	Gln-4	Thr-7	Gly-7	Gln-4	Thr-7	Trp-3	Leu-9	Gly-6	Trp-3	Leu-9	Gly-6	Ala-5	Ser-8	His-2	Ala-5	Ser-8	His-2	myLys	Ala-3	Sec-2	myLys	Ala-3	Sec-2
Ser-4	myIle	Val-8	Ser-4	myIle	Val-8	Ile-5	Met-6	Ala-6	Ile-5	Met-6	Ala-6	myArg-1	Leu-14	Ser-10	myArg-1	Leu-14	Ser-10	Ser-10	Gln-2	Asp-2	Ser-10	Gln-2	Asp-2
Thr-7	Gly-7	Gln-4	Thr-7	Gly-7	Gln-4	Gly-6	Trp-3	Leu-9	Gly-6	Trp-3	Leu-9	His-2	Ala-5	Ser-8	His-2	Ala-5	Ser-8	Sec-2	myLys	Ala-3	Sec-2	myLys	Ala-3
Asn-2	Gly-6	Tyr-2	Asn-2	Gly-6	Tyr-2	Phe-3	Met-3	Val-6	Phe-3	Met-3	Val-6	Tyr-3	Leu-6	Asp-2	Tyr-3	Leu-6	Asp-2	myTyr	Ile-6	myleu	myTyr	Ile-6	myleu
Lys-3	myTrp	myMet	Lys-3	myTrp	myMet	Trp-2	Arg-10	mythr2	Trp-2	Arg-10	mythr2	Phe-2	Ser-7	myMet	Phe-2	Ser-7	myMet	Ile-6	His-3	mySec	Ile-6	His-3	mySec
Tyr-2	Asn-2	Gly-6	Tyr-2	Asn-2	Gly-6	Val-6	Phe-3	Met-3	Val-6	Phe-3	Met-3	Asp-2	Tyr-3	Leu-6	Asp-2	Tyr-3	Leu-6	myleu	myTyr	Ile-6	myleu	myTyr	Ile-6
myMet	Lys-3	myTrp	myMet	Lys-3	myTrp	mythr2	Trp-2	Arg-10	mythr2	Trp-2	Arg-10	myMet	Phe-2	Ser-7	myMet	Phe-2	Ser-7	mySec	Ile-6	His-3	mySec	Ile-6	His-3
Cys-3	Glu-2	Met-6	Cys-3	Glu-2	Met-6	Arg-11	Thr-3	Ser-4	Arg-11	Thr-3	Ser-4	Leu-10	mythr2	Ala-6	Leu-10	mythr2	Ala-6	Arg-10	Asn-3	Arg-7	Arg-10	Asn-3	Arg-7
His-2	Pro-2	mygln	His-2	Pro-2	mygln	Leu-13	Arg-11	myGlu	Leu-13	Arg-11	myGlu	Asp-3	Gln-2	myAsn	Asp-3	Gln-2	myAsn	Thr-7	Thr-8	Thr-8	Thr-7	Thr-8	Thr-8
Met-6	Cys-3	Glu-2	Met-6	Cys-3	Glu-2	Ser-4	Arg-11	Thr-3	Ser-4	Arg-11	Thr-3	Ala-6	Leu-10	mythr2	Ala-6	Leu-10	mythr2	Arg-7	Arg-10	Asn-3	Arg-7	Arg-10	Asn-3
mygln	His-2	Pro-2	mygln	His-2	Pro-2	myGlu	Leu-13	Arg-11	myGlu	Leu-13	Arg-11	myAsn	Asp-3	Gln-2	myAsn	Asp-3	Gln-2	Thr-8	Thr-7	Thr-8	Thr-8	Thr-7	Thr-8
Gly-8	myGlu	Arg-6	Gly-8	myGlu	Arg-6	Val-3	Leu-13	Arg-6	Val-3	Leu-13	Arg-6	His-3	myLys	myMeti	His-3	myLys	myMeti	myAla	tm-2	Leu-6	myAla	tm-2	Leu-6
Ile-5	mySec	Gly-5	Ile-5	mySec	Gly-5	Val-7	Leu-14	Leu-11	Val-7	Leu-14	Leu-11	Gly-3	mySer	Met-4	Gly-3	mySer	Met-4	Val-8	Phe-2	Tyr-2	Val-8	Phe-2	Tyr-2
Arg-6	Gly-8	myGlu	Arg-6	Gly-8	myGlu	Arg-6	Val-3	Leu-13	Arg-6	Val-3	Leu-13	myMeti	His-3	myLys	myMeti	His-3	myLys	Leu-6	myAla	tm-2	Leu-6	myAla	tm-2
Gly-5	Ile-5	mySec	Gly-5	Ile-5	mySec	Leu-11	Val-7	Leu-14	Leu-11	Val-7	Leu-14	Met-4	Gly-3	mySer	Met-4	Gly-3	mySer	Tyr-2	Val-8	Phe-2	Tyr-2	Val-8	Phe-2

bottom right

Figure A5 - Layout of the *S.cerevisiae* microarray

Table A2 - *S.cerevisiae* nuclear-encoded tRNA microarray probes.

Amino acid	tRNA probe	Anticodon
Ala	Ala-5	AGC
	Ala-6	TGC
Arg	Arg-12	TCT
	Arg-10	CCG
	Arg-9	ACG
	Arg-11	CCT
Asn	Asn-3	GTT
Asp	Asp-3	GTC
Cys	Cys-3	GCA
Gln	Gln-4	CTG
Glu	Glu-3	CTC
Gly	Gly-7	GCC
	Gly-6	CCC
	Gly-8	TCC
His	His-3	GTG
Ile	Ile-5	AAT
	Ile-6	TAT
Leu	Leu-12	GAG
	Leu-11	CAA
	Leu-13	TAA
	Leu-14	TAG

Amino acid	tRNA probe	Anticodon
Lys	Lys-4	TTT
	Lys-3	CTT
Met	Met-6	CAT(i)
	Met-5	CAT(e)
Phe	Phe-3	GAA
Pro	Pro-6	TGG
	Pro-5	AGG
Sec	Sec-2	TCA
Ser	Ser-8	AGA
	Ser-10	GCT
	Ser-11	TGA
Thr	Thr-6	AGT
	Thr-7	CGT
	Thr-8	TGT
Trp	Trp-3	CCA
Tyr	Tyr-3	GTA
Val	Val-6	AAC
	Val-7	CAC
	Val-8	TAC

Four arrays were performed for the selected RNA samples: a regular (total RNA is hybridized directly), a cross-hybridization control (excess of DNA probes of Met-tRNAs are included in hybridization), a modification control (total RNA is first deacylated at pH 9 45 min) and a peptidyl-tRNA control (total RNA is treated with Aminopeptidase-M at room temperature for 25 min) (see section 3.2.10). Figure A6 shows the results obtained with the regular array.

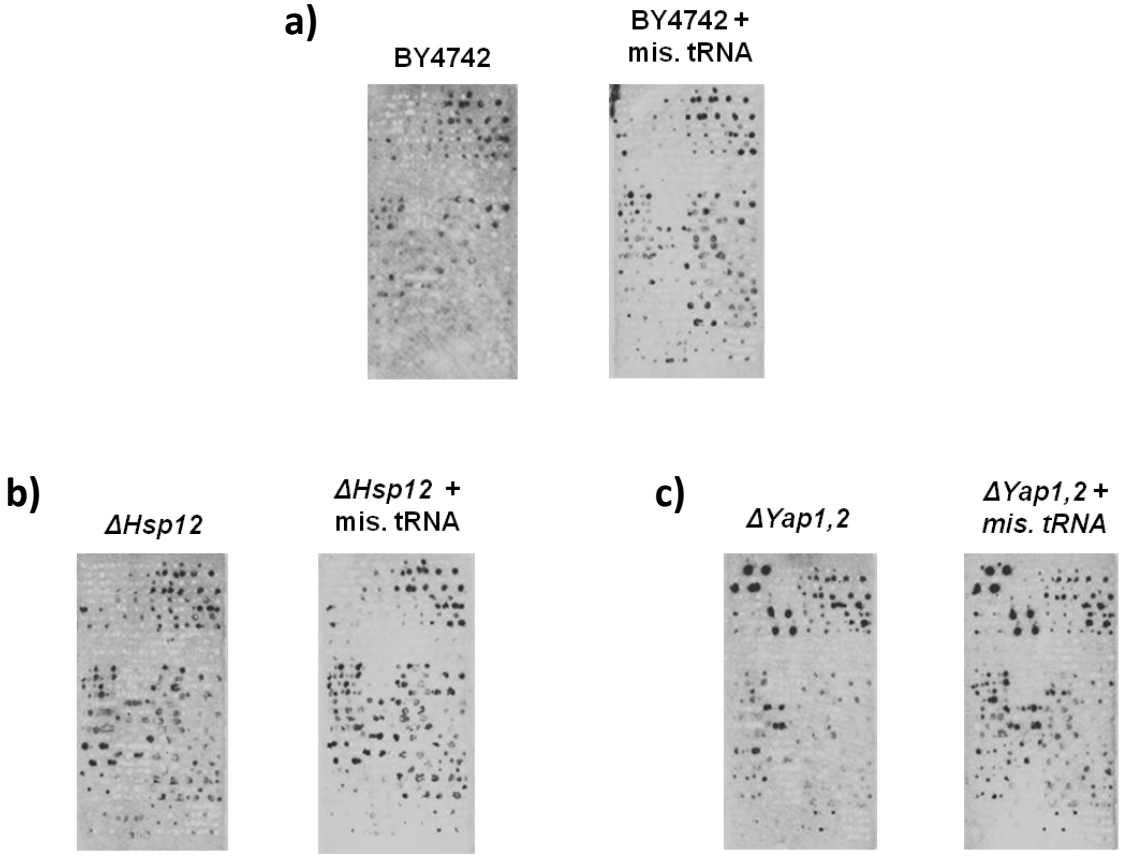

Figure A6 – Total RNA from the ^{35}S-Met pulse-labeled exponential phase *S.cerevisiae* cells was hybridized to a microarray with the layout showed in Figure A5. Potentially misacylated tRNAs are showed for a) BY4742 contro and mistranslating cells b) Δ*hsp12* control and mistranslating cells and c) Δ*yap1,2* control and mistranslating cells.